Bulletin

of

The Geological Society of America

VOLUME 69 August 1958 NUMBER 8

CONTENTS

	Pages
Stratigraphy of Ocoee series, Great Smoky Mountains, Tennessee and North Carolina. By Philip B. King, Jarvis B. Hadley, Robert B. Neuman, and Warren Hamilton	947–966
Submarine abrasion and wave-cut platforms. By William C. Bradley	967–974
Erosional processes and landforms in Badlands National Monument, South Dakota. By Kenneth G. Smith	975–1008
Radiocarbon chronology of Lake Lahontan and Lake Bonneville. By Wallace S. Broecker and Phil C. Orr	1009–1032
Pocono paleocurrents in Pennsylvania and Maryland. By Bernard R. Pelletier	1033–1064
Short Notes	
Crater Hill lava flow, Zion National Park, Utah. By Richard L. Threet	1065–1070
Definition of volcanic breccia. By Richard V. Fisher	1071–1074

Subscription $15.00 per year.
Printing Office: Mt. Royal & Guilford Aves., Baltimore 2, Md.
Communications for publications should be addressed to The Geological Society of America, Dr. H. R. Aldrich, Secretary, 419 West 117 Street, New York, N. Y.
Please give notice of change of address 4 weeks in advance. Claims for nonreceipt of the Bulletin of a given month must be sent to the Secretary of the Society before the end of the second succeeding month.

Entered as second-class matter at the Post Office at Baltimore, Md.
under the Act of Congress of July 16, 1894.
Accepted for mailing at special rate of postage provided for in Section 1103
Act of October 3, 1917, authorized on July 8, 1918.

PAPERS IN PRESS FOR FORTHCOMING ISSUES

Utuado Pluton, Puerto Rico. By J. D. Weaver

Stratigraphy and Structure of the Northern Sangre De Cristo Mountains, Colorado. By Linus R. Litsey

Rebound in the Bearpaw Shale, Western Canada. By R. Peterson

Uranium Emplacement in the Colorado Plateau. By Paul F. Kerr

Older Precambrian Rocks of the Diamond Butte Quadrangle, Gila County, Arizona. By Gordon Gastil

BULLETIN OF THE GEOLOGICAL SOCIETY OF AMERICA
VOL. 69, PP. 947-966, 4 FIGS. AUGUST 1958

STRATIGRAPHY OF OCOEE SERIES, GREAT SMOKY MOUNTAINS, TENNESSEE AND NORTH CAROLINA

BY PHILIP B. KING, JARVIS B. HADLEY, ROBERT B. NEUMAN, AND WARREN HAMILTON

ABSTRACT

Much of the Great Smoky Mountains, which span the boundary between Tennessee and North Carolina, is formed of the Ocoee series, of later Precambrian age. This is a body of terrigenous clastic sedimentary rocks, which has minor intercalations of limestone and dolomite but no volcanic components or known fossils. The series is probably 30,000 feet or more thick. It lies unconformably on a basement of earlier Precambrian granitic and gneissic rocks, and on the northwest side of the mountains it is overlain by the Cochran formation, or basal unit of the Chilhowee group, which is of Cambrian and Precambrian(?) age. South of the mountains it is overlain by rocks of the Murphy marble belt; here, the top of the Ocoee is placed tentatively at the base of the Nantahala slate.

The Ocoee series is divisible into three broad units of regional extent and contrasting lithologic character, which are herewith designated groups and named the Snowbird group, the Great Smoky group, and the Walden Creek group. The groups consist of local intergrading and intertonguing formations and have complex stratigraphic and structural relations. The Ocoee series is split by major thrust faults into three sequences, a southern, central, and northern, none of which contains more than two groups of the series.

The lowest group, the Snowbird, is best developed in the central sequence where it is more than 13,000 feet thick; it is much thinner in the southern sequence. In both sequences it lies unconformably on granites and gneisses. Toward the east it is largely sandstone, but this is interbedded with and intertongues westward into finer-grained sandstone, siltstone, and argillaceous rocks. These differences permit the Snowbird group to be divided, in ascending order, into the Wading Branch formation, Longarm quartzite, Roaring Fork sandstone, and Pigeon siltstone. Toward the west the Snowbird is represented by more strongly metamorphosed rocks termed the Metcalf phyllite.

Above the Snowbird group in the southern sequence is the Great Smoky group, more than 25,000 feet thick. The lower part, termed the Elkmont sandstone, is fine-grained sandstone. The middle part, termed the Thunderhead sandstone, is poorly sorted, coarse, feldspathic sandstone in graded beds. The upper part, termed the Anakeesta formation, includes many beds of dark argillaceous and silty rocks. South of the Great Smoky Mountains the Great Smoky group is overlain by the rocks of the Murphy marble belt.

The Snowbird group in the central sequence is overlain in a few places by coarser-grained rocks. These somewhat resemble those of the Great Smoky group, but their stratigraphic relations to it are not demonstrable, so that they are left as unclassified parts of the Ocoee series. In one area such rocks are named the Rich Butt sandstone, in another the Cades sandstone.

In the northern sequence the Walden Creek group, about 8000 feet thick, forms a varied assemblage of argillaceous and silty rocks and quartz-pebble conglomerate, with locally prominent quartzite, limestone, and dolomite. The Walden Creek group is divided, in ascending order, into the Licklog formation, Shields formation, Wilhite formation, and Sandsuck formation; the Wilhite is in turn divided into the Dixon Mountain member and Yellow Breeches member. The Walden Creek is overlain by the Chilhowee group of Cambrian and Precambrian(?) age but is in fault contact with the Snowbird group on the southeast; it is not in contact with the Great Smoky group. Northeast of the Great Smoky Mountains, the Walden Creek group is reported to overlie the Snowbird group as part of a sedimentary sequence from the basement rocks upward through the Chilhowee group into the overlying Paleozoic.

CONTENTS

TEXT

	Page
Introduction	948
Present investigation	948
Acknowledgments	948
Purpose of paper	948
Stratigraphic terminology	949
Previous terminology	949

	Page
Ocoee series defined	951
Groups of Ocoee series	951
Formations of Ocoee series	953
Snowbird group	954
General features	954
Wading Branch formation	954
Longarm quartzite	954
Roaring Fork sandstone	954
Pigeon siltstone	956
Metcalf phyllite	957
Great Smoky group	957
General features	957
Elkmont sandstone	958
Thunderhead sandstone	958
Anakeesta formation	959
Unclassified formations of Ocoee series	960
General features	960
Rich Butt sandstone	960
Rocks of Webb Mountain and Big Ridge	960
Cades sandstone	960
Walden Creek group	961
General features	961
Licklog formation	962
Shields formation	962
Wilhite formation	962
Sandsuck formation	962
General problems	963
Broader relations of Ocoee series	963
Age of Chilhowee group	964
Age of rocks of Murphy marble belt	964
Age of Ocoee series	965
References cited	965

ILLUSTRATIONS

Figure	Page
1. Index map of Great Smoky Mountains and vicinity	950
2. Geologic map of Great Smoky mountains and vicinity	952
3. Restored stratigraphic section of Snowbird group from southeast to northwest, across eastern Great Smoky Mountains	956
4. Fence diagram along northwest side of eastern and central Great Smoky Mountains	959

TABLE

Table	Page
1. Stratigraphic units of Ocoee series of Great Smoky Mountains	955

Introduction

Present Investigation

Between 1946 and 1955 a group of geologists with the U. S. Geological Survey investigated the Great Smoky Mountains of Tennessee and North Carolina, a project originally requested by the National Park Service. During this period an area of 1300 square miles was mapped geologically, including most of Great Smoky Mountains National Park and considerable surrounding territory. Results are being assembled in a series of reports (Fig. 1), which will be published by the U. S. Geological Survey.

Acknowledgments

We gratefully acknowledge assistance rendered and information given by other geologists who have taken part in the project for the Geological Survey—Richard Goldsmith, Andrew Griscom, John K. Lydecker, Harold E. Malde, Willis H. Nelson, Steven S. Oriel, Charlie A. Tucker, Jr., and Robert F. Yerkes. In addition, important contributions were made during the first 3 years of the investigation by Herman W. Ferguson and George D. Swingle, at that time on the staff of the Tennessee Division of Geology, whose work was generously contributed by that organization.

Besides mapping in the project area we have either jointly or singly taken part in many field excursions in surrounding areas, on some occasions under the guidance of other geologists working in the Southeastern States. Especially pertinent to the present paper was our participation in some of the reconnaissance done by John Rodgers in the mountains southeast of the Appalachian Valley, during preparation of his geologic map of east Tennessee (Rodgers, 1953).

Purpose of Paper

An important phase of this investigation has been untangling the stratigraphy of the Ocoee series, the great mass of sedimentary rocks that forms most of the Great Smoky Mountains. Although some problems remained at the close of the investigation, great progress was made in understanding the relations and geologic history of the Ocoee. This new understanding is expressed in a revised stratigraphic classification which has been worked out jointly among us (Table 1).

As it will be some years before completion and publication of our detailed reports, it seems desirable to place this preliminary summary before geologists working in this part of the Appalachians. The various stratigraphic names agreed on are based on type localities in different report areas, so that it is best to set them forth jointly in a single account, rather than present them piecemeal in the several reports.

This paper therefore deals primarily with the stratigraphy and nomenclature of the Ocoee

series. Treatment of the origin, structure, and subsequent history of the Ocoee, and geologic maps thereof, are reserved for the detailed reports. The general geology of the region is here mentioned only incidentally; it has been outlined in previous papers (Hadley, King, Neuman, and Goldsmith, 1955; Neuman, 1951).

In the present paper, localities referred to in the text are indicated on an index map (Fig. 1). For further geographic details the reader is referred to the topographic map of Great Smoky Mountains National Park and vicinity (U. S. Geological Survey, 1950, scale 1:125,000). Distribution of the Ocoee series is shown on a generalized geologic map (Fig. 2).

Stratigraphic Terminology

Previous Terminology

The Ocoee series corresponds to the "Ocoee conglomerate and slate", which Safford (1856, p. 151–152; 1869, p. 183–198) named for exposures in the gorge of the Ocoee River, Polk County, Tennessee, southwest of the Great Smoky Mountains, and recognized as constituting much of the Unaka Range from there to northeastern Tennessee. In the same region, Safford also recognized an overlying unit, the "Chilhowee sandstone", now termed the Chilhowee group.

Keith, in his series of geologic folios on the southern Appalachians, divided the rocks of the Unaka Range into formations that he attempted to trace over the whole region, but he did not formally use Safford's names "Ocoee" and "Chilhowee". Keith's interpretations evolved as his mapping of widening areas brought increasing understanding, so that in later folios the stratigraphic terminology and conclusions as to age, sequence, and structure differ greatly from those of the earlier publications. This evolution is difficult for the uninitiated reader to follow in the publications, because Keith made no general summary and did not explain fully in the folios the reasons for changes made in terminology and interpretation. A summary of Keith's results attempted by Barrell (1925) is unsatisfactory because he did not have access to unpublished maps of critical parts of the region.

Keith's initial interpretation of the rocks of the Ocoee series was set forth in his Knoxville and Loudon folios (1895; 1896) and was also used by Hayes in the Cleveland folio (1895). Rocks now placed in the Ocoee series were divided, in supposed ascending order, into the Wilhite slate, Citico conglomerate, Pigeon slate, Cades conglomerate, Thunderhead conglomerate, Hazel slate, and Clingman conglomerate. Although Safford surmised that the Ocoee underlay the Chilhowee and formed the base of the sedimentary column, Keith classed its rocks as of "age unknown" and showed them as lying unconformably on the Sandsuck shale, the Chilhowee group, and various "Silurian" (*i.e.*, Ordovician) formations. A statement by Bailey Willis, Keith's supervisor (*in* Walcott, 1891, p. 299–300), shows that they were unaware of the large low-angle faults in the region, which disorder the stratigraphic sequence.

As folio mapping was extended into surrounding areas, Keith discovered that the units of the Knoxville quadrangle were not only inapplicable regionally, but that the sequence, structure, and regional pattern of the rocks were different from that first supposed. About 1901 he therefore developed a new classification and interpretation (U. S. Geol. Survey, 1901, p. 69; 1902, p. 49), which was used in the Asheville and subsequent folios (Keith, 1904; 1907; U. S. Geol. Survey open-file reports, Mount Guyot, Cowee, and Murphy quadrangles):

Cambrian
- Overlying formations in Murphy marble belt
- *Nantahala slate*
  - (Type, Nantahala Gorge, Nantahala quadrangle).
- *Great Smoky conglomerate*
  - (Type, Great Smoky Mountains, Knoxville and Mount Guyot quadrangles)
- *Hiwassee slate*
  - (Type, gorge of Hiwassee River, Murphy quadrangle)
- *Snowbird formation*
  - (Type, Snowbird Mountain, Mount Guyot quadrangle

Unconformity

Archean
- Carolina and Roan gneisses, and Max Patch and Cranberry granites

Keith transferred these units from an "unknown" to a Cambrian age because he concluded that the Nantahala slate and Great Smoky conglomerate were the southeastern equivalents of the Nichols shale and Cochran conglomerate of the Chilhowee group, and because the remaining units lay conformably beneath them.

Keith's revised terminology and interpretation were remarkably perceptive for their

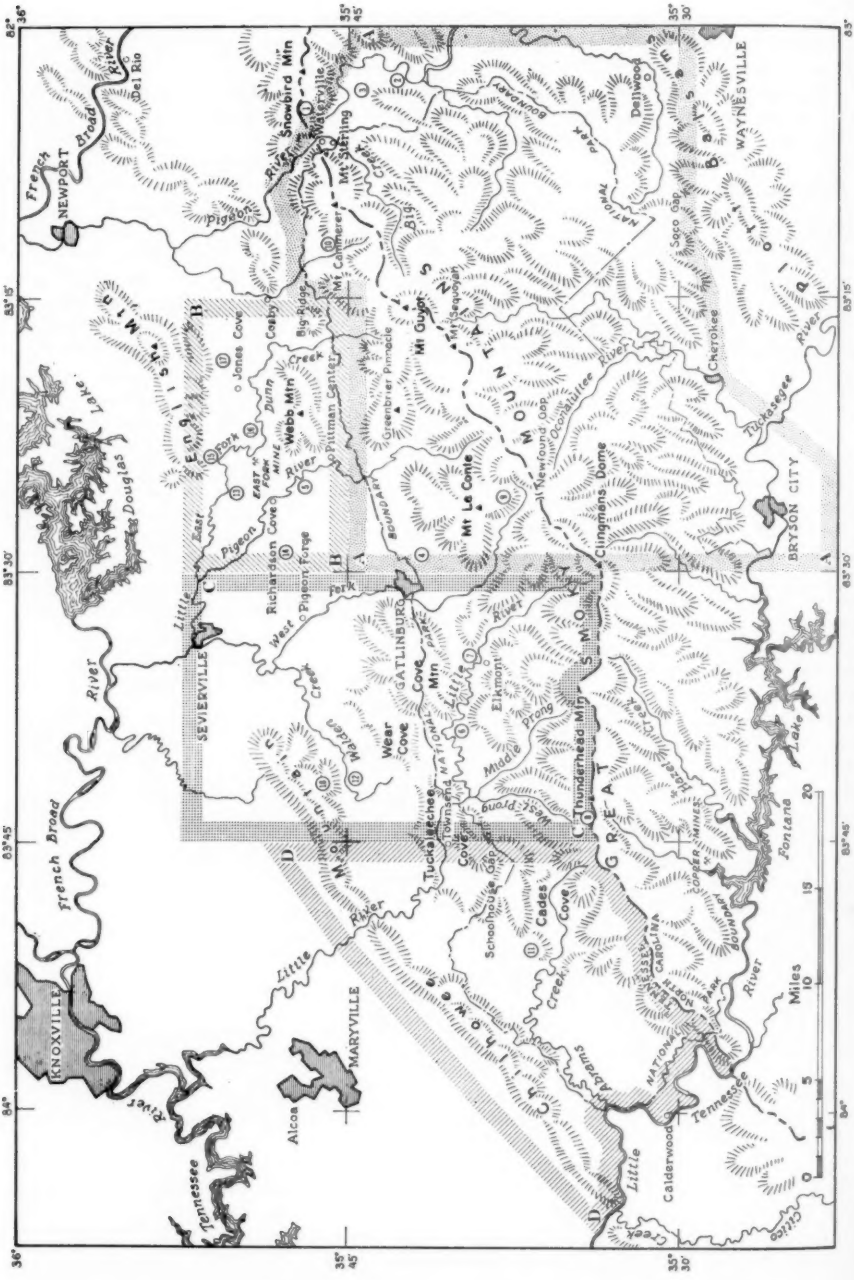

FIGURE 1. INDEX MAP OF GREAT SMOKY MOUNTAINS AND VICINITY
(See front of facing page for detailed caption)

time. His formations have proved to be useful lithologic entities, recognizable over wide areas in much the manner originally shown, and most were placed in correct sequence. Later work has shown the need for revision and amplification because of more detailed mapping and because of more sophisticated concepts of structure, metamorphism, sedimentation, and regional relations. Nevertheless, his stratigraphy forms a basis on which modern terminology of the Ocoee series can be established.

Much later, Stose and Stose (1949, p. 273) proposed that the Ocoee series of the Great Smoky Mountains be divided into a Hurricane graywacke, a Great Smoky quartzite, and a Nantahala slate, but these units as they were defined and mapped are not considered further here.

Ocoee Series Defined

Rocks of the Great Smoky Mountains which are now termed the Ocoee series (Stose and Stose, 1944, p. 401; 1949, p. 270; King, 1949, p. 622; Rodgers, 1953, p. 24) are a body of terrigenous clastic sedimentary rocks that have minor intercalations of limestone and dolomite but no volcanic components or known fossils. Many of the clastic rocks are coarse-grained, most are poorly sorted texturally and mineralogically, and few are cleanly washed. Many parts are monotonous sequences; changes from one rock type to another are commonly gradational vertically and laterally, with few mappable key beds. Aggregate thickness of the series is comparable to that of all the Paleozoic rocks of the adjacent Appalachian Valley.

The rocks of the Ocoee series are of sedimentary origin but have been metamorphosed to varying degrees. At the northwest edge of the foothills, shales are unaltered or are represented by slates; these give way southeastward to phyllites and schists. Mineral assemblages of the amphibolite facies are developed over wide areas; staurolite and kyanite are common, but metamorphic grain sizes are smaller, and obliteration of sedimentary structures less, than in rocks of similar grade in most regions. Sandstones are recrystallized and their grain size modified, but their sedimentary aspect and the distinctiveness of their beds are clearly preserved almost everywhere. In the discussion that follows, the rocks will generally be referred to in terms of their initial sedimentary rock types.

Throughout most of the outcrop area of the Ocoee series, no base or top is visible. On the southeast side of the Great Smoky Mountains, however, its basal beds lie unconformably on earlier granites and gneisses. In the northwest part of the mountains its upper beds are believed to be succeeded by the Cochran formation at the base of the Chilhowee group. To the south, also, it is succeeded by formations of the Murphy marble belt. Some geologists have included the Nantahala slate and even some of or all the higher units of this belt in the Ocoee. (*See* Wilmarth, 1938, p. 1528; King, 1949, p. 638.) In recent years, however, geologists of the Georgia Geological Survey have considered the Nantahala to be the basal formation of a succeeding and contrasting stratigraphic sequence excluded from the Ocoee (Furcron, 1953, p. 34–38; Hurst, 1955, p. 8). This interpretation seems reasonable, and we therefore tentatively place the top of the Ocoee series at the base of the Nantahala slate. The Ocoee is classed by the U. S. Geological Survey as a provincial series comparable to other series of the Precambrian such as the Keweenawan, Belt, and Grand Canyon.

Groups of Ocoee Series

The rocks of the Ocoee are divisible into broad mappable lithologic units. Such divisions were recognized by Keith, who designated them as formations, but as each can be divided into different component units, it is more appropriate to rank them as groups. Adapting Keith's classification to our knowledge, we divide the Ocoee series into the Snowbird group, the Great Smoky group, and the Walden Creek group. A few formations of the Ocoee series do not fit conveniently into these groups and are therefore left unclassified.

FIGURE 1. INDEX MAP OF GREAT SMOKY MOUNTAINS AND VICINITY
(See front of facing page for detailed explanation)

FIGURE 1. INDEX MAP OF GREAT SMOKY MOUNTAINS AND VICINITY

Areas covered by reports now in preparation are indicated by capital letters as follows: A, Eastern Great Smoky Mountains, by J. B. Hadley and R. Goldsmith; B, Richardson Cove and Jones Cove quadrangles, by W. B. Hamilton; C, Central Great Smoky Mountains, by P. B. King; D, Western Great Smoky Mountains, by R. B. Neuman and W. H. Nelson.

Type localities of stratigraphic units in Ocoee series are indicated by circled numbers as follows: 1, Snowbird Mountain; 2, Wading Branch Ridge; 3, Longarm Mountain; 4, Roaring Fork; 5, Little Pigeon River; 6, Metcalf Bottoms; unnumbered, Great Smoky Mountains; 7, Elkmont; 8, Thunderhead Mountain; 9, Anakeesta Ridge; 10, Rich Butt Mountain; 11, Cades Cove; 12, Walden Creek; 13, Licklog Hollow; 14, Shields Mountain; 15, Wilhite Creek; 16, Dixon Mountain; 17, Yellow Breeches Creek; 18, Sandsuck Branch.

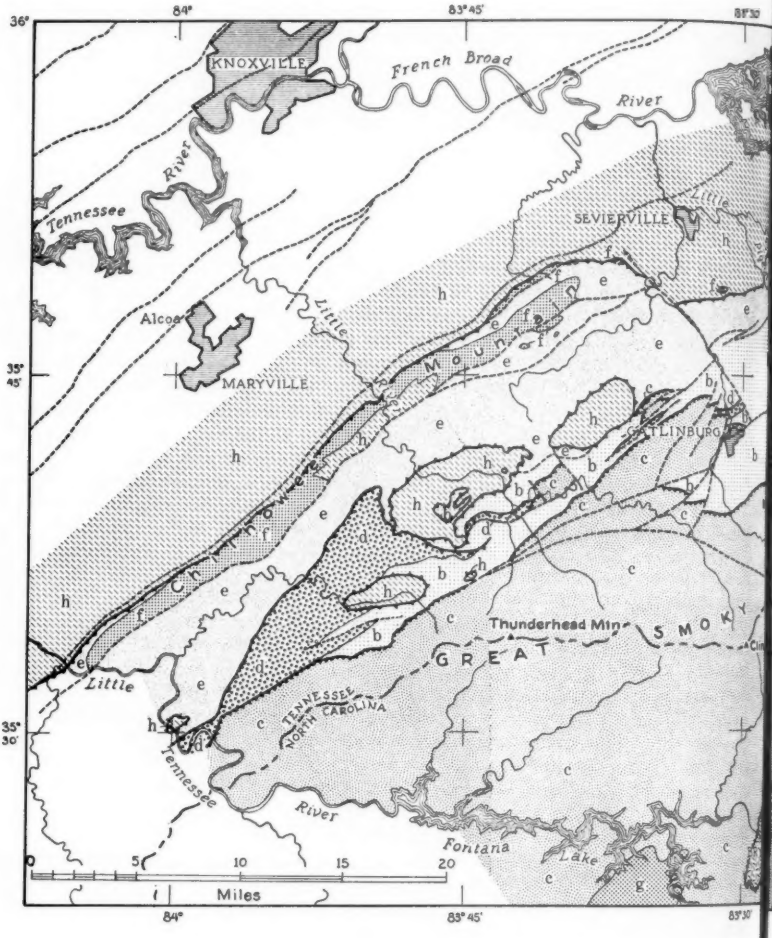

FIGURE 2. GEOLOGIC MAP OF GREAT S
Showing Ocoee series and adjacent formations and the groups into which the Ocoee is divided. Most of ge
between 1946 and 1955. Faults outside patterned area from Rodgers (1953).

Two of the groups, the Snowbird and Great Smoky, are adapted from Keith's formations of those names; they were sufficiently defined in the original descriptions, and their type localities are in the Great Smoky Mountains, where they have been restudied. One of them, the Great Smoky, has already been accorded group status in northern Georgia (Hurst, 1955, p. 8–9). The third group, Walden Creek, corresponds approximately to Keith's Hiwassee slate, but for reasons stated below the name Hiwassee has been abandoned and a new name substituted.

The rocks of the Ocoee series have complex stratigraphic and structural relations so that they do not form a single sequence. In the Great Smoky Mountains they are instead divided by major thrust faults into three separate sequences: northern, including the Walden Creek group and the overlying Chil-

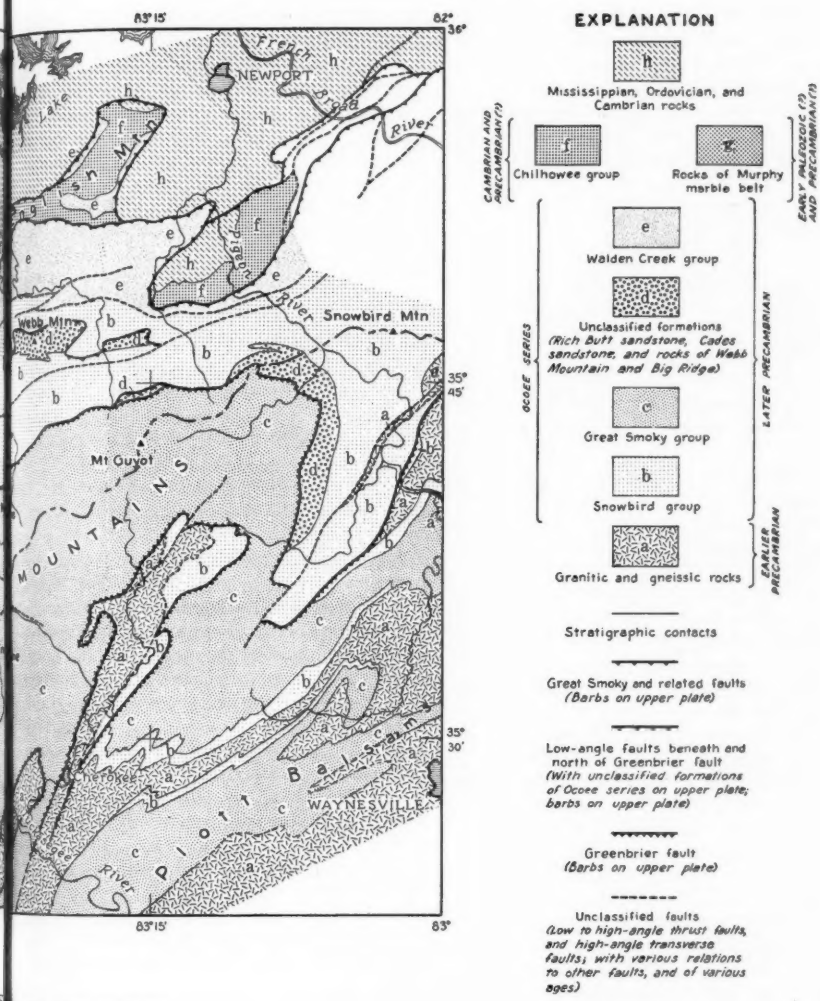

GREAT S
NTAINS AND VICINITY
Most of g
n patterned area by P. B. King, J. B. Hadley, R. B. Neuman, W. B. Hamilton, and others; surveyed

howee group; central, in which the Snowbird group is principally developed and is overlain by formations unclassified as to group; southern, in which a much thinned Snowbird group is overlain by the Great Smoky group.

Formations of Ocoee Series

The groups into which the Ocoee series is divided are of regional extent, but formations within the groups are local; they interfinger and intergrade with each other along the strike, and some do not persist throughout the area studied. Many of these formations are newly named here, but for some of them formation names used by Keith in the Knoxville folio (1895) can be adapted, although these names require redefinition, and the formations do not lie in the stratigraphic order originally assumed. Four of them, the Wilhite, Pigeon, Cades, and

Thunderhead are thus adapted and redefined. Three others, the Citico, Hazel, and Clingman, as used by Keith, are for various reasons unsuitable for further use and are abandoned.

The terminology here used for the groups and formations of the Ocoee series in the Great Smoky Mountains is summarized in Table 1.

Snowbird Group

General Features

The Snowbird formation was named by Keith (1904, p. 5) for Snowbird Mountain, northeast of the Great Smoky Mountains across the Pigeon River (Fig. 1); the term was applied to a conformable sequence of feldspathic sandstones, siltstones, and argillaceous rocks that lie unconformably on basement rocks.

The rocks of this assemblage are distinctive in the Ocoee series and can be divided into four intertonguing formations; they are here named the Snowbird group. The type section of the group is along the Pigeon River at the southwest and south base of Snowbird Mountain, where the group rests on granitic rocks and is succeeded conformably by the Rich Butt sandstone. In this section, the Snowbird group is at least 13,000 feet thick, but it may be thicker farther northwest.

Most of the Snowbird group occurs in the foothills immediately north of the main Great Smoky Mountains, where it lies beneath the Greenbrier fault (Fig. 2). Here it extends southwestward as far as Cades Cove, where it pinches out between other units; it probably does not reappear beyond. Northeastward from Snowbird Mountain the unit has been mapped across the French Broad River (Oriel, 1950, p. 23–30; Ferguson and Jewell, 1951, p. 16–21), although it is interrupted in places by faulting. Patches of the Snowbird reappear within and southeast of the Great Smoky Mountains, some in the central, some in the southern sequence.

In the southeast part of the mountains, above the Greenbrier fault, the Snowbird group is about a tenth as thick as in the type area. Southeastward near Waynesville it pinches out between the underlying granites and gneisses and overlying Great Smoky group. In this region the Snowbird is overlain conformably by the Great Smoky.

Wading Branch Formation

The Wading Branch, or basal formation of the Snowbird group, is here named for Wading Branch Ridge west of the Pigeon River about 5 miles southeast of Waterville (Fig. 1). The type section is somewhat to the north along the river, 4½ miles southeast of Waterville. The formation is traceable thence southwestward through several belts of outcrop as far as Cherokee and everywhere lies unconformably on granitic rocks (Max Patch granite of Keith). At the type locality it is about 1500 feet thick, but it thins greatly in the southwestern belts.

The Wading Branch formation consists of medium-bedded, dark clastic rocks, including sandy argillaceous rocks, siltstone, and coarse pebbly feldspathic sandstone. The coarser rocks are poorly sorted, have a dark micaceous matrix, and are somewhat graded. A distinctive basal unit generally less than 100 feet thick, representing reworked residual clay (Goldsmith and Hadley, 1955), is exposed throughout much of the extent of the formation.

Longarm Quartzite

The Longarm quartzite is here named for Longarm Mountain lying west of the Pigeon River about 4 miles southeast of Waterville (Fig. 1) and is typically exposed along the river at the north base of the mountain. The Longarm forms a substantial part of the Snowbird group near the Pigeon River and eastward, where it projects in ridges of intermediate height. It also appears in more limited areas as far southwest as Cherokee.

In contrast to the Wading Branch formation, the Longarm quartzite consists largely of clean feldspathic quartzite and arkose, dominantly light, medium-bedded, and medium- to very coarse-grained. Most layers are current-bedded. Interbedded with the quartzite and arkose, especially in the upper part, are many beds 1–3 feet thick of darker finer-grained sandstone.

The Longarm succeeds the Wading Branch conformably and rather abruptly, although the contact is gradational over several tens of feet. At the type locality the formation is about 5000 feet thick; but, like the other formations of the Snowbird group, it thins and eventually pinches out a short distance southeast of the Great Smoky Mountains.

Roaring Fork Sandstone

The Longarm quartzite on the Pigeon River is succeeded by a thick unit of darker sandstone and interbedded pelitic rocks to which the name Roaring Fork sandstone is here given, from a more typical section on Roaring Fork, 1-3

TABLE 1.—STRATIGRAPHIC UNITS OF OCOEE SERIES OF GREAT SMOKY MOUNTAINS

AGE	NORTH OF AND BELOW GREENBRIER FAULT			SOUTH OF AND ABOVE GREENBRIER FAULT	
CAMBRIAN AND PRECAMBRIAN (?)	CHILHOWEE GROUP	Cochran formation and higher units		ROCKS OF MURPHY MARBLE BELT	Nantahala slate and higher units
		DISCONFORMITY?		(PRECAMBRIAN (?) AND EARLY PALEOZOIC (?))	
					LITHOLOGIC BREAK, BUT PROBABLY CONFORMABLE
LATER PRECAMBRIAN	OCOEE SERIES			OCOEE SERIES	
	WALDEN CREEK GROUP *	Sandsuck formation		GREAT SMOKY GROUP	Unnamed higher strata
		Wilhite formation ☆ { Yellow Breeches member * / Dixon Mountain member *			Anakeesta formation *
		Shields formation *			Thunderhead sandstone
		Licklog formation *			Elkmont sandstone *
		FAULT CONTACT, SEQUENCE UNCERTAIN			
		WESTERN PART OF AREA	EASTERN PART OF AREA		
	UNCLASSIFIED FORMATIONS	Cades sandstone ☆	Rocks of Webb Mountain and Big Ridge / Rich Butt * sandstone	SNOWBIRD GROUP	Roaring Fork sandstone *
	SNOWBIRD GROUP	Metcalf phyllite *	Pigeon siltstone ☆ / Roaring Fork sandstone * / Longarm quartzite * / Wading Branch formation *		Longarm quartzite *
					Wading Branch formation *
		BASE NOT EXPOSED	UNCONFORMITY		UNCONFORMITY
EARLIER PRECAMBRIAN		Granitic and gneissic rocks			Granitic and gneissic rocks

Correlation between these sequences not established

New stratigraphic names * Old stratigraphic names, with major redefinitions ☆

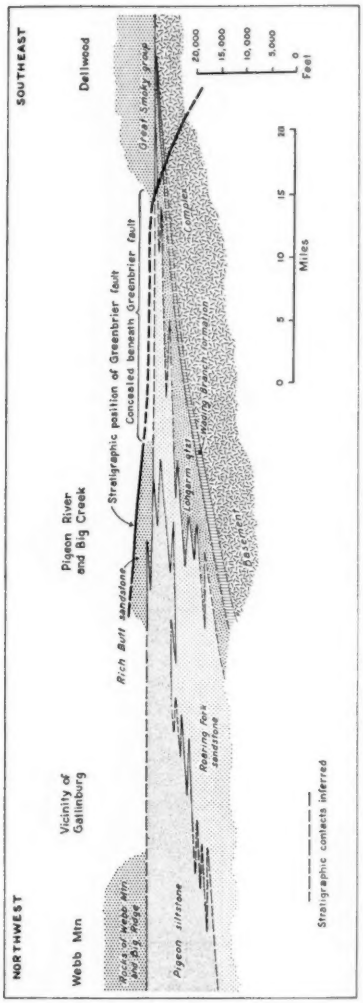

FIGURE 3.—RESTORED STRATIGRAPHIC SECTION OF SNOWBIRD GROUP FROM SOUTHEAST TO NORTHWEST, ACROSS EASTERN GREAT SMOKY MOUNTAINS
Showing relations of its formations and its relations to earlier Precambrian rocks, to Great Smoky group, and to unclassified formations of Ocoee series.

miles southeast of Gatlinburg (Fig. 1). In the vicinity of Roaring Fork, somewhat less than half of the formation consists of massive light-greenish-gray sandstone beds 5–50 feet thick, which are fine- to medium-grained, highly feldspathic, and moderately well sorted. Interbedded with them are thick- to thin-bedded finer-grained sandstone, siltstone, and argillaceous rocks. Current bedding, although much less evident than in the Longarm, is fairly common, especially in the finer-grained and thinner-bedded sandstone.

At the type locality about 8000 feet of Roaring Fork sandstone lies conformably below the Pigeon siltstone, but its base is cut off by faults. On the Pigeon River, where a complete section of the formation is present, it is only 2700 feet thick, and this marked decrease is interpreted as resulting from intertonguing eastward with the Longarm quartzite through an interval of several thousand feet (Fig. 3).

Pigeon Siltstone

The Pigeon siltstone (King, 1949, p. 639-640) was adapted from the Pigeon slate of Keith (1895) and named for exposures along the Little Pigeon River and its West Fork (Fig. 1). The Pigeon crops out in a wide band across the northern foothills of the mountains from near the meridian of Gatlinburg eastward. The type section is here designated as along the Little Pigeon River between Richardson Cove and Pittman Center, where it is 10,000 or 15,000 feet thick. The formation is also well exposed along the Pigeon River northwest of Waterville; it is not represented in the Snowbird group farther south, where it disappears by intertonguing with the Roaring Fork sandstone.

The contact between the Pigeon and Roaring Fork is placed at the top of the highest persistent sandstone bed at any locality, but the sandstones finger out westward so that the base of the Pigeon as thus defined descends in this direction. At the east end of the mountains the Pigeon is overlain conformably by the Rich Butt sandstone and other unclassified formations.

The Pigeon is a remarkably uniform body of gray to greenish-gray thin- to thick-bedded siltstone, composed of recrystallized quartz and feldspar silt, in a matrix altered to sericite and chlorite. Most of the siltstone is laminated in light- and dark-greenish-gray layers a few millimeters thick and is partly current-laminated; many of the laminae bear calcite or other

carbonates. Much of the formation, particularly the upper part along the north edge of its belt of outcrop, is dark gray rather than greenish, and the carbonate-bearing laminae are there more numerous than elsewhere. At wide intervals the siltstone is interbedded with units of slate or fine-grained feldspathic sandstone as much as several hundred feet thick, and thin laminae of slate and fine-grained sandstone are abundant.

Metcalf Phyllite

In the western part of the Great Smoky Mountains the Snowbird group is represented by the Metcalf phyllite, here named for Metcalf Bottoms on the Little River, where it is typically exposed along Tennessee Highway 73 (Fig. 1). The Metcalf crops out between the high ridges of the Great Smoky Mountains and the cove areas on the northwest in a belt extending from near the meridian of Gatlinburg southwestward to Cades Cove.

In most places the Metcalf phyllite is faulted against other rocks with which it is in contact and is itself thoroughly foliated, much contorted, and pervasively sheared; its thickness is thus indeterminable but may be thousands of feet. Relations with the remainder of the Snowbird group are uncertain; it joins the Pigeon siltstone at the northeast end of its outcrop belt, but the contact relations are obscure. The Metcalf is probably equivalent to the Pigeon siltstone and perhaps in part to the Roaring Fork sandstone but is differentiated because of its greater physical metamorphism and uncertain stratigraphic relations.

Before metamorphism, much of the Metcalf was probably like the Pigeon, although silty components seem to be somewhat less and argillaceous components greater. A characteristic rock of the formation is lustrous, thinly fissile, gray-green or gray phyllite, but almost half of the unit is more silty and resembles the siltstone of the Pigeon except for its stronger cleavage. Bedding laminae in the argillaceous rocks are everywhere subordinate to cleavage and have been obliterated in part, but they are better preserved in the siltstones; at a few places the siltstone is current-bedded, but carbonate-bearing laminae are uncommon. Sandstone beds resembling those in the Pigeon and Roaring Fork are widely spaced and generally thin, but northwest of Schoolhouse Gap they constitute much of the exposed section.

Great Smoky Group

General Features

The Great Smoky conglomerate was named by Keith (1904, p. 6) for the Great Smoky Mountains; the term was applied to the great mass of fine conglomerates, coarse sandstones, and argillaceous rocks that forms most of the main range.

This body of rocks is divisible into several formations and is here termed the Great Smoky group. The Great Smoky had previously been termed a group in northern Georgia (Hurst, 1955, p. 8–9) and divided into formations; although these formations are made up of rocks similar to those of the Great Smoky group of the Great Smoky Mountains, correlation between units of the two areas is not yet possible.

The Great Smoky group lies in the upper plate of the Greenbrier fault, terminates northwestward along the trace of the fault, and extends thence 20 or 25 miles southeastward (Fig. 2). Southwestward, the outcrop belt continues more than 100 miles with about the same width into northern Georgia. East of the Great Smoky Mountains the group is preserved only in isolated downfolds in older Precambrian rocks.

Through most of its extent in the Great Smoky Mountains the base of the Great Smoky group is cut off by the Greenbrier fault, but in the southeast part of the mountains it lies conformably on the Snowbird group. The top of the group is not present in the project area, but the overlying sequence of the Murphy marble belt has been mapped a little to the south (Keith, 1907). Although part of the Great Smoky group is tightly folded, that along the northern slope of the mountains generally dips at moderate angles southeastward and forms a homoclinal sequence of great thickness. Near the Middle Prong of the Little River as much as 25,000 feet of the Great Smoky is present, but its base and top are not exposed.

The Great Smoky group is a mass of clastic rocks—fine conglomerate, coarse to fine sandstone, and silty or argillaceous slates, phyllites, and schists. The group is monotonous in character through great thicknesses but is sufficiently different from one part to another to be divided broadly into three intergrading and intertonguing formations (Fig. 4). This subdivision is most apparent in the northern part of the mountains and has not been distinguished farther south.

Keith (1895) originally placed the upper part of the sequence here termed the Great Smoky group in the Hazel slate and Clingman conglomerate, but these names are now abandoned:

The Hazel slate was named for outcrops on Hazel Creek, Swain County, North Carolina, on the south slope of the Great Smoky Mountains, but Keith (1907) subsequently connected the outcrops here with those of the Nantahala slate and assumed they were correlative. Later, the name Hazel was approved by the U. S. Geological Survey for a unit in Texas (Dumble, 1902; King, 1940, p. 147–148). Recent mapping by Espenshade (U. S. Geol. Survey open-file report, 1946) in the Hazel Creek area failed to disclose any well-defined unit of argillaceous rocks. As mapped by Keith in the northern Great Smoky Mountains, the Hazel corresponds to argillaceous rocks that are now placed in the Anakeesta formation.

The Clingman conglomerate was named for Clingmans Dome, on the State-Line divide, and was supposed to be the highest stratigraphic unit in the Great Smoky Mountains. Keith subsequently (1907) merged it with his Great Smoky conglomerate, apparently on the assumption that it had been duplicated structurally. At Clingmans Dome and some other parts of the mountains, however, coarse sandstone overlies in stratigraphic sequence argillaceous rocks that are here classed as parts of the Anakeesta formation. We believe that these units of coarse sandstone are layers of Thunderhead lithology that intertongue at varying stratigraphic levels with the Anakeesta formation (Fig. 4). The type Clingman is probably equivalent to the upper beds of the Thunderhead sandstone and the lower part of the Anakeesta formation on Mount Le Conte, but other units mapped as Clingman lie at different and higher levels. For present purposes, therefore, it seems best to class these, depending on locality, as beds in the Anakeesta formation, as tongues of the Thunderhead sandstone, or as unnamed parts of the Great Smoky group.

Elkmont Sandstone

The Elkmont sandstone is here named for the community of Elkmont, 5 miles southwest of Gatlinburg, in the midst of an outcrop area of the formation (Fig. 1). Typical exposures of the formation occur along the Little River from Tennessee Highway 73 southeastward past Elkmont to the base of the Thunderhead sandstone; here a section may be worked out, although there is some repetition of beds by faulting. The Elkmont crops out on the lower northern spurs of the Great Smoky Mountains, from Greenbrier Pinnacle on the east, westward past the type locality, and beyond Cades Cove.

As the Elkmont sandstone is the first formation above the Greenbrier fault, its base is not visible, and a variable thickness is preserved under the Thunderhead sandstone—a few thousand feet on the east, about 5000 feet near Elkmont, and as much as 9000 feet south of Cades Cove. The Elkmont intertongues laterally with the Thunderhead, so that its top in the eastern exposures lies at least several thousand feet higher than in the western; much of the thick western section, moreover, differs only slightly from the overlying Thunderhead. In the southeastern part of the mountains, where the stratigraphic base of the Great Smoky group emerges, the Elkmont has not been identified, and it is uncertain to what part of this sequence it is related.

Most of the Elkmont, like the overlying Thunderhead, is composed of feldspathic sandstones, but those of the Elkmont are generally finer-grained and thinner-bedded, with fewer gritty or pebbly layers than in the Thunderhead; silty and argillaceous layers are generally thicker and more numerous. Graded bedding is visible in some of the sandstones but is rather obscure because of their fine texture. Near Elkmont, blue quartz grains like those in the Thunderhead are common in the upper 2000 feet, but they become sparse downward and are lacking in the lower part.

Thunderhead Sandstone

Thunderhead sandstone is named for Thunderhead Mountain, on the State-Line divide in the western part of the mountains (Fig. 1), where Keith (1895) distinguished the Thunderhead conglomerate with about the same limits as the present unit. Thunderhead Mountain is in a remote part of the region; the formation is better exposed on Mount Le Conte farther east, where a full section is present. Excellent outcrops of the Thunderhead occur along U. S. Highway 441 along the southwestern base of Mount Le Conte.

The Thunderhead sandstone is the most prominently exposed formation of the Ocoee series and forms great ledges and cliffs along the northern face of the Great Smoky Mountains. It is about 8000 feet thick near Thunderhead Mountain, 6000 feet on Mount Le Conte, and

more than 10,000 feet in the northeastern part of the mountains. These thicknesses are not of wholly contemporaneous beds, as the span of the formation becomes progressively higher eastward; the lower part in the west is equivalent to Elkmont sandstone farther east, and the upper part in the east is equivalent to Anakeesta formation farther west (Fig. 4).

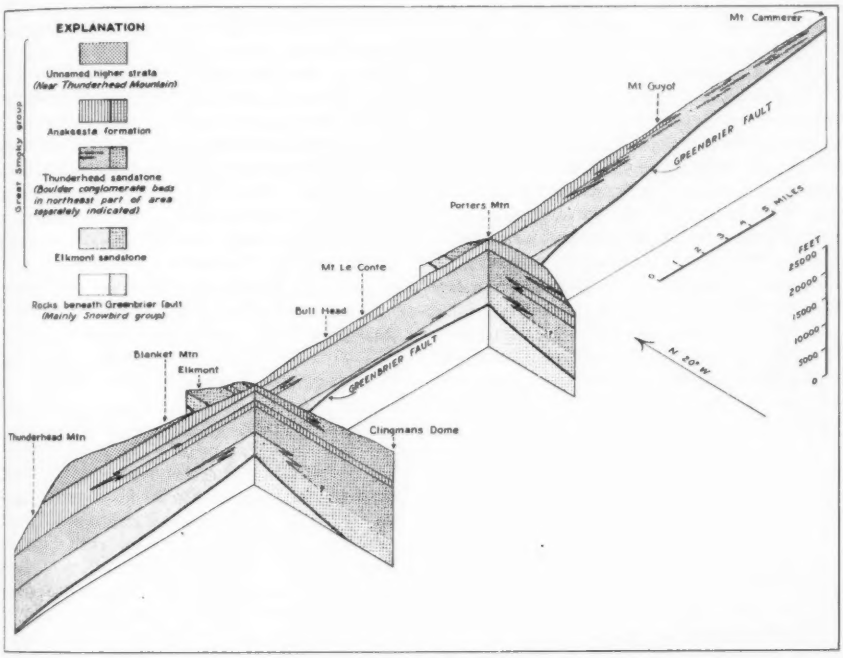

FIGURE 4.—FENCE DIAGRAM ALONG NORTHWEST SIDE OF EASTERN AND CENTRAL GREAT SMOKY MOUNTAINS
Showing restored relations of formations of Great Smoky group

The Thunderhead sandstone is thicker-bedded and coarser-grained than the remainder of the Great Smoky group. It is formed throughout of graded layers 5–25 feet thick, which range from fine conglomerate or coarse sandstone at the base, through medium and fine sandstone, to silty and argillaceous rocks at the top; the latter form partings between the sandstone beds. The conglomerate and sandstone are light to medium gray, composed principally of quartz and potassic feldspar grains, with lesser quantities of plagioclase and a few pebbles of leucogranite and quartzite. Part of the quartz is colorless, but an important component is blue-tinted. In many places the sandstone contains faint subspherical concretionary structures several inches in diameter, with carbonate-impregnated rims.

Anakeesta Formation

The Anakeesta formation is here named for Anakeesta Ridge, a high spur between Mount Le Conte and Newfound Gap (Fig. 1), and is typically exposed along U. S. Highway 441 from the base of the ridge up to the gap. The formation occurs only well back in the Great Smoky Mountains, where it crops out in narrow, steep-sided ridges and craggy pinnacles. A synclinal belt of the formation extends westward from Mount Sequoyah past Anakeesta Ridge to the meridian of Gatlinburg, most of the belt being north of the State-Line divide. The formation reappears farther west in a homoclinal sequence in the head drainages of the prongs of the Little River.

The Anakeesta formation is a body of dark silty and argillaceous rocks that overlie and intertongue extensively with the Thunderhead sandstone (Fig. 4). Individual tongues do not

exceed 2000 feet in thickness but range through a stratigraphic interval of nearly 5000 feet. Immediately east of Thunderhead Mountain all the tongues of Thunderhead sandstone have disappeared, and the Anakeesta forms an unbroken unit about 4500 feet thick, underlain by Thunderhead sandstone and overlain by a similar but unnamed coarse sandstone. Keith (1907; U. S. Geol. Survey open-file report, Mount Guyot geologic map) confused the Anakeesta with the Nantahala slate, but much of it lies several thousand feet lower than the typical Nantahala in Nantahala Gorge.

The Anakeesta formation consists mainly of dark-gray or black silty and argillaceous rocks, variously metamorphosed and generally rich in carbon and sulfides; the latter produce rusty weathered surfaces. These rocks are interbedded with thick beds of lighter-gray, coarser feldspathic sandstone like that in the Thunderhead. Many of the lighter beds form single layers in the darker rocks, but some form units of considerable thickness that are classed as tongues of the Thunderhead sandstone. In a few places the Anakeesta contains thin discontinuous beds of dark-gray sandy dolomite and limestone, the only carbonate rocks in the Great Smoky group.

Unclassified Formations of Ocoee Series

General Features

At various places in the foothills immediately north of the Great Smoky Mountains are rocks that lie either immediately beneath the Greenbrier fault or north of it and, where least disturbed, lie conformably on the Snowbird group; elsewhere they are semiallochthonous or allochthonous (Fig. 2). Most of these rocks differ markedly from the Snowbird group and resemble various parts of the Great Smoky group. Stratigraphic relations to the Great Smoky are not demonstrable, however, and the rocks in question are not included in either group.

Rich Butt Sandstone

The Rich Butt sandstone is here named for Rich Butt Mountain, a northwestern spur of Mount Cammerer, near the northeast end of the Great Smoky Mountains (Fig. 1); the type section of the formation is southeast of Mount Cammerer on Big Creek, above the community of Mount Sterling. The Rich Butt lies conformably on, and intertongues somewhat with, the Pigeon siltstone of the Snowbird group, but its top is cut off by the Greenbrier fault. Along Big Creek about 3000 feet of the formation is preserved beneath the fault, and on Rich Butt Mountain about 1800 feet.

The most characteristic rock of the Rich Butt sandstone in its type area is light feldspathic sandstone, medium- to fine-grained and medium- to thick-bedded, that contains sharply contrasting pelitic layers. On Rich Butt Mountain the sandstone is coarser-grained and thicker-bedded and contains a few lenses of very coarse feldspathic sandstone and fine arkosic conglomerate. Dark argillaceous rocks, conspicuous in the formation locally, are generally thinly and evenly layered and in places are interbedded with fine, reddish-weathering ankeritic sandstone. Thick-bedded sandstone containing intraformational fragments of argillaceous rock appears in a few places.

The standstones of the Rich Butt closely resemble those of the Elkmont sandstone which overlies the Greenbrier fault not far away, and the conglomeratic lenses are like the coarser phases of the Great Smoky group. Some siltstones and sandstones of the Rich Butt resemble parts of the Snowbird group.

Rocks of Webb Mountain and Big Ridge

Northwest of the outcrops of Rich Butt sandstone and several miles north of the front of the Great Smoky Mountains, Webb Mountain and Big Ridge rise prominently from the foothills (Fig. 1). The ridges are composed of rocks that lie conformably on the Pigeon siltstone on the south but are thrust over the Pigeon on the north. The lower 1000 feet of beds consists of thin- to thick-bedded feldspathic sandstone, with interbedded slates and siltstone, and the upper 3000 feet is thick-bedded, coarse, graded, feldspathic sandstone with interbedded dark siltstone. The lower part of the section resembles and is probably correlative with the Rich Butt sandstone, but the upper part is more like the coarser parts of the Great Smoky group; it might be higher stratigraphically than any of the beds of the Rich Butt section.

Cades Sandstone

The Cades sandstone is named for Cades Cove in the western part of the Great Smoky Mountains (Fig. 1) and is adapted from the Cades conglomerate of Keith (1895). Keith, however, mapped the Cades north and south of Cades Cove and widely elsewhere in the

mountains; the term is here restricted to rocks mainly north and west of the cove and beneath the Greenbrier fault.

The Cades sandstone lies in a similar position to the rocks of Webb Mountain and Big Ridge, but the structural complexities in the western part of the mountains are so much greater that its relations are not so plain. Around most of its periphery the Cades is thrust over adjacent rocks, but it may lie with sedimentary contact on the Metcalf phyllite on the south. Its strata are inverted over wide areas. Total thickness of the formation is unknown, but in some sections as much as 4000 feet of beds is exposed.

Most of the Cades is coarse-grained feldspathic sandstone, in graded beds as much as 3 feet thick, commonly containing chips of dark fine-grained rock and pebbles of leucogranite but no grains of blue quartz. Dark-gray argillaceous and silty rocks form partings between sandstone beds, as well as a few units nearly 1000 feet thick. The Cades also contains beds 10–50 feet thick of conglomerate characterized by well-rounded cobbles of quartzite, granite, and gneiss.

The Cades sandstone more closely resembles the Great Smoky group than any part of the Snowbird group, but it differs from the Elkmont and Thunderhead sandstones of the Great Smoky which adjoin it south of Cades Cove. It is much more like the rocks of Webb Mountain and Big Ridge to the east and is somewhat like the Rich Butt sandstone; originally it may have had stratigraphic relations similar to the unclassified rocks farther east.

Walden Creek Group

General Features

The Walden Creek group corresponds approximately to the Wilhite slate, Citico conglomerate, and Pigeon slate, as mapped by Keith in the northwestern foothills of the Knoxville quadrangle (1895) and also to the more inclusive Hiwassee slate of his later terminology (1904, p. 5). The term Citico conglomerate expresses a characteristic rock type of the group, a type that occurs at so many different levels that neither the conglomerate nor the supposedly underlying and overlying slates have stratigraphic meaning; the name Citico is here abandoned. The Hiwassee was named for a locality in the Murphy quadrangle, for which no description was published, and the name was used so confusingly elsewhere that it is properly abandoned.

The Walden Creek group is here named for Walden Creek, a western tributary of the West Fork of the Little Pigeon River, which drains the southeast slope of Chilhowee Mountain and the northern foothill belt, an area underlain by rocks of the group (Fig. 1). The Walden Creek crops out in a belt a few miles to 8 miles wide in the northwesternmost foothills of the Great Smoky Mountains (Fig. 2) and extends along the strike for many miles farther northeast and southwest.

The Walden Creek group is a heterogeneous body of shales and siltstones which contains discontinuous masses of conglomerate and sandstone and minor layers of quartzite, limestone, and dolomite. Many of its rock types are unique in the Ocoee series; especially noteworthy are its conglomerates made up of large rounded white quartz pebbles.

Structural disorder of the Walden Creek group exceeds that of the other groups of the Ocoee series, and structural and stratigraphic interpretations are uncertain. The conglomerates and other competent beds form discontinuous layers that were either structurally broken, originally lenticular, or both. The incompetent silty and argillaceous rocks are nearly everywhere so folded and crumpled that they give little idea of the over-all structure and sequence.

The best-defined sequence in the Walden Creek group is that south of English Mountain in the eastern part of the foothills, where despite much small-scale deformation the rocks form a broad pattern of northeast-plunging folds that expose a section perhaps 8000 feet thick. The formations of the group are therefore defined in this area. The stratigraphy of more broken sequences in the Walden Creek farther southwest is less well understood.

On Chilhowee and English Mountains the Cochran formation of the Chilhowee group lies on the Sandsuck formation of the Walden Creek group. The Sandsuck of these areas is in different fault blocks from the sequence of the remainder of the group south of English Mountain, but the Sandsuck is apparently represented at the top of the latter.

In the Great Smoky Mountains the Walden Creek group is adjoined on the south by the Snowbird group (Fig. 2) but is separated from it by faults, so that their relations cannot be established. As the Walden Creek group underlies the Chilhowee group and the Snowbird group overlies the basement complex, there is a presumption that Walden Creek overlies Snowbird. This relation is further suggested near the

French Broad River, northeast of the Great Smoky Mountains, where "Hiwassee slate" ("Sandsuck formation") overlies "Snowbird formation" according to other geologists (Keith, 1904, p. 5; Oriel, 1950, p. 23–30; Ferguson and Jewell, 1951, p. 16–21).

Relations just summarized suggest that the Walden Creek group is the highest part of the Ocoee series in the northwestern foothills, that the Sandsuck is its highest formation, that they are succeeded by the Chilhowee group, of known Cambrian age at its top, and that this part of the Ocoee is a sequence of beds lying beneath the Paleozoic rocks.

Licklog Formation

The Licklog formation is here named for Licklog Hollow where it is typically exposed, near the edge of the foothills southwest of the East Fork of the Little Pigeon River (Fig. 1). The Licklog is exposed only in the northwest part of the outcrop belt of the Walden Creek group, where it lies on the Great Smoky fault so that its basal relations are unknown. A variable thickness of the formation, nowhere more than a few hundred feet, is preserved above the fault.

Most of the Licklog is siltstone and shale, dark gray, laminated to crudely layered, and micaceous. These rocks are interbedded in places with sandstone and quartz-pebble conglomerate resembling those of the overlying Shields formation.

Shields Formation

The Shields formation is here named for Shields Mountain, a high ridge along the northwest edge of the foothills west of the Little Pigeon River (Fig. 1), which is made up of a southeastward-dipping sequence of the formation 2000 to 2500 feet thick. Typical exposures may be seen along the road at the east end of the mountain.

The most prominent rocks of the Shields are sandstone and conglomerate of "Citico" type, which form units a few feet to more than 1000 feet thick that project in ledges and ridges. The sandstones are coarse-grained, feldspathic, and not graded. The conglomerates are interbedded with the sandstones as seams, lenses, and thick beds. Most pebbles are of white vein-quartz and quartzite with a common maximum size of 1 inch.

Associated with the sandstone and conglomerate is argillaceous shale, which contains thin lenses of gritty sandstone. In the type area, shales dominate the upper half of the formation but intertongue at their base with the sandstones and conglomerates of the lower half.

Wilhite Formation

The Whilhite formation is named for Wilhite Creek, which drains southward from English Mountain into East Fork (Fig. 1). The name is adapted from the Wilhite slate of Keith (1895) but with very different interpretation of sequence and stratigraphic relations. Characteristic outcrops of the formation occur on Wilhite Creek and on Long Branch immediately to the south. The Wilhite is the most varied formation of the Ocoee series, and although it contains most of the carbonate rocks of the series it is generally dominated by clastic rocks. In the eastern part of the foothill area, near the type locality, the formation is divisible into two members:

The lower, or Dixon Mountain member, about 1500 feet thick, is named for Dixon Mountain west of Jones Cove and is dominantly siltstone, mostly micaceous and sandy, containing much carbonate that is mainly concentrated along certain laminae; some sandstone is interbedded. Similar and probably correlative siltstones farther west, north of Wear Cove, contain lenticular beds of light-gray quartzite.

The upper, or Yellow Breeches member, about 2000 feet thick, is named for Yellow Breeches Creek east of Jones Cove. It is characterized especially by limestone and dolomite which in places form units more than 100 feet thick, many of which are sandy and conglomeratic; these are interbedded with varied argillaceous, silty, and sandy rocks. Such limestone was the host rock for the manganese mineralization at the East Fork mine (Stose and Schrader, 1923, p. 102–105).

Sandsuck Formation

The Sandsuck shale was named by Keith (1895) for Sandsuck Branch, southeast of Chilhowee Mountain near its northeastern end (Fig. 1). The shale lies beneath sandstone and conglomerate, which Keith considered to be basal Cochran formation, but it intertongues widely with these coarser rocks. The base of the Cochran is therefore now redefined at a higher level, at the base of persistent beds of arkose and quartzite, in part maroon; the shale, sandstone, and conglomerate beneath is redefined as the Sandsuck formation. The best section of the

formation is not along the branch but on the opposite northwest slope of Chilhowee Mountain; there 2500 feet is exposed, but the base is cut off by the Great Smoky fault.

The Sandsuck formation is the lowest unit of the sequence on Chilhowee Mountain and occurs in the same position on English Mountain farther east; in both places its base is cut off by faults, and it is overlain by the Cochran formation of the Chilhowee group. These two occurrences are in fault blocks along the front of the Great Smoky thrust sheet and are not in sequence with the main body of the Walden Creek group to the southeast. However, rocks very similar to the Sandsuck of these areas, and probably correlative, form the top of the section of the remainder of the Walden Creek group in the plunging folds south of English Mountain.

On Chilhowee Mountain most of the Sandsuck formation is gray or greenish, thinly fissile silty shale with sandy laminae. As stated, the shale intertongues at various levels with units of coarse sandstone and quartz-pebble conglomerate, some of which, in the upper part, are as much as 1000 feet thick. The persistent arkose and quartzite beds at the base of the overlying Cochran lie either on shale or coarser beds, which suggests that the contact may be disconformable.

In the section south of English Mountain about 4000 feet of beds identified as Sandsuck overlies the Wilhite formation; the top is not preserved. Here the formation is made up of shaly siltstone with laminae of fine-grained sandstone, which is interbedded, especially in the middle, with coarse sandstone and quartz-pebble conglomerate.

General Problems

Broader Relations of Ocoee Series

In the preceding account, various local relations of the groups of the Ocoee series to each other and to adjacent rocks have been noted:

(1) The Snowbird group lies unconformably on earlier Precambrian basement rocks and is the oldest unit of the Ocoee series. (2) In the southern sequence above and southeast of the Greenbrier fault the Snowbird group is thin and is overlain conformably by the Great Smoky group. (3) In the central sequence beneath and northwest of the Greenbrier fault, where the Snowbird group is thick, it is overlain conformably by unclassified formations which may represent a vertical transition between the Snowbird and Great Smoky groups. (4) In the foothills northwest of the Great Smoky Mountains the Walden Creek group adjoins the Snowbird group with faulted contact but probably originally overlay it. (5) The Walden Creek group is overlain on the northwest by the Chilhowee group. (6) The Great Smoky group is overlain on the south by the Nantahala slate, at the base of the sequence in the Murphy marble belt.

These observations are insufficient to clarify the broader relations of the Ocoee series. Its three groups do not form a single stratigraphic sequence; the upper two, the Great Smoky and Walden Creek, are not in contact. What is the relation of the great mass of clastic rocks of the Great Smoky group to the very different rocks on the northwest? A definite answer cannot be given, because the Ocoee series has been split into different parts by faulting, and the connections between the parts are concealed or eroded; nevertheless, some suggestions can be made.

The Snowbird group of the sequence above the Greenbrier fault is thin and wedges out southeastward between basement rocks and the Great Smoky group; in the sequence below the Greenbrier fault it is about 13,000 feet thick near the type locality; its uppermost unit, the Pigeon siltstone, itself attains this thickness farther northwest. Most of the southeastward thinning of the Snowbird is clearly due to an overlap of its basal beds toward the edge of the depositional basin, as shown by dominance of coarse sandstones and arkoses typical of the Longarm quartzite in this direction. Some thinning, however, can be interpreted as caused by intertonguing of the upper part with the Rich Butt sandstone and possibly the rocks of Webb Mountain and Big Ridge. These in turn may pass southward into the Great Smoky group, as inferred from resemblance of the sandstones of the Rich Butt to those of the Elkmont sandstone on the south, and of some of the siltstones of the Rich Butt to the upper part of the Pigeon siltstone on the north.

The relation of the Great Smoky group to higher units on the northwest is much less certain, because they not only are of very different character but also are everywhere separated by a belt that is now several miles wide and was many times that before the folding and thrusting. Part of the Great Smoky group may be equivalent to part or all of the Walden Creek group. We believe it less likely that the Great Smoky could be equivalent to

any part of the Chilhowee group, although a correlation of the Great Smoky "conglomerate" with the Cochran "conglomerate" of the latter was asserted by Keith (1904, p. 6; 1907, p. 3) and has been accepted by many subsequent authors.

The Great Smoky group is more than 25,000 feet thick, and the Cochran formation is at most no more than a few thousand feet. The Great Smoky is a coarse, poorly sorted deposit with characteristic graded beds; the Cochran is not truly a "conglomerate", as Keith termed it, but an evenly bedded deposit of arkose, sandstone, and quartzite. The Cochran and associated formations of the Chilhowee group are traceable for hundreds of miles along the strike and in northeastern Tennessee are traceable across the strike in successive outcrop belts to a breadth of 35 miles (King and Ferguson, in preparation); distance before deformation was at least twice as great. The rocks of the Chilhowee group vary between these outcrop belts but remain recognizably Chilhowee throughout and never assume an aspect similar to the Great Smoky southeastward.

Age of Chilhowee Group

In order to establish the age of the Ocoee series, it is necessary to analyze the ages of the overlying units—the Chilhowee group and the rocks of the Murphy marble belt.

The Chilhowee group has for many years been classed by the U. S. Geological Survey as Cambrian on the basis of the occurrence of trilobites, brachiopods, and other fossils in its upper part, the occurrence of *Scolithus* in the upper and middle parts, the sedimentary homogeneity of the group, and the presence in many places of a well-marked unconformity at its base.

Relations are confused, however, because in places the Chilhowee lies on earlier sedimentary and volcanic rocks with only a minor unconformity, or even conformably, and many geologists have termed these earlier rocks Cambrian also; the Ocoee was thus placed in the Cambrian by Keith.

Paleontological data to fix as Cambrian the age of the Chilhowee group itself are decisive only for its upper part. A small lot of fossils, including *Olenellus*, was collected many years ago by Walcott (1890, p. 570; Resser, 1938, p. 25) from the topmost beds of the Chilhowee group, now termed the Helenmode formation, in Little River Gap in Chilhowee Mountain. A few fossils were also obtained at the same locality during the present investigation, and the same general zone has yielded fossils in other areas. Keith (1895) reported similar fossils from the Murray shale, at another locality on Chilhowee Mountain lower in the section, but careful search at that place during the present investigation failed to yield any others, and their occurrence requires verification. In addition, *Olenellus* has been reported from the still lower Nichols shale, in about the middle of the Chilhowee section (Butts, 1940, p. 5), but this claim is probably erroneous. Much more abundant throughout the Chilhowee group than trilobites or other fossils is *Scolithus*, a tubular structure perhaps formed by worms; it occurs as low in the section as the Nichols shale and equivalent formations. Although *Scolithus* indicates some form of life and was cited by Walcott and others as supporting the Cambrian age of the containing beds, it is not now regarded as diagnostic by most paleontologists.

The problems of the Chilhowee group are thus the same as those of units at the bottom of the lowest Cambrian in many other regions. Fossils that indicate a Cambrian age decrease downward in conformable sequences of beds; hundreds or thousands of feet beneath them there may be a decisive unconformity—or, as in the Great Smoky Mountains, the fossiliferous beds may overlie a vast sequence of earlier deposits. In the absence of fossils, designation of the absolute base of the Cambrian, if there is any, in such sequences is not possible.

In view of these circumstances, the U. S. Geological Survey now restricts beds classed as Cambrian to those for which paleontological data are available. The Helenmode formation, at the top of the Chilhowee group, is therefore classed as Cambrian, and its remaining unfossiliferous formations are termed Precambrian(?); the Chilhowee group as a whole is classed as Cambrian and Precambrian(?).

Age of Rocks of Murphy Marble Belt

Rocks of the Murphy marble belt were interpreted by Keith (1907) as a set of higher formations synclinally infolded in the Great Smoky group, and although different alternative interpretations have been suggested (Stose and Stose, 1944, p. 377; Van Horn, 1948, p. 18–20), this interpretation seems to be well established (Hurst, 1955, p. 72). These higher formations were correlated by Keith (1907, p. 11) with parts of the Chilhowee group and higher Cambrian strata farther northwest, and this view has been adopted by some later

authors (Furcron, 1953, p. 37–38; Hurst, 1955, p. 7–8). This correlation was based only on comparisons of the sequence and lithology of the two sections—for example, between the Murphy marble and the Shady dolomite. The report of fossils from the Murphy marble (McCallie, 1907, p. 34) cannot be verified, and its significance remains to be appraised. The age of the beds overlying the Great Smoky group on the south is thus not determined, and although part of them may plausibly be of early Paleozoic age, proof by fossils or other means has not yet been obtained.

Age of Ocoee Series

Since the first description of the Ocoee series by Safford nearly 100 years ago, its age has been variously interpreted, the spectrum ranging from Precambrian to well up in the Paleozoic (King, 1949, Table 2, p. 622–623). The most recent U. S. Geological Survey classification of the Ocoee series before the present report is Precambrian(?), as given in a report by Rodgers (1953, p. 34). Rodgers himself designated the Ocoee as "Cambrian or Precambrian" in a subsequent paper (1956, p. 410).

Evidence and inferences so far set forth indicate that the Ocoee is older than the Chilhowee group of Cambrian and Precambrian(?) age, as well as older than the rocks of the Murphy marble belt. It lies unconformably on Precambrian granitic and gneissic rocks. These considerations indicate that the Ocoee is older than the Cambrian as now defined yet is younger than the Precambrian basement rocks. The U. S. Geological Survey therefore now classifies the Ocoee as later Precambrian.

References Cited

Barrell, Joseph, 1925, The nature and environment of the Lower Cambrian sediments of the southern Appalachians: Am. Jour. Sci., 5th ser., v. 9, p. 1–20

Butts, Charles, 1940, Description of the Montevallo and Columbiana quadrangles (Alabama): U. S. Geol. Survey Geol. Atlas, folio 226, 20 p.

Dumble, E. T., 1902, The red sandstone of the Diabolo Mountains, Texas: Texas Acad. Sci. Trans., v. 4, p. 103–105

Ferguson, H. W., and Jewell, W. B., 1951, Geology and barite deposits of the Del Rio district, Cocke County, Tennessee: Tenn. Dept. Conserv., Div. Geol. Bull. 57, 235 p.

Furcron, A. S., 1953, Comments on the geology of the Ellijay quadrangle, Georgia, North Carolina, Tennessee: Georgia Geol. Survey Bull. 60, p. 32–40

Goldsmith, Richard, and Hadley, J. B., 1955, Pre-Ocoee erosion surface in the Great Smoky Mountains, North Carolina (Abstract): Geol. Soc. America Bull., v. 66, p. 1687–1688

Hadley, J. B., King, P. B., Neuman, R. B., and Goldsmith, Richard, 1955, Outline of the geology of the Great Smoky Mountains area, *in* Russell, R. J., *Editor*, Guides to southeastern geology: Geol. Soc. America, p. 390–411

Hayes, C. W., 1895, Description of the Cleveland sheet (Tennessee): U. S. Geol. Survey Geol. Atlas, folio 20, 4 p.

Hurst, V. J., 1955, Stratigraphy, structure, and mineral resources of the Mineral Bluff quadrangle, Georgia: Georgia Geol. Survey Bull. 63, 137 p.

Keith, Arthur, 1895, Description of the Knoxville sheet (Tennessee and North Carolina): U. S. Geol. Survey Geol. Atlas, folio 16, 6 p.

——1896, Description of the Loudon sheet (Tennessee): U. S. Geol. Survey Geol. Atlas, folio 25, 6 p.

——1904, Description of the Asheville quadrangle (Tennessee and North Carolina): U. S. Geol. Survey Geol. Atlas, folio 116, 10 p.

——1907, Description of the Nantahala quadrangle (North Carolina and Tennessee): U. S. Geol. Survey Geol. Atlas, folio 143, 11 p.

King, P. B., 1940, Older rocks of the Van Horn region, Texas: Am. Assoc. Petroleum Geologists Bull., v. 24, p. 143–156

——1949, The base of the Cambrian in the southern Appalachians: Am. Jour. Sci., v. 247, p. 513–530, 622–645

King, P. B., and Ferguson, H. W., in preparation, Geology of northeasternmost Tennessee: U. S. Geol. Survey Prof. Paper 311

McCallie, S. W., 1907, A preliminary report on the marbles of Georgia: Georgia Geol. Survey Bull. 1, 126 p.

Neuman, R. B., 1951, The Great Smoky fault: Am. Jour. Sci., v. 249, p. 740–754

Oriel, S. S., 1950, Geology and mineral resources of the Hot Springs window, Madison County, North Carolina: N. C. Dept. Conserv. Devel., Div. Min. Res., Bull. 60, 70 p.

Resser, C. E., 1938, Cambrian system (restricted) of the southern Appalachians: Geol. Soc. America Special Paper 15, 140 p.

Rodgers, John, 1953, Geologic map of east Tennessee, with explanatory text: Tenn. Dept. Conserv., Div. Geol. Bull. 58, pt. 2, 168 p.

——1956, The clastic sequence basal to the Cambrian system in the central and southern Appalachians: 20th Internat. Geol. Cong., El sistema Cámbrico, su paleogeographía y el problema de su base, symposium, pt. 2, p. 385–413

Safford, J. M., 1856, A geological reconnaissance of the State of Tennessee: Nashville, 1st Bienn. Rept., State Geologist, 164 p.

——1869, Geology of Tennessee: Nashville, 550 p.

Stose, G. W., and Schrader, F. C., 1923, Manganese deposits of east Tennessee: U. S. Geol. Survey Bull. 737, 154 p.

Stose, G. W., and Stose, A. J., 1944, The Chilhowee group and Ocoee series of the southern Appalachians: Am. Jour. Sci., v. 242, p. 367–390, 401–416

——1949, Ocoee series of the southern Appalachians: Geol. Soc. America Bull., v. 60, p. 267–320

U. S. Geological Survey, 1901, Twenty-second annual report of the United States Geological Survey to the Secretary of the Interior, 1900–1901; Part 1, Director's report, p. 13–207

——1902, Twenty-third annual report of the Director of the United States Geological Survey to the Secretary of the Interior, 1901–1902, 217 p.

Van Horn, E. C., 1948, Talc deposits of the Murphy marble belt: N. C. Dept. Conserv. Devel., Div. Min. Res. Bull. 56, 54 p.

Walcott, C. D., 1890, The fauna of the Lower Cambrian, or *Olenellus* zone: U. S. Geol. Survey 10th Ann. Rept., pt. 1, p. 509–760

Walcott, C. D., 1891, Correlation papers; Cambrian: U. S. Geol. Survey Bull. 81, 447 p.

Wilmarth, M. G., 1938, Lexicon of geologic names of the United States: U. S. Geol. Survey Bull. 896, 2396 p.

U. S. Geological Survey, Menlo Park, Calif.; U. S. Geological Survey, Denver, Colo.; U. S. Geological Survey, Washington, D. C.; U. S. Geological Survey, Denver, Colo.

Manuscript Received by the Secretary of the Society, October 23, 1957.

Publication Authorized by the Director, U. S. Geological Survey

BULLETIN OF THE GEOLOGICAL SOCIETY OF AMERICA
VOL. 69, PP. 967–974, 6 FIGS. AUGUST 1958

SUBMARINE ABRASION AND WAVE-CUT PLATFORMS

BY WILLIAM C. BRADLEY

ABSTRACT

According to classical theory, wave-cut platforms are developed by deep submarine abrasion while sea level is stationary. Modern writers, however, believe that wave erosion takes place only in shallow water. Fragile, subaerially etched pyroxene sand grains are mechanically unstable at depths of less than about 30 feet in the Santa Cruz area of California but are mechanically stable at greater depths, supporting the conclusion that significant wave-produced submarine abrasion is restricted to the surf zone with a maximum depth of about 30 feet. Most sediment in transit beyond the surf zone is too fine-grained to act as an abrasive. If sea level is stationary, marine planation may produce a wave-cut platform up to about one-third of a mile wide; a wider platform can be cut only during slow submergence. The modern and former platforms in the Santa Cruz area were carved while sea level was rising.

CONTENTS

TEXT

	Page
Introduction and problem	967
Acknowledgments	969
Platform cutting	969
Classical theory	969
Submarine abrasion: a review	969
Evidence from Santa Cruz area	970
Grain size	970
Abrasion of fragile grains	970
Submarine abrasion: a summary	972
Platform cutting and sea level	972
Summary	973
References cited	973

ILLUSTRATIONS

Figure	Page
1. Map of Santa Cruz area, California	968
2. Profile of modern wave-cut platform at Santa Cruz	968
3. Classical theory of platform cutting	969
4. Etched and blunted pyroxene sand grains	971
5. Per cent of freshly etched grains of total pyroxenes	971
6. Platform extension during slow submergence	973

TABLE

Table	Page
1. Estimations of the limiting depth of submarine abrasion	970

INTRODUCTION AND PROBLEM

The sea floor in the vicinity of Santa Cruz, California (Fig. 1), is a modern wave-cut platform carved into the Miocene Monterey formation (Fig. 2; Bradley, 1957). Between sea level and an altitude of 850 feet on adjacent Ben Lomond Mountain, five prominent marine terraces (described by Lawson, 1893, Wilson, 1907; Branner *et al.*, 1909; Rode, 1930; Page and Holmes, 1945; Alexander, 1953; Bradley, 1957) have wave-cut platforms that, except for subsequent warping, are sufficiently similar to the modern platform to warrant the belief that all were developed in the same manner. Although in places the former platforms are carved into older rocks, for the most part they too cut the Monterey formation.

A fundamental problem in the genesis of wave-cut platforms is whether sea level is stationary or rising while cutting takes place. The classical theory, to be reviewed in this paper, considers sea level stationary. Most authors have either been noncommittal or have supported the classical theory, but a few have related platform cutting to submergence. The submarine terrace bordering islands off southern California (Smith, 1900, p. 216), the modern and former platforms in the near-by Santa Monica Mountains (Davis, 1933, p. 1044), and some old platforms in Florida (Cooke, 1945, p. 273–311), have been correlated with submergence; both Smith and

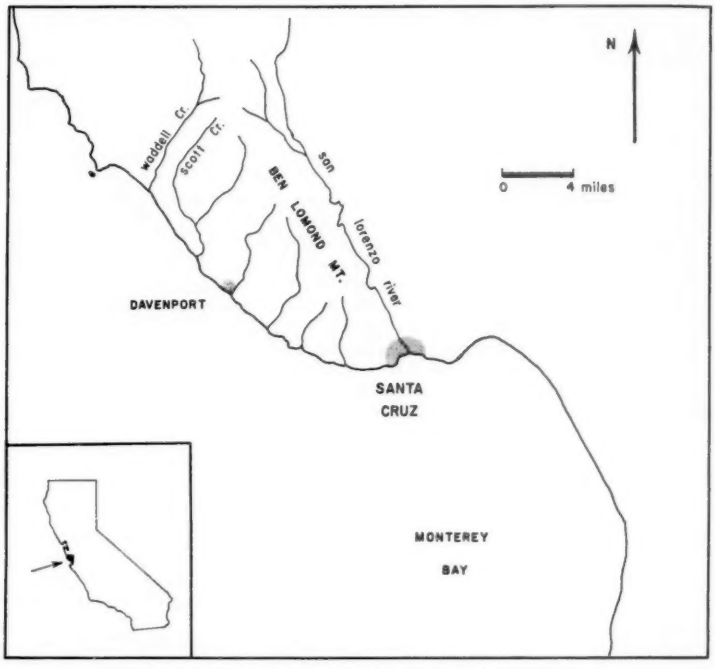

FIGURE 1.—MAP OF SANTA CRUZ AREA, CALIFORNIA

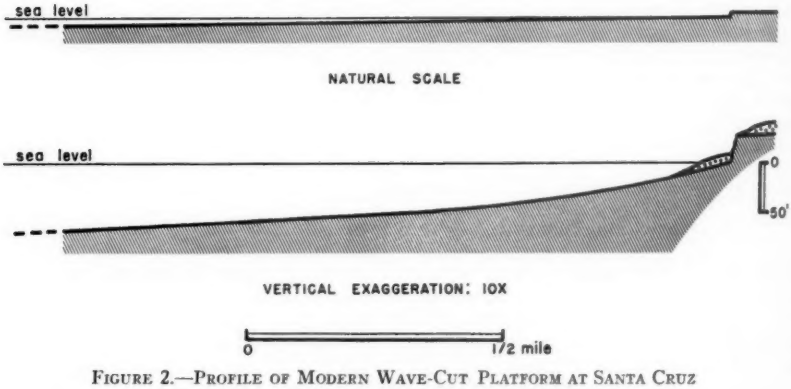

FIGURE 2.—PROFILE OF MODERN WAVE-CUT PLATFORM AT SANTA CRUZ
Irregularities of less than 5 feet have been smoothed

Davis based their conclusions on the amount of erosion necessary to produce broad platforms. Alexander (1953, p. 35–36) decided that the marine-terrace platforms east of Santa Cruz, California, were carved by a rising sea. He found (p. 36–37) that each marine terrace is associated with a stream terrace representing the valley floor of a stream graded to sea level at the shore-line angle.[1] The stream terraces are composed of fill, which led Alexander to conclude that submergence and valley alluviation occurred

[1] The shore-line angle, or sea-level line, is the junction between sea cliff and wave-cut platform (Davis, 1933, p. 1051).

simultaneously with platform development. Although suggestive, this evidence does not prove the platforms were cut while sea level was rising, because the same relationships would have evolved if each platform had been cut after submergence ceased.

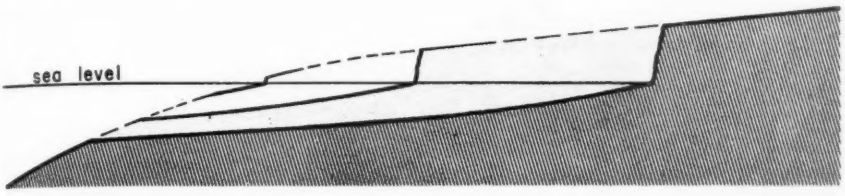

FIGURE 3.—CLASSICAL THEORY OF PLATFORM CUTTING
Sea level is stationary. Platform is lowered as it is extended landward.

The present paper reviews the sea-level problem in platform cutting and discusses pertinent evidence from the Santa Cruz area of California.

ACKNOWLEDGMENTS

Special thanks are due A. D. Howard, Stanford University, who supervised the study of the Santa Cruz marine terraces, and G. A. Thompson, Stanford University, and Sheldon Judson, Princeton University, for their numerous fruitful discussions. H. W. Menard of Scripps Institution of Oceanography read the manuscript and made thoughtful criticisms. R. E. Garrison, T. C. Silver, R. A. Sands, D. E. Feltham, R. L. Christiansen, and D. E. Lee helped collect samples of neritic, beach, and terrace deposits. A. D. Russell, Santa Cruz city engineer, made available some of the submarine data used in this paper. Grants from the Shell Fund for Fundamental Research at Stanford University supported the study.

PLATFORM CUTTING

Classical Theory

In the ideal view of platform cutting (Davis, 1909, p. 702–703; Johnson, 1919, p. 201–215; Barrell, 1920, p. 354–356; Twenhofel, 1939, p. 213–216; Cotton, 1942, p. 412–413; von Engeln, 1949, p. 521–526; Kuenen, 1950, p. 302–306; and Thornbury, 1954, p. 433–437), sea level is considered stationary (Fig. 3). Wave attack creates and drives landward a sea cliff, leaving under shallow water a wave-cut platform thinly veneered with detritus. The platform slopes seaward at whatever declivity is necessary for the removal of debris supplied by the sea cliff and streams. Platform extension (landward) depends on continued platform lowering, because unless a platform gradient sufficient for the transportation of erosional debris is maintained, sea-cliff erosion stops. Platform lowering results from abrasion as the debris shifts across it.

Submarine abrasion therefore is a key process in the carving of wave-cut platforms, and how far landward a platform can be extended while sea level is stationary depends directly on the limiting depth of submarine abrasion. The modern platform at Santa Cruz is at least 1½ miles wide and extends to a depth of 75 feet (Fig. 2; Bradley, 1957, p. 426–427); if this platform was eroded by the sea at its present level, submarine abrasion must be effective to a depth of at least 75 feet. An adjacent marine terrace contains a former platform[2] that is 2 miles wide at Santa Cruz; if it was eroded at a time when sea level was static, submarine abrasion must be effective to a depth of 100 feet. The problem becomes intensified where platforms are even wider (Hanna, 1926, p. 196; Pardee, 1934, p. 9–10; Alexander, 1953, p. 13; Emery, 1958, p. 43). Belief that broad platforms can be carved while sea level is stationary implies acceptance of deep submarine abrasion. It is thus pertinent to establish the limiting depth of significant wave-produced submarine abrasion.

Submarine Abrasion: A Review

Many foreign writers around the beginning of the Twentieth Century believed that submarine abrasion was restricted to shallow water and that extensive marine plantation required

[2] Shore-line angle now approximately 100 feet above sea level.

a rising sea; these views have been summarized by Johnson (1919, p. 234) and Fairbridge (1952, p. 352–355). Opposed to this "shallow water view" of submarine erosion was a "deep water view" implied by Gulliver (1899), Fenneman (1902), and Davis (1909, p. 702–703), and firmly expressed by Johnson (1919, p. 80–83, 225) who concluded that erosion might occur at depths as great as 600 feet. Johnson believed that orbital motion of water particles would extend to such a depth, and any fine sediment that would be thus moved would act as an abrasive. With deep submarine erosion and unlimited time, these men felt extensive marine planation was possible with a static sea level.

TABLE 1.—ESTIMATIONS OF THE LIMITING DEPTH OF SUBMARINE ABRASION
(In feet)

Author	Depth
Johnson (1919)	600
Barrell (1920)	300
Rode (1930)	150–300
Miller (1939)	100
Dietz and Menard (1951)	30
Dietz (1952)	30
Fairbridge (1952)	Few fathoms
Shumway *et al.* (1954)	50–60
Longwell and Flint (1955)	30
Newell and Imbrie (1955)	24
Russell (1958)	36
Bradley (This paper)	30

Since 1919 writers have become more conservative in estimating the depth at which important marine abrasion occurs (Table 1). Barrell (1920, p. 355–356) agreed that fine sediment could be moved in deep water but felt that 300 feet was probably the greatest depth at which sediment competent to erode could be moved. Rode (1930, p. 55–70) further stressed that the lower limit of wave motion is not the same as the lower limit of destructive wave action and emphasized that sand must be of a certain minimum size (he believed 1 mm) before it can act as an effective abrasive. Using available data on the transportation of debris by running water, on the orbital motion of water particles, and on wave conditions and bottom sediments along the central California coast, he theoretically calculated that the lower limit of significant abrasion in the Santa Cruz area was between 150 and 300 feet. Further reductions in the estimated limiting depth of abrasion have been made by Miller (1939, p. 97), Fairbridge (1952, p. 348, 352), Shumway *et al.* (1954, p. 1304), Newell and Imbrie (1955, p. 12), and Russell (1958, p. 3). Dietz and Menard (1951, p. 2011), Dietz (1952, p. 1808), and Longwell and Flint (1955, p. 244) have concluded that vigorous abrasion is restricted to the surf zone, which has a maximum depth, except in rare cases, of about 30 feet. Thus the "deep water view" of Johnson's time has been gradually brought back into agreement with the old "shallow water view".

Twenhofel's (1945) studies of the rounding of beach sand grains have emphasized the point that sand must be of a certain minimum size before it can act as an abrasive. He concluded (p. 66) that abrasion of quartz grains on a beach is almost infinitesimal if the grains are smaller than 0.5 mm.

Evidence From Santa Cruz Area

Grain size.—Neritic deposits beyond the surf zone in the Santa Cruz area tend to be finer-grained than 0.2 mm (Galliher, 1932; 1935; Bradley, 1957, p. 427–428). In light of Twenhofel's (1945, p. 66) conclusion that quartz beach sand must be at least 0.5 mm before it will suffer significant abrasion, sand in the Santa Cruz area coarse enough to be capable of abrading the modern wave-cut platform is found principally within the surf zone and on the beach.

Abrasion of fragile grains.—The modern sea cliff, the outer edge of the lowest prominent marine terrace, exposes a former platform and 5–15 feet of overlying beach deposits. Pyroxene[3] grains within the terrace deposits have been subaerially etched into delicate forms (Fig. 4); etching of this sort has been described by Ross *et al.* (1929), Edelman and Doeglas (1931), van Baren and Kiel (1950, p. 191, 202), Hutton (1952), Hay (1957, p. 34–37), and Bradley (1957, p. 433–434). Sea-cliff erosion releases these fragile grains to the surf zone, where their sharp points become blunted[4] (Fig. 4). Using freshly etched pyroxene grains as an index of abra-

[3] Augite, titanaugite, and hypersthene.

[4] Grains smaller than about 0.06 mm retain their etching even in the surf zone, apparently because of their small size (Hutton, 1952, p. 73–74; Bradley, 1957, p. 434). Etched grains discussed in this paper are larger than 0.06 mm.

sion, a study of their survival in beach and neritic deposits yields clues to the depth of submarine abrasion.

Ten shallow neritic and 23 beach samples were examined to determine what proportion is too deep to represent the early stages of solution. (2) In marine-terrace deposits the quantity of pyroxene decreases as the degree of etching increases (Bradley, 1957, p. 433–434), whereas no such relationship exists

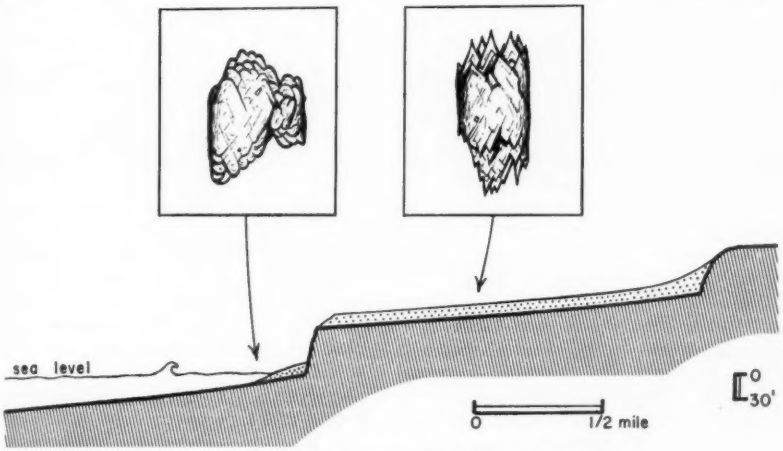

FIGURE 4.—ETCHED AND BLUNTED PYROXENE SAND GRAINS (0.147–0.104 mm.)

of pyroxene in the 0.147–0.104 mm size range consists of the freshly etched variety[5] (Fig. 5). Less than 2 per cent of pyroxene grains in beaches and in 3 neritic samples from depths of 10, 20, and 25 feet retain their fragile etching. At a depth of about 30 feet, however, etched grains become more abundant. In 2 samples from 30 feet, etched grains constitute 5 and 18 per cent of the pyroxene, and in 5 deeper samples the etched grains constitute 10–25 per cent of the pyroxene. Although 10 neritic samples can hardly furnish conclusive evidence, they do suggest an important environmental change at about 30 feet, a figure that Dietz and Menard (1951, p. 2011) suggested as the maximum depth of the surf zone.

Three lines of evidence indicate that the etched pyroxene grains in neritic and beach deposits are land-derived and not the product of leaching in place on the sea floor: (1) in marine-terrace deposits where leaching is known to occur, all pyroxene grains are etched. In neritic deposits, however, only a few grains show fresh etching, and with these the etching

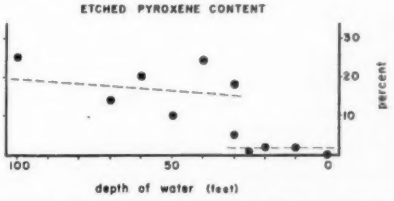

FIGURE 5.—PER CENT OF FRESHLY ETCHED GRAINS OF TOTAL PYROXENES (0.147–0.104 mm.)

within neritic deposits. (3) Chemically unstable minerals such as apatite and olivine, rare in terrace deposits, are present with the etched grains on the sea floor.

How such delicate grains get from the sea cliff to water deeper than 30 feet is not clear; they may pass through the surf zone in rip currents before abrasion can occur.[6] However, regardless of their origin in neritic deposits, their importance as an indicator of submarine abrasion remains the same. Their mechanical instability at depths less than 30 feet indicates

[5] The 0.147–0.104 mm size was selected because pyroxene is especially abundant in this range (Bradley, 1957, p. 426).

[6] The amount of time necessary for blunting is unknown. Shaking for 20 minutes in the RoTap machine produced a faint blunting, but this was abrasion in a dry state.

that this is an abrasion environment, and their preservation at greater depths suggests that these deeper neritic deposits are experiencing little abrasion at present. The deeper deposits, therefore, cannot be significantly abrading the underlying wave-cut platform.

Submarine Abrasion: A Summary

Geologically important wave-produced submarine abrasion is restricted to the surf zone, which has a maximum depth of about 30 feet, as Dietz and Menard (1951, p. 2011) have suggested. Here, sediments are sufficiently coarse to act as abrasives. Beyond the surf zone, sediments are transported without marked abrasion, because the environment is less rigorous and the grain size of the material is too small.

Agents other than waves may cause submarine erosion at depths greater than 30 feet. Tidal currents and turbidity currents can transport debris coarse enough to serve as an abrasive in deeper water. Rocks exposed on the shallow California sea floor are riddled with holes of rock-boring organisms (Menard *et al.*, 1954, p. 134), and such biologic activity may be important in submarine erosion (Shumway *et al.*, 1954, p. 1305; H. W. Menard, Personal communication). Although currents and organisms may modify a platform once it is developed, they are not believed competent to carve it initially. Currents must necessarily be localized to be erosively effective, and hence cannot uniformly bevel bedrock over great lateral distances. Organisms alone can hardly be expected to chew bedrock into the shape of a platform that slopes gently seaward and has a near-shore concavity. In addition, for organisms to cause a substantial lowering of the bedrock sea floor, the inter-hole fragments would have to be continually removed to allow fresh rock to be attacked, and transportation of such relatively large fragments would be difficult. Wave-induced erosion is considered the only mechanism capable of cutting the Santa Cruz area platforms.

Platform Cutting and Sea Level

The evidence presented indicates that platform cutting takes place only within the surf zone. The modern platform is about 0.3 miles wide at a depth of 30 feet, and the five prominent marine-terrace platforms at their calculated 30-foot depths, when corrected for subsequent deformation, are 0.30–0.33 miles wide. It is therefore concluded that with rocks and wave conditions as in the Santa Cruz area, a sea with static level may carve a platform up to about one-third of a mile wide; a platform wider than one-third of a mile can be carved only during submergence. The modern and five former platforms are all wider than one-third of a mile in places, and it is therefore also concluded that each of these platforms was cut, at least in part, at a time when sea level was rising (relatively).

Santa Cruz area platform profiles are best explained by erosion during slow submergence. They are concave only within about half a mile of the sea cliff, and farther seaward their gradients are essentially constant (Fig. 2; Bradley, 1957, p. 426, 430, 441). Thus the sharpest part of the platform concavity coincides with the erosive surf zone. Figure 6 illustrates platform extension during slow submergence. As sea level rises, the actively cutting surf zone continually carries the platform concavity up and into the land; beyond the surf zone the platform is simply extended landward at its uniform gradient, with little alteration required to maintain a continuous smooth platform profile. In this way it would be possible for the surf zone to carve a broad and deep platform that at every stage of development would show a smooth profile hinged at the shore-line angle.

It is natural to associate platform cutting with submergence brought about by deglaciation. However, even ignoring the possibility of submergence due to diastrophism, it does not necessarily follow that each wide platform in a terrace sequence was cut during a separate interglacial interval, as was supposed by Davis (1933) and Alexander (1953). In an unstable area like the west coast of North America, slow and continuous submergence during deglaciation could from time to time be offset by more rapid mountain building. During each tectonically quiet period the rising sea could carve a platform, and during each tectonic pulse, emergence could produce a marine terrace. More than one platform might therefore be cut during the same interglacial interval. This theoretical consideration is introduced solely as a caution against the hasty correlation of single marine terraces with interglacial intervals.

Although it seems reasonable that the Santa Cruz area platforms were carved during inter-

glacial intervals, the author has little evidence by which to relate platforms to specific intervals. The platform of the lowest prominent terrace was cut prior to 39,000 years ago (Bradley, 1956), and it is easy to speculate that the cutting took place during the Sangamon Interval; Alexander (1953, p. 38) supported a Sangamon age, but Carter (1957, p. 13, 16) might favor a Yarmouth age. The modern platform has certainly been cut in part during post-Wisconsin time and is presumably being expanded today as sea level is rising (Marmer, 1949; Studds, 1951, p. 112). Drowned river valleys in the Santa Cruz area (Alexander, 1953, p. 8) must be at least partly post-Wisconsin features.

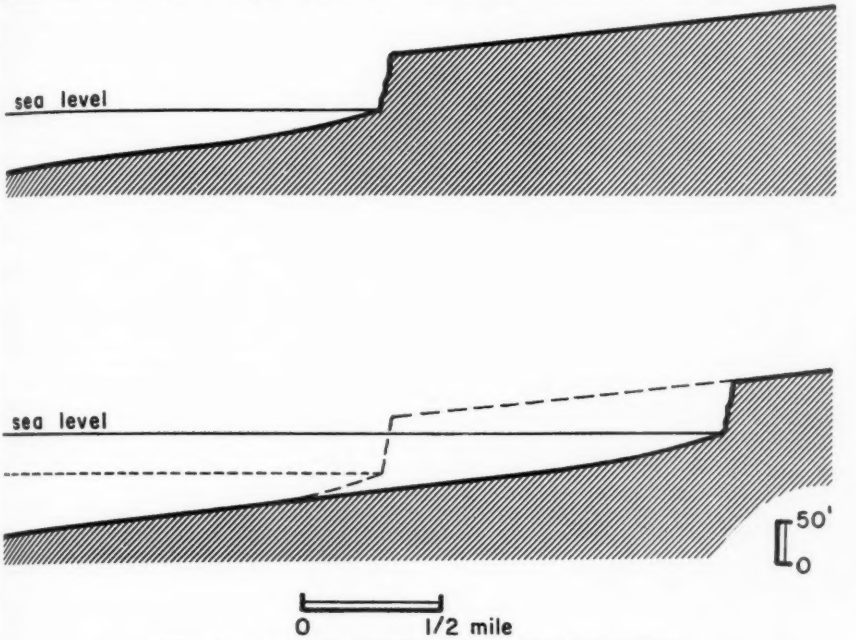

FIGURE 6.—PLATFORM EXTENSION DURING SLOW SUBMERGENCE

SUMMARY

Geologically significant wave-produced submarine abrasion is confined to the surf zone, which has a maximum depth of about 30 feet, as has been suggested by Dietz and Menard (1951), and contains sediment coarse enough to serve as an abrasive. If sea level is stationary, relative to the land, marine planation of perhaps one-third of a mile is all that may reasonably be expected. More extensive marine planation is possible only during submergence, and the shaping of a continuous smooth wave-cut platform probably requires that submergence be slow (although not necessarily continuous). Extensive marine planation cannot occur during emergence, and emergence of a sea floor that had a slope related to sediment transport induces beach progradation rather than planation (Bradley, 1957). It seems well to keep in mind the possibility that smooth unconformities overlain by marine sediments may result from marine planation during the transgression that led to marine deposition.

REFERENCES CITED

Alexander, C. S., 1953, The marine and stream terraces of the Capitola-Watsonville area: Univ. Calif. Pub. Geography, v. 10, p. 1–44

Barrell, Joseph, 1920, The piedmont terraces of the northern Appalachians: Am. Jour. Sci., v. 199, p. 227–258, 327–362, 407–428

Bradley, W. C., 1956, Carbon-14 date for a marine terrace at Santa Cruz, California: Geol. Soc. America Bull., v. 67, p. 675–677

—— 1957, Origin of marine-terrace deposits in the Santa Cruz area, California: Geol. Soc. America Bull., v. 68, p. 421–444

Branner, J. C., Newsom, J. F., and Arnold, Ralph, 1909, Santa Cruz folio: U. S. Geol. Survey Geol. Atlas, Folio 163, 11 p.

Carter, G. F., 1957, Pleistocene man at San Diego: Baltimore, Johns Hopkins Press, 400 p.

Cooke, C. W., 1945, Geology of Florida: Florida Geol. Survey Bull. 29, 339 p.

Cotton, C. A., 1942, Geomorphology: N. Y., John Wiley & Sons, 505 p.

Davis, W. M., 1909, The outline of Cape Cod: p. 690–724 *in* Johnson, D. W., *Editor*, Geographical essays: Boston, Ginn and Co., 777 p.

—— 1933, Glacial epochs of the Santa Monica Mountains, California: Geol. Soc. America Bull., v. 44, p. 1041–1133

Dietz, R. S., 1952, Geomorphic evolution of continental terrace (continental shelf and slope): Am. Assoc. Petroleum Geologists Bull., v. 36, p. 1802–1819

Dietz, R. S., and Menard, H. W., 1951, Origin of abrupt change in slope at continental shelf margin: Am. Assoc. Petroleum Geologists Bull., v. 35, p. 1994–2016

Edelman, C. H., and Doeglas, D. J., 1931, Reliktstrukturen detritischen Pyroxenen und Amphibolen: Min. pet. Mitt., v. 42, p. 482–490

Emery, K. O., 1958, Shallow submerged marine terraces of Southern California: Geol. Soc. America Bull., v. 69, p. 39–60

Fairbridge, R. W., 1952, Marine erosion: 7th Pacific Sci. Cong., Pacific Sci. Assoc. Proc., v. 3, p. 347–358

Fenneman, N. M., 1902, Development of the profile of equilibrium of the subaqueous shore terrace: Jour. Geology, v. 10, p. 1–32

Galliher, E. W., 1932, Sediments of Monterey Bay, California: Rept. 28, State Mineralogist Calif., v. 28, p. 42–79

—— 1935, Glauconite genesis: Geol. Soc. America Bull., v. 46, p. 1351–1366

Gulliver, F. P., 1899, Shoreline topography: Am. Acad. Arts and Sciences Proc., v. 34, p. 151–258

Hanna, M. A., 1926, Geology of the La Jolla quadrangle, California: Univ. Calif. Dept. Geol. Sci. Bull., v. 16, p. 187–233

Hay, R. L., 1957, Mineral alteration in rocks of middle Eocene age, Absaroka Range, Wyoming: Jour. Sed. Petrology, v. 27, p. 32–40

Hutton, C. O., 1952, Accessory mineral studies of some California beach sands: U. S. Atomic Energy Comm., RMO-981, 112 p.

Johnson, D. W., 1919, Shore processes and shoreline development: N. Y., John Wiley & Sons, 584 p.

Kuenen, Ph. H., 1950, Marine geology: N. Y., John Wiley & Sons, 568 p.

Lawson, A. C., 1893, The post-Pliocene diastrophism of the coast of Southern California: Univ. Calif. Dept. Geol. Sci. Bull., v. 1, p. 115–160

Longwell, C. R., and Flint, R. F., 1955, Physical geology: N. Y., John Wiley & Sons, 432 p.

Marmer, H. A., 1949, Sea level changes along the coasts of the United States in recent years: Am. Geophys. Union Trans., v. 30, p. 201–204

Menard, H. W., *et al.*, 1954, Underwater mapping by diving geologists: Am. Assoc. Petroleum Geologists Bull., v. 38, p. 129–147

Miller, A. A., 1939, Attainable standards of accuracy in the determination of preglacial sea levels by physiographic methods: Jour. Geomorphology, v. 2, p. 95–115

Newell, N. D., and Imbrie, John, 1955, Biogeological reconnaissance in the Bimini area, Great Bahama Bank: N. Y. Acad. Sci. Trans., ser. 2, v. 18, p. 3–14

Page, B. M., and Holmes, C. N., 1945, Geology of the bituminous sandstone deposits near Santa Cruz, Santa Cruz County, California: U. S. Geol. Survey Oil and Gas Investig., prelim. map 27

Pardee, J. T., 1934, Beach placers of the Oregon coast: U. S. Geol. Survey, Circ. 8, 41 p.

Rode, Karl, 1930, Geomorphogenie des Ben Lomond (Kalifornien) eine Studie uber Terrassenbildung durch marine Abrasion: Zeitschr. Geomorph., v. 5, p. 16–78

Ross, C. S., Miser, H. D., and Stephenson, L. W., 1929, Water-laid volcanic rocks of early upper Cretaceous age in southwestern Arkansas, southeastern Oklahoma, and northeastern Texas: U. S. Geol. Survey Prof. Paper 154-F, p. 175–202

Russell, R. J., 1958, Geological geomorphology: Geol. Soc. America Bull., v. 69, p. 1–22

Shumway, George, *et al.*, 1954, Observations by diving geologists of bedrock off southern California (Abstract): Geol. Soc. America Bull., v. 65, p. 1304–1305

Smith, W. S. T., 1900, A topographic study of the islands of Southern California: Univ. Calif. Dept. Geol. Sci. Bull., v. 2, p. 179–230

Studds, R. F. A., 1951, Coast and Geodetic Survey data—an aid to the coastal engineer: 1st Conf. Coastal Eng. Proc., Wave Research Council, Univ. Calif., Berkeley, p. 102–125

Thornbury, W. D., 1954, Principles of geomorphology: N. Y., John Wiley & Sons, 619 p.

Twenhofel, W. H., 1939, Principles of sedimentation: N. Y., McGraw-Hill Book Co., 610 p.

—— 1945, The rounding of sand grains: Jour. Sed. Petrology, v. 15, p. 59–71

van Baren, F. A., and Kiel, H., 1950, Contribution to the sedimentary petrology of the Sunda shelf: Jour. Sed. Petrology, v. 20, p. 185–213

von Engeln, O. D., 1949, Geomorphology: N. Y., Macmillan Co., 655 p.

Wilson, M. E., 1907, Shore topography near Davenport, Santa Cruz County: Calif. Phys. Geog. Club Bull., v. 1, p. 11–17

University of Colorado, Boulder, Colorado

Manuscript Received by the Secretary of the Society, August 5, 1957

BULLETIN OF THE GEOLOGICAL SOCIETY OF AMERICA
VOL. 69, PP. 975-1008, 21 FIGS., 2 PLS. AUGUST 1958

EROSIONAL PROCESSES AND LANDFORMS IN BADLANDS NATIONAL MONUMENT, SOUTH DAKOTA

By Kenneth G. Smith

Abstract

Small-scale erosional features in the Big Badlands of South Dakota include miniature mountain ranges and pediments, with morphology resembling that of mature mountainous desert regions of the southwestern United States. Miniature badland pediments have steeper gradients than large-scale pediments of the arid southwest, but angles of mountain fronts average about the same for both—approximately 35°.

There is an abrupt reduction of slope where the miniature mountain front meets its bordering pediment. The miniature mountain drainage is poorly integrated; it consists of closely spaced rill channels having the same gradient as the mountain slope.

At the expense of the retreating miniature mountain front the pediment is extended headward by erosion at the margins of spreading sheetwash. The escarpment retreats by disaggregation through absorption and desiccation and by rill erosion.

Topographic texture varies with underlying bedrock. Topography developed on the Chadron formation is fine-textured; that on the Brule formation is ultra-fine-textured. Badlands drainage is typically dendritic with regularly bifurcating finger-tip tributaries.

The mean maximum angle of slope in typical Chadron topography is 26.2°, with estimated standard deviation of 4.2°. For the Brule formation mean maximum slope angles of 56.0°, 49.5°, and 51.0° were obtained in three areas. A *t* test revealed that the differences between means of Brule and Chadron are significant.

Each slope mean represents an equilibrium condition in which the slope has been adjusted to achieve a steady state between the resistivity of the material to erosion and the intensity of erosional processes.

CONTENTS

TEXT

	Page
Introduction	976
General statement	976
Field methods	976
Acknowledgments	977
Regional setting	977
Location	977
Climate and vegetation	977
Stratigraphy	977
Structural geology	980
Topographic subdivisions	980
Miniature pediments and associated features	981
Definitions	981
Theories of large-scale desert-pediment origin	982
Theories of miniature pediment origin in badlands	983
Miniature pediments of White River Badlands	984
Description of areas	984
Morphology and development of miniature badlands pediments	992
Regrading of pediment surface	994
Pediment embayments and pediment passes	994
Pediment domes	995
Morphology of small-scale pediments and large-scale pediments compared	996
Conclusions concerning origin of miniature pediments	997
Topographic texture of badlands topography	998
Derivation of texture ratio	998
Texture ratios for typical badlands topography	998
Relation of texture ratio to drainage density	1000
Factors controlling topographic texture	1001
Bifurcation ratios for dendritic drainage of badlands	1002
Stream-order numbers in the Badlands	1002
Statistical methods applied to Badlands	1003
Slope analysis	1003
Relation of slope angle to slope length	1005
Conclusions	1006
References cited	1007

ILLUSTRATIONS

Figure	Page
1. Base map of Badlands National Monument, South Dakota	978

Figure — Page
2. Generalized stratigraphic column of the Oligocene White River beds, Badlands of South Dakota ... 980
3. Topographic subdivisions of White River Badlands ... 981
4. Topographic map of Area 1 ... 984
5. Topographic map of Area 2 ... 986
6. Topographic profile across hanging pass in Area 2 ... 986
7. Topographic map of Area 3 ... 987
8. Topographic map of Area 4 ... 988
9. Topographic map of Area 5 ... 989
10. Topographic map of Area 6 ... 990
11. Topographic map of Area 7 ... 991
12. Encroaching silt wedge in area of rising base level ... 994
13. Comparison of large-scale and small-scale pediment profiles ... 997
14. Topographic map of drainage area studied ... 999
15. Logrithmic graph of drainage density-texture ratio ... 1000
16. Stream-order-number graph for three small fourth-order drainage basins ... 1002
17. Stream-order-number graph for the two major divisions of drainage area studied ... 1002
18. Topographic profiles of large remnant buttes on Lower Prairie level ... 1004
19. Typical slope profile developed on Chadron formation ... 1005
20. Slope length–slope angle graph ... 1005
21. Sketch diagram of relationship of badlands escarpment to pediment surface at rill-channel mouth ... 1006

Plate — Facing page
1. Miniature pediments and associated erosional landforms ... 984
2. Typical large- and small-scale badlands erosional features ... 985

TABLES

Table — Page
1. Monthly rainfall, in inches, 1948–1951 ... 978
2. Generalized stratigraphic column ... 979
3. Texture-ratio data for the Chadron formation ... 999
4. Texture-ratio data for the Brule formation ... 999
5. Mean-texture ratios and drainage-density values for seven general areas ... 1001
6. Stream-order number data for Figure 9 and 10 ... 1003
7. Summary of slope-analysis data ... 1004

INTRODUCTION

General Statement

Factors that have contributed to the erosion of the Big Badlands of South Dakota are semiarid climate, general lack of vegetation, torrential summer rains, and homogeneous clays of the Oligocene White River group. Rapid erosion causes the isolation of small buttes which develop into minature mountain ranges and pediment systems. These display well-formed pediments, pediment embayments, pediment passes, panfans, and inselbergs. The morphology of the miniature mountain pediments is similar to that of mature mountainous desert regions.

Large-scale contour maps of several miniature pediment areas were drawn from instrumental field surveys as a means of comparing them with large-scale desert forms. These maps closely resemble conventional maps of mountainous desert regions. One map was prepared to measure and illustrate the dense drainage network in the higher areas.

The higher parts of the badlands offer longer slopes and well-developed dendritic drainage, to which quantitative geomorphic methods of slope analysis and drainage density-texture determinations were applied.

Field Methods

Seven maps of miniature mountain-pediment areas were drawn in the field, using a plane table and explorer's alidade. The following mapping procedure was used: (1) Instrument stations were set up at opposite ends of a 100-foot base line. (2) A station at one end of the base line was given the arbitrary elevation of 100.0 feet as a reference point. (3) All additional instrument and rod stations were sighted in with the alidade, and the distances were measured with a steel tape. (4) All rod stations were made at points where the rod could be sighted in with the instrument carefully leveled with the striding level. Elevations were determined by standard leveling procedures of addition or subtraction from the level sight line.

The drainage-area map was surveyed on a scale of 50 feet to the inch, using conventional plane-table procedure. All elevations were determined with reference to a United States Coast and Geodetic Survey bench mark.

Slope angles of the pediments and of the steeper adjacent badland slopes were determined at the junction of the two. An Abney hand level, set in a 3-foot length of board, was used to measure all angles. Wood blocks 2 inches high are attached under the ends of the board. This gives an average angle for a slope

of that length and eliminates the effect of minor irregularities on the surface. This combination of hand level with a 3-foot board is called a slope sloth.

The slope sloth was also used to survey longitudinal pediment profiles and profiles of the steeper slopes adjacent to pediments. Slopes were also measured with a steel tape to determine the length of slope furnishing debris to the pediment at its base and the relationship between slope length and angle of slope.

After rain storms the runoff pattern on the pediment surfaces indicated the type of flow. The distribution of silt on the pediment surface soon after runoff periods indicated how water transports material down-slope across the pediment.

Acknowledgments

Field work was carried out as part of a Columbia University research program in quantitative geomorphology, supported by the Geography Branch of the Office of Naval Research under Project No. 389-042, contract N6 ONR 271, Task Order 30, and was directed by Professor Arthur N. Strahler, who suggested the research problem and supervised the field work and laboratory studies.

The author wishes to acknowledge the patient understanding and help of his wife, Eleanor G. Smith, who served as full-time field assistant during the summer of 1950 and part-time assistant in 1951. Mr. Philip H. Lamberton, of the University of Michigan, served most capably as a regular field assistant during the summer of 1951.

Field work in the Badlands National Monument was made possible through the kind co-operation of Mr. Harry J. Liek, Co-ordinating Superintendent, National Park Service, South Dakota, who issued a permit for the geomorphic study. Mr. J. Estes Suter, Superintendent of the Badlands National Monument, and his assistants gave the author all available recent meteorologic data and aided in the location of bench marks and other features.

Professor Donaldson Koons, of Colby College, Maine, made several pertinent suggestions in the field concerning methods of approaching the problem, as did also Professor Brainerd Mears, Jr., of the University of Wyoming.

The author wishes to thank especially Mr. and Mrs. E. J. Harvey, of Interior, South Dakota, for their kindness while accommodating the field party.

Regional Setting

Location

Badlands National Monument is in southwestern South Dakota, in Pennington and Jackson counties. The town of Interior was used as a base of operations. All maps and observations were made in the eastern part of the National Monument area, near Cedar Pass, Norbeck Pass, and Big Foot Pass (Fig. 1).

The Big Badlands, or White River Badlands, of South Dakota are the most extensive badlands known. They are 120 miles long and range from 30 to 50 miles wide, with a total area of nearly 4000 square miles (Darton, 1921, p. 2).

Climate and Vegetation

The climate is semiarid, with an average annual precipitation of 15 inches. Most of the precipitation falls between April 1 and October 1. Summer rainfall is torrential, occurring as convectional storms. Rainfall data are available from old meteorological records for stations at Kadoka, Cottonwood, and Interior. Until recently no rainfall records were maintained at Monument Headquarters; a rainfall-recording station was established in March of 1948 (Table 1).

The year 1951 was exceptionally wet for this part of the west, with a total of 20.73 inches of rain. Although this figure does not appear excessive, 7.30 inches of rain fell during the month of June. The increased rainfall caused exposure of many new fossil-bone areas. An increase in vertical erosion occurred in many of the major gullies, resulting in the development of vertical embankments along the channel courses.

Temperature extremes are common. Summers are hot, with maximum daily temperatures exceeding 100° F. Winters are cold, with temperatures as low as −30° F.

Vegetation in the Badlands is sparse. The steeper slopes are barren, but prairie grasses are abundant on some of the lower or more level areas, with accompanying sage brush and various types of cacti. The slump topography adjacent to the steeper slopes retains moisture, which facilitates the growth of scrub cedar trees.

Stratigraphy

Upper Cretaceous, Oligocene, Pleistocene, and Recent formations are exposed. Although all areas mapped are located on outcrops of the

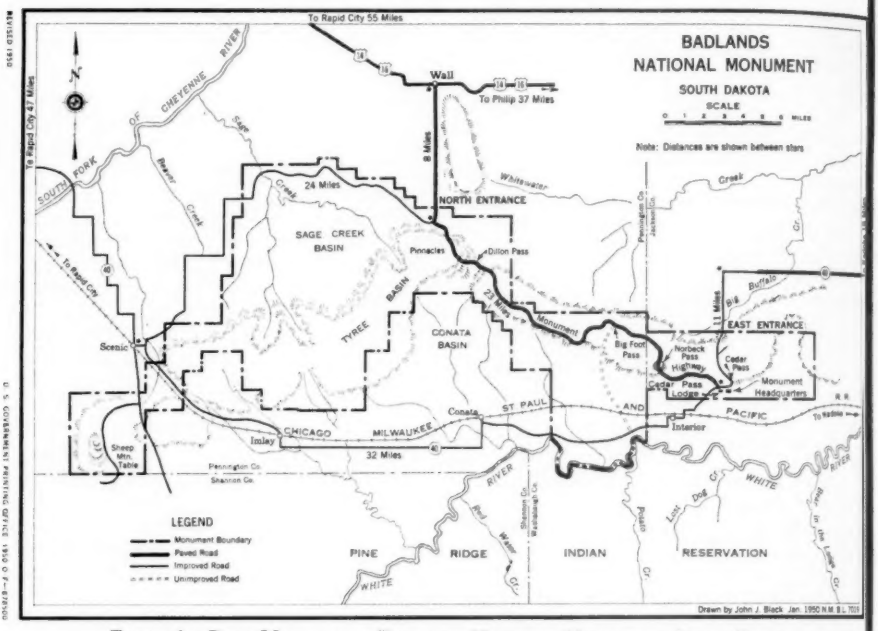

FIGURE 1.—BASE MAP OF THE BADLANDS NATIONAL MONUMENT, SOUTH DAKOTA
From Soc. Vert. Paleontologists Field Conf. in Western South Dakota, Guidebook, 1951, p. 61

Oligocene White River group, a brief description of all formations is necessary to aid in visualizing the general regional setting (Table 2).

The oldest rocks exposed are the "Interior" beds—rusty and lavender shales and clays. They represent a weathered zone developed on the Upper Cretaceous Pierre shale during the long pre-Oligocene erosion period. Red, brown, and lavender result from a concentration of iron compounds by weathering and leaching (Bump, 1951, p. 38).

Formations of the Oligocene White River group outcrop throughout most of the Badlands. The White River group has been divided into the Chadron formation (older) and the Brule formation (younger). Both are characterized by poorly consolidated clays and silts, with some channel sandstones. There are several marker zones of nodular clays containing large calcareous concretions, and a few local conglomerates. Both volcanic ash and bentonite clay are present. The predominant clay minerals are illite and montmorillonite (Van Houten, 1953, p. 73).

The Chadron formation contains thin, freshwater limestones in the upper part. Over this lies the Brule formation whose upper part contains dense volcanic ash beds constituting the Whitney member (Fig. 2). Maximum thickness of the Oligocene formations is approximately 500 feet.

Pleistocene sands and gravels are scattered over the area and have a maximum thickness

TABLE 1.—MONTHLY RAINFALL IN INCHES* 1948–1951
Badlands National Monument, South Dakota

	1948	1949	1950	1951
Jan.	....	....	.06	.10
Feb.	....	....	....	.15
March	....	.86	....	2.18
April	2.64	1.19	.31	.35
May	2.51	2.46	.28	1.80
June	5.80	1.19	.84	7.30
July	1.52	.10	2.08	2.36
August	1.08	2.81	2.25	2.59
Sept.	....	.57	2.47	2.24
Oct.	.95	2.10	.40	.80
Nov.	.30	....	.35	....
Dec.	.05	....	....	.91

* Information courtesy of J. Estes Suter, Superintendent, Badlands National Monument.

of 20 feet (Ward, 1922, p. 31). Much of the Pleistocene has been eroded.

Recent deposits are chiefly reworked Oligocene sediments, forming piedmont slopes around the larger buttes and at the base of the highland area of the Badlands, known as the Wall. The Recent deposits range from 10 to 20 feet thick. Ward (1922, p. 33) believes that the Recent piedmont deposits originated as coalescing alluvial fans, as evidenced by gradual slope diminution.

TABLE 2.—STRATIGRAPHIC COLUMN
Badlands National Monument, South Dakota

Recent			Piedmont deposits around all large buttes and abrupt higher ground; reworked Tertiary sandstones and shales; unconsolidated; thickness 10–20 feet.
Pleistocene			Scattered sands and gravels, mostly subangular fragments, 1–4 inches in diameter, some cobbles and boulders up to 12 or 14 inches in diameter; maximum thickness, 20 feet.
Oligocene (White River group)	Brule	Whitney	Massive volcanic ash beds, light pink clays with numerous concretions (Leptauchenia nodular layer), gray to creamy-colored clays, occasionally tinged with red. Thickness 60–100 feet.
		Orella	Massive, arenaceous clays, lenticular sandstones, and conglomerates, with layers of nodules or concretions; generally yellowish gray to buff. Thickness consistently about 200 feet.
	Chadron		Largely gray, spongy clays and silt with numerous sandstones, conglomerates, and fresh-water, limestones. Maximum thickness, 190 feet.
Upper Cretaceous	"Interior beds" (Pierre shale)		Possibly a weathered zone of Pierre shale; rusty and lavender shales; thickness 2–40 feet.

Structural Geology

Structurally, the White River Badlands area is one of essentially horizontal sedimentary rocks, with a few minor flexures and faults. There is a slight regional dip of 1°–2° in the Tertiary formations, which Clark (1937, p. 270) interprets as original southeast dip.

Four faults, 1–1½ miles long, occur near Cedar Pass (Fig. 1). All are normal faults trending northwest, with a maximum vertical displacement of 25 feet. There are also several smaller faults, many less than a quarter of a mile long, with a maximum throw of 18 feet (Ward, 1922, p. 42).

One major fold in the area (Clark, 1937, p. 270) is an anticline that trends N. 70°W., approximately parallel with the Wall (Fig. 3), and extends from the Sage Creek drainage basin as far east as Interior (Fig. 1). The anticline is asymmetrical; the northeast limb dips 3°. The steeper dips on the southern limb are as high as 14° in some places.

Minature pediment areas selected for study were in areas where the rocks are almost horizontal. Because the forms mapped are small, they could be restricted both horizontally and vertically to layers of nearly homogeneous rock. The careful selection of miniature pediment areas in this manner reduces the possibility of including structural features as important controlling factors in pediment development.

Topographic Subdivisions

The Big Badlands are in the Great Plains geomorphic province; locally they have been designated as the Tertiary Table Lands of the Missouri Plateau (Rothrock, 1943, p. 59). Ward (1922, p. 12–14) divides the Big Badlands in the vicinity of Interior into four approximately parallel topographic subdivisions that trend approximately east-west: (1) the Flood Plain of the White River, (2) the Lower Prairie, (3) the Wall, and (4) the Upper Prairie.

The Wall is outlined on the map (Fig. 3).

The Flood Plain lies along the southern boundary of the area. It consists chiefly of recent sands and gravels. No typical badlands develop on the coarse flood-plain deposits.

The Lower Prairie is an area of subdued topography that slopes from the Wall on the north to the White River Flood Plain on the south. Most of the area has a sod cover with abundant grass; it is used as a grazing area for cattle. Isolated buttes and groups of buttes rise above the general level of the Lower

Prairie as outliers of the retreating Wall to the north. The buttes have steep slopes and lack vegetation.

The Lower Prairie level has been deeply dissected by intermittent streams flowing southward from the Wall to the White River. The deep dissection has caused several of the buttes to be surrounded by moatlike trenches. Ward (1922, p. 50) believes this detail of erosion followed the partial burial of the buttes and the development of a sod cover up their sides, and in many cases over the tops. He explains (Ward, 1922, p. 50):

"The stripping process went forward readily on the upper slopes where the cover was thin. Once started, the runoff could move down these bare rock slopes almost unimpeded, and so would be able to dig deeply into the peripheral lower fill material, which would thus be cut back concentrically and carried out through breaks in the moat wall."

Northern extensions of the Lower Prairie form deep embayments in the Wall. These have been stripped of their sod cover by erosion, and miniature pediment areas have developed on the newly exposed bedrock beneath.

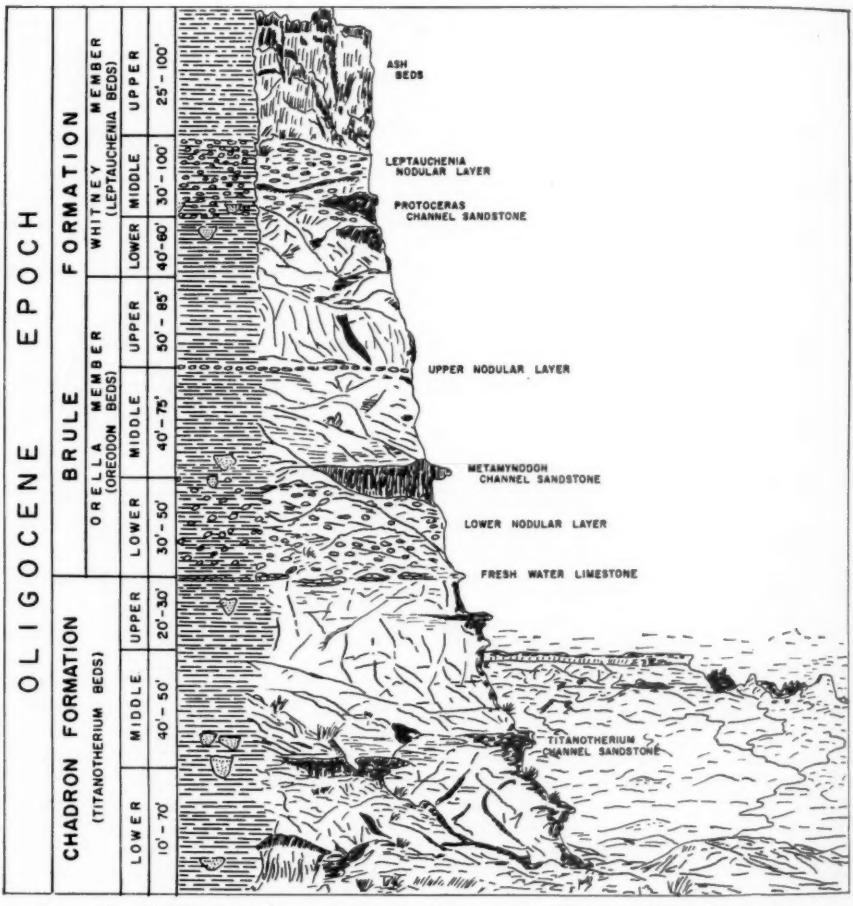

FIGURE 2.—GENERALIZED STRATIGRAPHIC COLUMN OF THE OLIGOCENE WHITE RIVER BEDS, BADLANDS OF SOUTH DAKOTA

From Soc. Vert. Paleontologists Field Conference in Western South Dakota, Guidebook, 1951, p. 34

The Wall is an irregular erosional scarp of the Badlands trending east-west between the Lower Prairie and Upper Prairie. The highest elevations in the Badlands occur in this area; the Wall has a maximum width of 3 miles. At a few points elongate spurs of badlands topography extend southward from the Wall, but in general it presents a straight front along the southern side. The highest points of the Wall are capped by dense, resistant volcanic ash.

The Wall is about 60 miles long and is typically associated with the term "badlands." It presents a barrier to north-south travel, except for a few passes now utilized by the federal highway.

The Upper Prairie, north of the Wall, is a sod-covered surface of relatively low relief similar to the Lower Prairie. However, remnant buttes surrounded by moatlike trenches are found only on the Lower Prairie.

Along the north side of the Wall the drainage on the Upper Prairie level is northward to the Cheyenne River and Bad River. On the Lower Prairie drainage originates within the Wall and flows southward to the White River. All tributary streams draining the Badlands are intermittent or ephemeral, although many of the channels and valley floors are wide, indicating a large discharge during periods of runoff.

Rothrock (1943, p. 63) points out that badlands are common on the Missouri Plateau and usually occupy bluffs of the large river valleys or the sides of the larger buttes. He describes four major factors in the development of badlands:

(1) Alternation of easily eroded clays with less easily eroded beds of sand and volcanic ash. Sand and ash beds protect the softer underlying clays causing differential erosion.

(2) Gumbo in the clay dries, cracks, and leaves a mass of loose rubble a foot or more deep. This loose material is rapidly washed away during thunder showers, leaving steep bare slopes.

(3) Height of the Badlands above the White River causes rapid downcutting in the Wall, and few of the stream beds are graded.

(4) Summer rainfall, largely thunder showers, deepen gullies more quickly than they can be widened.

Darton (1921, p. 6) considers the barren, steep slopes in the Badlands a result of erosion more rapid than soil development.

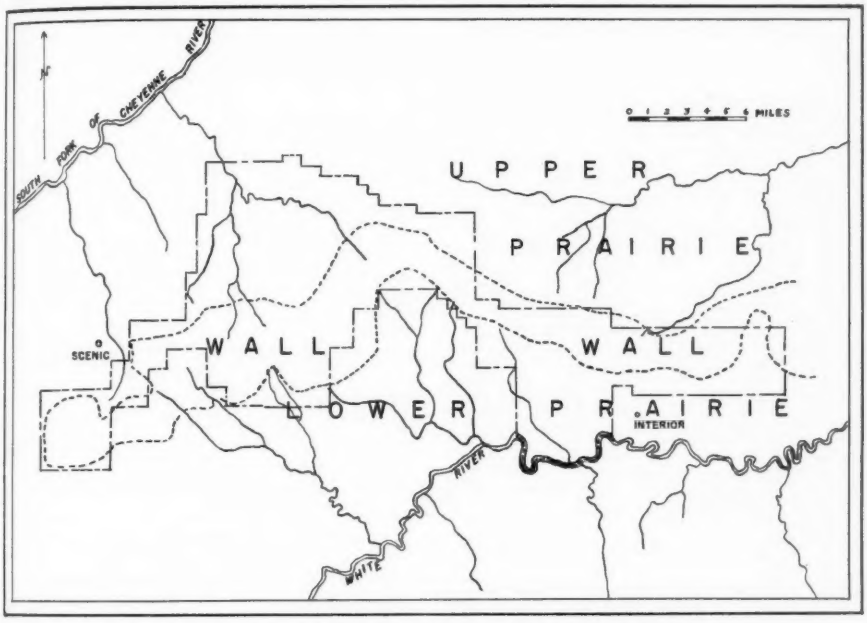

FIGURE 3.—TOPOGRAPHIC SUBDIVISIONS OF THE WHITE RIVER BADLANDS
Showing position of the "Wall' as related to the Upper and Lower Prairies

Miniature Pediments and Associated Features

Definitions

To avoid confusion over some terminology used in this paper, definitions are given.

DESERT PEDIMENTS: Rock surfaces of low relief, often veneered with fluvial gravels, sloping away from the base of mountains or escarpments in arid and semiarid climates (Von Engeln, 1942, p. 433). A pediment may or may not completely encircle a single mountain peak or small mountain range.

CONOPLAIN: A circular, cone-shaped pediment surface symmetrically distributed about a single mountain remnant or a closely spaced group of remnant mountain peaks (Ogilvie, 1905, p. 28). Several small buttes of the Big Badlands illustrate this form in miniature.

PEDIMENT EMBAYMENTS: Tonguelike extensions of pediments that penetrate mountain valleys like bays along an indented coast (Howard, 1942, p. 3). The floors of pediment embayments are confluent with the pediment surface.

PEDIMENT PASSES: Low gaps formed where pediment embayments, projecting inward from opposite sides of a mountain range, meet at the divide in broad cols (Howard, 1942, p. 3).

PANFAN: As defined by Lawson (1915, p. 33), the ultimate surface after the last remnants of a range in a region of rising base level have disappeared and the flanking alluvial fans coalesce at the divide. Blackwelder (1931, p. 138) objects to the term panfan because the crests may be barren for some distance outward. The writer found this true of the end stages of the Badlands miniature pediments. The term *pediment dome* is suggested here for the ultimate surface attained in an area of pedimentation, regardless of whether the rock surface is bare or covered by alluvium.

INSELBERGS: Islandlike erosional remnants of mountain masses which have become separated from the main body of the retreating escarpment or mountain front and stand as isolated peaks surrounded by the pediment surface.

SHEETWASH: Runoff that is not concentrated in definite channels, sometimes used synonymously with unconcentrated rill wash or sheet flood. Howard (1942, p. 15) prefers to use the term sheet flood for unconcentrated runoff of greater depth than sheetwash. By his definition there would probably be no occurrence of sheet flood on the miniature pediment surfaces of the Badlands. *Rill wash* is considered with sheetwash in that the badlands rill channels are not permanent features. They disappear, reappear, and change position on the steeper slopes, depending upon the amount of rainfall and degree of concentration of sheet runoff. If a rill channel develops a permanent channel and initiates a grading of its course differing from the angle of slope on which it originated, it may then be considered an intermittent stream channel.

BADLANDS SCARP: Retreating escarpment at the head of the miniature badlands pediments, which would correspond with the retreating mountain front of the large-scale desert pediment regions.

DISAGGREGATION: Disintegration of the surface material of the Badlands as a result of saturation by heavy rains followed by desiccation and breaking up of the material in place by cracking during dry periods. The loose rubble thus formed is rapidly removed by succeeding rainfalls. The process takes place repeatedly over short periods of time, depending upon the frequency of precipitation. Freezing and thawing may play an important role in disaggregation during winter months.

Theories of Large-Scale Desert-Pediment Origin

Lateral corrasion by streams, rill wash, or sheetwash and sheet flood, and the weathering of slopes with removal of debris by rills (Gilluly, 1937, p. 340) are active in the formation of large-scale desert pediments. Two general hypotheses have been advanced to explain the origin of pediments: the "weathering-removal hypothesis" and the "lateral planation hypothesis" (Howard, 1942, p. 14).

The weathering-removal hypothesis relies largely upon weathering of the upland front and removal of the weathered debris by any erosional agency, including both sheet flood and streams. McGee (1897, p. 108) was one of the first proponents of this hypothesis; he considered sheet flood an efficient agency in transportation, corrasion, and deposition.

The lateral-planation hypothesis attributes recession of the mountain front to lateral cutting by graded streams which issue from the adjacent mountains and impinge against the foot of the slope at the mountain-pediment junction. The idea was first advanced by G. K. Gilbert (1877, p. 126) and was fully developed by Sidney Paige (1912, p. 450) and later by Douglas Johnson (1931, p. 175; 1932a, p. 391; 1932b, p. 656).

Howard, Johnson, and Paige strongly favor lateral corrasion as the principal erosional pro-

cess in the formation of pediments. Rich (1935, p. 1024) discards lateral erosion as unnecessary and strongly advocates pedimentation by weathering and sheetwash, in conjunction with the blanketing effect of alluvial debris. McGee (1897, p. 108) and Lawson (1915, p. 28) favored sheet flood and rill wash respectively as the dominant erosional agents in pediment formation.

In his study of the Papago Country of Arizona, Bryan (1922, p. 96) recognized three processes which were combining to form pediments in the region: (1) lateral planation by streams issuing from the canyons, (2) rill cutting at the foot of the mountain slopes, and (3) weathering of outliers and unreduced remnants, with transportation of the debris by rills.

After further studies of pediments at Granite Gap, New Mexico, however, Bryan (1936, p. 135) stated that, as far as evidence obtainable in the area was valid, it indicated that pediments are formed by the retreat of mountain slopes induced by weathering and rain wash, and that lateral planation was ineffective in the area. He goes on to say, though:

> "Doubtless in the production of extensive areas of pediment, lateral planation is the most effective process but the importance of the retreat of slopes under weathering and the work of flood rills should not be unduly minimized."

Bryan thus confirms his belief in the necessity of processes given under both hypotheses. W. M. Davis (1930, p. 15) agreed with Bryan.

Gilluly (1937, p. 347) concluded that processes given under both hypotheses are necessary for pediments surrounding the Little Ajo Mountains in Arizona. He agrees with Bryan and states:

> "Pediments are slopes of transportation peculiar to arid regions and formed by cooperation of lateral corrosion, rill wash, and weathering, with subsequent removal of detritus by rills. One process may dominate in one place and another elsewhere, but all are operative."

V. C. Miller (1950, p. 643) studied small pediments cut on weak shales in the vicinity of House Rock, Arizona. Miller's conclusions are essentially the same as those of Bryan and Gilluly.

Theories of Miniature Pediment Origin in Badlands

The morphology of the miniature mountain-pediment systems observed in the White River Badlands is similar to that of mature mountainous desert regions of the southwestern United States. The erosional processes causing the development of both large-scale and small-scale pediments may be similar. One purpose of this study is to determine what analogies exist between the two.

Wilmot Bradley and Douglas Johnson came to different conclusions concerning the miniature pediment origin. Both agreed on the similarity in form to the pediment areas of the arid southwest.

Bradley (1940, p. 248) observed miniature pediments in southwestern Wyoming and concluded that the small-scale forms are developed by unconcentrated rill wash accompanied by pelting rain and sheet-flood erosion, and that lateral corrasion was ineffective. Bradley observed that the miniature and large-scale forms had much in common, but that processes differed in degree and in kind.

Bradley (1940, p. 254) states that badlands miniature pediments are carved by the combined action of unconcentrated rill wash and pelting rain within a narrow zone at the foot of a retreating badlands escarpment. Thereafter the pediment gradients are lowered by sheet-flood erosion and integrated into an extensive surface. The pediment surface, once formed, serves as a graded shelf across which debris from the wasting hills is transported.

Douglas Johnson (1932c, p. 546) studied the White River Badlands of South Dakota and compared the miniature forms and large-scale forms both in form and mode of development. Johnson states:

> "The distribution of these features in relation to drainage lines, and their delicate adjustment to miniature stream profiles, seem to exclude the weathering hypothesis and to render the sheet flood interpretation of doubtful application and to favor the ascription of these forms to normal stream erosion."

Johnson published this in an abstract and did not discuss his major points, nor did he present evidence for his conclusions. In the study of miniature pediments he has applied his earlier theory of pediment origin—lateral corrasion by normal stream erosion—to the miniature badlands forms as well as to the large-scale mountainous desert pediments.

The writer's observations in part substantiate Bradley's views. Lateral corrasion by streams, however, cannot be overlooked as a possible starting mechanism. A narrow plain of lateral corrasion formed adjacent to a steeper badlands scarp permits other agents of erosion to become active. This may be of considerable importance, because there are no fault scarps to provide initial relief. Some initiating mecha-

nism, such as lateral corrasion, is necessary to start the other erosional processes and maintain the abrupt junction between the steeper slope and the flood plain.

Field evidence indicates that lateral corrasion by streams plays a minor role in the development of miniature pediments. Instead, within elongate small pediment embayments adjacent upland slopes may be steepened at the junction with the pediment surface by a different type of lateral erosion at the margin of sheetwash.

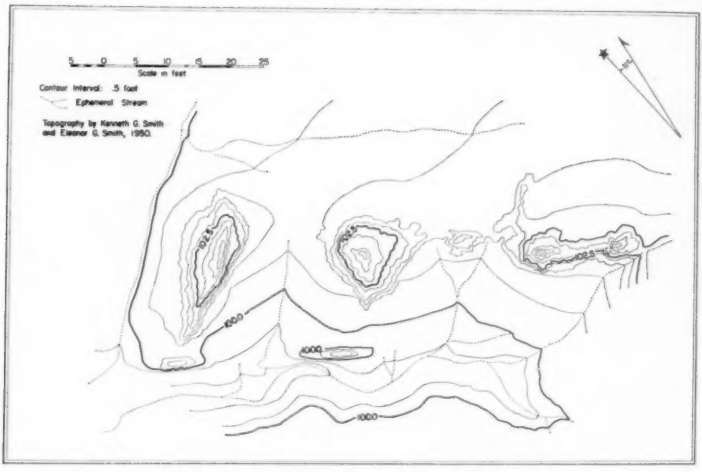

FIGURE 4.—TOPOGRAPHIC MAP OF AREA 1

Miniature Pediments of White River Badlands

No systematic differences were noted at different stratigraphic levels in the Big Badlands, although minor features differ in detail. This held true in spite of marked differences between the slope forms of valley walls and divides in the Chadron formation and those in the Brule formation.

The Chadron formation (Fig. 2) is easily eroded and causes the development of a subdued badlands topography with small, well-rounded convex hills, commonly referred to as "haystacks." The Brule formation has several dense ash beds near the top and several well-consolidated layers scattered throughout the section; consequently its topography is complex and rugged, with many ridges and high terraces.

The miniature pediments developed on the softer clay layers and are especially prominent in the lower Brule formation and in the Leptauchenia nodular layer of the upper part of the Brule formation (Fig. 2). Complete miniature mountain-pediment systems are less numerous in the Chadron outcrops; field mapping was restricted therefore to the Brule formation.

Description of Areas

Area 1.—Area 1 (Fig. 4), 1 mile north of Monument Headquarters, provides a typical example of the miniature mountain ranges and pediments resembling the mature mountainous desert terrain of the southwestern United States. The area is in a mature stage of development, with three major remnant mountain

PLATE 1.—MINIATURE PEDIMENTS AND ASSOCIATED EROSIONAL LANDFORMS

FIGURE 1.—General view of Area 1, looking west

FIGURE 2.—Miniature pediment embayment, Area 2

FIGURE 3.—Miniature hanging pass, Area 2

FIGURE 4.—Miniature drainage basin of Area 3

FIGURE 5.—Inselberg encircled by small-scale conoplain, Area 4

FIGURE 6.—Run-off pattern on miniature pediment surface as shown by silt streaks, Area 4

FIGURE 7.—Run-off pattern on pediment surface as formed by water poured down rill channels, Area 4

FIGURE 8.—Pediment-badlands escarpment junction in Area 4, illustrating abrupt change in gradient

FIGURE 1

FIGURE 2

FIGURE 3

FIGURE 4

FIGURE 5

FIGURE 6

FIGURE 7

FIGURE 8

MINIATURE PEDIMENTS AND ASSOCIATED EROSIONAL LANDFORMS

FIGURE 1

FIGURE 2

FIGURE 3

FIGURE 4

FIGURE 5

FIGURE 6

FIGURE 7

FIGURE 8

TYPICAL LARGE- AND SMALL-SCALE BADLANDS EROSIONAL FEATURES

masses about 3 feet high and one smaller inselberg, all of which form a belt of highlands 80 feet long trending approximately east-west (Pl. 1, fig. 1). The total area mapped is about 5000 square feet.

The miniature topography has developed upon poorly consolidated buff clays containing large calcareous nodules. This nodular clay is the Leptauchenia layer of the Brule formation. Although the clay appears relatively unconsolidated, it is quite strong and hard when dry, except for a thin layer of disaggregated rubble at the surface. When wet, the clay becomes plastic, and the surface layer of rubble, which is fragmented by numerous mud cracks, is easily removed by runoff. The plastic wet clay results in some local downslope sliding of the outer layer as a form of slope adjustment along the margins of rapidly downcutting valleys. The nodular character of the clay and general morphology of the area is readily apparent in a general longitudinal view of the area (Pl. 1, fig. 1).

Two major pediments slope away from the miniature remnant mountain range in opposite directions with slightly different gradients. The northward-sloping pediment has a lower gradient because the base-level stream is higher and farther away; the gradient of the southward-sloping pediment surface is greater because the base-level stream is closer and lower. The higher base level on the north may be explained by the fact that a westward-flowing stream along the northern margin of the area has been silting-in its channel. The silting-in process has not yet developed a silt wedge encroaching on the pediment, such as occur elsewhere in the Badlands.

The southward-sloping pediment suface is graded to a stream channel which is serpentine on a narrow flood plain. The stream cannot encroach northward onto the pediment surface because a sandstone dike, 1 foot thick, trends parallel to the stream course. The clastic dike stands out as a discontinuous remnant linear ridge on the southwestern portion of the pediment (Fig. 4).

A clastic dike also controls the drainage of the western part of the area, where the straight course of the southward-flowing stream is readily apparent. The dike lies along the east side of the stream and prevents the stream from migrating laterally eastward upon the adjacent pediment surface. This dike is only 1 inch thick; it rises less than half a foot above the level of the stream bed and thus does not appear on the topographic map. The two clastic dikes intersect in the southwestern corner of the area.

Area 2.—Area 2, approximately 3½ miles west of Monument Headquarters, shows well-developed pediments, pediment embayments, and pediment passes (Fig. 5). The topographic map is on a larger scale (1 inch = 3 feet) than those for other areas. To show more clearly the outline of the pediment embayments (Pl. 1, fig. 2), a contour interval of 0.1 foot was used on the pediment surfaces and 0.5 foot on the steeper slopes.

The area is stratigraphically lower than Area 1; the miniature topography has developed on massive gray clays of the lower Brule or upper Chadron formation. In some places the two formations are not readily separated.

Of the two well-developed pediment passes, one is a hanging pass (Pl. 1, fig. 3); a third pediment pass is almost completely developed (Fig. 6).

The large, semicircular embayment (Fig. 5) is cut on a bedrock surface. The southward-sloping surface of the pediment embayment truncates a thin, horizontal layer of more resistant rock. This embayment extends nearly 12 feet into the remnant upland masses. Although sheet flood may be predominant in the

---

PLATE 2.—TYPICAL LARGE- AND SMALL-SCALE BADLANDS EROSIONAL FEATURES

FIGURE 1.—General view of miniature mountains and pediments of Area 5, looking west

FIGURE 2.—Major remnant butte of Area 6, showing silt streaks on pediment surface in foreground

FIGURE 3.—Pediment embayment, Area 6, showing slopes adjacent to the pediment surface with an absence of rill channels due to the nodular character of the clay

FIGURE 4.—Deep miniature pediment embayment on west side of Area 6, with minute longitudinal drainage channel and concave transverse profile

FIGURE 5.—Mud cracks at pediment–badlands escarpment, Area 6

FIGURE 6.—Pediment embayment, Area 7, showing a flat transverse profile

FIGURE 7.—General view of steep-sloped spurs of drainage map area, looking west from instrument station "A"

FIGURE 8.—Remnant butte of Brule formation, north of town of Interior, on Lower Prairie level, showing breached, grass-capped piedmont slope

embayment during runoff, the constriction at the embayment mouth channels some flow through it during heavy rains. The channel does not, however, continue outward on the pediment surface to the south.

flow in the last stages of runoff periods, a condition also noted in Area 1.

Area 3.—Area 3 (Fig. 7), a good example of a minute drainage basin, is the smallest well-developed basin observed in mountain fronts

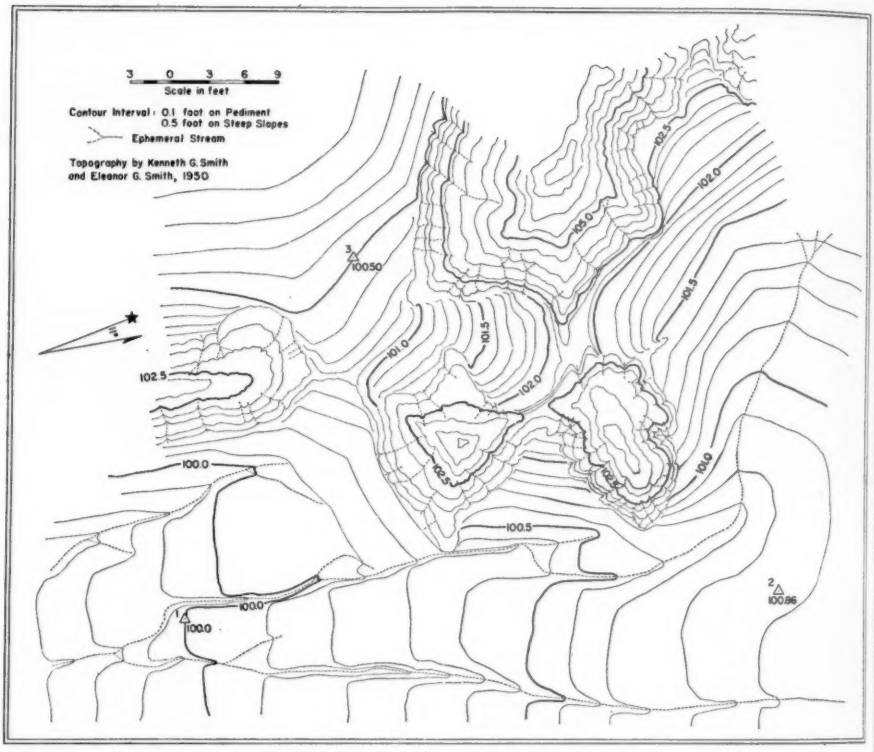

FIGURE 5.—TOPOGRAPHIC MAP OF AREA 2

In both Area 2 and Area 3 the buttes have poorly integrated drainage systems and their numerous rill marks terminate at the junction between the pediment and the badlands escarpment. There are two exceptions to this in Area 2: in the east-facing pediment embayment on the eastern side of the area a minute third-order drainage basin has developed; on the north side of the most northeasterly butte a second-order drainage basin has developed. Such miniature drainage basins are not common on the small-scale topographic forms.

The pediment surfaces of Area 2 slope gently from adjacent badlands escarpments, and no drainage lines cross them to join the local base-level streams. A few streaks of silt on the pediment surfaces suggest rill wash, ending as mud-

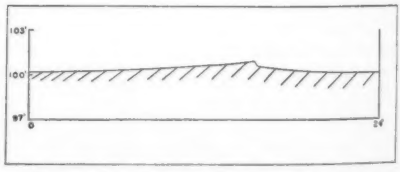

FIGURE 6.—TOPOGRAPHIC PROFILE ACROSS HANGING PASS IN AREA 2

bordering miniature pediments within the Badlands. It is about 300 feet east of Area 2, on a long, low spur extending southward from the Wall. Pediment surfaces slope away from the spur on either side throughout its length. In places the crest of the spur rises as high as 10 feet above the adjoining pediments. The

drainage basin is third order, with a dendritic drainage pattern (Pl. 1, fig. 4). Rill channels drain the steeper slopes of most of the spur; only one small drainage basin was mapped on the southeast side of the spur.

of clay developed over the main stream. The writer first thought this was due to solution of the calcareous cementing material in the clay and subsequent development of subterranean drainage. It seems more likely, however, that

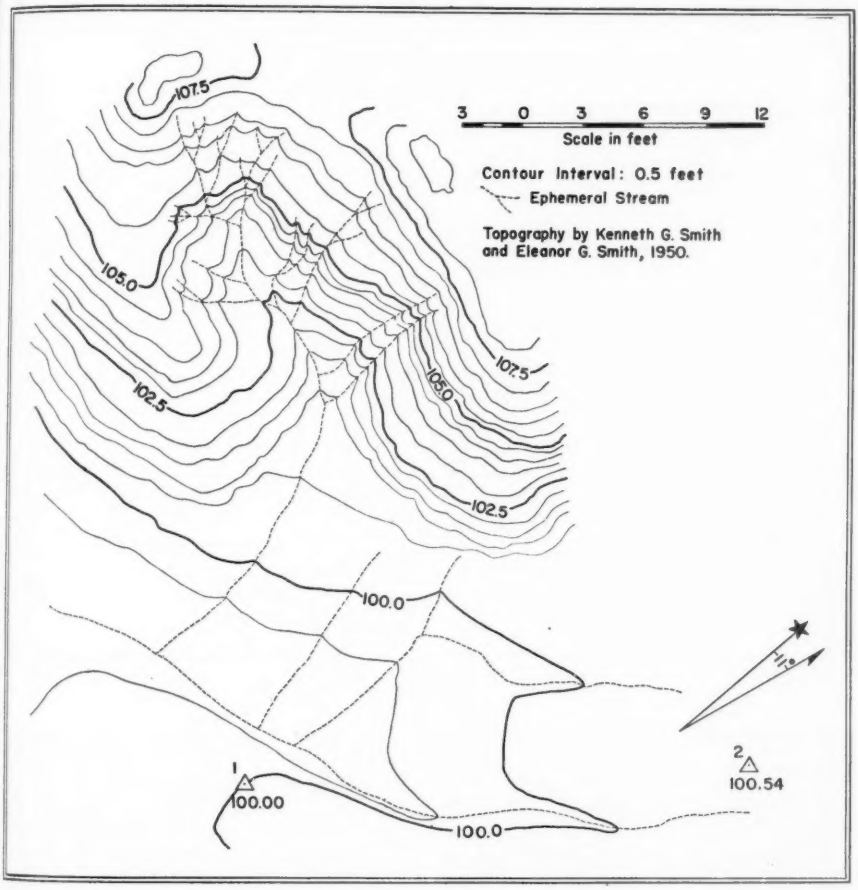

FIGURE 7.—TOPOGRAPHIC MAP OF AREA 3

The miniature pediment east of the basin was one of the few observed in the Badlands on which a stream originated within the bordering upland area and extended across the pediment surface. The pediment embayment extending headward at the mouth of the small basin may be affected by this drainage line; it represents the only evidence of embayment widening by lateral planation of a stream.

Between August 1950 and August 1951, near the mouth of the basin, a natural bridge the increased rainfall in June 1951 (Table 1) deepened the minute steep-walled channels, oversteepening them, and that slope adjustment by highly viscous mudflows on the valley sides partially covered the deeper main channels, but allowed the deeper main stream to continue beneath the clay bridge.

Area 4.—Area 4 (Fig. 8), approximately 4 miles west of Monument Headquarters, is an excellent example of a well-developed conoplain.

The butte in the center of the area rises slightly more than 5 feet above the pediment or conoplain. The proximity of a local base-level stream east of the butte causes the pediment to be shorter and slightly steeper on that side.

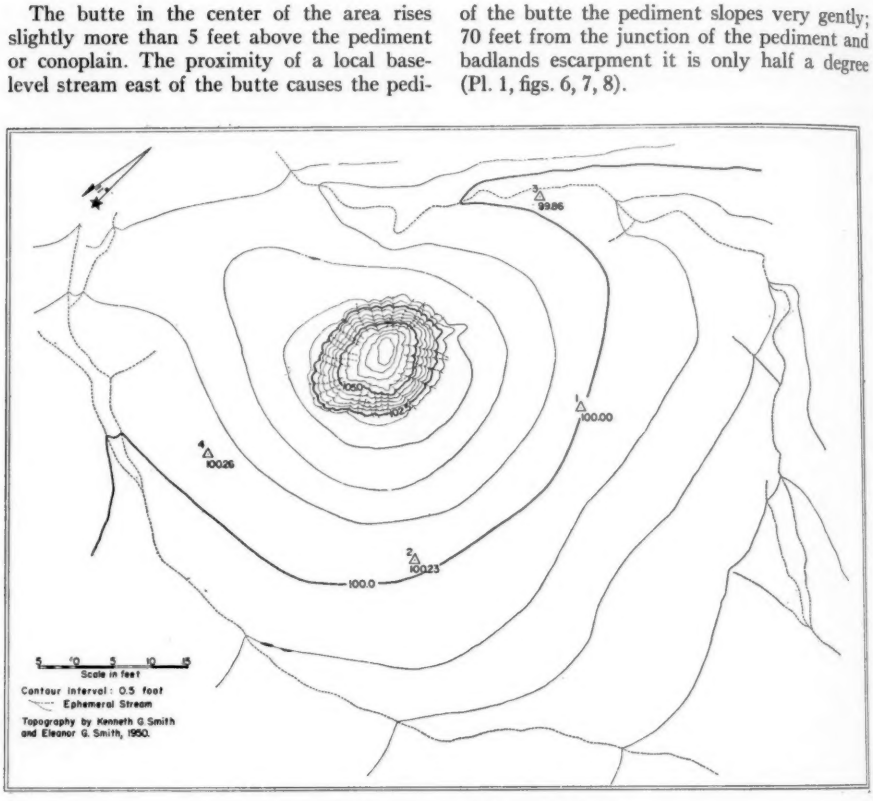

FIGURE 8.—TOPOGRAPHIC MAP OF AREA 4

The butte is convex with a well-rounded crest (Pl. 1, fig. 5). Rill channels are closely spaced on its flank; 48 rill channels join the pediment surface around the perimeter of the butte. Only 30 of the rill channels are large enough to be mappable. The steeper slopes of the butte range from 34° to 46° at the junction between the pediment and retreating badlands escarpment.

Around the base of the butte the pediment slopes about 7°. None of the rill channels supplies sufficient concentration of runoff to form drainage lines across the conoplain surface.

Although the conoplain surface at first appears convex, the longitudinal profiles on three sides of the butte are actually concave, while the shorter pediment surface on the southeast side is straight. Southwest and east of the butte the pediment slopes very gently; 70 feet from the junction of the pediment and badlands escarpment it is only half a degree (Pl. 1, figs. 6, 7, 8).

Area 5.—Area 5, north of Cedar Pass, is a region of mature miniature mountainous desert topography developed on nodular buff clays of the Brule formation. The area is about 100 feet long and 70 feet wide; less than 25 per cent of the region consists of buttes (Fig. 9; Pl. 2, fig. 1).

In Area 5 a network of streams has developed upon the pediment surface. Close examination showed that ephemeral streams trending northward on the pediment surface are extending themselves headward on the pediment owing to the more rapid vertical erosion in their main-trunk stream. The northward-flowing stream in the eastern part of the map is subsequent, growing headward along the contact between the less resistant buff nodular clay and an overlying recent layer of a more resistant fill of angular material, derived from erosion of dense ash beds.

Large calcareous clay nodules exposed on the pediment surface suggest that this surface has

been cut on bedrock. The lone inselberg, west of instrument station *C*, is largely nodular material, and no rill channels are present on its slopes. Erosion of the inselberg is chiefly by unconcentrated flow, for channels are absent.

rounding pediment to a height of 5½ feet. The topography has developed on buff, nodular clays of the Brule formation similar to that of Areas 1 and 5. The central inselberg has several small rill channels on its slopes, although fewer

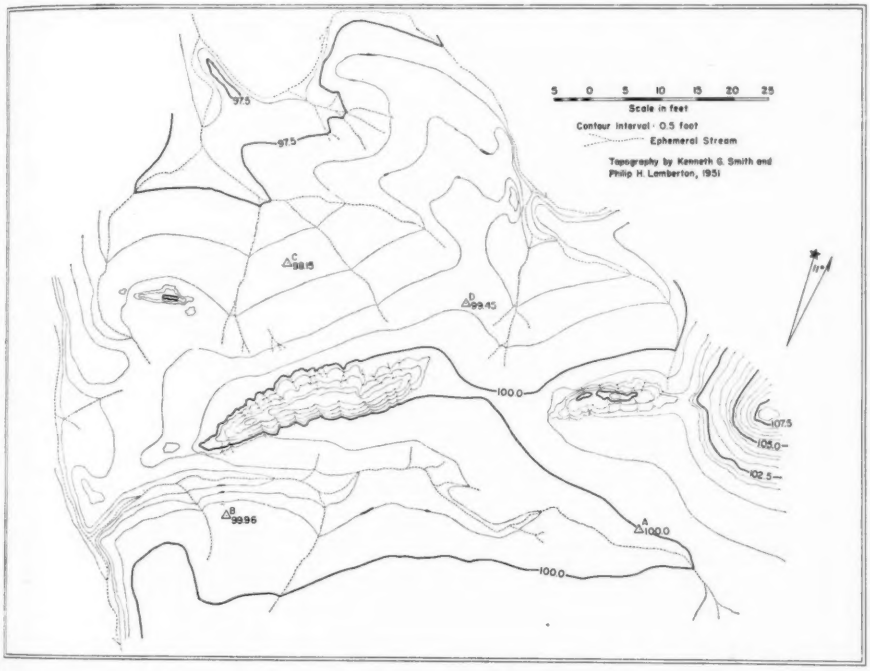

FIGURE 9.—TOPOGRAPHIC MAP OF AREA 5

Extensive mud cracks cover the pediment surfaces of Area 5, indicating bedrock clay beneath. Traces of silt on the pediment represent material in transit across the graded pediment profile. The silt is generally only a fraction of an inch thick and shows direction of flow. The silt thickens slightly toward the local base-level streams, but, as most of the streams are actively eroding their channels vertically at a fairly rapid rate, there is no pronounced permanent thickening of the silt cover on the pediment.

Area 6.—Area 6, west of Norbeck Pass, consists of one major butte in the center of the map and several minor inselbergs with extensive pediments (Fig. 10). For this larger area a scale of 1 inch to 10 feet was used, and the contour interval of half a foot was retained.

The major, central butte is about 45 feet long, 20 feet wide, and rises abruptly above the surrill channels develop on buttes in nodular beds than on those formed in the clays of the Brule formation. The clays of Areas 2, 3, 4, and 7 are more nearly homogeneous, with an occasional thin, resistant layer, and almost no calcareous nodules (Pl. 2, fig. 2).

The smaller inselbergs of Area 6 are characterized by the absence of rill channels; runoff evidently occurs only as sheetwash on the slopes.

No well-developed drainage systems have been formed on the miniature mountains. The slopes adjacent to the pediments have a mean angle of 46°, and the rill channels maintain the same gradient.

The pediments are well developed and extremely dissected by minute stream channels—a marked contrast to the small amount of pediment dissection noted in all other areas except Area 5. North and south of the area, large

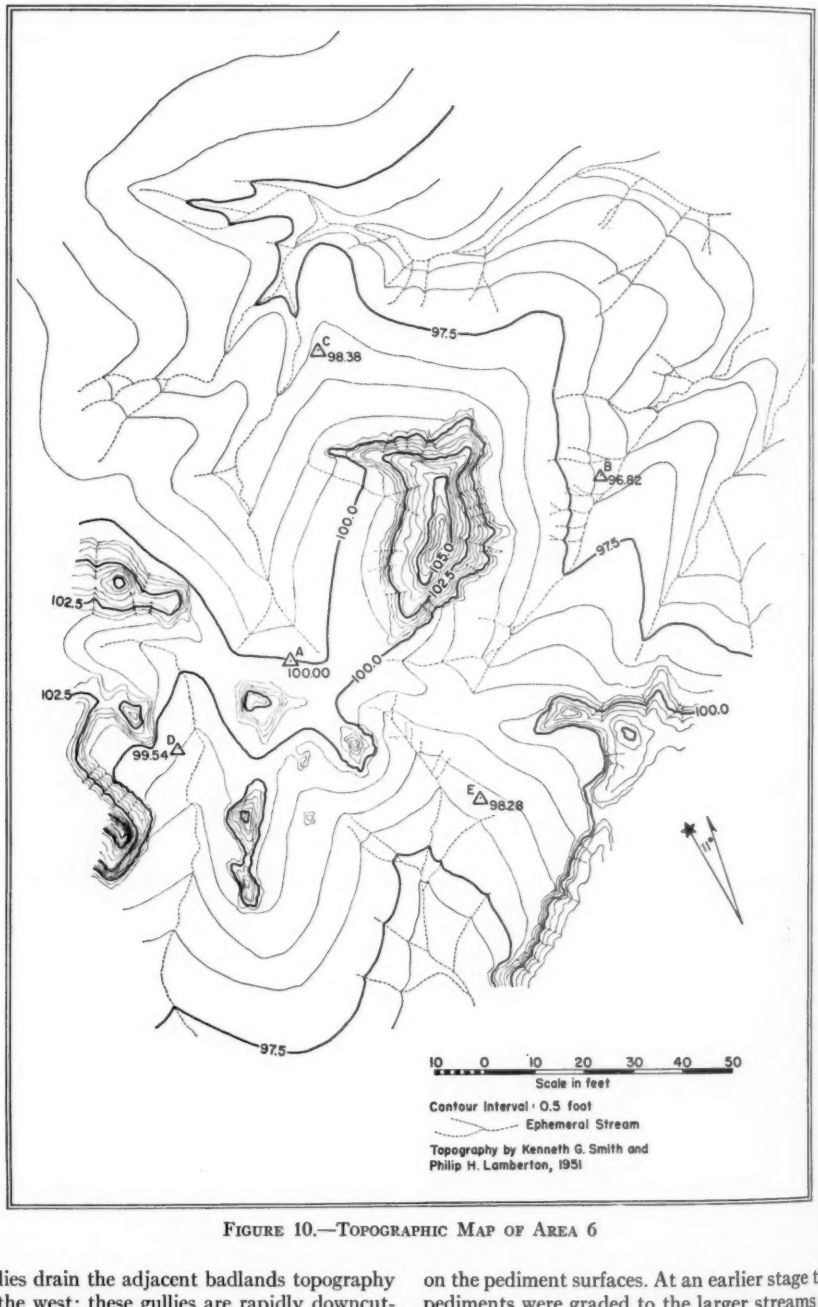

FIGURE 10.—TOPOGRAPHIC MAP OF AREA 6

gullies drain the adjacent badlands topography to the west; these gullies are rapidly downcutting their channels and have caused headward growth of the network of streams now present on the pediment surfaces. At an earlier stage the pediments were graded to the larger streams of the gullies, which served as local base levels prior to their rejuvenation.

Pediment passes and pediment embayments are well developed in Area 6. Three pediment embayments are found in the southern part of the area, two in the west, and one in the east. fig. 6). The transverse profiles of each pediment embayment on the map is straight.

At the head of each embayment, where the pediment ends abruptly at the junction with

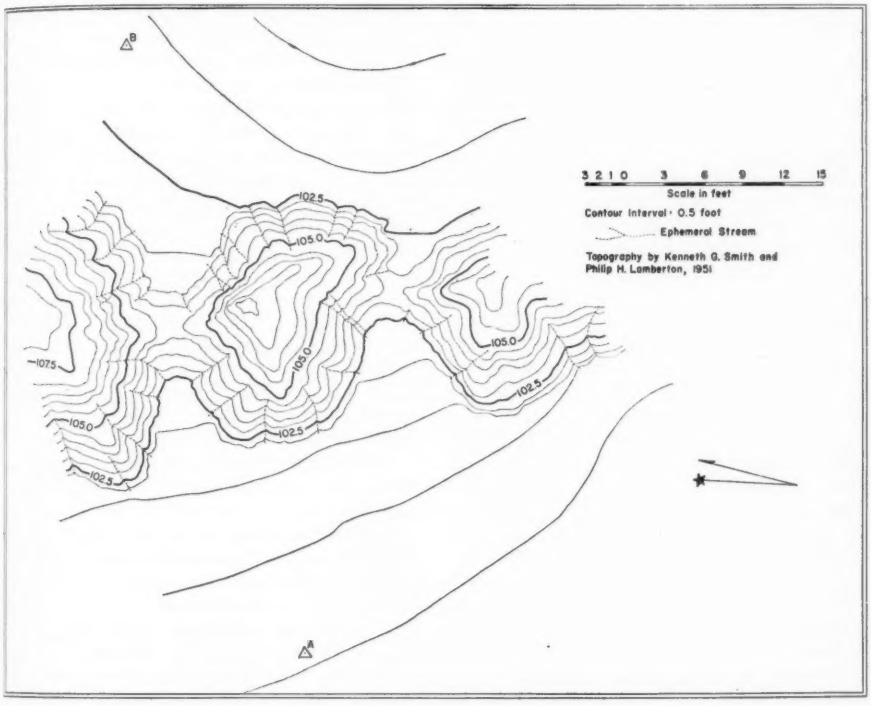

FIGURE 11.—TOPOGRAPHIC MAP OF AREA 7

Only one of the embayments has a well-defined stream channel draining it, and the stream does not extend upward onto the badlands escarpment at the embayment head.

The pediment embayment in the southeastern corner of the area has rather steep marginal slopes, and there is a slight trace of a drainage line down the center of the embayment (Pl. 2, fig. 3). Area 6 affords several opportunities to study the development of pediment embayments and the relation of the pediment surfaces to the steeper slopes of the badlands escarpments (Pl. 2, fig. 4; Pl. 2, fig. 5).

Area 7.—Area 7 lies north of and adjacent to Area 2. Two sets of opposing pediments in the central part of the area extend well into the remnant upland masses from opposite sides (Fig. 11). The embayments have accordant junctions with the main pediments, and all have concave longitudinal profiles (Pl. 2, the badlands escarpment, the embayment surfaces have gradients of 6°–7°. None of the miniature pediment embayments has developed a convex transverse profile.

Pediment embayments extending inward from opposite sides of the mountain masses may be separated at their heads by a low, col-like divide (Howard, 1942, p. 99). This form develops in the late stages of embayment formation, finally resulting in a pediment pass. The two sets of opposing pediment embayments in Area 7 are still separated by the low col-like divides. Weathering and erosion will eventually form the pediment pass.

The lowest point along the crest of the divide separating the embayments of Area 7 rises as little as 1 foot above the pediment surface at the embayment head (Fig. 11). No drainage lines have developed on the embayment surfaces in this area; scattered clay lumps on the

pediments suggest strong sheet-flood action during runoff periods.

Morphology and Development of Miniature Badlands Pediments

The miniature pediments develop as smooth surfaces, sloping gently away from the buttes. The longitudinal profile of a badlands pediment is typically concave-up, resembling the longitudinal profile of a graded stream. The pediment profile represents a graded surface of transportation adjusted to the discharge of water and debris supplied from adjacent upland source areas. The gradient of a miniature pediment may be 7° or 8° immediately below the junction with the badlands escarpment, decreasing outward from that point to as low as 1° adjacent to the local base-level stream.

In places streaks of silt on the pediment surfaces represent fine clay and silt deposited during the final stages of runoff. These flow lines suggest a change from a continuous layer of sheet wash to subdivided rill wash. The silt streaks change position on the pediment surface with successive periods of runoff and are temporary features. Silt streaks were observed in all the areas mapped but are clearest in Areas 4 and 6 (Pl. 1, fig. 6; Pl. 2, fig. 2).

The junction between the badlands escarpment and a bordering pediment is sharply defined and would be classed as an angular junction by Howard (1942, p. 30). The weathered or disaggregated material present at the surface is usually a fine silt or rubble and does not accumulate at the bases of the steeper slopes as talus cones or alluvial fans, but is rapidly removed by rill wash during rainfall periods.

No evidence suggested downslope movement of loose material on the badlands escarpments during dry periods, except for occasional rolling of larger fragments; evidently most of the loose rubble on the steeper slopes is moved only by rain-storm runoff.

The calcareous nodules in some of the clays generally disintegrate into smaller fragments as they move down the steeper slopes. Occasionally, however, larger fragments of nodules are scattered on the pediment surface by exceptionally strong sheet wash.

The nodules are too small to cause major variations in topography, except to form miniature pedestal rocks. They may have diminished the number of rill channels on the remnant buttes of Areas 1, 5, and 6. The nodules suggest that the pediments are cut surfaces rather than depositional forms. In Area 1 many nodules are in place on the pediment surface, surrounded by massive clay. The relation between the massive clay and the nodules is the same on the badlands escarpments; the clay exposed on the pediment is evidently bedrock.

The mud cracks at the pediment-badlands escarpment junction (Pl. 2, fig. 5) curve upward at the junction. The same material is present at the surface both on the pediment and on the steeper slope. As the mud cracks are similarly spaced on both surfaces, it is assumed that the material in which they have formed, in this instance the bedrock clay, is the same. In areas where silt covers the pediment surfaces (Areas 2 and 7), the silt consists of the coarser material present in the original clay, and the spacing of mud cracks differs from that on the clay. Those mud cracks formed on the original clay bedrock are more closely spaced than those formed on the silt cover; the boundary between the two on the pediment surface may thus be readily recognized in the field.

Miniature badlands pediment systems are graded to local base-level streams which form part of a drainage network in and around the miniature landforms. It was first noted in Area 1 (Fig. 4), however, and substantiated by observations in the other areas mapped, that miniature landforms are characterized by absence of well-integrated drainage comparable to the stream systems draining large-scale mountainous desert regions. Instead, runoff on the steeper slopes of the miniature buttes is confined to sheet wash and rill-channel flow. The rill channels may be straight, extending from near the top of the badlands escarpment to the junction with the pediment surface, but few, if any, continue as intermittent stream channels on the pediment surface. A few rill channels bifurcate into two or more separate channels in their upper extremities, but all maintain the same gradient as the average slope angle of the badlands scarp.

The steeper slopes of the buttes of Area 1 (Fig. 4) average about 35°. The rill channels do not continuously erode their channels more rapidly than the recession of the steeper slopes by disaggregation and sheet wash. Consequently, the rill channels maintain the same gradient as the receding slope on which they form and do not grade their channels to a normal profile of equilibrium, as to true stream channels.

Except in Area 3 (Fig. 7), no minute stream

which originates within the miniature mountains continues across the adjacent pediment to join the local base-level stream. An abrupt change in gradient occurs where each rill channel joins the pediment surface. During runoff the rill channels are concentration lines for discharge, and the water flowing in the channels would normally be heavily laden with silt and debris derived from up-slope areas.

The rill channels are probably so steep that the capacity of the rill is never fully met when discharge is copious. Upon reaching the pediment surface, the heavily loaded discharge of the rill channel is checked abruptly in velocity because of the abrupt change in gradient. Assuming that the pediment surface is a graded slope of transportation, the rill flow abruptly reaches a graded slope when it contacts the pediment. It cannot erode this surface to a lower slope because this would upset the condition of grade; it does not steepen the slope by aggradation because the slope is already adjusted to transport the normal detrital load. The sudden decrease in gradient causes a spreading of the water on the pediment surface, changing to sheet flow or sheet wash, and exerting a strong lateral shear where the spreading sheet is banked up against the junction between the pediment and badlands escarpment. Additional rainfall adds to the total discharge of sheet wash on the pediment, but the pediment-surface profile has been adjusted to account for increased erosional and transportational capacity by a steadily reduced, or concave-up profile.

The lateral shear exerted by spreading rill water at the junction may explain the undercutting at the mouth of each rill channel (Pl. 2, figs. 2, 3, 4).

The extension and widening of the miniature pediment is evidently due to the manner in which the rill channel mouths are formed. Since no streams (as distinct from rills) originate within the miniature mountains and cross the pediment surfaces, a theory of pedimentation by lateral corrasion of graded streams is not applicable to the development of the miniature badlands forms. The location of the inselberg in Area 4 (Fig. 8) suggests the absence of lateral corrasion by streams as an active process in the formation of the surrounding pediment (Pl. 1, fig. 5). The conoplain encircles the butte, and no major stream flows near enough to the butte to effect any undercutting at the pediment-butte junction. The major inselbergs of the other area mapped are similarly located with respect to major streams draining the surrounding areas. The absence of drainage lines originating within the miniature mountain systems and extending across the adjacent pediments requires some explanation for pediment formation other than lateral planation.

A plausible working hypothesis for the widening and extension of the miniature pediments must consider the nature of the rill-channel mouths and the junction between pediment and badlands escarpment.

During field work, the writer did not observe runoff in a heavy rainfall. He did, however, observe the last stages of runoff following one storm in Area 4 (Fig. 8); the flow on the conoplain surface was discontinuous, fan-shaped sheets of water, the apex of each fan pointing at an individual rill-channel mouth. Sheet wash emanating from a given rill channel overlapped that of adjacent rill channels. After runoff had ceased thin, fan-shaped silt deposits remained on the conoplain surface (Pl. 1, fig. 6). The depositional silt is not a permanent alluvial form but represents material in transit which will be removed and replaced by new debris during the next heavy runoff.

Near the inselberg of Area 4 larger fragments of clay were found on the pediment surface. It was first assumed that these clay fragments indicated an earlier stronger period of sheet flow, at which time coarser material could be transported by the greater volume of discharge. Closer observation, however, showed that the larger fragments of clay were the remains of blocks of bedrock which had fallen downslope on the flank of the inselberg. Large cavities on the sides of the butte indicate the position from which fragments were derived. The clay blocks are evidently loosened by swelling when the ground becomes saturated. Once on the pediment surface, sheet wash disintegrates the clay fragments, and the finer material is transported down the pediment slope.

Water poured into three adjacent rill channels on the inselberg of Area 4 verified the distribution of runoff on the pediment surface as inferred from surface markings. Although conditions of natural runoff could not be duplicated, the results were considered significant. A change was observed from normal channel flow in the rills to a thin sheet of water on the pediment-badland scarp junction, with a marked decrease in velocity on the pediment surface. The sheet wash carried a heavy load of silt and clay and on the pediment terminated

in a mudflow. Under normal rainfall conditions, increased precipitation over the pediment surface evidently enables the sheetwash to transport the heavy load of sediment down the lesser gradient of the pediment and prevents the permanent deposition of a silt layer (Pl. 1, fig. 7).

Lateral corrasion by normal stream erosion may be the initiating factor in the development of miniature pediment areas, but, once a butte becomes separated from the retreating badlands escarpment, the steeper slopes of the butte continue to retreat by disaggregation of the material exposed on its flanks, with removal of the material by sheetwash. The pediment is extended headward in this manner, and its surface is graded to the stream channel which originally separated the butte from the retreating badlands scarp.

Regrading of the Pediment Surface

A change in the condition of the local base-level stream to which the pediment surface is graded will be followed by changes on the pediment. If downcutting increases along the local base-level stream, the pediment will be dissected by new streams extending themselves headward from the major stream. On the other hand, a rise in local base level will cause a silt wedge to encroach on the pediment surface, thickening outward from the badlands escarpment.

The pediments of Areas 1, 5, and 6 (Figs. 4, 9, 10) are dissected by numerous streams which head on the pediment at points well downslope from the mountain–pediment junction. The major streams to which the pediments of these areas are graded are cutting down actively because they do not have large amounts of silt along their channels, and in places they flow on bedrock. The pediment surfaces become convex at their outer margin where they join the local base-level streams; the streams are deepening their channels so rapidly that sheetwash removal of material from the pediment surface cannot keep pace with them. As a result new stream channels begin to incise the pediment. As the base-level stream continues to erode its channel more rapidly, these streams continue to grow headward, and the pediment becomes more and more dissected.

In contrast, the northward-sloping pediments of Areas 2 and 7 (Figs. 5, 11) are being encroached upon by a silt wedge, which first becomes evident as a thin film of coarser material approximately 3 feet from the badlands escarpment. From the point where the silt first appears the wedge gradually thickens outward on the pediment surface toward the local base-level stream. The silt layer is finely laminated and appears to be a permanent depositional feature rather than material in transit.

FIGURE 12.—ENCROACHING SILT WEDGE IN AREA OF RISING BASE LEVEL

Silt wedge, in black, is exaggerated to indicate a thickening from zero to 0.44 inch. Pediment surface in Area.

Small blocks were carefully cut from the pediment surface to determine the increase in thickness outward on the pediment. The wedge thickens from zero, 3 feet from the mountain-pediment junction, to 0.44 inch, 12 feet out on the pediment surface (Fig. 12).

The absence of a sedimentary cover on several of the pediments suggests that there is a delicate balance between the activity of the local base-level stream and the erosional processes which are extending the pediment headward. Consequently, a sedimentary wedge such as in Areas 2 and 7 apparently indicates the encroachment of the depositional feature due to the inability of the local base-level stream to accommodate the load of debris supplied to it. Base level is rising, and the pediment profile is being regraded to the higher base level.

The rise of base level adjacent to Areas 2 and 7 was apparently caused by recent growths of vegetation along the axial stream channel, causing a decrease in velocity of discharge. A subsequent silting-in along the small valley has caused a rise in elevation of the stream-channel bottom. The longitudinal profile of the pediment must be regraded to the higher level to retain equilibrium. The new profile is still concave-up but is at a higher level than the earlier pediment profile.

Pediment Embayments and Pediment Passes

Typical pediment embayments of Areas 2 and 7 (Pl. 1, fig. 2; Pl. 2, fig. 6) are adjacent to one another and have had similar histories.

Pediment embayments of these two areas have concave-up longitudinal profiles, but the transverse profiles are straight. The embayments lack a longitudinal stream, which eliminates a theory of origin by lateral corrasion of streams originating in the miniature-mountain area at the heads of the embayments.

Along the margins of the pediment embayments of Areas 2 and 7 the slope of the adjacent miniature mountain flanks ranges from 40° to 47°, with a pronounced steepening at the junction with the embayment surface; here the scarp becomes nearly vertical, forming a miniature cliff 1–2 inches high. Since there are no drainage lines on the embayment surface, the steep slope along its margins suggests undercutting by sheet wash.

The origin of miniature pediment embayments may be related to variations in intensity of the undercutting effect observed at the mouths of all rill channels throughout the area. Should a rill channel become overly enlarged as a result of the coalescence of two channels at its head, the immediate effect may be more rapid backcutting at the pediment–escarpment junction, causing the development of a deeper indentation in the scarp at the rill-channel mouth, the floor of which is accordant with the pediment surface. Once initiated, marginal rill channels would be deflected into the small embayment first formed, permitting the main rill channel to increase its rate of backcutting at the junction. In the newly developed embayment debris from the steeper adjacent slopes would continue to be removed by sheet wash. The increase in load would accompany the increase in discharge, offsetting downcutting action on the surface of the new embayment; hence no drainage channel would develop on the pediment surface. The pediment embayment maintains the graded slope and represents a tonguelike extension of the surrounding pediment into the bordering mountains.

The widening and headward extension will continue by the same erosional processes until the divide between the embayment and an opposing pediment embayment is lowered so much that the central rill channels disappear and a low, col-like divide is formed. The pediment embayments of Area 7 (Fig. 11) are at this stage of development. Once this stage has been attained, runoff from the divide at the embayment head is unconcentrated sheet wash, but the marginal rill channels remain active and, with the aid of marginal erosion by sheet wash, continue to widen the pediment embayment. In time adjacent pediment embayments will unite to form a continuous pediment surface separated from an opposing pediment by a low, linear ridge. As erosion continues, the linear ridge will disappear, and a linear pediment dome will form.

The pediment embayments of Area 6 (Fig. 10) differ from those of Areas 2 and 7 in that the transverse profiles are concave rather than straight, and a central drainage channel may be present, although longitudinal streams were never found as far up the embayment as the mountain–pediment junction at its head (Pl. 2, figs. 3, 4). The longitudinal profiles of pediment embayments in Area 6 are concave also, and there is no apparent change in gradient where the embayment surface joins the main pediment.

The relations between the central longitudinal streams and the concave transverse profiles of the Area 6 pediment embayments do not support a theory of development by lateral stream corrasion. The concave transverse profile prevents lateral migration by the central stream, so that it cannot impinge against the steeper marginal slopes of the embayment.

The steeper marginal slopes of the pediment embayments of Area 6 range from 45° to 54°, with a pronounced steepening at the junction with the embayment surface, where a miniature vertical wall is developed.

If opposing pediment embayments are extended headward so that no low col-like divide separates them and the pediment slopes intersect, a pediment pass is formed. A well-rounded pediment pass occurs between the two westernmost buttes of Area 1 (Fig. 4). Pediment passes are characterized by bedrock exposures along their surfaces with minor amounts of silt present. If, as opposing embayments are extending headward, the surface of one develops at a lower level than the other, the end product may be a hanging pass (Pl. 1, fig. 3).

Pediment Domes

In Area 5 (Fig. 9), north of instrument station *D*, the butte has been removed by erosion, and this portion of the area is in the final stage of pedimentation. It resembles the panfan defined by Lawson (1915, p. 33) but differs in that an encroaching sedimentary wedge is not present.

Rich (1935, p. 1022) describes similar forms without encroaching alluvial cover which are comparable to a panfan in morphology. Since no true panfan areas, according to Lawson's definition, were observed, the term *pediment dome* is suggested to describe the comparable

feature which lacks only the encroaching alluvial cover.

Morphology of Small-scale Pediments and Large-scale Pediments Compared

The large-scale topographic maps of the miniature pediment systems closely resemble conventional topographic maps of large-scale mountainous desert regions. To clarify similarities and differences, the miniature badlands pediments are compared with the large-scale corms of the Sacaton Mountains of Arizona, as described by Howard (1942, p. 16).

The longitudinal profiles of large-scale pediments and miniature pediments are directly comparable, as both are concave-up. The angle of slope of the pediment differs considerably, however, especially at the mountain–pediment junction. Miniature pediments slope away from adjacent escarpments at angles of 5° to 7°, exceptionally at 9° or 10°. They are much steeper than those of the Sacaton Mountain area, where the pediments slope away from the mountain front at angles of less than 1° in most places, with a maximum angle of 2½° (Fig. 13). The concave longitudinal profiles of both the large-scale and small-scale forms represent an adjustment of the pediment surfaces to the transportation of debris derived from adjacent highland areas.

The badlands scarps adjacent to miniature pediments have an average slope of 35°, which is also true for major portions of the Sacaton Mountains. Variations in mountain-slope angles in the Sacaton Mountains are the result of differences in lithology. In the Badlands the bedrock is essentially homogeneous, and a more constant angle holds.

Badlands escarpments adjacent to pediments lack integrated drainage and depend upon rill channels and slope wash for removal of runoff. The rill channels may change positions seasonally, or even with each heavy rainfall. In contrast, the Sacaton mountain fronts are well dissected by several major streams.

The miniature pediments are seldom crossed by a stream channel originating within the bordering highland areas. If a stream is present on the pediment surface, it is usually extending headward from a point of origin along the local base-level stream. In contrast, the pediments of the Sacaton Mountains are dissected by streams that originate within the bordering mountain ranges. Increased vertical erosion by the main base-level stream causes the development of strongly dissected miniature pediments.

The junction between the upland slopes and the miniature pediment is generally sharp and angular, except where the badlands escarpment has ceased to recede and the mountain slope is reclining. Curved, faceted, and concealed junctions, as described by Howard (1942, p. 24) in the Sacaton Mountains, were not observed in the miniature landforms. The variations in types of mountain–pediment junctions of the Sacaton Mountains are due to the weathering and erosional characteristics of the underlying bedrock. The constant angular junctions of the miniature badland forms are evidently caused by the relative homogeneity of the underlying bedrock; the small size of areas mapped restricted the forms to homogeneous units within the Oligocene White River group.

Opposing miniature pediment embayments of the badlands, extending inward from opposite sides of the small-scale mountain ranges, are similar to the large-scale embayments of the Sacaton Mountains. The miniature embayments may intersect at a pediment pass, in a low, col-like divide, or a low remnant upland ridge may separate one embayment from another. The floor of a pediment pass generally has a convex-up longitudinal profile. The longitudinal profiles of pediment embayments, on the other hand, are concave-up. The miniature pediment embayments may have either a concave-up or straight transverse profile. None, however, was observed with a convex-up transverse profile, although Howard (1942, p. 135) reported several among the large-scale pediment embayments of the Sacaton Mountains.

The escarpments adjacent to miniature pediment embayments commonly steepen at the junction with the floor of the embayment, as do those of the Sacaton Mountains. This steepening cannot, however, be attributed to the same erosional processes in both regions. The steep margins of the large-scale pediment embayments probably originated through undercutting by lateral swinging of the trunk stream and free swinging of the tributary streams against the mountain front. The absence of central longitudinal streams draining the miniature pediment embayments and the absence of small streams draining marginal escarpments suggests lateral erosion at the margins of sheet wash rather than stream planation.

Panfan areas, as described by Lawson (1915, p. 33), do not develop in the miniature mountain-pediment forms. Where the ultimate stage of pediment formation is reached within the

badlands areas, a pediment dome resembles a true panfan. The presence of a silt wedge, analogous to the alluvial cover of large-scale panfans, depends upon the activity of the local base-level streams. Pediment domes in Area 5 agent of deposition except when confined to a valley where it can undercut the margins. Undercutting at the margins of sheet wash is readily apparent in the miniature pediment embayments and causes steeper mountain slopes

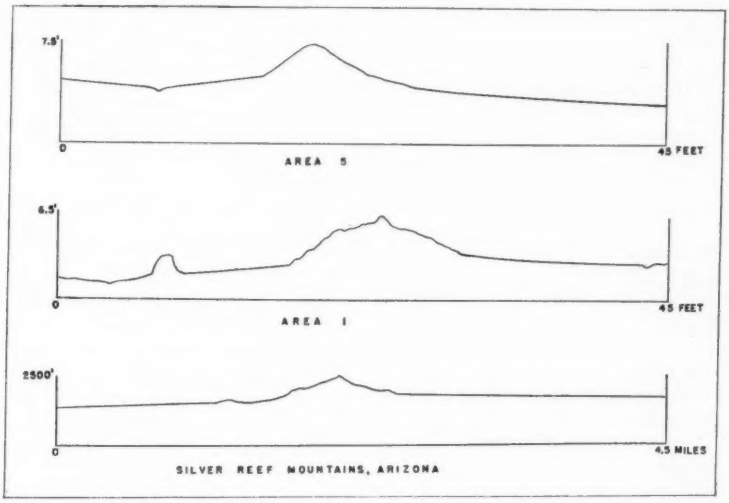

FIGURE 13.—COMPARISON OF LARGE-SCALE AND SMALL-SCALE PEDIMENT PROFILES
Illustrating the similarity in morphology between large-scale pediment forms and miniature pediment areas

(Fig. 9) were surrounded by local base-level streams, which eroded their channels vertically without silt deposition.

Howard (1942, p. 125) pointed out that in the Sacaton Mountains slopes recede uniformly in all parts. This is also true for the miniature badland pediment forms. The rapid parallel recession of slopes in the badlands forms may explain why rill channels maintain the same gradients as the average angle of slope. Slope retreat is evidently so rapid it prevents vertical erosion by the rill channels, and consequently the upland drainage cannot become integrated.

Howard (1942, p. 134) concluded that undercutting by lateral planation is necessary for parallel slope retreat; the upper portions of the slopes recede by weathering-removal processes. Undercutting by erosional processes is essential for the maintenance of the angular junction in both types of areas, but in miniature pediment forms back-cutting at the rill channel mouths is induced by spreading of the water sheet.

Tolman (1909, p. 147) believed that the erosional importance of sheet flood was overemphasized; he considered the sheet flood an at the junction between the pediment floor and the marginal badlands escarpment. Paige's conclusion (1912, p. 450) that sheet floods are the result of rock-cut plains, and not the cause, is not tenable in the miniature badland pediment areas, where sheet wash, or sheet flood, is both a cause and an effect in relation to the pediment surface. Although produced by the pediment, the sheet wash extends the pediment and keeps its junction with the escarpment sharp.

The main difference in erosional processes between large- and small-scale pediment areas lies in the mechanism of erosion at the inner margin of the pediment.

Conclusions Concerning Origin of Miniature Pediments

(1) Miniature pediments grow as the badlands escarpment retreats by weathering (disaggregation), slumping, and sheet and rill erosion. Erosion extends the pediment at the margins of spreading sheet wash close to rill-channel mouths, where each rill terminates at the mountain–pediment junction.

(2) Sheet wash is apparently not a major erosional agency on the surface of the miniature pediment once the surface has been developed, but is chiefly an agent of transportation and maintains the graded profile of the pediment by removing debris derived from adjacent buttes. Larger scattered fragments and broken nodules common on the pediment surface are derived from the slope above. Sheet wash may cause a slow lowering of the pediment to maintain a graded profile with respect to a slowly falling base-level stream.

(3) The concave-up profile of the pediment reflects equilibrium attained as the pediment is formed and graded to its local base-level stream.

(4) Abrupt changes of base level will be met by a readjustment of the longitudinal profile of the pediment. A rise in local base level results in deposition on the pediment surface of a silt layer that thickens outward from the miniature mountain front. Ultimately this layer will be of uniform thickness, restoring the original grade to the pediment. With lowering of local base level streams will extend headward on the pediment surface.

(5) Lateral corrasion by a major intermittent stream initiates the pediment surface development, and sheet wash becomes the major agent of transportation; slumping and backwearing by spreading sheet wash at rill-channel mouths continue the retreat of the escarpment base.

(6) Pediment embayments are formed by the processes that act elsewhere along the miniature pediments and badland escarpments. Embayments evidently develop along preexisting rill channels which were larger than the average rill channel and were characterized by deeper indentations at the junction with the pediment surface. No stream channels drain the embayments longitudinally, and the steep marginal slopes are interpreted as the result of lateral erosion at the margins of sheet wash.

(7) In late stages, when the upland areas have been removed, miniature pediment domes are formed. The miniature domes are free of depositional material.

Topographic Texture of Badlands Topography

Derivation of Texture Ratio

In an earlier study of topography (Smith, 1950, p. 657), a texture ratio, T, was established,

$$T = N/P.$$

Texture of an area is then defined as the ratio of the number of crenulations N on that contour having the maximum number within a given drainage basin to the length (in miles) of the perimeter P of the basin. Texture ratios for drainage basins in different areas might be used to designate coarse-, medium-, or fine-textured topography: Coarse T_m = less than 4.0; Medium T_m = 4.0–10.0; Fine T_m = greater than 10.0, in which T_m represents the weighted mean texture ratio for a given area and is obtained by the following equation (Smith, 1950, p. 660):

$$T_m = \sum (AN/P)/\sum A.$$

The weighted mean texture ratio is the ratio of the sum of the products of the basin area times the texture ratio for each basin, $\sum(AN/P)$, to the sum of the areas of the basins, $\sum A$.

A conclusive study of topographic texture requires highly accurate, large-scale maps. Air photos should be used conjunctively.

Texture Ratios for Typical Badlands Typography

A strongly dissected area near Big Foot Pass (Fig. 1) was mapped on a scale of 50 feet to the inch, with a contour interval of 20 feet (Fig. 14). Maximum relief is about 200 feet. The area is maturely dissected and has a fine-textured, dendritic drainage pattern.

Exposures of massive clays and ash beds of the Brule formation form steep high slopes; the lower slopes, underlain by the Chadron formation, form gentle, rounded, typical haystack topography (Pl. 2, fig. 7).

Texture ratios for the basins developed on the Chadron formation range from 13.7 to 33.0. Seven small basins were selected for the measurements on the Chadron formation, all of which were first- or second-order basins. The writer concluded that development of basins higher than second order is prevented because the Chadron clays, when saturated, may be extremely plastic to a depth of 1 foot or more, which causes a constant slow flowage for slope adjustment. This fills in any gullies which might develop. At times the plastic clay covers a small gully, leaving a short segment of channel beneath (Table 3).

The Brule formation is more massive than the Chadron, with nodular layers at several horizons and dense ash beds in the upper portion. It produces a more rugged topography and has more first-order streams. Formations are essentially horizontal, and there is no apparent

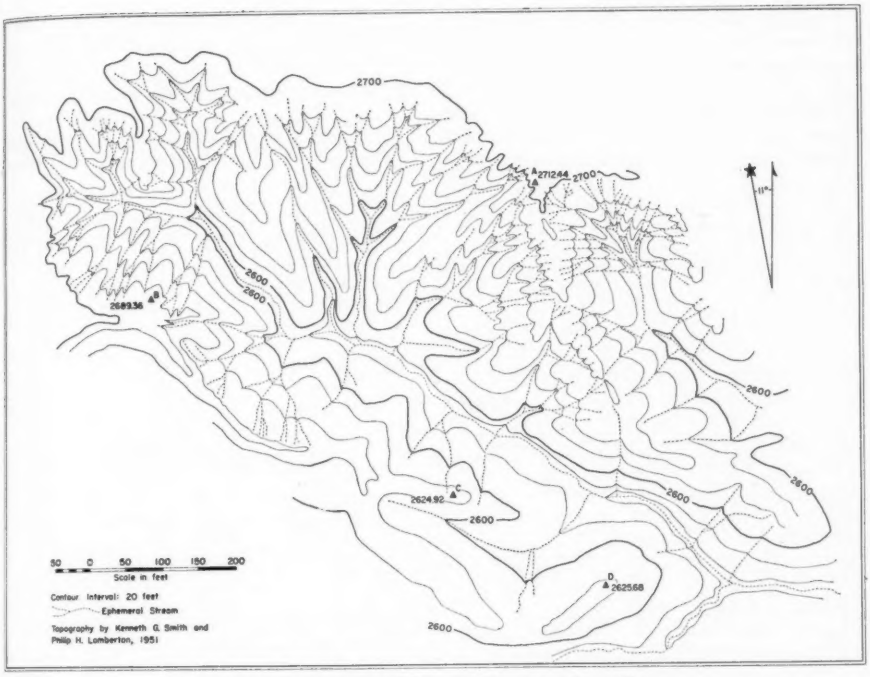

FIGURE 14.—TOPOGRAPHIC MAP OF DRAINAGE AREA STUDIED

TABLE 3.—TEXTURE RATIO DATA FOR SOUTH DAKOTA BADLANDS (CHADRON FORMATION)

Texture ratio	Drainage density*
13.9	38.8
26.1	81.6
17.9	59.2
33.0	149.4
20.3	132.2
17.3	90.03
13.7	93.7

* Drainage density is number of miles of channel length per square mile of basin area.

structural control of drainage development, thus allowing the dendritic drainage pattern to prevail. Texture-ratio values range from 7.6 to 124.3 (Table 4).

The weighted mean texture ratios (T_m) for the 7 basins on the Chadron is 26.9, while the mean texture ratio for the 21 basins developed on the Brule is 69.7. These values are considerably lower than those developed on a clay-sand back-fill area near Perth Amboy, New

TABLE 4.—TEXTURE RATIO DATA FOR SOUTH DAKOTA BADLANDS (BRULE FORMATION)

Texture ratio	Drainage density
49.2	243
34.8	229
71.7	295
42.8	198
28.6	229
32.5	256
63.2	316
45.0	159
113.3	252
101.5	169
7.6	114
34.3	170
61.3	135
84.2	194
88.0	211
66.1	243
97.8	410
49.1	418
103.2	418
92.8	383
124.3	379

Jersey (Fig. 15) (Smith, 1950, p. 666), where the texture ratios for individual drainage basins range from 149 to 254, with the lowest value for N/P exceeding the highest value recorded on the Brule formation. The weighted mean texture ratio for the Perth Amboy area is 230. Texture-ratio values recorded from topographic maps surveyed by Professor Brainerd Mears, of the University of Wyoming, in the Chinle Badlands, Petrified Forest National Monument, Arizona, are of the same order of magnitude as the higher values for the Brule drainage basins and range from 106 to 127, with a mean texture ratio of 111 (Table 5).

A study of weighted mean texture by the writer (1950, p. 667) suggested that for texture ratios exceeding 50 an "ultra-fine" texture grade should be established. Under this classification the drainage basins developed on the Chadron formation are considered fine-textured, while approximately half the Brule drainage basins are ultra-fine. If only the mean texture ratio is considered the entire Brule formation outcrop area, with T_m = 69.7, is ultra-fine-textured. The Chadron area, with a mean texture ratio of 26.9, is fine-textured.

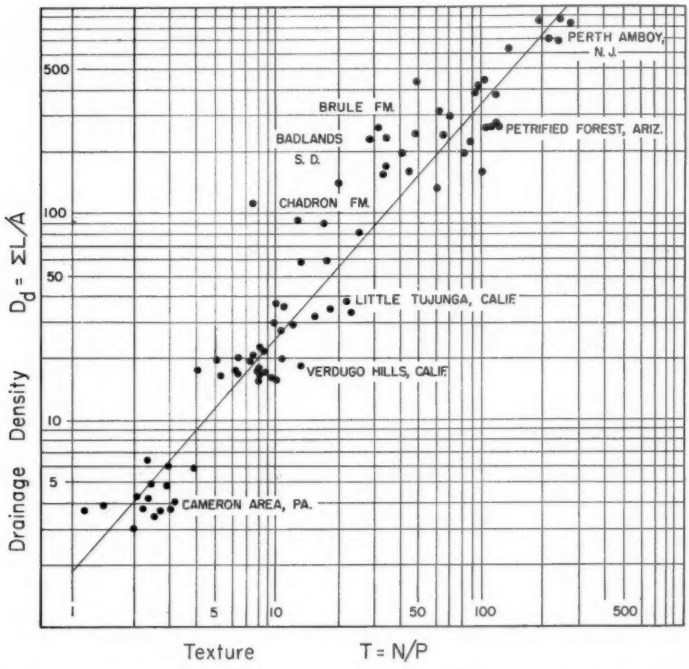

FIGURE 15.—LOGARITHMIC GRAPH OF DRAINAGE DENSITY–TEXTURE RATIO
Estimating equation was derived from this.

Relation of Texture Ratio to Drainage Density

Drainage density, "the length of stream per unit area in a given drainage basin" (Horton, 1945, p. 283), was also determined for individual basins of the drainage-map area (Fig. 14), so that a comparison could be made between drainage density and texture-ratio values. Drainage density may be expressed by the equation:

$$D_d = \sum L/A,$$

in which $\sum L$ represents the total length of streams in the basin, and A represents the area, both in units of the same system.

Drainage-density values range from 113.5 to 418 for the Brule formation drainage basins, and from 58.8 to 149.4 for the Chadron formation. Because the Chadron basins have lower texture-ratio values, lower drainage densities would be expected.

The data obtained from the Badlands National Monument were plotted on log-log paper (Fig. 15) for a comparison with the data from the earlier texture study (Smith, 1950, p. 667). Drainage-density values were plotted as ordinates, texture ratios as abscissas. The data

TABLE 5.—MEAN TEXTURE RATIOS AND DRAINAGE-DENSITY VALUES FOR SEVEN GENERAL AREAS

Locality	Mean texture ratio	Mean drainage density
Pennsylvania	2.64	4.08
Verdugo Hills, Calif.	8.65	18.10
Little Tujunga, Calif.	17.83	31.50
Badlands, South Dakota (Chadron formation)	26.90	77.60
Badlands, South Dakota (Brule formation)	69.70	258.00
Petrified Forest, Ariz. (Chinle formation)	111.00	230.00
Perth Amboy, N. J. (Clay-sand back fill)	230.00	747.00

from the five areas of the earlier texture study form a scatter zone which approximates a straight line, and the South Dakota Badlands drainage density–texture ratio points fill the gap between the Perth Amboy, New Jersey, data and the California data. A scatter zone fitted by a straight line is still maintained, suggesting that drainage density is a power function of the texture ratio.

Using the general form:

$$\log Y_c = \log a + b \log X,$$

which is the logarithmic form of:

$$Y_c = aX^b,$$

constants were derived from the earlier data by the method of least squares to give $\log Y_c = .220 + 1.11 \log X$.

The Badlands data, although filling the gap on the original graph (Fig. 15), tend also to alter the trend of the fitted line. By inspection a straight line was fitted to the point and new constants were derived for the power function, giving $\log Y_c = .255 + 1.15 \log X$. This equation estimates drainage-density values when only texture ratios are known, and vice versa. It does not relate cause and effect as in regression studies.

Factors Controlling Topographic Texture

Texture of topography depends upon both natural and map factors. The most important natural factors include climate, vegetation, rock or soil type, rainfall intensity, infiltration capacity, relief, and stage of development in the landmass cycle. Weak rocks produce fine-textured topography; resistant rocks cause coarse textures. The sparse vegetation of arid climates causes finer textures than those developed on similar rocks in a humid climate. Textures are coarse in the initial and early stages of erosion, finest in early maturity when relief is the greatest.

Data from the South Dakota Badlands drainage map (Fig. 14) increase the general knowledge concerning the texture ratio–drainage density relationship and suggest general conclusions concerning the natural factors controlling topographic texture and the reasons for the variations in texture and drainage density. Table 5 summarizes weighted mean texture ratios and drainage densities.

The Petrified Forest topography (Fig. 15), with a mean texture ratio of 111.0, has an ultra-fine texture. The underlying Chinle formation is essentially a massive, unconsolidated clay or shale, relatively homogeneous. Weakness of the formation and absence of a vegetal cover, combined with the torrential summer rains, form the finely dissected badlands topography.

The highest mean texture ratio, 230, was recorded in the clay-sand backfill area near Perth Amboy, New Jersey (Fig. 15). Absence of vegetation, weakness of the homogeneous clay-sand material, a low infiltration capacity, and the more frequent rainfall of the humid marine climate are important factors in the more extensive dissection of this badlands topography as compared to that in the Chinle badlands and the White River Badlands. The additional rainfall may be a key factor in this region, but, once vegetation gains a foothold, which is inevitable in such a climate, the surface becomes highly resistant, and texture ratio decreases.

The normal stream-eroded topography of the White River Badlands Brule formation, with a mean texture ratio of 69.7, is ultra-fine-textured. The lower mean texture ratio, as compared with the Chinle badlands (111.0), reflects the greater resistance of the Brule formation. The Brule formation in the drainage-map area consists of alternating beds of

weak clay and nodular clay, with more resistant volcanic ash beds exposed in the higher levels. Torrential summer rainfall and lack of vegetation are common to both this area and the Petrified Forest region.

Badlands developed on the Chadron formations are fine-textured, with a mean texture ratio of 26.9. Climatic conditions are those of the adjacent Brule formation and the Chinle badlands. Vegetal cover is absent. The poorly consolidated clays, on which slopes tend to adjust themselves by plastic flow when saturated, prevent the development of the extremely fine textures observed in the Brule and Chinle badland topography.

Thus variations in texture ratios in the semiarid badlands areas of Arizona and South Dakota, with similar climatic conditions and vegetation dispersement, are due to differences in the erosional characteristics of the underlying bedrock.

Bifurcation Ratios for Dendritic Drainage of Badlands

Stream-Order Number in Badlands

Horton (1945, p. 286) demonstrated that in a typical dendritic drainage pattern the streams of a given drainage basin may bifurcate in such a manner that, when plotted on semi-log paper, the number of streams of a given order on the logarithmic ordinate and stream order numbers on the abscissa, form an approximate straight line. This may be expressed by the equation:

$$N_u = R_b^{(s-u)}$$

in which N_u represents the number of streams of a given order, R_b is the bifurcation ratio for the basin, s is the highest order number stream in the basin, and u is the given order.

A study of the bifurcation ratios in the drainage-map area (Fig. 14) was undertaken to evaluate Horton's (1945, p. 286) concept. Three fourth-order basins were outlined on the map so that the numbers of streams of each order number could be determined and the data plotted on semi-log paper. The three basins were designated *A*, *B*, and *C* as shown in Figure 16. Then, because a major drainage divide extends southward from instrument station *A* on the map (Fig. 14), the map area was separated into an eastern drainage basin and western drainage basin, from which the same data were compiled and plotted on semi-log paper (Fig. 17). Table 6 presents a summary of the data for the two figures.

Both sets of graphs (Figs. 16, 17) illustrate the straight-line relationship. The two sets of

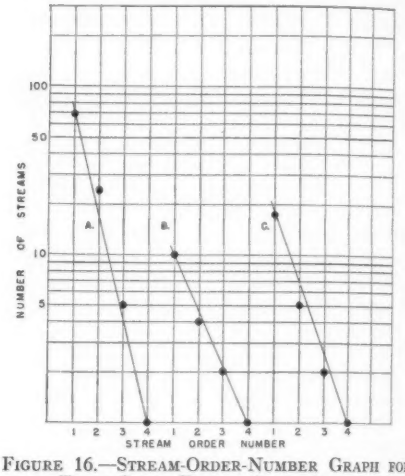

Figure 16.—Stream-Order-Number Graph for Three Small Fourth-Order Basins

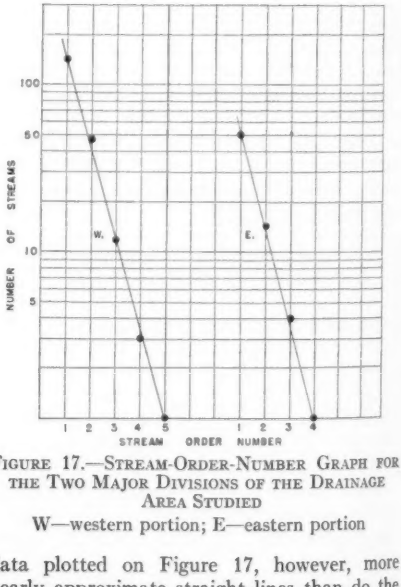

Figure 17.—Stream-Order-Number Graph for the Two Major Divisions of the Drainage Area Studied

W—western portion; E—eastern portion

data plotted on Figure 17, however, more nearly approximate straight lines than do the data plotted on Figure 16. This suggests that, the larger the area considered in such a study, the greater the possibility that the stream order–stream number relationship will approximate a straight line on semi-log paper.

The relationship shown by the two graphs (Figs. 16, 17) suggests an orderly development of dendritic drainage in the relatively homogeneous badlands clays, conforming with Horton's concept of the bifurcation ratio. This relationship will evidently continue so long as the drainage system remains constant. The introduction of structural control of drainage may cause an increase in the number of first-order streams and render the bifurcation-ratio concept untenable in specific instances.

TABLE 6.—STREAM-ORDER NUMBER DATA FOR FIGURES 9, 10

Stream-Order Number	Number of streams					Bifurcation ratio
	1	2	3	4	5	
Figure 9						
Basin "A"	68	24	6	1		4.21
Basin "B"	10	4	2	1		2.16
Basin "C"	17	5	2	1		2.63
Figure 10						
Eastern Area (E)	50	14	4	1		3.57
Western Area (W)	139	46	12	3	1	3.40

STATISTICAL METHODS APPLIED TO BADLANDS

Slope Analysis

The Brule formation forms the high areas of the Badlands within the Wall and is expressed in rugged ridges, spires, and pinnacles. On the Chadron formation low, rounded hills—haystacks—usually develop. On the Brule formation slopes are steeper than on the Chadron formation. The ash beds of the Brule cause vertical faces, whereas lower slopes predominate on the Chadron formation.

Recent deposits underlying the grass-capped piedmont surface (Pl. 2, fig. 8) are unconsolidated and easily eroded when exposed. Under normal conditions the mean-slope angle of 52.7° (Table 7) seems high for such material. The high average slope angle may be attributed to the grass-covered surface directly above the steeper slope which protects the subjacent material. The grass surface acts in the same capacity as a layer of more resistant rock, and the weaker underlying material is removed from beneath by sapping action during run-off periods, thus maintaining the steeper slope angle.

Steeper slopes on the exposures of Brule formation are high-cohesion slopes (Strahler, 1950, p. 693) and are typical of many badlands regions. High-cohesion slopes are formed in areas underlain by cohesive fine-textured materials such as clays or clay-rich soils (Strahler, 1950, p. 693). Slope angles were sampled in three areas underlain by the lower portion of the Brule formation so that the steepening effect of an overlying ash bed did not have to be taken into consideration (Table 7, *A*, *C*, *E*). Mean angles of slope for the three areas sampled were 56.07°, 49.53°, and 51.00° respectively.

Two sets of data from the lower Brule formation (Table 7, *A*, *C*) were obtained from two large remnant buttes of similar lithology on the Lower Prairie. Mean slope angles were determined by a frequency-distribution analysis of slope angles recorded in the field for each. Slope-angle data were then tested to determine whether or not the differences in means were significant. The level of probability was obtained by means of the *t* test (Dixon and Massey, 1951, p. 103):

$$t = \frac{\bar{X}_1 - \bar{X}_2}{S_p \sqrt{1/N_1 + 1/N_2}}$$

in which S_p is the pooled estimate of variance of the two samples, $\bar{X}_1$ and $\bar{X}_2$ are the means for each group of data, and N_1 and N_2 are the numbers of variates in each sample. A value of 6.82 was obtained for *t*, which, with 151 degrees of freedom, gives a probability of less than .001. This means that the observed differences in means would be expected to occur by chance variations in sampling considerably less than 1 time in 1000, and therefore the differences may be considered significant.

The significant differences in mean slope angles developed on similar buttes can only be attributed to existing field conditions. Both *A* and *C* are typical Lower Prairie remnant buttes surrounded by moatlike trenches (Ward, 1922, p. 50). Butte *A* is close to a major drainage line extending southward from the Wall and actively downcutting its channel. Consequently, the streams which flow parallel to the base of the butte are also downcutting their channels rapidly, and the old grass-capped piedmont surface has not receded so far from the base of the butte as on butte *C*, where more extensive pediments have developed (Fig. 18). The wider trench, with extensive pediment at

the base of the butte, has resulted in a lower mean angle of slope on butte *C*, whereas active downcutting along the narrower trench parallel to butte *A* has maintained a steeper angle of slope.

this gives a probability of less than .001; the differences are judged significant.

The Chadron formation, where overlain by the more resistant Brule formation, tends to be sapped from beneath it thus resulting in a

TABLE 7.—SUMMARY OF SLOPE-ANALYSIS DATA

	Class Mid-Values (in degrees)																		
	36.5	38.5	40.5	42.5	44.5	46.5	48.5	50.5	52.5	54.5	56.5	58.5	60.5	62.5	64.5	66.5	68.5	X	s
A	0	0	0	0	1	3	3	3	9	18	9	11	10	4	2	1	1	56.07°	4.75°
B	0	0	0	1	2	2	6	7	5	7	8	1	1	1	0	1	0	52.69°	4.88°
C	0	1	7	8	11	7	5	10	6	5	5	4	6	2	0	1	0	49.53°	5.67°
	33.5	35.5	37.5	39.5	41.5	43.5	45.5	47.5	49.5	51.5	53.5	55.5	57.5	59.5	61.5	63.5	65.5		
D	2	0	0	1	2	2	4	1	0	0	0	0	0	0	0	0	0	42.00°	4.48°
E	0	0	0	0	1	1	3	1	2	2	2	1	3	1	0	1	0	51.00°	6.06°
	11.5	13.5	15.5	17.5	19.5	21.5	23.5	25.5	27.5	29.5	31.5	33.5	35.5	37.5	39.5	41.5	43.5		
F	0	0	0	0	7	14	8	23	13	14	7	6	0	0	1	1	0	26.19°	4.24°

A. Brule formation—remnant butte north of Interior.
B. Slope angles beneath grass cover of breached piedmont slope.
C. Brule formation—remnant butte west of Interior.
D. Chadron formation in drainage map area.
E. Brule formation in drainage map area.
F. Chadron formation slope angles.

Within the drainage-map area (Fig. 21) slope angles were determined for both the Brule and Chadron formations (Table 7, *D*, *E*). A value of 4.4 was obtained for *t*, which, with 28 degrees of freedom, gives a probability of less than .001; the differences in means may be considered significant. In this area differences in mean slope angles are directly related to the variations in lithology between the two formations, the nodular clays of the Brule formation maintaining higher average angles of slope than the more nearly homogeneous clays of the Chadron formation, which adjust to lower slopes by plastic flow when saturated.

A frequency-distribution analysis of the typical Chadron haystack topography, which develops south of the Wall, gave a mean slope angle of 26.19° (Table 7, *F*) as compared with 42.00° in areas where the Chadron is overlain by the Brule formation. Typical Chadron haystacks are low round convex hills with long gentle slopes (Fig. 19). Testing the differences in means for significance, a value of 12.0 was obtained for *t*. With 104 degrees of freedom,

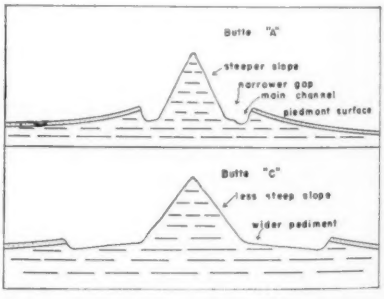

FIGURE 18.—TOPOGRAPHIC PROFILES OF LARGE REMNANT BUTTES ON LOWER PRAIRIE LEVEL
Buttes "A" and "C", illustrating differences in width of moatlike trenches surrounding each butte.

higher mean slope angle (Table 7, *D*). Once the Brule formation has been eroded, the Chadron slopes adjust more rapidly by plastic flowage when wet, causing the development of lower average slope angles and the more rounded haystack topography.

The value of a slope-analysis study depends upon the determination of the existing relationships between slope angle and controlling factors in a given area. Strahler (1950, p. 675) points out that slopes reflect a steady state in its value is zero (Croxton and Cowden, 1946, p. 660).

The closer the value for r approaches 1, the stronger the degree of correlation indicated. The correlation coefficient obtained, 0.485,

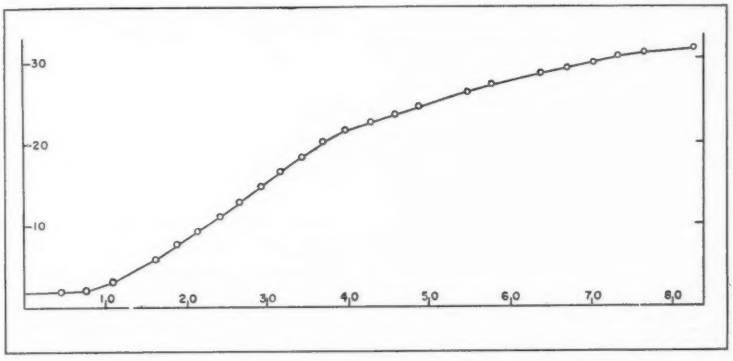

FIGURE 19.—TYPICAL SLOPE PROFILE DEVELOPED ON CHADRON FORMATION
Scale in feet

the rate of removal of debris. The almost constant angle assumed by slopes in a given area is directly related to conditions within the area. This is substantiated to a certain degree by the steeper angle maintained by that slope developed beneath the grass-capped piedmont surface (Table 7, *B*) and by the differences between the Chadron haystack topography and the Chadron slopes where overlain by the more resistant Brule formation (Table 7, *D*, *F*).

Relation of Slope Angle to Slope Length

Additional statistical data were obtained in areas underlain by the nodular clays of the lower Brule formation (Table 2, Orella member), in which small-scale pediment surfaces are present at the base of the retreating badlands escarpment. The writer measured and plotted escarpment angles and escarpment-slope lengths, from pediment to crest, at 134 points along the pediment–escarpment junction (Fig. 20). The points form a broad scatter with an ascending slope, suggesting a simple linear relationship between slope length and slope angle; slope length increases with slope angle.

The coefficient of correlation, r, is 0.485. The correlation coefficient indicates the relationship between the two variables in simple linear correlation, independent of the units or terms in which they were originally expressed, and if there is no relationship between the variables

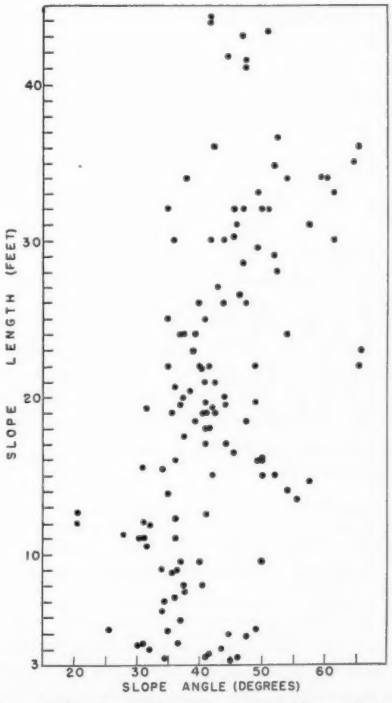

FIGURE 20.—SLOPE LENGTH–SLOPE ANGLE GRAPH
Correlation coefficient, 0.485.

seemed large enough to indicate some relation between escarpment-slope length and escarpment-slope angle but is not a high enough value to rule out the possibility of a chance relationship in the particular samples at hand.

cutting along the margins of sheet wash spreading fanwise at the mouth of each rill (Fig. 21).

In the Badlands area stream gradients, pediment surfaces, and retreating badlands escarpments are adjusted to runoff discharge and

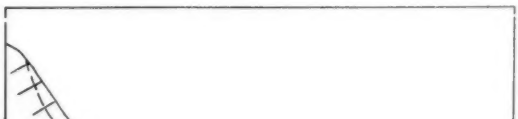

FIGURE 21.—SKETCH DIAGRAM OF RELATIONSHIP OF BADLANDS ESCARPMENT TO PEDIMENT SURFACE AT RILL-CHANNEL MOUTH

(1) Graded slope of sheet-wash transport. (2) Slope representing equilibrium (steady state) between rapid downwear by rill and sheet wash plus mass movements, and rapid steepening induced by backwearing at foot of scarp. (3) Point of undercutting where escarpment is undermined and flowage or sliding is instigated.

The significance of the correlation was then tested by means of the t test, which determines whether or not the observed correlation coefficient is significantly greater than zero (Croxton and Cowden, 1946, p. 682). The equation used is:

$$t = \frac{r\sqrt{N-2}}{\sqrt{1-r^2}}$$

in which N is the number of variates. This yields a value of 6.37 for t with an associated probability of less than .001, which means that there is less than 1 chance in 1000 that the correlation coefficient, 0.485, could be due to chance alone, if based on a sample drawn from a population having zero correlation. The writer concludes, therefore, that slope angles increase with increasing slope lengths.

Conclusions

Field observations justify three conclusions: (1) badland pediments are graded slopes adjusted to permit transportation of debris by sheet wash across the surface with minimum slope; (2) badland escarpments are steep, rapidly retreating slopes reduced by the action of sheet wash and rill wash combined with creep, flowage, or sliding movements; (3) pediments are extended upgrade by backamount of debris supplied. Rapid removal of debris from the slope base does not produce talus accumulations nor do slopes reduce to low angles by long-continued creep or slow flowage. This is directly due to the weathering characteristics of the underlying formations, the material of which disintegrates into pieces small enough to be removed by rill wash. The theory applies to the Brule formation and to the Chadron, except that Chadron formation slopes adjust rapidly by flowage when saturated and would be lower. The theory would apply as well to the dense ash beds of the upper part of the Brule formation, which stand as vertical cliffs, because where strength of material is greater a steeper slope is needed to bring about the necessary wasting of the slope.

The steep escarpment slope represents an equilibrium between the intensity of downwearing by sheet- and rill wash and mass movements, which tend to reduce the slope to lower angles, and backwearing at the scarp base, which tends to develop a steeper slope.

A long escarpment slope produces a heavy discharge of the rills at the foot of the scarp; hence the backcutting by spreading water sheets is strong, and the escarpment will steepen rapidly and maintain a greater average steepness. With a short escarpment there will be less backcutting. Consequently erosion on the steep escarpment will continue until a new equilibrium is in operation.

If an increase in slope length is associated with an increase in slope angle—then in a badlands area the steepest angles of slope would be developed in the mature stage of dissection of the landmass. After the mature stage of development is attained, the streams grade and reduce vertical erosion of their valleys; rapid downcutting at the slope base is replaced by backcutting at the inner edge of pediments which form on both sides of the main graded streams. Once the flat interstream divide areas have been consumed, the escarpment slopes shorten and become progressively lower. A lowering of the divide results in reduction of the escarpment angle.

The statistical data have revealed significant correlations and differences in means which must then be explained by geomorphic conditions. Data presented in this paper can all be related by general theory to existing conditions within a local area in which controlling factors are readily apparent in the field.

Within the White River Badlands differences in topography merely observed and recorded descriptively provide no means of stating the magnitude of the quantities or of the differences between areas. Statistical analysis offers a means of quantitative expression as well as a means of ascertaining that the observed differences could not be due to chance alone. Once this has been demonstrated, the geomorphologist must determine the causative factors from field evidence. The method of analysis is not an end in itself, but may be used to strengthen ideas and hypotheses which contribute an understanding to the dynamics of geomorphic processes.

References Cited

Blackwelder, Eliot, 1931, Desert plains: Jour. Geology, v. 39, p. 133–140

Bradley, W. H., 1940, Pediments and pedestals in miniature: Jour. Geomorphology, v. 3, p. 244–254.

Bryan, Kirk, 1922, Erosion and sedimentation in the Papago country, Arizona: U. S. Geol. Survey Bull. 730-B, p. 19–90

——1936, Processes of formation of pediments at Granite Gap, New Mexico: Zeitschr. Geomorphologie, Band 9, Heft 4, p. 125–135

Bump, James D., 1951, The White River Badlands of South Dakota: Soc. Vert. Paleontologists Field Conf. in Western South Dakota, Aug. 29, Sept. 1, 1951, Guide Book, p. 35–46

Clark, John, 1937, The stratigraphy and paleontology of the Chadron formation in the Big Badlands of South Dakota: Carnegie Mus. Annals, v. 25, art. 21, p. 261–350

Croxton, F. E., and Cowden, D. J., 1946, Applied general statistics: New York, Prentice-Hall, Inc., 944 p.

Darton, N. H., 1921, Badlands of South Dakota and Nebraska: Geol. Charakterbilder (K. Andree), Heft 25, Berlin, 7 p.

Davis, W. M., 1930, Rock floors in arid and humid climates: Jour. Geology, v. 38, p. 1–27, 136–157

Dixon, W. J., and Massey, F. J. Jr., 1951, Introduction to statistical analysis, New York, McGraw Hill Book Co., 370 p.

Gilbert, G. K., 1877, Report on the geology of the Henry Mountains (Utah): U. S. Geol. Survey of the Rocky Mountain Region (Powell), 160 p.

Gilluly, James, 1937, Physiography of the Ajo region, Arizona: Geol. Soc. America Bull. v. 48, p. 323–347

Horton, R. E., 1945, Erosional development of streams and their drainage basins: Hydrophysical approach to quantitative morphology: Geol. Soc. America Bull., v. 56, p. 275–370

Howard, A. D., 1942, Pediment passes and the pediment problem: Jour. Geomorphology, v. 5, p. 1–31, 95–136

Johnson, Douglas, 1931, Planes of lateral corrasion: Science, n. ser., v. 73, p. 174–177

——1932a, Rock fans of arid regions: Am. Jour. Sci., 5th ser., v. 23, p. 389–416

——1932b, Rock planes of arid regions: Geog. Review, v. 22, p. 656–665

——1932c, Miniature rock fans and pediments: Science, n. ser., v. 76, p. 546

Lawson, A. C., 1915, The epigene profiles of the desert: Univ. Calif. Bull. 9, p. 25–48

McGee, W J, 1897, Sheetflood erosion: Geol. Soc. America Bull., v. 8, p. 87–112

Miller, Victor C., 1950, Pediments and pediment-forming processes near House Rock, Arizona: Jour. Geology, v. 58, p. 634–645

Ogilvie, Ida H., 1905, The high-altitude conoplain: Am. Geologist, v. 36, p. 27–34.

Paige, Sidney, 1912, Rock-cut surfaces in the desert ranges: Jour. Geology, v. 20, p. 442–450

Rich, John L., 1935, Origin and evolution of rock fans and pediments: Geol. Soc. America Bull., v. 46, p. 999–1024

Rothrock, E. P., 1943, A geology of South Dakota. Part I: The surface: S. D. Geol. Survey Bull. 13, 88 p.

Smith, Kenneth G., 1950, Standards for grading texture of erosional topography: Am. Jour. Sci., v. 248, p. 655–668

Strahler, Arthur N., 1950, Equilibrium theory of erosional slopes approached by frequency distribution analysis: Am. Jour. Sci., v. 248, p. 673–696

Tolman, C. F., 1909, Erosion and deposition in southern Arizona bolson region: Jour. Geology, v. 17, p. 136–163

Van Houten, Franklyn B., 1953, Clay minerals in sedimentary rocks and derived soils: Jm. Jour. Sci., v. 251, p. 61–82

Von Engeln, C. D., 1942, Geomorphology, New York, The Macmillan Company, 655 p.

Ward, Freeman, 1922, The geology of a portion of the Badlands: S. D. Geol. and Nat. Hist. Survey, Circ. 8 (S.D. Univ. Bull., Ser. 21, no. 7), 80 p.

Continental Oil Co., Durango, Colo.

Manuscript Received by the Secretary of the Society, May 27, 1953

BULLETIN OF THE GEOLOGICAL SOCIETY OF AMERICA
VOLUME 69, PP. 1009–1032, 10 FIGS. AUGUST 1958

RADIOCARBON CHRONOLOGY OF LAKE LAHONTAN AND LAKE BONNEVILLE

BY WALLACE S. BROECKER AND PHIL C. ORR

ABSTRACT

Radiocarbon measurements on fresh-water carbonates have been used to determine the absolute chronology of the two largest fossil lakes in the Great Basin. The possibility of systematic errors due to exchange and to low initial C^{14} concentration has been considered with the conclusion that most of the measurements reported have not been affected by more than 10 per cent.

The results of the study suggest a high-water period from 25,000 to about 14,000 years ago. This period was preceded by an interval of moderately low water level extending back to at least 34,000 years before present. Following a recession to a moderately low water level close to 13,000 years ago Lake Lahontan and possibly Lake Bonneville rose to their maximum levels close to 11,700 years ago. This rapid rise was followed by an equally rapid fall close to 11,000 years ago. This latter decline is recorded by terrestrial deposits in many of the wave-cut caves on the shore lines of the ancient lakes. There is some evidence for another maximum close to 10,000 years ago. The lakes have probably remained low since 9000 years ago.

Consideration of the factors influencing the response of the lakes to climate change suggests that response is sufficiently rapid that the lake levels can be used as direct estimates of the relative climates. The lake-level chronology is hence a climate chronology for the Great Basin.

CONTENTS

TEXT

	Page
Introduction	1010
General statement	1010
Acknowledgments	1011
Nature of samples	1011
Uncertainties in the radiocarbon ages	1011
Composite samples	1011
Initial C^{14}/C^{12} ratio	1011
Postdepositional exchange	1012
Internal consistency	1015
Radiocarbon results	1015
General	1015
Samples from lake sediments	1018
Samples from terrace deposits	1021
Samples from cave deposits	1024
Discussion	1027
Chronology	1027
Relation of lake level to climate	1029
Conclusions	1031
References cited	1032

ILLUSTRATIONS

Figure	Page
1. Map of Great Basin with outline of lakes Bonneville and Lahontan	1010
2. Concentration as a function of depth in an infinite slab for various degrees of penetration of a material diffusing in from the surface	1015
3. Map showing sample locations in the Lahontan area	1018
4. Map showing sample locations in the Bonneville area	1019
5. Lake-sediment sections	1020
6. Idealized section of Lahontan shore line	1022
7. Section of a concentric tufa dome located in the Needles area on Pyramid Lake	1022
8. Diagram showing the evolution of Fishbone Cave	1025
9. Height of lakes Lahontan and Bonneville as a function of time based on radiocarbon data	1028
10. Conditions under which Lake Lahontan could be maintained at its highest level	1030

TABLES

Table	Page
1. Measurements of contemporary materials from the Lahontan area	1012
2. Estimates of contamination due to exchange with atmospheric CO_2	1013
3. Radiocarbon dates on Great Basin samples	1016
4 Comparison of the heights of the main Lahontan and Bonneville terraces	1023

Introduction

General Statement

Since the explorations of the Great Basin by Fremont in 1842 geologists have been interested in the history of the numerous dry and near-dry lakes of this region. To even the casual observer it is obvious that the level of these lakes was once far higher than at present. The problem has been to determine when these high levels occurred and how the climatic changes they signify correlate with the general pattern of world-wide events in the late Quaternary. Although most geologists believe that the times of higher lake level correspond to times of glaciation, the sequence of high stands and their correlation with individual glacial periods has proven difficult to determine without some absolute dating technique. Radiocarbon dating provides a solution to this problem, and the primary aim of this work is, therefore, to establish by radiocarbon dating a chronology for lake-level fluctuations that might be precisely correlated with other events in the late Pleistocene and Recent periods.

The two lakes chosen for this study were Lahontan and Bonneville, which are now represented by their far smaller remnants such as Pyramid Lake in Nevada and Great Salt Lake in Utah. The outline of these lakes is given on the map of the Great Basin (Fig. 1). This choice was made partly because they are the largest and hence most representative of the so-called "pluvial lakes" and partly because extensive studies of their deposits have been made. The importance of the early surveys conducted by Russell (1885) in the Lahontan area and Gilbert (1890) in the Bonneville area cannot be overemphasized. Their work supplied maps of the area, elevations of the main terraces, and descriptions of the significant deposits and provided the relative chronologies that have been the starting points for all subsequent investigations. The authors are

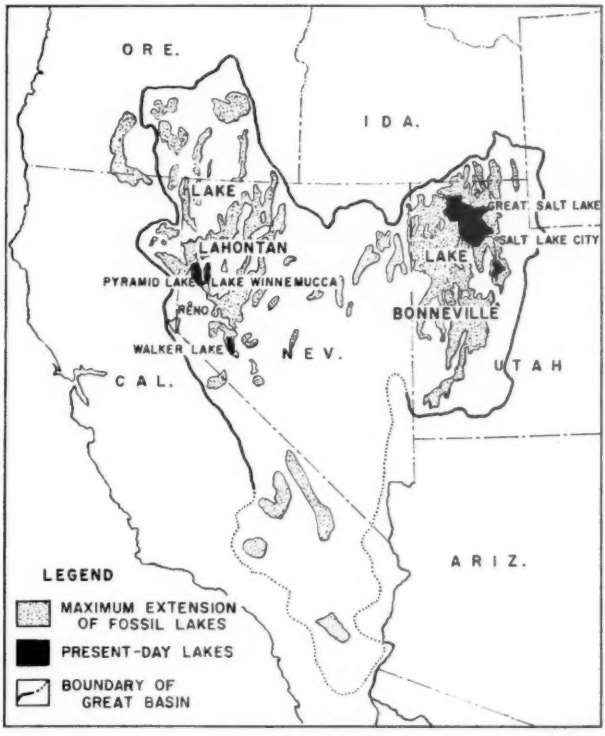

FIGURE 1.—MAP OF GREAT BASIN WITH OUTLINE OF LAKES BONNEVILLE AND LAHONTAN

actively continuing their research, and this paper should be considered a preliminary report.

Acknowledgments

The investigations of the history of Lake Lahontan reported in this paper began with the discovery of the Winnemucca Caves by G. E. Rollins. Field work in the area was supported by funds provided by the Max C. Fleischman Foundation of Nevada and O. H. Truman, President of the Western Speleological Institute. The authors express their appreciation to the following for their active interest in the program: J. W. Calhoun of the Nevada State Museum; Julius Bergen and S. S. Wheeler of the Fleischman Foundation; A. S. Coggeshall and Harold S. Chase of the Santa Barbara Museum of Natural History; Thomas Trelease of the Nevada Fish and Game Commission; Louise G. Reed of the Western Speleological Institute.

A. J. Eardley of the University of Utah and O. A. Schaeffer and Raymond Davis, Jr., of the Brookhaven Laboratories aided the authors in obtaining samples in the Bonneville region.

Bench marks established in critical areas by the U. S. Geological Survey allowed instrument surveys of sample elevations to be made.

The radiocarbon measurements were made at the Lamont Observatory. The authors would like to express their thanks to C. S. Tucek, James Hubbard, and Marylou Zickl for their assistance in this part of the work. A large part of the financial support for these measurements was provided by the National Science Foundation.

Nature of Samples

Most of the samples measured in this study were fresh-water carbonates. These include shell, marl, and fine-grained lithified carbonates, or tufas. Tufa consists of relatively pure $CaCO_3$ in many forms, from massive or coralline in structure to prismatic crystals of fine-grained calcite. It is found as thick coatings on the rock outcrops of wave-cut terraces, as grotesque castles extending up to 300 feet above ground surface, as speliothems inside the caves, and as pure carbonate lenses or conglomerate cement in sequences of sedimentary deposits.

Geologists agree that these carbonate masses were deposited from the lake waters, but there have been two conflicting opinions as to the processes involved. Early workers (Russell, 1885; Gilbert, 1890) considered tufa deposits to be the result of inorganic precipitation primarily from the evaporation of wave spray. Jones (1925, p. 6–13) pointed out that tufa forming today in both Pyramid Lake and the Salton Sea is covered with blue-green algae, and his suggestion that the precipitation is organic is generally accepted at present. The presence of algae remains within ancient tufas, as determined by the examination of acid residues (Flowers, 1956, personal communication), lends support to this hypothesis.

Whereas this mode of origin fits the coralline and massive tufa forms, it is less acceptable for the thinolite variety. Dana (*in* Russell, 1885, p. 214) suggested that this form is a pseudomorph after some pre-existing salt but could not identify its predecessor. Jones (1925, p. 24) claims, however, to have precipitated minute crystals with the form of thinolite prisms from Pyramid Lake water saturated with $CaCO_3$. Another possibility is the recrystallization of pre-existing carbonates. This mode of origin is suggested by the occurrence of thinolite crystals in the inner layers of large carbonate mushrooms and spherical masses.

Uncertainties in the Radiocarbon Ages

Composite Samples

Several uncertainties arise in converting the measured C^{14} concentration in fresh-water carbonate materials into absolute ages. One of these is the possibility that the sample measured consisted of two generations of tufa. In this case the age obtained from the C^{14} data would lie between the true ages of the two component parts. Since, in cases where these ages differ by more than 1000 years the use of the composite age could lead to false conclusions, care has been taken in selecting homogeneous samples for measurement. In most localities where sampling was done only one generation was present. Where more than one was present the boundaries were apparent, and a separation was made. Although tufa of only one age was present in most of the samples measured the possibility of error due to composite samples must not be overlooked.

Initial C^{14}/C^{12} Ratio

A fundamental problem in all C^{14} age work is the estimation of the C^{14}/C^{12} ratio for a material at the time of its formation. This

problem is more acute with fresh-water carbonates than with terrestrial organic materials or marine shells. In the latter cases the materials receive their carbon from the large rather well-mixed reservoirs of the atmosphere and the surface ocean, so that measurement of wood or oceanic shell in one area allows an estimate of the modern value in other areas which is accurate to at least 3 per cent. In the case of lakes, however, each body must be considered separately. The C^{14}/C^{12} ratio for a given lake is dependent on the C^{14}/C^{12} ratio of the dissolved carbonate in the river waters supplying the lake and the ratio of the flushing rate of the lake to the rate of exchange between the CO_2 in the atmosphere and the carbonate in the water. Since these factors vary from lake to lake, carbonates from different lakes may be expected to range widely in C^{14} concentration. Measurements available to date (Deevey, 1954, p. 286) range down to a value 20 per cent below that in atmospheric CO_2.

An estimate of the initial C^{14}/C^{12} ratio in ancient samples can be made by measuring the C^{14}/C^{12} ratios in currently forming materials from a similar environment. Measurements on currently forming tufa from Pyramid Lake give a ratio (normalized for C^{13}/C^{12} differences) 5 per cent lower than in wood grown on the shores of the lake. The measurements on which this value is based are summarized in Table 1. For simplicity of presentation the contemporary modern values are normalized to the same C^{13}/C^{12} ratio. The tufa measured formed during the past 40 years.

Lake Lahontan was much larger during deposition of many of the samples studied. Possibly the conditions that caused these high lake levels also affected the C^{14}/C^{12} ratio in the lake waters. Because of the large number of unknowns it is difficult to estimate the magnitude of such effects. An attempt is currently being made to obtain quantitative estimates of the possible variations.

TABLE 1.—MEASUREMENTS OF CONTEMPORARY MATERIALS FROM THE LAHONTAN AREA

		C^{14}/C^{12}*	C^{13}/C^{12}*	C^{14}/C^{12}*†
L 288-M	Sage wood (Winnemucca Cave area)	0.0	0.00	0.0
L 288-C	Recently formed carbonate (base of pyramid, Pyramid Lake)	−1.0±0.8	+1.85	−4.7±0.8
L 288-I	Living algae (Pyramid Lake)	−8.0±2.0	∼ +0.20	−8.4±2.0

* Per cent difference from Lahontan wood (L 288-M).
† Normalized to a common C^{13}/C^{12} ratio.

Pending the results of these studies the ages of carbonate materials deposited from the waters of Lake Bonneville and Lake Lahontan were calculated using the values obtained on current materials from Pyramid Lake. This corresponds to a value about 1 per cent lower than modern wood uncorrected for C^{13}/C^{12} ratio differences and 6 per cent lower than the normalized modern wood value. If, as is probably the case, the variation did not exceed 5 per cent the age uncertainty introduced is less than 400 years. In no case can the error be more than 500 years on the positive side, since this would represent static equilibrium with the atmosphere. The addition of 500 years to the ages quoted hence provides a maximum age as far as the initial C^{14}/C^{12} ratio is concerned.

Postdepositional Exchange

Another possible source of error in ages based on the C^{14} content of carbonates is exchange of the carbon atoms in the sample with those in the surroundings subsequent to the formation of the material. Since most of the samples studied were exposed to the atmosphere continuously over the past 10,000 years, one possible avenue for exchange is transfer of C^{14} from the CO_2 molecules in the atmosphere to the carbonate ions of the $CaCO_3$. Such a transfer probably involves two steps. The first step is the replacement of the CO_2 in a $CO_3^{=}$ ion on the surface of a crystal by a CO_2 molecule from the atmosphere during a collision. The

second step is the diffusion of these carbonate ions from the surface into the crystal.

One of two possible approaches could determine the extent of such exchange: (1) calculate the amount of exchange expected using the bonate, the interatomic distances in $CaCO_3$, and the C^{14}/C^{12} ratio in the atmosphere allows the former to be computed. Using empirical surface-area data obtained by the gas-adsorption method used by Kulp and Carr (1952), an

TABLE 2.—ESTIMATES OF CONTAMINATION WITH ATMOSPHERIC CO_2

Description	Locality	Surface area (m^2/gm)	First* fraction $\times 10^3$	Last* fraction $\times 10^3$	Measured† contamination $\times 10^3$	Predicted† contamination (Surface exchange) $\times 10^3$	Predicted† contamination (Diffusion) $\times 10^3$	Predicted† contamination (Total) $\times 10^3$
1-inch-thick layer of massive tufa	Within 50 feet of the Lahontan Beach level in the cave area of Lake Winnemucca	~0.5	305 ± 10 (9550 ± 250)** (11 per cent)††	308 ± 10 (9450 ± 250)** (9 per cent)††	−0.3 ± 1.4	0.15	0.01	0.16
Massive intermediate layer in an 8-inch thick tufa mass	100 feet above Crypt Cave on top of large granite outcrop	.075	224 ± 10 (12,000 ± 300)** (9 per cent)††	198 ± 10 (13,000 ± 400)** (19 per cent)††	2.3 ± 1.3	0.02	0.0012	0.02
4-inch-thick layer of porous tufa	Coating on outcropping limestone on the broad Provo terrace at the north end of the Oquirrh Mountains	7.5	334 ± 10 (8800 ± 200)** (12 per cent)††	265 ± 15 (10,700 ± 400)** (12 per cent)††	8.3 ± 2.1	7.5	0.12	7.6

* C^{14}/C^{12} sample: C^{14}/C^{12} atmospheric CO_2.

† $C^{14'}/C^{12}$ sample: C^{14}/C^{12} atmospheric CO_2 where $C^{14'}$ represents the amount of C^{14} in a bulk sample due to post-depositional contamination.

** "Apparent age" of sample from its C^{14}/C^{12} ratio.

†† Size of fraction in the per cent of total sample.

available diffusion coefficients and empirical surface-area data, or (2) examine natural carbonates directly for the effects of exchange. Both approaches have been attempted in the course of this study.

If it is assumed that the rate of exchange between the surface carbonate molecules and the CO_2 in the atmosphere is rapid, an estimate of the maximum amount of contamination can be made without extreme mathematical difficulty. In this case the surface carbonate molecules would at all times have a C^{14}/C^{12} ratio close to that in the CO_2 in the atmosphere. The calculation then becomes a matter of computing the contamination due to this surface layer and adding to it the net contribution of C^{14} due to transfer by diffusion from the surface to the interior layers of the crystal.

Knowledge of the surface area of the carbonate, the interatomic distances in $CaCO_3$, and the C^{14}/C^{12} ratio in the atmosphere allows the former to be computed. Using empirical surface-area data obtained by the gas-adsorption method used by Kulp and Carr (1952), an average CO_3 spacing of 4.0 Å, and a specific C^{14} activity of 160 disintegrations per mole for atmospheric CO_2, estimates of the contribution of surface contamination have been made for three tufa samples. The results (Table 2, column 7) are expressed as the ratio of the concentration of surface contaminant $C^{14}O_3^=$ ions in a homogenized sample to the $C^{14}O_2$ concentration in atmospheric CO_2. Even in the case of sample L-363D which is unusually porous (hence high in surface area) the age error for a measurement made on bulk material would be only about 300 years. For a sample of similar surface area 20,000 years in age the error due to surface contamination would be about 700 years. As will be shown below the sample can be pretreated so that this error is eliminated. Even if this were not done such errors are negligible for most applications and

become important only for samples greater than 25,000 years in age or where extremely high precision is necessary.

The contribution due to diffusion can be estimated as follows. The fact that none of the tufas under consideration have bulk C^{14} concentrations of more than 30 per cent of the C^{14} concentration in the atmospheric CO_2 allows the problem to be adequately approximated as that of diffusion into a semi-infinite solid. The surface layer of this solid can be considered to have a constant C^{14} concentration equal to that in atmospheric CO_2. Taking into account the radioactive decay of the diffusing substance the differential equation for such a process is:

$$\frac{\partial C}{\partial t} = D\frac{\partial^2 C}{\partial x^2} - \lambda C$$

where C is the concentration of the radioactive species, D the diffusion coefficient, and λ the decay constant of the radioactive species.

Following Crank (1956, p. 124–131) the solution of this equation (for times greater than two half lives of C^{14}, *i.e.*, 11,000 years) expressed as the average concentration of diffused C^{14} ($\overline{C}$) in a homogenized sample is closely approximated by

$$\overline{C} = S\sqrt{\frac{D}{\lambda}}(1 - e^{-\lambda t})C_O$$

where S is the surface area, and C_O is the C^{14} concentration in the surface layer and hence the atmosphere.

The room-temperature diffusion constant D can be obtained by extrapolation of high-temperature data through the use of the Arrhenius equation:

$$D = D_O e^{-\Delta H_{act}/RT}$$

Haul *et al.* (1953, p. 619) carried out diffusion experiments at 600°C. and 800°C. on calcite crystals of known surface area using CO_2 enriched in C^{13}. From their data they computed values for the two constants, D_O and ΔH_{act}, and obtained values of 1.81×10^{-10} cm²/sec. and 27,700 cal./mole respectively. The room-temperature value for D would then be 1.8×10^{-30} cm²/sec.

Using this value of D, the empirical surface areas mentioned above and the specific activity of atmospheric CO_2 estimates of the contamination levels are given for three tufa samples in column 8 of Table 2. The results are expressed in the same way as those for surface contamination. The term containing t is a second-order correction; hence the order of magnitude of the results is independent of the age assigned. Thus the amount of contamination due to diffusion should be negligible for all applications.

In order to check these predictions three samples of tufa were examined for contamination. Such checks are feasible, since the C^{14} added by surface exchange and diffusion is concentrated close to the surface of the crystals. Whereas this is the case by definition for surface exchange, it is not so obvious in the case of diffusion. To make this clear, the distribution of diffused contamination as a function of depth below the surface layer has been calculated as a function of time for a slab. As shown in Figure 2 the concentration falls off very rapidly with depth. The curves represent the distribution for progressively longer periods of time. This figure indicates that for exchange in the range of 5 to 50 per cent there should be a pronounced difference in the C^{14}/C^{12} ratio in the outer 10 per cent or surface material from that of the inner 10 per cent or core material. For exchange amounting to less than 20 per cent the inner 10 per cent is unaffected.

The experimental problem is to devise a method by which the surface material and the inner material can be separated. Since mechanical separation is not possible, two other methods were considered: acid leaching and thermal decomposition. The two methods were tested by determining their respective efficiencies of separation for tufas which had been purposely contaminated by placing them in an enriched $C^{14}O_2$ atmosphere at elevated temperatures. Although both methods gave good results, thermal decomposition was superior. More than 95 per cent of the contamination was removed with the first few per cent of the CO_2 released (at 700°C.).

Three samples were checked by this method. The C^{14}/C^{12} ratio in the first 10 per cent of the CO_2 released was compared in each case with that of the last 10 per cent, on the assumption that more than 95 per cent of the C^{14} introduced by surface exchange should be in the first fraction and almost none in the last. Since the concentration of primary C^{14} (that present at the time of deposition) should be the same in each of the two fractions the difference between them can be attributed to contamination. The results are shown in Table 2. For each fraction the ratio of the C^{14} concentration in the sample to that in atmospheric CO_2 is given (columns 4 and 5). The apparent ages calculated from these

ratios are also given. From these results the amount of contamination in a homogeneous or bulk sample can be computed (column 6). If the theoretical predictions are correct this last set of numbers should closely approximate the sum of the values calculated for diffusion and surface exchange (column 9). In each of the three cases the agreement is within the measurement error indicating that the error due to exchange with the atmosphere is (as concluded above) small. The use of "core" material obtained by either thermal decomposition or acid leaching eliminates the problem.

No laboratory experiments have been done to establish the extent of contamination by solution and redeposition in the presence of rain water or ground water. Since the region is and has been rather dry it is hoped that these effects are also small. Further work is needed before any reliable conclusions can be drawn.

From the above considerations it is clear that no evidence has been found that points to any large systematic errors in the C^{14} ages on fresh-water carbonate samples. Although this does not prove that such errors do not exist it makes the probability small.

Internal Consistency

The internal consistency of the ages obtained provides additional evidence for the reliability of the samples. The age obtained on shell material separated from a marl gave the same age as the marl (L-364CR and L-364CS). Organic and inorganic material separated from a core sample (L-376D) taken in Great Salt Lake gave ages of 26,300 ± 1100 and 25,300 ± 1000 respectively. Samples of tufa (L-289D) and shell (L-289P) in Fishbone Cave differed in age by less than 400 years.

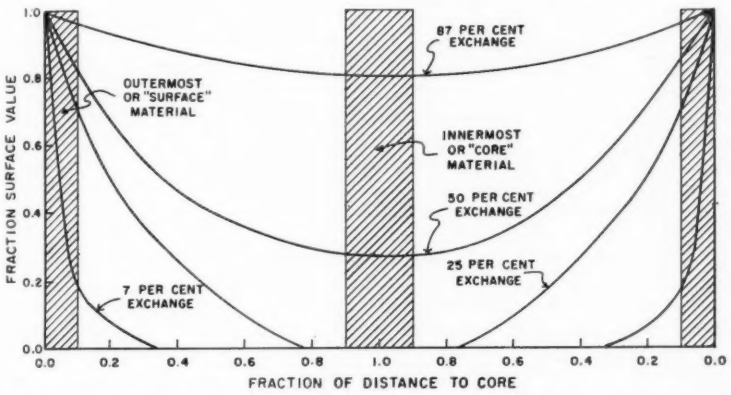

FIGURE 2.—CONCENTRATION AS A FUNCTION OF DEPTH IN AN INFINITE SLAB FOR VARIOUS DEGREES OF PENETRATION OF A MATERIAL DIFFUSING IN FROM THE SURFACE
Ruled areas represent material sampled in laboratory contamination studies

RADIOCARBON RESULTS

General

Age determinations made on samples from the Bonneville and Lahontan areas are listed in Table 3. The modern control value used for carbonate samples is that obtained on recent materials from Pyramid Lake. As mentioned above, this value is 5 per cent below maximum possible or static equilibrium value. The value used for organic materials is based on the average for recently grown woods. Errors quoted include only uncertainties in the laboratory measurements and not those associated with the problems discussed above.

Figures 3 and 4 show the geographical location of the samples. The location of a sample may be determined by noting the number given in parenthesis for each sample in Table 3. These numbers correspond to those on the maps.

The results are most easily discussed by dividing them into three categories: those on materials from lake sediments, those from terrace deposits, and those from wave-cut caves. Such a division will emphasize the correlation between the events in different lake basins.

TABLE 3.—RADIOCARBON DATES ON GREAT BASIN SAMPLES

Location†	Elevation*	Description	Age	Sample number
		LAHONTAN SAMPLES		
Needles (Pyramid Lake) (1)	60	Large oölites	1100±200	L 288-F
Anaho Island (3)	50	Shell from extensive beach	2100±200	L 288-H
Crypt Cave (Winnemucca) (8)	305	Basketry from upper deposits	2400±200	L 289-II
Hidden Cave Fallon area (6)	304	Wood fragments 32 inches below surface	3050±200	L 289-BB
Guano Cave (Winnemucca) (8)	245	Twigs from habitation level 22–28 inches below surface	3200±130	L 356-B
Diaphragm Cave (Pyramid Lake) (2)	10	Shell from lake sediments	3200±250	L 289-R
Fishbone Cave (Winnemucca) (8)	250	"Amberat" from cave ceiling	4150±150	L 364-BI
Cowbone Cave (Winnemucca) (8)	220	Matting associated with a human burial	5970±150	L 289-FF
Fishbone Cave (Winnemucca) (8)	250	Fragments of netting from lowest habitation level	7830±350	L 289-KK
Needles (Pyramid Lake) (1)	90	Outermost layer of tufa mushroom	8500±200	L 364-CE
Above Crypt Cave (Winnemucca) (8)	525	Lithoid tufa	9700±200	L 289-G
Above Crypt Cave (Winnemucca) (8)	411	Lithoid tufa	9700±200	L 356-H
Lahontan Beach (Winnemucca) (8)	560	Lithoid tufa, highest observed in area	9500±200	L 364-AA
Above Crypt Cave (8)	525	Lithoid tufa (duplicate of L 289-G)	10,000±220	L 356-G
Fishbone Cave (Winnemucca) (8)	250	Juniper roots and bark	11,200±250	L 245
Anaho Island (3)	570	Lithoid tufa	11,800±200	L 289-N
Mullen Pass (4)	560	Lithoid tufa	11,250±350	L 289-I
Anaho Island (3)	520	Lithoid tufa	11,700±200	L 289-M
Anaho Island (3)	390	Lithoid tufa	11,570±250	L 289-L
Entrance Fishbone Cave (Winnemucca) (8)	250	Lithoid tufa	11,700±500	L 289-C
Diaphragm Cave (Pyramid Lake) (2)	10	Multi-layer tufa diaphragm	12,700±300	L 289-H
Truckee River Canyon (5)	202	Radiating material from tufa pavement in lake sediments	12,900±350	L 289-S
Truckee River Canyon (5)	210	Radiating material from tufa pavement in lake sediments	12,700±300	L 364-AM
Truckee River Canyon (5)	210	Mammillary material from base of tufa mushroom	13,700±300	L 364-AN
Above Crypt Cave (Winnemucca) (8)	411	Massive tufa from an intermediate layer in mass 8 inches thick	13,000±400	L 364-DA (2)
Needles (Pyramid Lake) (1)	90	Dendritic tufa from concentric dome	14,500±400	L 364-CI
Fishbone Cave (Winnemucca) (8)	250	Shell from sand below terrestrial deposits	15,130±550	L 289-P

TABLE 3.—CONCLUDED

Fishbone Cave (Winnemucca) (8)	250	Tufa from broken piece of diaphragm	14,800±500	L 289-D
Hidden Cave (Fallon area) (6)	300	Tufa from diaphragm	15,130±400	L 289-AA
Fishbone Cave (Winnemucca) (8)	250	Shells from lake sediments	15,670±700	L 289-O
Anaho Island (3)	~280	Dendritic tufa	16,130±750	L 289-K
Crypt Cave (Winnemucca) (8)	300	Shell from top of lake deposits	18,700±700	L 364-BR
Crypt Cave (Winnemucca) (8)	300	Microscopic shell from lake sediments	19,750±650	L 364-BS
Truckee River Canyon (5)	200	Impure marl from sediments cut by river	17,600±650	L 364-AL
Astor Pass (Pyramid Lake) (7)	~300	Marl deposited at head of valley	16,800±600	L 364-CR
Astor Pass (Pyramid Lake) (7)	~300	Shell from marl deposits	17,500±600	L 364-CS
Anaho Island (3)	170	Thinolite tufa	28,900±1400	L 289-J
Truckee River Canyon (5)	190	Shell from canyon sediments	>34,000	L 364-AK
		BONNEVILLE SAMPLES		
Oquirrh Mountains (North end) (10)	~660	Porous tufa coating outcrop on Provo Terrace	11,000±600	L 363-D
Great Salt Lake (10)	−40	Limy silt and clay from lake bottom core	12,500±250	L 376-C
Oquirrh Mountains (North end) (10)	~330	Tufa coating limestone outcrop on Stansbury Terrace	12,900±180	L 363-C
Oquirrh Mountains (North end) (10)	~330	Massive tufa from gravel sequence associated with Stansbury Terrace	13,200±300	L 363-B
West Mountain area (11)	490	Tufa from intermediate level between Provo and Stansbury Terrace	15,200±400	L 333-C
Oquirrh Mountains (North end) (10)	~660	Massive tufa coating cliff below Provo Terrace	15,530±280	L 363-E
Oquirrh Mountains (North end) (10)	~1000	Fine-grained massive white tufa from the Bonneville level	16,100±350	L 363-G
Reservoir Butte Area (9)	~300	Finely laminated marl from the Old River bed sequence	21,200±450	L 363-J
Reservoir Butte Area (9)	~300	Poorly laminated marl from the Old River bed sequence	23,300±800	L 363-I
Oquirrh Mountains (North end) (10)	~1000	Thin tufa coating boulder near Bonneville level	23,150±1000	L 363-H
West Mountain area (11)	320	Tufa	25,500±1300	L 333-A
Great Salt Lake (10)	−55	Organic fraction; limy silty clay lake bottom core	26,300±1100	L 376-D
Great Salt Lake (10)	−55	Inorganic fraction; limy silty clay from lake bottom core	25,300±1000	L 376-D
West Mountain area (11)	580	Tufa from limestone conglomerate	33,200±4000	L 333-B

* Height in feet above the present level of Pyramid Lake (3800 feet) for the Lahontan samples and above the present level of Great Salt Lake (4200 feet) for the Bonneville samples.

† Numbers in parentheses after the locations indicate the areas from which the samples were taken as shown on the maps (Figs. 3, 4).

Samples from Lake Sediments

Although lake sediments in general do not give information as to the exact position of the water level at specific times in the past, they do indicate the sequence of periods of high and low lake level. Vertical sections of sediments from three of the pluvial lakes in the Great Basin (Fig. 5) show distinct changes in types of sediment. These changes mark the transitions from high- to low-water stages.

The first radiocarbon measurements on such deposits were made by Libby (1955, p. 116–117) on a series of samples submitted by Flint and Gale from a core taken in Searles Lake, California. These samples were from a mud layer between the first and second salt bodies. These salt bodies record successive periods of desiccation, and the intervening mud layer indicates a period of high water level. The results obtained from radiocarbon measurements on organic material extracted from various levels in the mud layer are shown in Figure 5. Their ages range from 10,500 years for a sample from the top of the section to 23,900 years for a sample from the base. The measurement on the latter sample has been rechecked by the Yale University Radiocarbon Laboratory giving an age of 21,200 years (Preston *et al.*, 1955, p. 958).

Even though no core samples are available from the sediments in the Lahontan area, excellent vertical exposures of the lake sediments in river valleys provide stratigraphic data as well as samples suitable for C^{14} dating. An exposure in the canyon of the Truckee River about 5 miles south of the point where it empties into Pyramid Lake proved particularly informative. The sequence of beds is shown in Figure 5.

Somewhat similar sections have been published by Russell (1885, p. 136) and by Antevs (1925, p. 83–85). The section in Figure 5 comes from nearly the same location as Antevs' section 12. The only difference in the section constructed for this paper is the inclusion of the clay layer above the tufa pavement. In many sections poor preservation and a covering of wind-blown sand makes this unit difficult to recognize, but as shown by Russell (1885, p. 143) and observed by the authors it is present.

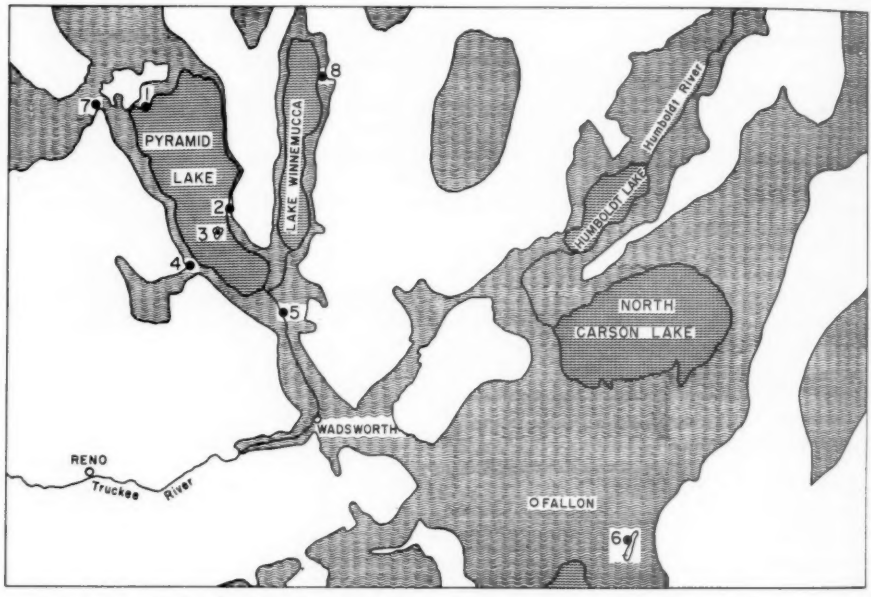

FIGURE 3.—MAP SHOWING SAMPLE LOCATIONS IN THE LAHONTAN AREA

Larger patterned area represents the maximum area covered by the fossil lake and the smaller areas represent the present size of the remnant lakes. The numbers designate areas where sample collections were made.

The three main clay units A, B, and C represent times at which the lake level was more than 200 feet above the present Pyramid Lake level, and the gravel and sand layers represent times at which it was close to or below the 200-foot level. Within the upper clay unit (A) is a layer of tufa 6 inches thick. Two samples (L-364AM, L-289S) of this material were collected from exposures about 1 mile apart. On one sample (L-364AM) two C^{14} measurements were made: one on the radiating material forming the top of the layer and one on the massive mammillary material that forms the base. The ages were respectively 12,700 ± 300 and 13,700 ± 300 years. Only the radiating or upper portion of the tufa was run from the second sample; the age obtained was 12,900 ± 300 years.

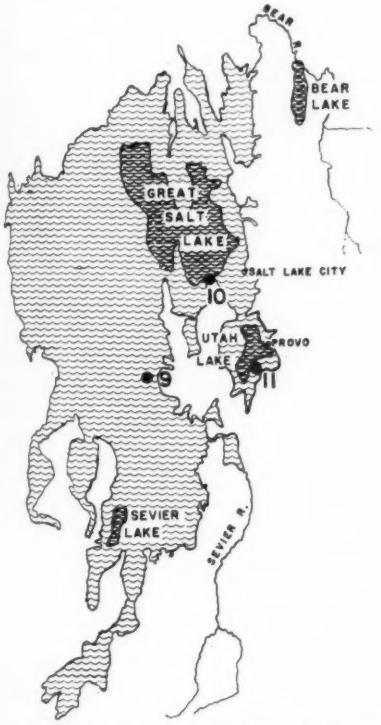

FIGURE 4.—MAP SHOWING SAMPLE LOCATIONS IN THE BONNEVILLE AREA

Larger patterned area represents the maximum area covered by the fossil lake; smaller areas represent the present size of the remnant lakes. Numbers designate areas where sample collections were made.

Four feet below the tufa within the clay layer (A) a sample (L-364AL) was taken from a thin layer of rather impure marl. The age obtained on the bulk carbonate from this material was 17,600 years.

The only other datable material found in the sequence was a layer of shell (L-364AK) from near the base of the sand layer located between clay units A and B. The age of this sample is greater than 34,000 years.

From this sequence it appears that an early extensive high-water stage of unknown age (C) was followed by a rather long low-water stage during which the gravel deposits between units C and B were deposited. Following this the lake again rose to a high level and deposited clay unit B. The base of the overlying sand, which presumably records a low-water interval, lies beyond the range of the measurement sensitivity. The upper clay unit records two high-water stages: one precedes 13,000 B.P., and the other follows 13,000 B.P. These high-water stages are separated by an interval (recorded by the tufa deposition) during which the water level was approximately 200 feet above its present level.

Numerous marl deposits are found in the Lahontan area associated with the so-called "dendritic terrace", which is approximately 300 feet above the present level of Pyramid Lake. These deposits are abundant near the old shore line and are either absent or very impure in areas where the water was deeper. A sample (L-364CR) obtained in the Astor Pass area north of Pyramid Lake had an age of 17,200 years. This result is based on two measurements: one on the bulk carbonate and the other on shells separated from the marl. The results were 16,800 and 17,500 respectively. This age is in good agreement with that on the thin marl layer in the Truckee sequence.

Two sections were sampled in the Bonneville area: one a sequence exposed in the Old River bed and the other that in a core from the bottom of Great Salt Lake. Two measurements were made on the white marl member of the standard sedimentary sequence as defined by Gilbert (1890, p. 190). The sequence as it appears in the Old River bed is shown in Figure 5. Gilbert recognized two high-water stages separated by a period of low water or even perhaps desiccation. The first of these pluvial periods is marked by a rather thick sequence of yellow clay, whereas the second left only white marl deposits. The portion of the section above the white marl consists of sands and gravels

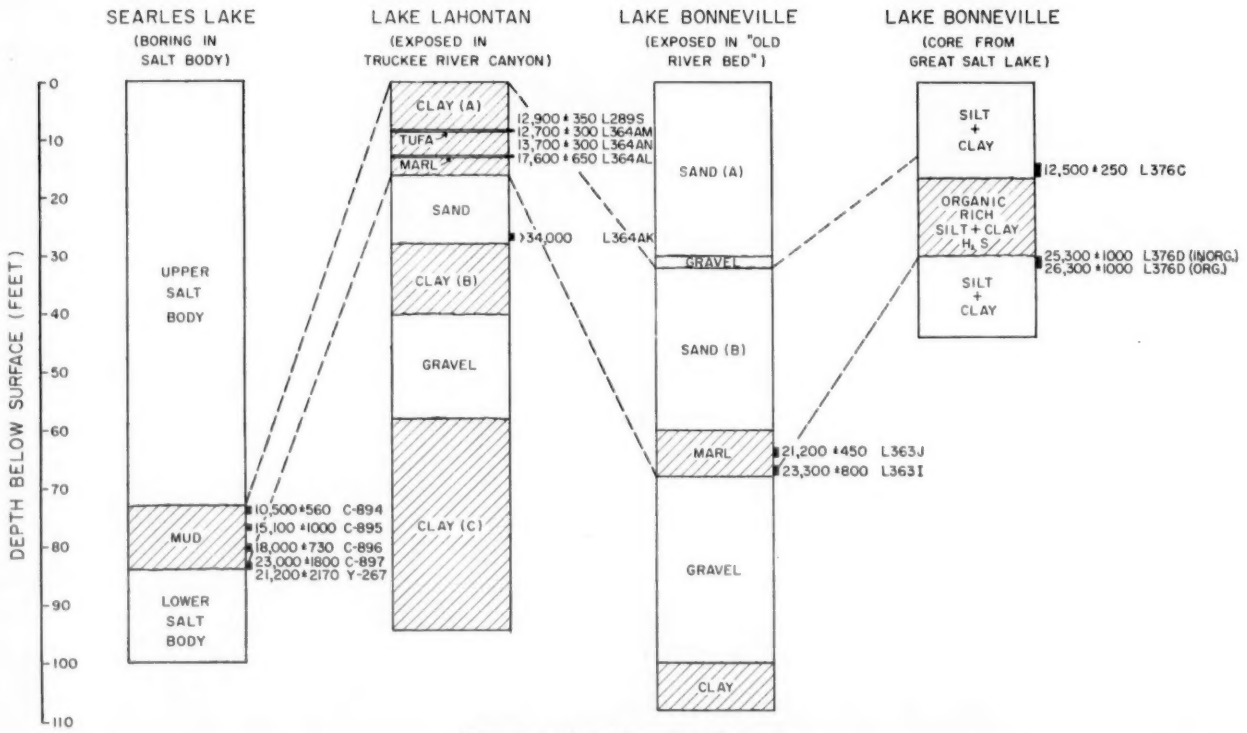

FIGURE 5.—LAKE-SEDIMENT SECTIONS

Correlation lines connect points in the cores corresponding to beginning and end of the last major high-water period for each lake. Age determinations on the Searles Lake core indicated by C were made by the Chicago Laboratory (Libby, 1955); Y indicates determinations made by the Yale Laboratory (Preston *et al.*, 1955).

(Fig. 5). Gilbert interpreted these to be low-water deposits except for the lower sand (B), which he felt marked an intermediate level. The radiocarbon dates (L-363I, L-363J) on the white marl from the Old River bed in the Dugway Proving Grounds area are internally consistent; this indicates that the deposition of this material occurred about 22,000 years ago.

Ives (1951, p. 787) estimated the time interval over which the white marl was deposited by counting varves. His estimate of 6000 years is not unreasonable. Since the two samples dated by C^{14} were from the middle and lower portion of the deposit possibly the deposition occurred between about 24,000 and 18,000 years ago.

The fourth section in Figure 5 is from a core taken near the south end of Great Salt Lake at a depth of about 28 feet. This core has been studied in detail by Schreiber and Eardley who submitted the samples to the authors for analysis. A detailed lithology and discussion can be found in Eardley *et al.*, (1957, p. 1170). The area where the core was taken has probably been covered with water for at least 30,000 years. The material in the 43-foot core consists primarily of silty clay. The section between a depth of 16.5 feet and 29.5 feet differs somewhat, however, in that it is higher in organic material and has a distinct odor of H_2S. Such a deposit is characteristic of stagnant bottom waters. It is possible that this layer was deposited during a period of rising lake level. In such a case precipitation would exceed evaporation, and a stable low salinity surface layer might prevent the renewal of the bottom water. This interpretation differs from that given by Eardley *et al.* (1957, p. 1167). They feel that the sulfide-rich layer records a stand of the lake at the Stansbury level.

If the former explanation is assumed, the two age measurements, one from material immediately above the layer (L-367C) and one from immediately below it (L-367D), suggest that the high-water period began less than 25,500 years ago. The estimate of the beginning is in good agreement with that obtained in the Searles Lake borings. The Bonneville date is exceptionally good, since independent measurement of the organic and the inorganic carbon in the sample gave the same result. The 12,500-year age is not strictly comparable with the Searles Lake dates, since it may establish the date when desiccation began rather than when it was completed.

The data from all three localities are internally consistent in that they indicate a general high-water interval from about 23,000 years to 10,000 years before present preceded and followed by low-water intervals. The only information available as to the time of the beginning of the earlier of these two low-water stages is that it was more than 34,000 years ago.

Samples from Terrace Deposits

A more detailed picture of the lake-level history is revealed by considering the dates obtained on materials associated with lake terraces. Although tufa deposits are abundant in the Lahontan Basin, they cover only a small percentage of the total area. Hence, there are only a limited number of localities where a sequence of tufa ranging from the highest known level to the present water surface can be observed. A summary of the vertical distribution based on such sections observed on Anaho Island and in the Fishbone Cave area of Lake Winnemucca, as well as on Jones' (1925, p. 18–23) observations at Marble Buttes, is given below and in Figure 6. Near the highest recognized lake level (Fig. 6, location 1) patches of lithoid tufa up to 6 inches thick are found in crevices in the rocks and in platelike fragments scattered on the slopes. Below this a more or less continuous layer of lithoid tufa 6–20 inches thick coats the rock outcrops (Fig. 6, location 2). Still lower (Fig. 6, location 3), beginning at about 400 feet above the present lake level, the tufa thickens into rounded or shinglelike growths. In some areas there are two distinct masses (Fig. 6, locations 3 and 4) of this thick tufa separated by a terrace. This type of tufa comes to an abrupt end 30–70 feet above the thinolite terrace. On and below this latter terrace, masses (Fig. 6, location 5) consisting of several layers of thinolite tufa, capped on the outside by dendriticlike tufa, occur in forms ranging from sandwichlike sequences to the grotesque tufa castles for which Pyramid Lake is famous.

Radiocarbon measurements on samples from each of the three major terrace deposits show that they were all deposited during the past 35,000 years.

The radiocarbon dates obtained on materials at or below the thinolite terrace range in age from 30,000 years to the present. If these carbonates were deposited when the water was less than 200 feet above its present level, the dates should establish periods of low lake level. The oldest of these samples is thinolite tufa

Correlation lines connect points in the cores corresponding to beginning and end of the last major high-water period for each lake. Age determinations on the Searles Lake core indicated by C were made by the Chicago Laboratory (Libby, 1955); Y indicates determinations made by the Yale Laboratory (Preston *et al.*, 1955).

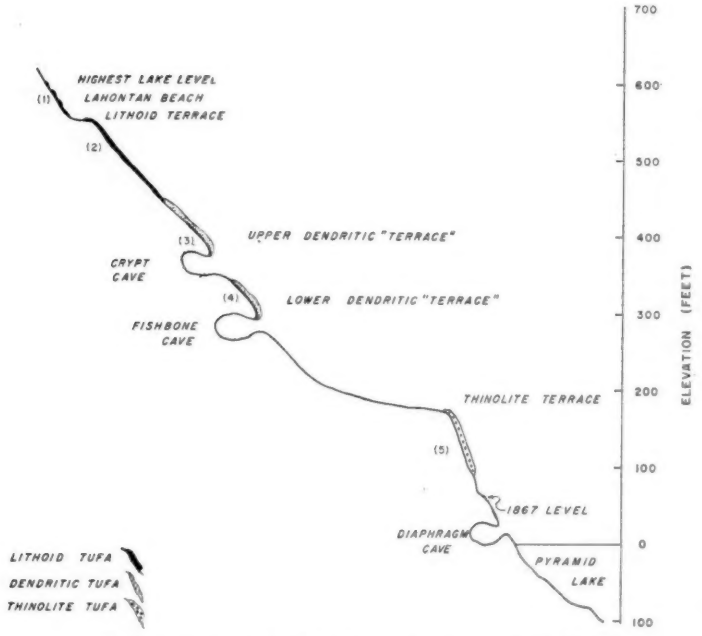

FIGURE 6.—IDEALIZED SECTION OF LAHONTAN SHORE LINE
Present elevation of Pyramid Lake is 3800 feet above sea level

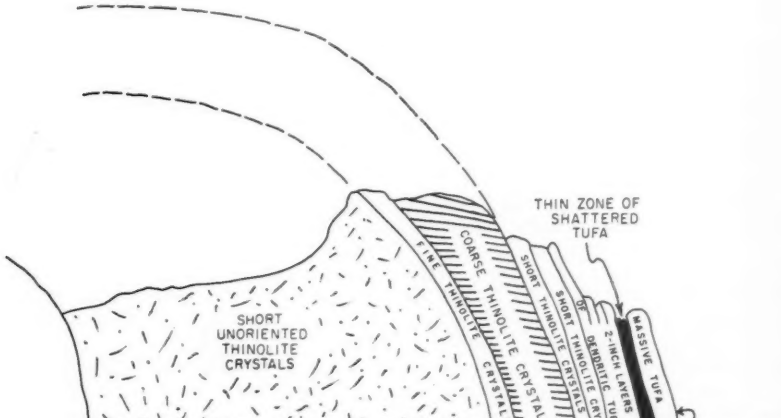

FIGURE 7.—SECTION OF A CONCENTRIC TUFA DOME LOCATED IN THE NEEDLES AREA ON PYRAMID LAKE

from Anaho Island. Its age (assuming no exchange or recrystallization) is close to 29,000 years.

A spherical mass of tufa which formed part of one of the large tufa castles in the Needles area north of Pyramid Lake was sampled from what Russell (1885, p. 190) calls lithoid tufa were obtained on Anaho Island from levels greater than 350 feet above the present lake level. Two of these were from within 100 feet of the highest recognized level of the lake. All the ages obtained were within one sigma of

TABLE 4.—COMPARISON OF HEIGHTS OF THE MAIN LAHONTAN AND BONNEVILLE TERRACES

Lahontan				Bonneville			
Name	Elevation	Height above 1890* lake level (3870 feet)	Fraction of maximum level	Name	Elevation	Height above 1890 lake level (4200 feet)	Fraction of maximum level
Lahontan beach	4400	530	1.00	Bonneville level	5150	950	1.00
Dendritic terrace	4190	320	.61	Provo level	4820	620	.65
Thinolite terrace	3980	110	.22	Stansbury level	4500	300	.32

*The level of Pyramid Lake has fallen 60 feet since 1890 as a result of use of Truckee River water for irrigation.

the surface to the core. The mass consists of concentric layers of a number of varieties of tufa surrounding a core 16 feet in diameter of short unoriented thinolite crystals. Figure 7 shows a cross-section of the mass pointing out the various layers and the ages obtained. To date only two of the samples have been measured; the sample from the outermost layer (L-364CE) has an age of 8500 years, and the sample (L-364CI) from the series of dendritic layers has an age of 14,500 years.

Samples taken from beaches within 100 feet above the present level of Pyramid Lake yielded recent dates. Shells from such a beach on Anaho Island dated 2100 years before present, and large oölites from the Pinnacles area dated 1100 years before present.

Only one sample of dendritic tufa has been measured from the level of the dendritic terrace. Material from about 300 feet above Pyramid Lake on Anaho Island has an age close to 16,000 years.

The ages obtained on samples from the highest level reached by Lake Lahontan indicate that such a level was reached very close to the end of the high-water period. The samples fall into two groups: those close to 11,700 years and those close to 10,000 years.

Three samples (L-289N, L-289M, L-289L) of 11,700 years. A sample (L-289I) from the 600-foot level in the Mullen Pass area on the west side of Pyramid Lake had an age close to 11,300 years.

Samples obtained on the east side of dry Lake Winnemucca, however, have significantly greater C^{14} concentrations and hence presumably lower ages. The ages of four such samples fell within 300 years of 10,000 years before present.

A set of measurements has been made on tufas collected from each of the three main Bonneville terraces: the Bonneville, the Provo, and the Stansbury. Although tufa is much less abundant than in the Lahontan area, deposits are fairly abundant on the latter two terraces and can be found with some difficulty on the highest or Bonneville terrace. The heights of the main terraces are compared with those at Lahontan in Table 4.

The two samples collected from the Bonneville level at the north end of the Oquirrh Mountains differed from all the other tufas measured. One consisted of rather dense, fine-grained, white material which formed the cement between large stream cobbles. The second sample formed a thin white coating of $CaCO_3$ approximately a quarter of an inch thick on a large boulder lodged in the alluvium

just below the Bonneville terrace. Both of these samples differed in that they lacked the distinct structure and color (from staining) typical of other tufa. Whether this difference in appearance represents a difference in origin is not clear.

The ages obtained on these samples were respectively 15,600 and 21,150 years. The latter date substantiates Gilbert's (1890, p. 193) conclusion that the white marl beds were deposited during one of the main periods of occupation of the Bonneville level. This conclusion is based on the correlation of the marl layers in a sediment section in the Lemington area with those in the Old River bed and on the fact that the Lemington marl reaches within 50 feet of the Bonneville level.

Three samples from the Provo level have been measured. One (L-333B) was collected at the authors' request by Dr. H. J. Bissel of Brigham Young University. This sample comes from the West Mountain area and consists of a limestone conglomerate cemented with tufa. Although extreme care was taken to select only pieces of tufa free of limestone fragments, the age of 33,200 obtained may be in error because of contamination with ancient carbonate. Since this measurement is close to the limit of reliable tufa ages perhaps the sample should merely be considered greater than 25,000 years old. Correction for as much as 50 per cent limestone contamination would not lower the age more than this.

The second sample (L-363E) was collected by the authors from the well-formed wave-cut Provo terrace at the northern end of the Oquirrh Mountains. The location was directly below the position on the Bonneville terrace where samples L-363G and L-363H were collected. The material formed a 4-inch coating on the face of a cliff formed by Paleozoic limestones near the Provo terrace level. The age obtained is 15,530 years.

A third sample (L-363D) was obtained from a tufa coating on outcrops projecting through the broad Provo terrace. This sample was located within a few hundred yards of sample L-363E discussed above. The two tufas differed in appearance as well as position with respect to the Provo terrace. Whereas L-363D was from the terrace, L-363E came from slightly below the terrace. Of the two, L-363D had a far more porous structure; L-363E was massive. L-363D was thermally decomposed. The age of the last 10 per cent of the CO_2 to be removed was 10,700 years. Bulk material, run in the same manner as most of the other tufas reported, had an age of 10,400 years. Since there is definite evidence for contamination in this sample, an age of 11,000 $\pm$ 600 has been selected for the best estimate of the true age. This sample provides the only evidence obtained to date for a high water level in the Bonneville region close to the end of the "pluvial" period.

A sample (L-333C) collected by Dr. Bissel in the West Mountain area from about 130 feet below the Provo terrace gave an age of 15,200 years.

Two samples of tufa from the Stansbury level in the Oquirrh Mountains area have been dated. The first (L-363C) formed a coating on Paleozoic limestones exposed on the terrace. Its age is 12,900 years. The second (L-363B) is from a large tufa mass found within a delta just below the Stansbury terrace. Its age is 13,200 years.

Comparison of the terrace data from the two lakes shows evidence in both cases of a stand at the level of the lowest terrace between 25,000 and 30,000 years ago and again close to 13,000 years ago. The evidence for the latter occupation in the Lahontan region does not come only from the terrace deposits but also from the tufa pavement in the Truckee sedimentary sequence mentioned above. The elevation of the tufa pavement in the Truckee sequence is very close to that of the Thinolite terrace. The Provo and Dendritic levels were both occupied between 15,000 and 16,000 years ago.

Whereas there is abundant evidence in the Lahontan region for one or possibly two occupations of this level between 12,000 and 9500 years ago, the only evidence for a high water level in the Bonneville region during this time is the date of 11,000 years for sample L-363D.

Although no tufa deposits have been found in the Lahontan region to indicate that relatively high water levels were occupied during the period 16,000 years ago and the period 23,000 years ago (as suggested by the samples from the Bonneville level), the marl deposits at the dendritic level indicate a relatively high level about 17,000 years ago; as shown below, evidence from cave deposits indicates that between 18,000 and 20,000 years ago the level was above the Dendritic terrace.

Samples from Cave Deposits

Studies on the deposits in wave-cut caves provide much information concerning the fossil levels of these lakes. They contain lacus-

trine deposits that provide estimates of the minimum lake level and terrestrial deposits that provide estimates of the maximum level.

The Lahontan caves can be divided into two groups: those associated with the dendritic tufa masses between 200 and 400 feet above the present lake level and those close to the present level. Although the two groups of caves contain similar deposits, indicating similar evolution, the difference in level requires different ages for many of the geological events suggested by the caves.

Fishbone Cave is a typical example of the upper caves. It is cut in a granite sea cliff on the northeast shore of Lake Winnemucca at an elevation of about 250 feet above Pyramid Lake. It consists of one room roughly 30 feet deep, 30 feet wide, and 5 feet high; the walls and ceiling are covered with large mammillary tufa deposits, and the floor is covered with dust and rat debris. The entrance is a slit 20 feet long located at the base of a large mass of comblike tufa which extends approximately 70 feet above the cave.

Excavation of the floor of the cave revealed a sequence of human and animal occupation debris lying above a thick layer of water-laid silts. A layer of broken plates of tufa and coarse granitic and shell sand separates the occupation layers from the lake deposits.

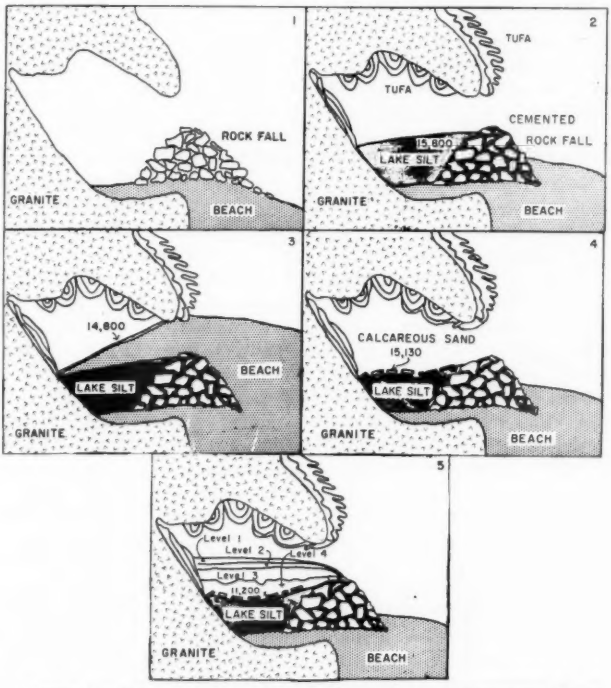

FIGURE 8.—DIAGRAM SHOWING THE EVOLUTION OF FISHBONE CAVE
Levels indicated in block 5 represent divisions of the terrestrial deposits based on archeological studies.

These deposits are behind a barrier of blocks of rock that restrict the cave entrance.

The events that occurred in the evolution of Fishbone Cave are depicted in Figure 8. The cave was cut in granite by wave erosion more than 19,700 years ago (the age of the oldest dated deposit in the caves). Subsequent to cutting, rock falls partially choked the entrance of the cave. With a lake level higher than 250 feet silts were deposited behind the barrier. Shells (L-2890) taken from these silts were dated at 15,670 years.

Continued deposition of silt behind the barrier and perhaps construction of a beach in front of the cave gradually sealed the entrance of the cave and left an isolated void inside. This void was then sealed off from the sediments below by the deposition of a flat layer of tufa on

the surface of the sediments. This "diaphragm" (L-289D) in Fishbone Cave has an age of 14,800 years, and a similar deposit (L-289AA) in Hidden Cave at about the same level but in the Fallon area has an age of 15,130 years. Similar diaphragms have been found in all the caves studied, including the one near the present Pyramid Lake level.

Following the formation of the diaphragm, the lake level dropped and removed a large portion of the supporting sediments in Fishbone Cave, causing the collapse of the diaphragm onto the lake sediments remaining behind the protective barrier. Shells (L-289P) from coarse sand deposited above the broken pieces of diaphragm are 15,130 years old. This date suggests that the time interval between the formation of the diaphragm and its collapse was small. The shells must be younger than the diaphragm, but the time interval between the two events is apparently smaller than the range of error in dating.

An 11,700-year date (L-289C) on tufa from the entrance of the cave indicated that the lake again flooded the cave at this time. Evidence for the events during the period from 15,000 to 12,000 years B.P. was probably removed from the cave by subsequent wave action.

The next event recorded in the cave deposits is the occupation by animals and man (Orr, 1956, p. 6–7). Wood fragments (L-245) from the base of level 4 (just above the broken pieces of diaphragm) are 11,2000 years old. Fragments of netting from higher in the same level were dated at 7830 years B.P.

Above level 4, which consisted of coarse sand, dust, and human debris including a limited amount of perishable artifacts, human bones, and horse and camel bones, a small change in composition and culture occurs. Level 3 contains a greater abundance of perishable material. Horse and camel bones are still present, but juniper and marmot are replaced by sagebrush and jack rabbit bones. From this information it is inferred that the climate became drier and perhaps the lake level lower than during the deposition of level 4.

The upper two levels consist of dust and rat debris; level 2 is compacted, suggesting a more moist climate, and level 1 is loose and typical of the present climate.

Additional information concerning the lake has been obtained from two measurements of material from the sediments of Crypt Cave. This cave is in the same area as Fishbone but at least 70 feet higher. Sediments consisting of microscopic ostracod shell (L-364BS) taken from the base of the lake deposits in the cave are 19,750 years old, and gastropod shell (L-364BR) from sediments near the top of the sequence is 18,700 years old. Since the lake level must have been somewhat above the cave during the deposition of these samples, the dates supply evidence for a near maximum level between 20,000 and 18,000 years ago.

Dates from archeological materials in other caves at the dendritic level add to the post-glacial history of the lakes. Measurements from Cowbone and Crypt caves show human occupation 5900 and 2400 years ago. Dates between 8500 and 1900 years on materials from caves in the Humboldt area (Libby, 1955, p. 118) also show that the lake level has almost certainly not risen to the 300-foot level in recent times.

A study of Diaphragm Cave, one of the group close to the present Pyramid Lake level, adds several significant facts to the picture. A nearly complete diaphragm of tufa divides the cave in half; the sediments on which the diaphragm formed have been removed. Since the diaphragm probably forms soon after the cave is sealed off by sediments, and since these sediments are presumably beach deposits near water level, the 12,700-year age on a piece of the diaphragm (L-289H) may date a low-water stage of the lake.

Remnants of lake silts (L-289R) containing shells and numerous fish scales were dated at 3200 years; they mark a level at least 20 feet above that of the present.

Radiocarbon dates are available for only one cave in the Bonneville region, Danger Cave. This cave is located 50 feet above the present level of Great Salt Lake in the western part of the Bonneville region. Libby (1955, p. 119) dated a number of organic samples from the deposits in the cave. His dates suggest that the water level of Lake Bonneville fell below the cave level about 11,200 years ago. There seems to be little reason to doubt the age: in addition to the duplicate analyses made by Libby, recent rechecks at the Yale Laboratory (Preston *et al.*, 1955, p. 958) give the same results.

This date is extremely important, as are the date of 11,200 years B.P. on the lowermost terrestrial deposits in Fishbone Cave and Libby's (1955, p. 119) age measurement of $11,200 \pm 570$ on bat guano from the base of the terrestrial deposits in Leonard Rock Shelter in the Humboldt area. (*See* Fig. 3). The three dates constitute excellent evidence for a fall in the levels of both lakes close to 11,000 years ago. The extreme importance of this age lies in the fact that tufas from the highest levels have ages slightly older and younger than 11,000 years.

Discussion

Chronology

Figure 9 shows a plot of the probable sequence of lake levels, as indicated by the radiocarbon dates, for Lake Lahontan and Lake Bonneville. The positions of the points with arrows directed upward may be considered as minimum lake levels at the indicated times. These points are obtained from radiocarbon dates on materials deposited from the lake waters. Whereas in most cases the deposits were probably formed near the lake surface, possibly some formed at considerable depth. The points with arrows pointing downward are based on dates on organic material from terrestrial deposits in wave-cut caves. These samples merely set an upper limit on the height of the lake.

In both lakes there is evidence for two main high-water stages within the past 35,000 years. These two stages are separated by a brief low-water stage and were followed by the near-desiccation levels of recent times. The first of these high levels appears to have been rather long, *i.e.*, from about 25,000 years to 15,000 years ago. The beginning of this event in the Bonneville region is dated by the sample from the Salt Lake core and perhaps by the one Stansbury level sample. In the Lahontan region no direct estimate is available, but the thinolite terrace date of 29,000 years may be used as a maximum and the 19,000 year date on the Crypt Cave shell as a minimum. The estimates from both lakes are in good agreement with that of 24,000 from the mud-layer dates determined by Libby (1955, p. 117) on samples from the Searles Lake boring.

Both lakes reached rather high levels during this period but perhaps not their maximum. The marl dates from Astor Pass and the cave-sediment dates from the Winnemucca area suggest that Lake Lahontan was above the Dendritic level during at least part of this period. The two Bonneville terrace dates and the white marl dates from the Old River bed provide evidence for near maximum levels in the Bonneville region.

The period between 16,000 and 13,000 years seems to have been one of declining water level in both lakes. In the Lahontan area the Crypt Cave sediments, the Fishbone Cave sediments and diaphragm, and the Truckee Canyon tufa pavement show a fall from the +400-foot level to approximately the +200-foot level between 17,000 and 13,000 years ago. The Diaphragm Cave diaphragm dates suggest an even lower level close to 12,500 years ago.

In the Bonneville area dates of 16,000 on the Bonneville terrace, 15,000 on the Provo terrace, 15,200 on a sample taken between the Provo and Stansbury levels, and finally two 13,000-year dates on Stansbury level samples suggest the same pattern. This decline may have been modulated by numerous oscillations, as suggested by the 14,500-year date on the large tufa mushroom from Pyramid Lake and the 13,000-year date on the tufa from above Crypt Cave.

Following the intermediate-low- to low-water stage of about 12,500 years ago, there appears to have been a sharp rise to the maximum levels attained by the lakes. The most probable time of the maximum is 11,700 years ago. Numerous tufa samples from Anaho Island and Mullen Pass record this event in the Pyramid Lake area.

To date only one sample in the 11,000-year range has been run from the Bonneville area. It was from the Provo terrace. Whether the lake rose above the Provo terrace at this time is not clear and depends on when the Red Rock Pass outlet was cut. If the 16,000-year Bonneville terrace tufa date is valid, it may be used as a maximum date for the cutting of the pass. Possibly the outlet formed during the 11,500-year maximum; the Lahontan evidence indicates that this high level exceeded that attained during the earlier broad maximum. More evidence is needed before this problem can be solved.

Evidence from terrestrial deposits in wave-cut caves indicates a rather sharp decline in lake level close to 11,000 years ago. Whether this decline marks the close of the pluvial period is not clear, since there is radiocarbon evidence for a post-11,000-year maximum in the Lahontan region. In the past most workers have concluded that the base of the terrestrial deposits in the caves marks the beginning of the continuous low-water stage of recent times. They reason that if the lakes had risen one would expect that the terrestrial deposits would have been removed from the caves by wave action or at least that the perishable materials would have decomposed. Since deposits (dating 11,000 years B.P.) which contain some perishable materials exist in most caves, the possibility of a post-11,000-year high-water stage has been excluded in the past.

Thus far no evidence for a major post-11,000-year oscillation has been found in the sediment sections. In the case of Searles Lake it would only show up if there were complete desiccation

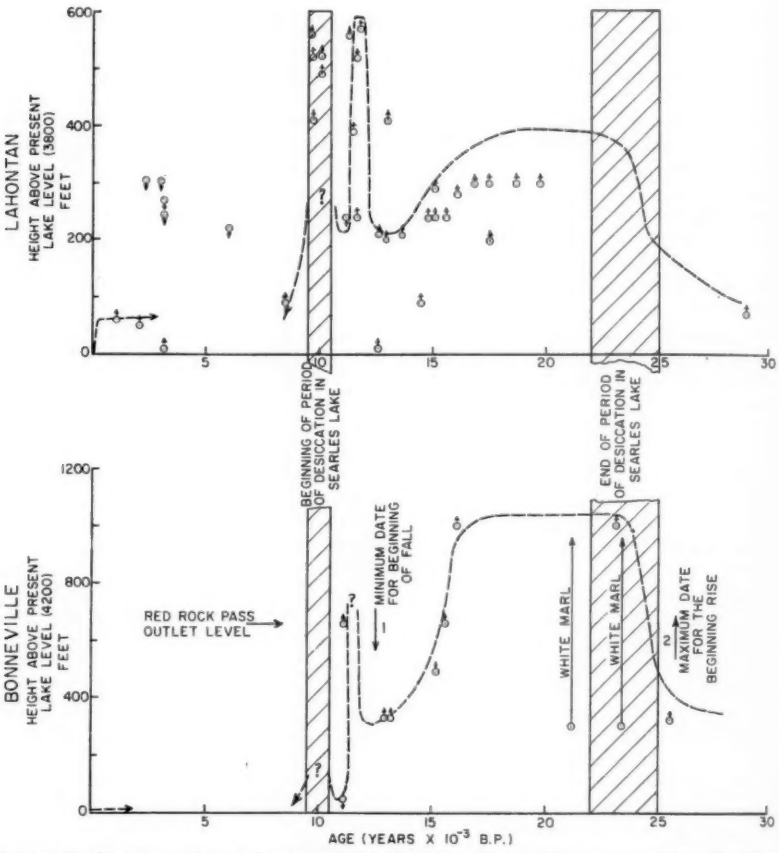

FIGURE 9.—HEIGHT OF LAKES LAHONTAN AND BONNEVILLE AS A FUNCTION OF TIME BASED ON RADIOCARBON DATA

Points with upward directed arrows represent samples deposited from the waters of the lake, and points with downward pointed arrows represent samples from terrestrial deposits. Ruled areas represent the periods of initial rise and desiccation of the waters in Searles Lake. Arrows 1 and 2 represent the ages obtained on material taken immediately above and below the organic rich layer in the Great Salt Lake core.

11,000 years ago. More careful examination of the Lahontan and Bonneville sections may help to answer the question.

On the positive side the four radiocarbon dates of close to 9700 years B.P. are internally consistent. These samples taken hundreds of feet apart and differing in size and texture give the same result. No evidence for exchange with the atmosphere exists. Using the maximum possible control value the age could be raised to only 10,500 years.

A more careful examination of the deposits in Crypt Cave shows that the lowest terrestrial level appears to have been partially eroded and disconformably covered by the more recent layers. Also the materials in this level are not nearly so well preserved. Further field studies and radiocarbon dating of these layers will yield valuable information on this problem.

Since neither argument is based on sufficiently strong evidence the problem remains unsolved. The post-11,000-year rise is hence indicated by a question mark in Figure 9.

The C^{14} chronology for Lake Lahontan presented in this paper is in agreement with the relative chronology given by Russell (1885, p. 237) with one exception. He felt that the deposition of the lithoid tufa at the highest lake levels preceded the deposition of either the thinolite or the dendritic tufa. He concludes, however,

that the lake stood at the high level once again after it deposited the thinolite and then the dendritic tufa. This agrees with the present findings. The only change that must be made in Russell's chronology is that the lithoid tufa on the highest terraces was deposited during his second rather than his first high stand. The first stand at the lithoid terrace probably precedes the radiocarbon record.

The agreement between the "classical" and radiocarbon chronologies at Bonneville is nowhere near so good. Data given here does not yield the accepted Bonneville-Provo-Stansbury sequence. One possible explanation for this disagreement is that the stands recorded by tufa deposits on wave-cut cliffs are not the same stands recorded in the sedimentary sequences. The latter could record major fluctuations that occurred much earlier than the events given here. The rapid fluctuation that appears to have occurred between 12,000 and 11,000 years ago may have left only minor geomorphic and sedimentary features.

The major purpose of this research was not to date the established stratigraphic units but to work out the pattern of lake fluctuations over the past 30,000 years. Most of the samples selected were chosen because they were directly related to the position of the lake. Where samples were run from sedimentary units the data was in agreement with the direct evidence from terrace deposits. The authors have not attempted to relate the measurements obtained to the more detailed stratigraphic units of the various alluvial and soil sequences. (*See* Eardley *et al.*, 1957; Hunt, 1953.) This is left to the geologists engaged in these studies.

A large amount of work will be needed to make the radiocarbon data from both lakes agree with detailed field relationships. Errors in both approaches will be found. The authors hope that their radiocarbon chronology will supply a stimulus for more research in this branch of Pleistocene history.

Relation of Lake Level to Climate

It is interesting to consider the climatic implications of such lake-level fluctuations. The area and height of a lake with no outlet are controlled by a delicate balance between input and evaporation. Three factors affect the input: (1) the rate of precipitation in the hydrographic basin, (2) the rate of evaporation, and (3) the net uptake or release of water by mountain glaciers within the basin. The loss from the lake depends only on the evaporation rate per unit area of lake surface and the total area of the lake.

Neglecting the contribution of mountain glaciers, the area of the lake can be related to three parameters: the average rainfall per year, l_r, the average evaporation per year, l_e, and the fraction of terrestrial precipitation reaching the lakes as runoff, f_r. The following equation is obtained for the equilibrium situation when the input of water per year due to direct precipitation and runoff equals the loss due to evaporation.

$$A_{lake} = \frac{f_r}{l_e/l_r + f_r - 1} A_{basin}$$

Estimates of the present values of the parameters in the Lahontan Basin are as follows:

l_e = 54 inches/year (Hardman and Venstrom, 1941, p. 82)
l_r = 10 inches/year (Jones, 1925, p. 32)
f_r = .20 (Jones, 1925, p. 33–39)

Combined with the area of 45,000 square miles for the basin, the present area of the lakes would be estimated as 1900 square miles. This compares favorably with Russell's (1885, p. 260) estimate of 1500 square miles.

What change in these parameters would be required to raise the level of the lake to its maximum? This represents an area increase of about a factor of five. If the increase were entirely due to increased precipitation with no corresponding change in evaporation rate or per cent runoff, an average rainfall of about 31 inches per year would be required. If evaporation rate alone were changed, a decrease to 17 inches per year would be required. Nearly 100 per cent runoff would be required if it alone were different. The increased lake level was, however, probably due to a change of all three of these factors.

The present value of f_r is certainly no greater than that during the high-water periods, since either decreased evaporation or increased rainfall would allow more runoff (Thornthwaite and Mather, 1955). The present value of rainfall can also be considered as a lower limit for periods of expanded lakes since the evaporation rates required would otherwise be extremely low ($\backsim$ 15 inches/year). It is also unreasonable to assume a higher evaporation rate during high-water periods than that observed at present. Combining these values with those calculated above, the following limits can be

placed on the three parameters during the maximum high-water stage:

$$l_e = 31 - 10 \text{ inches/year}$$
$$l_r = 17 - 54 \text{ inches/year}$$
$$f_r = 0.2 - 1.0$$

Figure 10 shows the possible combinations of these parameters capable of maintaining the high lake level. Any point within the field defines all three parameters.

to produce the necessary reduction in evaporation rate.

Another factor that must be considered is the rate of response of the lake to climatic change. A hypothetical example will point out that aside from the possible influence of mountain glaciers the response is rapid. If Lake Lahontan were filled to its maximum level today, calculations based on present evaporation and rainfall rates for Pyramid Lake show

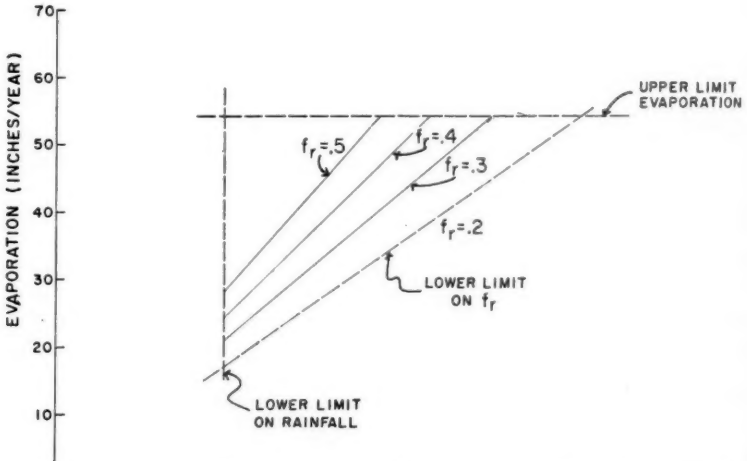

FIGURE 10.—CONDITIONS UNDER WHICH LAKE LAHONTAN COULD BE MAINTAINED AT ITS HIGHEST LEVEL
Any point within the triangular field denotes one possible set of rainfall, evaporation, and runoff conditions that could maintain the level of Lake Lahontan at an elevation of 4400 feet.

Whereas it is highly desirable to express the above parameters in terms of only mean annual temperature and precipitation rate, with the present state of knowledge this is not feasible. As shown by Thornthwaite and Mather (1955) the amount of runoff is a rather complex function not only of temperature and rainfall but also of their time distribution within a given year as well as of other factors such as soil moisture capacity and type of vegetation.

On the basis of present knowledge several conclusions can be drawn. Of these, the most important is that the climatic conditions required to produce maximum lake levels are not extreme. An increase in rainfall from 10 to 18 inches per year combined with a decrease in evaporation rate of about 30 per cent would be sufficient. A mean annual temperature decrease of 5°C. would probably be more than sufficient

that within 200 years the lake would have returned to close to its present size.

Before concluding that the lag between climatic change and adjustment of the lake level is negligible the role of mountain glaciers must be considered. Since a large portion of the water that supplies the existing lakes in both the Lahontan and Bonneville basins originates in the mountains, during times of expanding glaciers potential lake water sould be withheld. This water would then be released during times of glacial retreat. The question is whether the amount of water involved would be significant to the water budgets of the lakes. Evidence shows that the times of high lake level broadly correlate with times of expanded glaciers.

The effect of mountain glaciers on the lakes would be far less if glacial periods were primarily the result of increased precipitation rather than

decreased temperature. Although both are capable of producing simultaneous expansion of mountain glaciers and interior lakes, they would operate in different manners. In one case the glaciers would grow because of increased nourishment and the lakes because of increased inflow; in the other case, the glaciers would grow because of decreased melting rates and the lakes because of decreased evaporation loss over the lake and the basin. The rate of turnover in the lakes would be approximately a factor of three lower in one case than in the other. Hence any holdup or release of water by the mountain glaciers would be three times as effective in a temperature-controlled glacial period as in a precipitation-controlled glacial period.

Another important factor in determining the influence of mountain glaciers on the response of the lakes to climatic change is the ratio of the volume of water in the glaciers at their maximum to that in the lakes at their maximum. Only mountain glaciers within the lake basin are important in this respect.

Although the volume of the lakes can be estimated accurately, that of the glacial ice is rather difficult, since only their areal extent is recorded and not their thickness. A crude estimate for the Lahontan Basin, based on an area of 4000 square miles and an average thickness of a quarter of a mile, gives a volume of 1000 cubic miles for the mountain glaciers. This is the same order of magnitude as that of about 600 cubic miles for Lake Lahontan at its maximum. Bearing in mind the uncertainty in the estimate, a ratio of the maximum volume of glacial ice to lake water of 2 to 1 will be assumed for the Lahontan Basin. The volume of the mountain ice is hence great enough that if it were either created or melted in a short period it could influence the lake level.

Since the rate of transfer of water through the Lake Lahontan system even during a temperature-controlled glacial period would be about 2 cubic miles per year, any such growth or melting would have to occur in less than 1000 years to produce a significant change in the lake regime. Spread over 5000 years it would produce only a minor perturbation.

Even a rapid expansion or melting would tend merely to create a lag in the response of the lakes and not any pronounced minima or maxima in their levels. This becomes clear by considering a hypothetical example. Assume that during a prolonged cold period both the lakes and glaciers have come to equilibrium with the climate and have reached their maximum size. The temperature is then changed suddenly to its present value. If the ice were to melt away at a constant rate over a period of 500 years, a simple calculation shows that the lake level would fall continuously. The increased loss by evaporation of lakes would more than balance the inflow of melt water. The only effect would be a slight lag in the response of the lake level to the climatic change. This lag would probably be no more than 500 years regardless of the rates involved. The influence of the mountain glaciers on the response of the lakes to climatic change is therefore negligible. The response of the lakes to any change in temperature or precipitation is completed in less than 500 years.

The fact that the lakes respond very rapidly to climate change means that the curves of lake level versus time are also an index of relative climate in the Great Basin. Detailed studies should allow oscillations in climate as small as 1000 years in duration to be established.

Conclusions

The following conclusions are drawn concerning the histories of the dry and near dry lakes in the Great Basin.

(1) Radiocarbon measurements on carbonate materials deposited from the waters of these lakes appear to give reliable estimates of the age of fossil lake levels. Possible error, as a result of variation in the C^{14}/C^{12} ratio in the lake carbonate and exchange of carbon between the carbonate material and the atmosphere after deposition, is probably less than 500 years.

(2) The major fluctuations in the levels of Lake Lahontan and Lake Bonneville over the past 25,000 years have been determined. Two pronounced maxima are recorded in each case: a broad maximum between 24,000 and 14,000 years B.P. and a rather sharp maximum close to 11,500 years ago. Although some evidence is available for a third maximum close to 10,000 years ago (separated from the 11,500 year maximum by a pronounced minimum), more data are needed before it can be established. The lakes have been comparatively low during the past 9000 years.

(3) The Bonneville outlet at Red Rock Pass appears to have been cut more recently than 16,000 years ago and perhaps during the 11,500-year maximum.

(4) The climatic changes required to produce the observed lake maxima are not extreme. A twofold increase in the precipitation rate and a

5°C. decrease in temperature would be adequate.

(5) The fluctuations in lake level are sensitive indices of climate. Lags in response and perturbations produced by expanding or retreating mountain glaciers are on the order of the uncertainty in the radiocarbon ages and hence negligible. Hence the lake-level curves provide a record of the climate in the Great Basin over the past 30,000 years.

References Cited

Antevs, E., 1925, On the Pleistocene history of the Great Basin: Carnegie Inst. Washington Pub. 352, p. 53–114

——1952, Cenozoic climates of the Great Basin: Geologische Rundschau, v. 40, p. 94–108

Crank, J., 1956, The mathematics of diffusion: Oxford, Clarendon Press, 347 p.

Deevey, E. S., Gross, M. S., Hutchinson, G. E., and Kraybill, H. L., 1954, The natural C^{14} contents of materials from hard-water lakes: Nat. Acad. Sci. Proc., v. 40, p. 285–288

Eardley, A. J., Gvosdetsky, Vasyl, and Marsell, R. E., 1957, Hydrology of Lake Bonneville and sediments and soils of its basin: Geol. Soc. America Bull., v. 68, p. 1141–1201

Gilbert, G. K., 1890, Lake Bonneville U. S. Geol. Survey Mon. 1, 375 p.

Hardman, G., and Venstrom, C., 1941, A 100-year record of Truckee River runoff estimated from changes in levels of Pyramid and Winnemucca Lakes: Am. Geophys. Union Trans., v. 22, p. 72–90

Haul, R. A. W., Stein, L. H., and de Villiers, J. W. L., 1953, Exchange of carbon-13 dioxide between calcite crystals and gaseous carbon dioxide: Nature, v. 171, p. 619

Hunt, C. B., Varnes, H. E., and Thomas, H. E., 1953, Lake Bonneville—Geology of northern Utah Valley, Utah: U. S. Geol. Survey Prof. Paper 257-A, 99 p.

Ives, R. L., 1951, Pleistocene valley sediments of the Dugway Area, Utah: Geol. Soc. America Bull., v. 62, p. 781–797

Jones, J. C., 1925, Geologic history of Lake Lahontan: Carnegie Inst. Washington Pub. 352, p. 3–50

Kulp, J. L., and Carr, D. R., 1952, Surface area of deep-sea sediments: Jour. Geology, v. 60, p. 148–149

Libby, W. F., 1955, Radiocarbon dating: Chicago, Univ. Chicago Press, 124 p.

Orr, P. C., 1956, Pleistocene man in Fishbone Cave, Pershing County, Nevada: Nev. State Mus. Dept. Archeology Bull. 2, p. 1–20

Preston, R. S., Person, E., and Deevey, E. S., 1955, Yale natural radiocarbon measurements II: Science, v. 122, p. 954–960

Russell, I. C., 1885, Geological history of Lake Lahontan: U. S. Geol. Survey Mon. 11, 287 p.

Thornthwaite, C. W., and Mather, J. R., 1955, The water balance: Climatology, v. 8, Drexel Inst. Tech., 63 p.

Lamont Geological Observatory, Columbia University, Palisades, N. Y.; Western Speleological Institute, Santa Barbara, Calif.

Manuscript Received by the Secretary of the Society, October 8, 1957

Lamont Geological Observatory Contribution No. 297

Western Speleological Institute Contribution No. 14

3 dioxide
s carbon

s, H. E.,
northern
vey Prof.

ments of
America

e Labon-
. 352, p.

ce area of
v. 60, p.

Chicago,

Fishbone
ev. State
20
S., 1955,
nents II:

of Lake
11, 287 p.
R., 1955,
8, Drexel

COLUMBIA
ERN SPE-
A, CALIF.
Y OF THE

TRIBUTION

ONTRIBU-

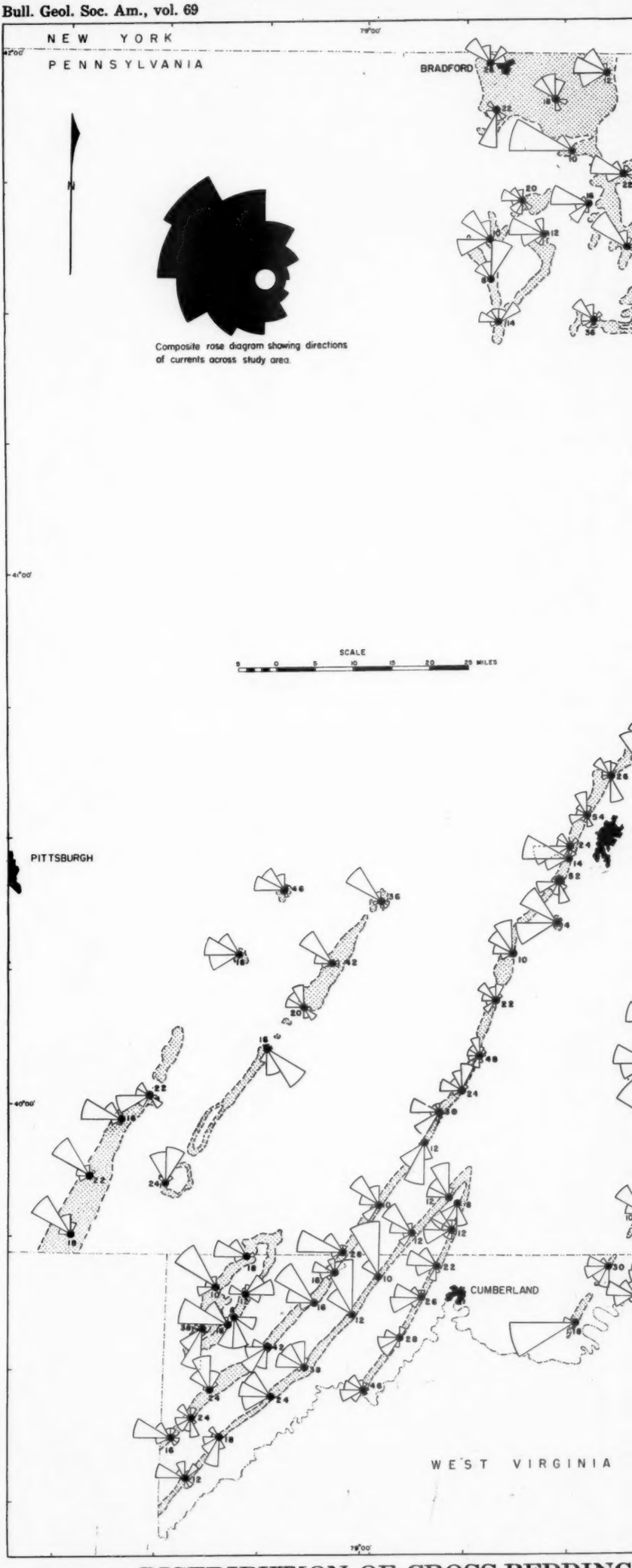

DISTRIBUTION OF CROSS-BEDDING

NG AZIMUTHS IN THE POCONO FORMATION IN PE

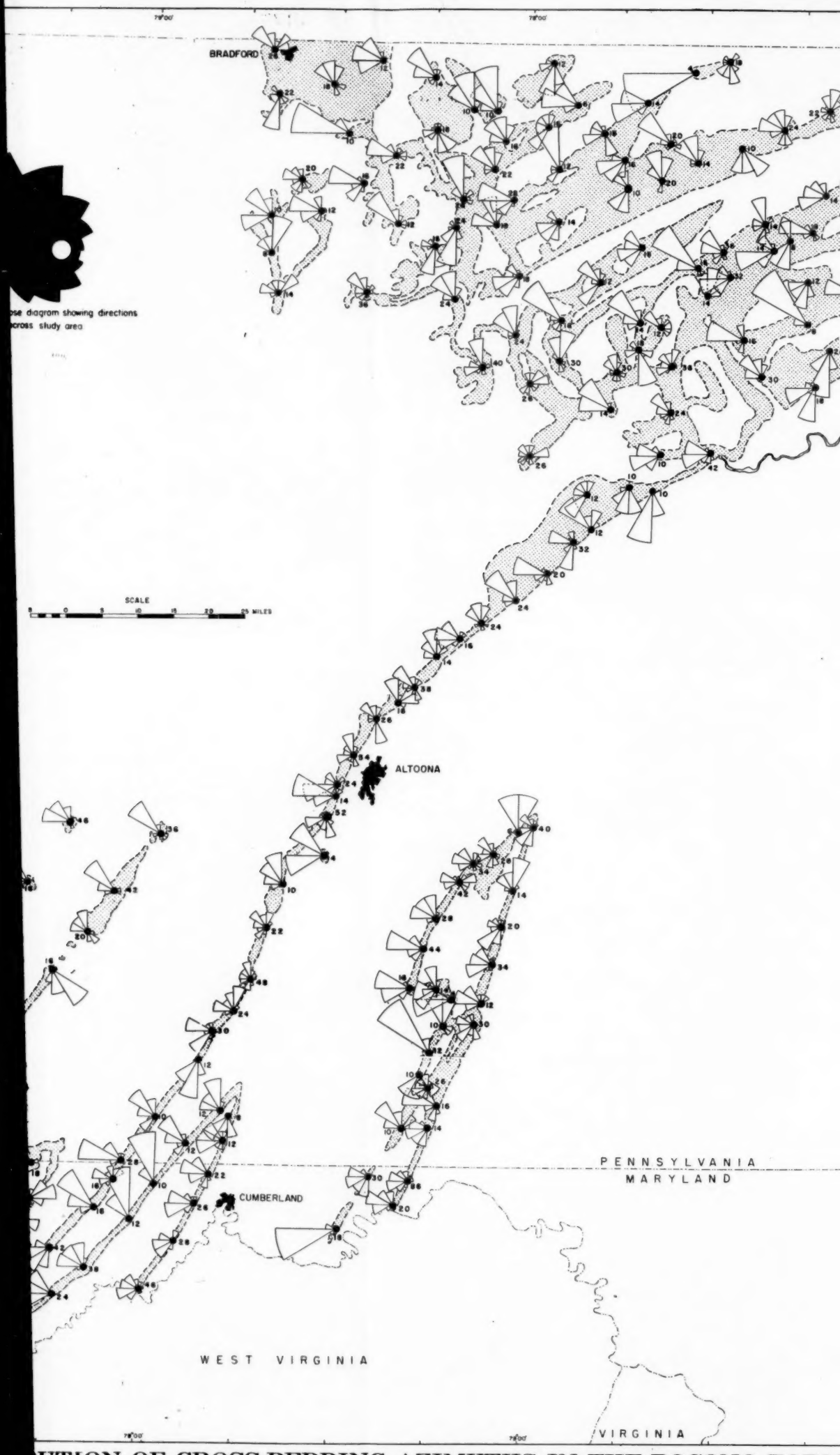

se diagram showing directions
across study area

UTION OF CROSS-BEDDING AZIMUTHS IN THE POCONO FORM

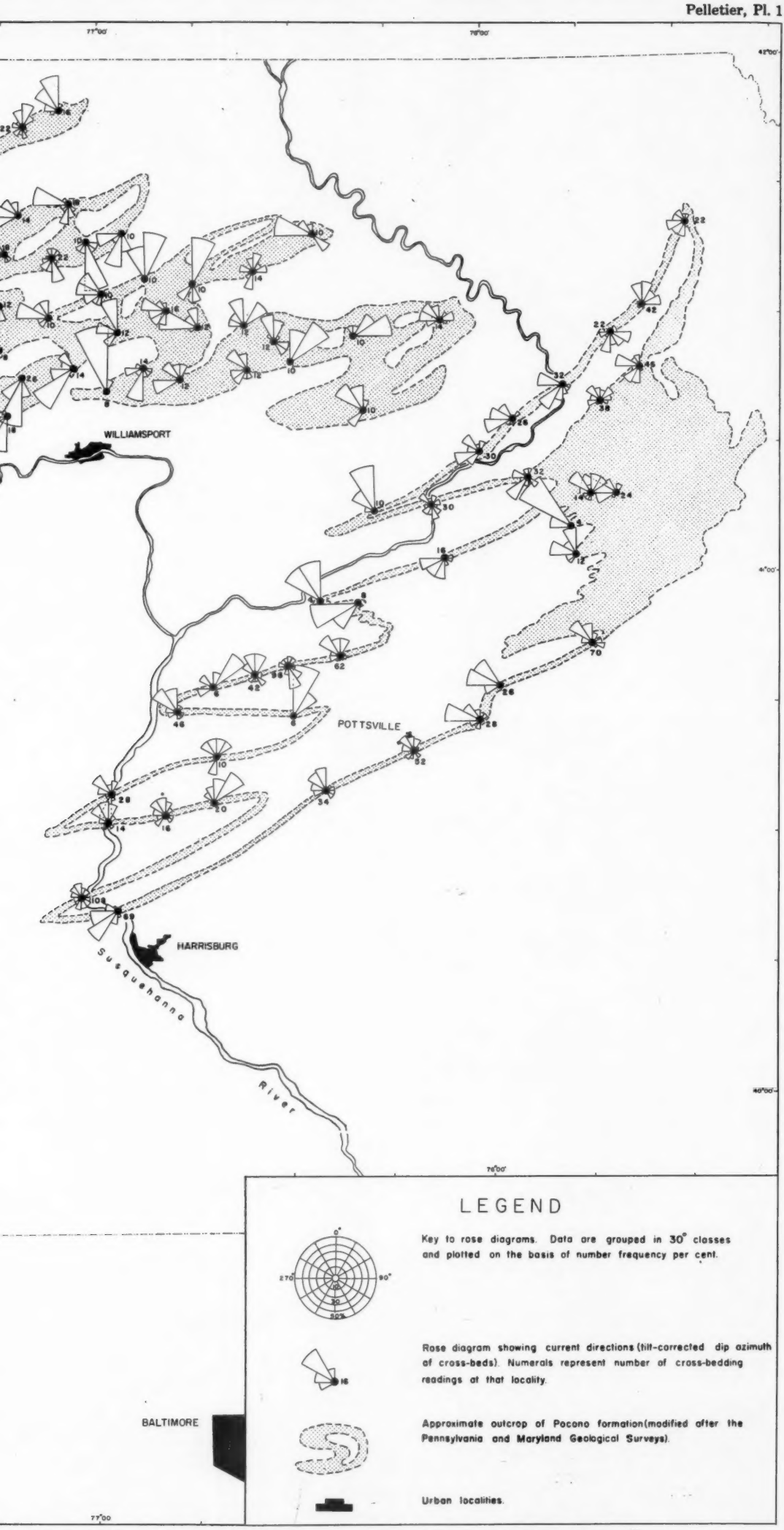

LEGEND

Key to rose diagrams. Data are grouped in 30° classes and plotted on the basis of number frequency per cent.

Rose diagram showing current directions (tilt-corrected dip azimuth of cross-beds). Numerals represent number of cross-bedding readings at that locality.

Approximate outcrop of Pocono formation (modified after the Pennsylvania and Maryland Geological Surveys).

Urban localities.

RMATION IN PENNSYLVANIA AND MARYLAND

BULLETIN OF THE GEOLOGICAL SOCIETY OF AMERICA
VOL. 69, PP. 1033-1064, 19 FIGS. AUGUST 1958

POCONO PALEOCURRENTS IN PENNSYLVANIA AND MARYLAND

BY BERNARD R. PELLETIER

ABSTRACT

A combined petrographic, stratigraphic and sedimentological study was made of the Pocono formation (Mississippian) of Pennsylvania and Maryland to determine the paleocurrent system, source area, and paleogeography of Pocono time.

Measurement of 5000 cross-bedding attitudes at 254 localities and studies of other current structures showed transport direction was toward the northwest. The paleoslope, reconstructed by contouring the moving average of the largest diameter of the 10 largest quartz pebbles at each outcrop, dipped west and northwest across Maryland, Virginia, West Virginia, Pennsylvania, and western New York. Tilt-corrected trends of 325 oriented plant remains in the anthracite region of Pennsylvania are about perpendicular to the regional current direction.

Extrapolation of the size-distance curve of the pebble diameters, after adjustment for crustal shortening, indicated the vicinity of Atlantic City, New Jersey, as a probable source area.

Stratigraphic studies, petrographic analyses, the paleocurrent pattern, and numerous current structures indicate that the Pocono formation was fluviatile and derived from clastic sediments and low-rank metamorphic rocks.

Measurements of cross-bedding in Upper Devonian, Mississippian Mauch Chunk, and Lower Pennsylvanian strata at 35 localities showed that the current pattern is essentially the same as that of the Pocono. Calculations based upon the southeastward increase in pebble size, corrected for crustal shortening, showed the Pottsville (Lower Pennsylvanian) source area was a few miles south of Philadelphia and about 100 miles northwest of that of the Pocono. The source region had migrated toward the northwest.

CONTENTS

TEXT

	Page
Introduction	1034
Purpose	1034
Method and scope	1034
Acknowledgments	1036
Stratigraphic nomenclature and earlier work	1037
Thickness and lithofacies	1037
Thickness	1037
Lithofacies	1037
Petrography	1038
Gross lithology	1038
Petrography of the sandstones	1040
Cross-bedding	1043
General statement	1043
Cross-bedding scale	1043
Cross-bedding azimuths	1043
Cross-bedding inclinations	1047
Origin of cross-bedding	1050
Primary linear structures	1051
Oriented plant remains	1051
Primary current lineation in sandstones	1052
Ripple marks	1053
Maximum pebble sizes	1053
Direction of transport	1053
Distance of transport	1054
Pocono sedimentation	1056
Sedimentary (depositional) strike	1056
Major facies	1057
Terrestrial facies	1057
Arthrophycus facies	1057
Marine facies	1057
Paleogeography	1058
General setting	1058
Fall line	1058
Coastal plain	1058
Shore line	1058
Summary of Pocono sedimentation	1058
Mid-Paleozoic sedimentation	1059
Outline of study	1059
Cross-bedding	1059
Maximum pebble size in the Pottsville conglomerate	1059
Shift of the fall line	1060
Summary of mid-Paleozoic sedimentation	1060
Conclusions	1061
References cited	1062

ILLUSTRATIONS

Figure	Page
1. Study area	1035
2. Construction of moving average	1036
3. Isopach map of Pocono formation	1038
4. Lithofacies map of Pocono formation	1039
5. Histograms showing distribution of detrital grain diameters in Pocono formation	1042

Figure Page
6. Petrographic classification of Pocono sandstones 1043
7. Histogram showing frequency distribution of cross-bedding thicknesses in Pocono formation 1043
8. Vertical distribution of cross-bedding dip azimuths at Susquehanna Water Gap, through Berry Mountain, Pennsylvania 1046
9. Vector means of tilt-corrected cross-bedding dip azimuths in Pocono formation 1047
10. Moving average of vector means showing regional current patterns 1048
11. Grouping of tilt-corrected dip azimuths of cross-bedding in relation to strike of true bedding 1048
12. Frequency distribution of tilt-corrected cross-bedding inclinations of Pocono formation grouped according to different amounts of tilt 1050
13. Orientation of plant remains in the Pocono formation, anthracite region 1052
14. Distribution of pebble sizes in the Pocono formation 1054
15. Log maximum pebble size and distance, Pocono formation 1055
16. Sedimentary trends and general physiographic divisions during Pocono time in the central Appalachians 1055
17. Variation of current directions in mid-Paleozoic times 1059
18. Log maximum pebble size and distance, Pottsville conglomerate 1060
19. Schematic diagram showing maximum pebble sizes, position of fall lines, and shore lines of Pocono and Pottsville 1061

Plate Facing page
1. Distribution of cross-bedding dip azimuths in the Pocono formation in Pennsylvania and Maryland 1033

TABLES

Table Page
1. Comparison of standard deviation and vector magnitude 1045
2. Variation of mean tilt-corrected cross-bedding inclinations 1049
3. Variation of mean cross-bedding inclinations 1049
4. Variations of mean cross-bedding inclinations in other formations 1050
5. Per cent of cross-beds with tilt-corrected inclinations greater than 30° (Pocono formation) 1051
6. Comparison of average quartz pebble sizes in the Pocono with those of the Pottsville 1060

Introduction

Purpose

The importance of the Appalachian geosyncline in geologic theory and in the geologic history of North America makes it desirable to integrate stratigraphic, petrographic, and paleocurrent analyses of one of its prominent deposits. The Pocono formation was chosen because of its widespread exposures, accessibility of outcrops, abundance of cross-bedding and conglomerates, and the extensive record of measured sections and well data available.

Similar work of lesser detail was done in the adjacent Upper Devonian, Mississippian Mauch Chunk, and Lower Pennsylvanian conglomerates to determine the history of sedimentation through geologic time.

The Pocono formation was investigated in the anthracite region of central Pennsylvania (Fig. 1) and in the northern anthracite region of the Lackawanna syncline, in the Broadtop coal basin of Bedford, Fulton, and Huntingdon counties, along the Allegheny front extending southwestward from Sullivan and Bradford counties, and across Lycoming, Clinton, Centre, Blair, Bedford, and Somerset counties. In western Pennsylvania, outcrops were examined on Laurel Hill and Chestnut Ridge and in part of the Allegheny Plateau extending west and north from the Allegheny front including parts of Sullivan, Bradford, Tioga, Lycoming, Centre, Clinton, Potter, Cameron, Elk, and McKean counties. In Maryland, studies were made along Meadow Mountain and in several ridges of western Maryland including all flanks of the Accident anticline, Backbone Mountain, and Big Savage Mountain in Garrett County, and Dans Mountain in Allegany County.

Method and Scope

An isopach map (Fig. 3) was constructed from the thicknesses of the Pocono formation obtained from published records. Sand-shale ratios were calculated from drill records and section measurements, and a lithofacies map (Fig. 4) was drawn.

From thin sections, a point count was made to estimate percentage composition and to classify the rock. Two hundred grains in each slide were measured to determine the size distribution. Results were classified into Udden size grades and presented in a series of histograms.

Outcrops were examined for primary structures, fossils, and conglomerates. Bedding and cross-bedding attitudes were measured at

each locality with the Brunton pocket transit. If a suitable cross-bedding surface was not exposed, the notebook was aligned with the traces of the cross-bedding on two nonparallel rock surfaces. As two intersecting lines form a plane, and as the traces examined constitute foreset planes per unit were measured. The number of readings was larger in most cases.

The average current direction for each locality was obtained by a vector summation of the individual cross-bedding dip azimuths. The vector mean at each locality was calcu-

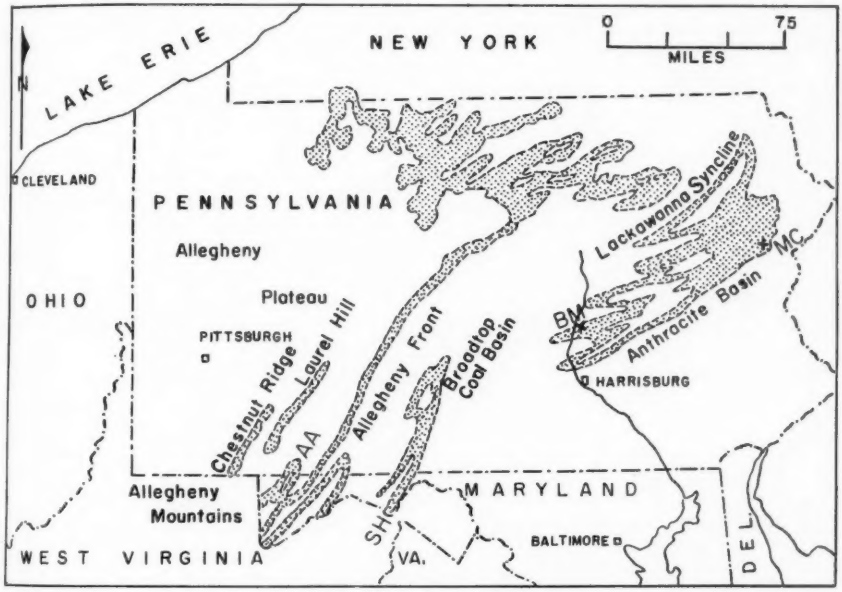

FIGURE 1.—STUDY AREA

Pocono outcrop area stippled. Abbreviations are as follows: AA—Accident Anticline; SH—Sideling Hill, BM—Berry Mountain; MC—Mauch Chunk.

such lines, the notebook must be in the plane of the cross-bed. The strike and dip of the notebook is then measured.

The cross-bedding readings were rotated to correct for the deformation or tilt of the Pocono beds. The Schmidt stereonet was used to correct for tilt. The cross-bedding poles were rotated about the strike of the true bedding through an angle equal to the dip of the bed. The stereonet procedures used are outlined by Haff (1938). Possible errors due to tilt correction have been discussed by Whitaker (1955, p. 765).

An attempt was made to secure a uniform areal density of observation points. As no similar study had been made of the Pocono formation, there was no guide to the spacing of observation points or to the number of measurements required. At least two cross-bedded units per outcrop and two different

lated from trigonometric functions in the same manner that latitude and longitude departures are computed for a transit traverse. To minimize local variations and erratic values a moving average was computed for four adjacent 15-minute quadrangles (Fig. 2). The average was plotted at the center of the group of four. This average value[1] was obtained by a trigonometrical summation of all the locality averages within the four quadrangles. By moving the unit area (four quadrangles) 15 minutes at a time both east-west and north-south, all quadrangles are utilized four times. In this manner the inferred paleocurrent pattern was constructed. Although Miller (1956) and Krumbein (1956) have proposed other methods of averaging regional data, the

[1] Locality averages were used to avoid unnecessary weighting by a more heavily sampled locality.

method used seemed adequate for this study. A less extensive reconstruction of paleocurrents was made for the Upper Devonian, Mauch Chunk, and Pottsville.

Tilt-corrected foreset inclinations were separately recorded to determine the effect of folding and tilting upon cross-bedding (Tables 2–5). Other directional indicators such as primary lineation and oriented plant stems were treated in the same manner as the cross-bedding. Data were reduced on the stereonet, and mean orientations were determined by vector summation and analyzed statistically.

Thicknesses of cross-bedded units were also measured at each locality. Averages were plotted, and a moving average was contoured. The log of the thickness plotted on logarithmic probability paper showed the distribution was essentially log normal.

As the mean grain size and maximum pebble size are presumed to be correlated (Kurk, p. 249 *in* Pettijohn, 1957b), the longest diameters of the 10 largest pebbles in the outcrop or in talus blocks derived therefrom, were averaged for each locality. These values were plotted, and a moving average contoured. From the pattern of size decrease, the paleoslope was inferred. From the spacing of the contours, a graphic plot of the log of the pebble diameters against distance (Figs. 15,18) was made. From Sternberg's Law, the coefficient of size reduction was determined.

Acknowledgments

The writer expresses thanks to F. J. Pettijohn, who suggested the problem, gave invaluable advice on field methods and presentation of data, and gave freely of his time for consultation. Many thanks are extended to A. C. Waters, who also read the paper and offered helpful suggestions.

The time and advice given by the following are greatly appreciated: F. Chayes, of the Geophysical Laboratory of the Carnegie Institution, Washington, D. C., discussed statistics with the writer; R. Brinkman of Bonn University, Germany, explained field methods and results at an informal meeting at The Johns Hopkins University; C. Gray, R. C. Bolger, and M. N. Shaffner of the Pennsylvania Geological Survey, Harrisburg, and G. H. Wood, J. P. Trexler, and H. H. Arndt of the U. S. Geological Survey, Mount Carmel, Pennsylvania, suggested localities where the Pocono formation could be easily reached and discussed the stratigraphic problems of the Pocono.

The writer is indebted to The Johns Hopkins University for scholarships and assist-

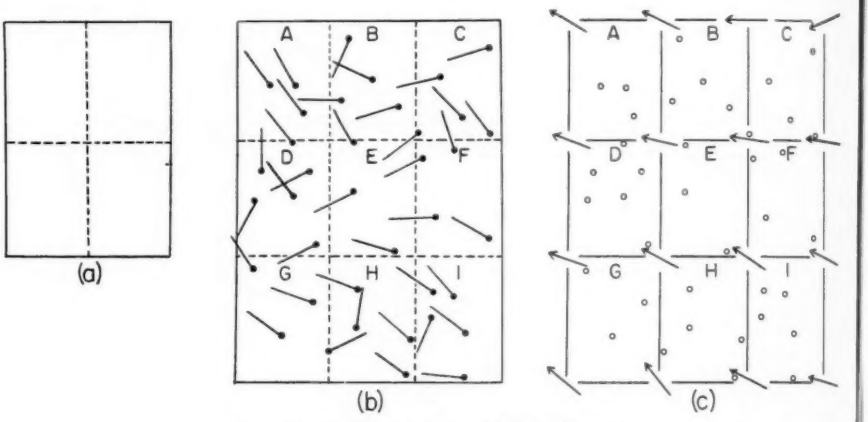

FIGURE 2.—CONSTRUCTION OF MOVING AVERAGE

All vector means (*b*) in *ABED* are summed trigonometrically, and the resultant is plotted in the center of the *ABED* grid unit (*c*) as shown by small arrow. Next, the unit grid (*a*) is moved to the east in (*b*) so as to include *BCFE*. All vector means in these quadrangles are summed trigonometrically, and the average value is plotted at the center of the *BCFE* grid unit in (*c*). This operation is repeated in an east-west and north-south direction, moving the unit grid 15 minutes at a time. In this manner each 15-minute quadrangle is utilized four times.

antships. For expenses of field work The Geological Society of America provided a grant from the Penrose Bequest.

Stratigraphic Nomenclature and Earlier Work

Pocono nomenclature is reviewed by Wilmarth (1938, p. 1687), and Read (1955, p. 4). The term Pocono formation is generally applied to the gray and buff conglomerate, sandstones, and shales that separate the red beds of the Mauch Chunk above from the red beds of the Catskill below.

Weller *et al.* (1948, p. 170) placed the Pocono and its subdivisions in the Lower Mississippian but mention that many authors are not in agreement on the lower boundary. Some designate the lower Pocono as Upper Devonian; if this is correct, a Devonian-Mississippian boundary may occur within that formation. Except in western Pennsylvania, fossil invertebrates are rare, and dating must be based upon plant remains.

Most of the earlier work on the Pocono was restricted to mapping and to stratigraphic problems, with special reference to oil and gas possibilities. Interpretations of the origin were based mainly on regional stratigraphic data. Barrell (1913) noted marine fossils in the Pocono of extreme western Pennsylvania and flora in the Pocono of the east and concluded that the Pocono was marine in the west and fluviatile in the east. The primary structures and gross lithology coincided with this interpretation.

Early workers noted pronounced eastward thickening of the Pocono across southern Pennsylvania and western Maryland and southward thickening across the anthracite basin. These observations suggested a highland source southeast of the present anthracite region. White (1934) restated this idea. Willard (1946) demonstrated from stratigraphic, lithologic, and paleontological data that the Pocono formation passes from a continental facies in the southeast to a marine facies in northwestern Pennsylvania.

Studies of the flora of the Pocono have been summarized by Read (1955, p. 2). In the present study, the paleocurrent pattern and its bearing on origin and paleogeography of the Pocono is emphasized.

Thickness and Lithofacies

Thickness

The Pocono formation is thickest in the southeast and thins to the west and north (Fig. 3).

An unconformity—possibly a result of southwesterly tilting and/or erosion (discussed by Ebright, 1952, p. 7; Bolger and Grouse, 1953, p. 5)—between Pocono (or equivalents) and Lower Pennsylvanian beds in central Ohio and adjacent West Virignia extends northeasterly into Pennsylvania for almost the entire length of the State. Therefore, the thickness is in part a function of post-Pocono erosion. The deepest downwarp in the area of deposition (as shown by the thickest accumulation of sediments) during Pocono sedimentation was probably in central Pennsylvania and western Maryland. Erosion has removed the Pocono southeast of the anthracite region. Westward and northwestward thinning suggests sediment transport from southeast to northwest.

Lithofacies

A lithofacies map (Fig. 4) of the Pocono formation was made from published sections and well-log data. Because of the doubtful logging methods and inconsistent nomenclature, only records of cores examined and correlated by a geologist were used.

Sand-shale ratios were plotted in Figure 4. Two ratios, 2:1 and 1:1, were used to divide the Pocono area into three major zones. Coarser clastics predominate in the east and southeast. From the anthracite region northwestward, the Pocono grades from a heavy conglomerate-sandstone-shale facies into a minor conglomerate-sandstone-shale facies, into a sandstone-predominant shale facies.

It is concluded, therefore, that a source area supplying clastics lay southeast of the anthracite region. Northwest of this area, a coastal plain (inferred from the stratigraphy) extended across western Maryland and western Pennsylvania and was bordered by a marine body (inferred from evidence of marine fauna) farther west. The sand-shale ratios in the area affected by the unconformity are misleading. The uppermost Pocono, where observed, is commonly the coarsest part. Therefore, where it has been removed, the ratios may be consistently low.

Petrography

Gross Lithology

The Pocono formation consists of interbedded shale, sandstone, and conglomerate. In a 1200-foot section through Berry Mountain at the Susquehanna Water Gap, 138 feet of shale, 1027 feet of sandstone, and 78 feet of conglomerate are exposed. These are the cumulative thicknesses of 31 shale intervals, 68 sandstone intervals, and 27 conglomerate intervals. In southeastern Pennsylvania sandstones and conglomerates are quantitatively more important than shales. In northwestern Pennsylvania the conglomerates are insignificant, and shales, with some sandstones, form most of the section.

At Berry Mountain most shale intervals are 4 feet or less thick. However, two shale intervals were 20 and 24 feet thick respectively; eight were 6–10 feet thick. Fine-grained sandstone is commonly associated with the shale.

The Pocono shales are dark gray to black and weather rusty brown. They contain carbonaceous material but do not reach the grade of a true coal. Pods and streaks of low-rank coal are widespread, but none are commercially important. The flora and coaly material are in general restricted to southeastern Pennsylvania. Plant remains occur along bedding planes. In the sandier ripple-marked facies, many fragments are oriented parallel to the ripples.

A marine fauna appears in McKean County northwest of the Allegheny front. The shales here contain worm burrows, structures similar to *Arthrophycus*, and small irregular polygons, which appear to be poorly preserved mud cracks. Ovoid clay stone concretions, up to 6 inches in diameter and lacking a visible nucleus, parallel the bedding planes.

Quartzose sandstones throughout the section at Berry Mountain are up to 10 feet thick, but most are less than 4 feet thick. Many of the sandstones contain quartz pebbles and are referred to as pebbly sandstones. If the pebbles form less than 10 per cent of the rock, the term sandstone was used. If the pebbles form more than 10 per cent, the rock was termed conglomerate.

The Pocono sandstones, commonly quartzitic, are gray to tan and weather grayish brown. Streaks of red hematite may be present. The gray and brown sandstone has a salt-and-

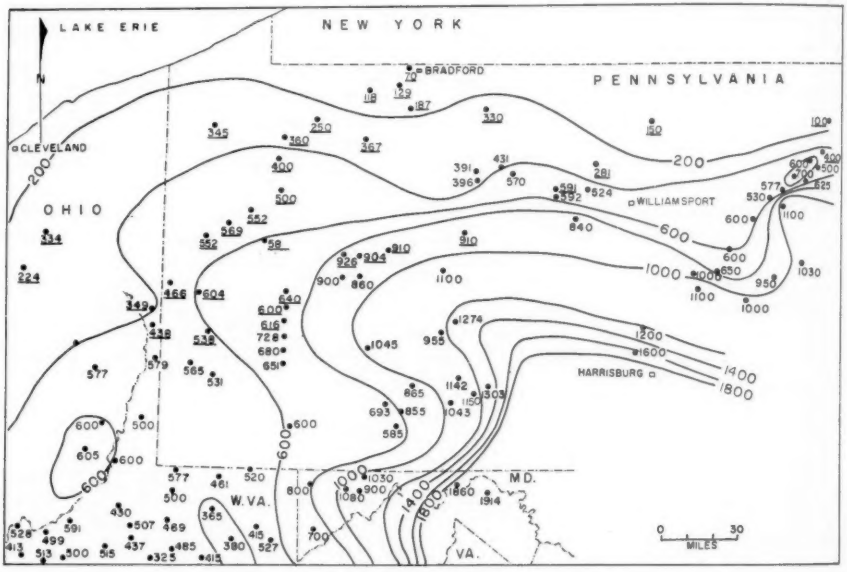

Figure 3.—Isopach Map of Pocono Formation

Contour interval is 200 feet. Numeral represents thickness of Pocono, and underscored numeral indicates unconformity at top of section.

pepper aspect, owing to a mixture of quartz grains, dark rock fragments, black flecks of iron oxide and organic material, and mica. Plant fragments are common and may parallel the trend of associated ripple marks.

Massive sandstones, found in most outcrops, are up to 4 feet thick; most are thinner.

wanna syncline and the northeastern Allegheny front. Bedding is regular but lacks the fine stratification of material deposited below wave base. Some outcrops show lenticularity in the bedding, and in some northwestern outcrops bedding exhibits penecontemporaneous slumps.

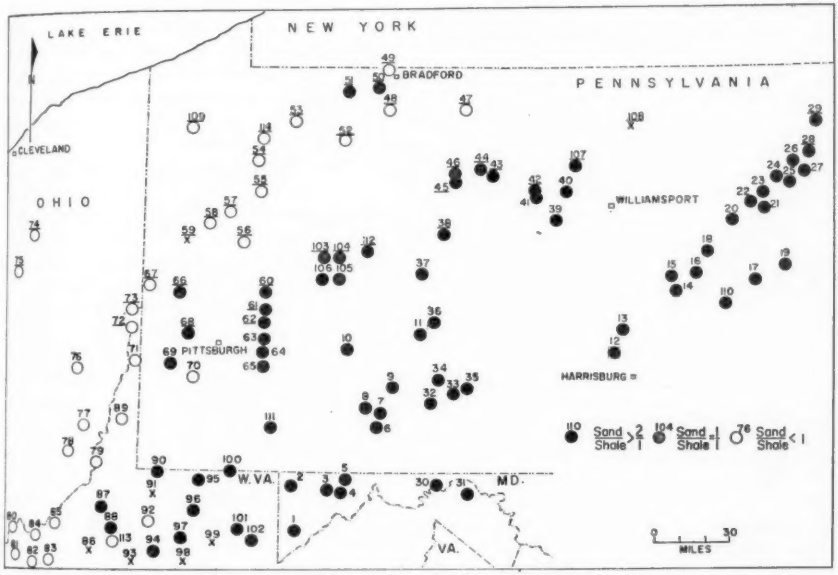

FIGURE 4.—LITHOFACIES MAP OF POCONO FORMATION

Numeral represents station number keyed to reference table by the author (Ph.D. thesis, The Johns Hopkins Univ.) for lithofacies and isopach maps. Underscored numeral indicates unconformity at top of section. X indicates thickness recorded but not lithofacies.

Local thicknesses of 10–12 feet of red sandstone are common. Cross-bedded sandstones are conspicuous and are common in most outcrops. Ripple marks are of all types in the Pocono but are not prominent. Symmetrical ripple marks south of Scranton have a wave length of 6 inches. Asymmetric ripple marks are not common, but a good example was noted in McKean County. Interference ripple marks were observed with a wave length of 6 inches and ripple striking 85°, and a wave length of 8 inches and ripple striking 18°. Amplitude of both ripples is 1½ inches.

Primary current lineation (Stokes 1947; H. Cloos, 1938)—Crowell's (1955) parting lineation—is also widespread but not abundant at a given outcrop. Scouring, although not pronounced, was observed at the base of the formation along the northern rim of the Lacka-

Shale-chip breccias, although present at nearly every outcrop, are not a major unit of the formation. No areal or vertical trend in size distribution of the contained shale fragments was noted. The breccias are in general restricted to the sandstones, but some are found in the quartz conglomerate beds. Shale fragments are up to 8 inches long but average from half an inch to 5 inches in most localities. All shale chips are flat, polygonal, angular to subrounded, and parallel to bedding planes.

At Berry Mountain, quartz conglomerates are more common in the lower half of the section than in the upper half. The first major conglomerate bed is 200 feet above the base of the Pocono. At certain localities in the anthracite region, such as at Mauch Chunk, Aristes, and north of Shamokin, the first major conglomerate occurs within 70

feet of the base. In the Hyner View section on the Allegheny Plateau northwest of Berry Mountain, the major conglomerate is in the upper part of the section. In western Maryland the major quartz conglomerate is also in the upper part of the section.

The position of the quartz conglomerates remains uncertain. The conglomerates, however, appear to ascend in the section toward the northwest. The equivalent positions of the older layers of conglomerate in the southeast are occupied by sandstone and shales in the northwest.

A. D. Leonard (1953, unpub. M. S. thesis, The Pennsylvania State Univ.) indicated that at least 10 per cent of the Pocono section at Mauch Chunk consisted of quartz conglomerate. The present writer estimated 3 per cent of quartz conglomerate at outcrops along the northwestern rim of the central anthracite region and less than 1 per cent along the Allegheny front and in western Maryland. The conglomerate decreases toward the west and northwest.

The conglomerate pebbles are chiefly white vein quartz cemented by silica. They are equidimensional to ovoid and commonly are well rounded. Pebbles of sandstone, quartzite, slate, schist, and rare chert are also found. These form less than 10 per cent of the conglomerates. In southeastern Pennsylvania quartz pebbles up to 80 mm long have been measured. They decrease in size to the northwest. No preferred orientation of the pebbles could be seen, except that the ovoid pebbles parallel the bedding. Some conglomerate beds exceed 8 feet in thickness. Large plant impressions and molds occur in these beds. Crossbedding is present in the moderately conglomeratic beds and pebbly layers but is not common. Massive structure is common.

The plants, coaly material, and heavy conglomerates in the southeast contrast markedly with the marine fauna, minor conglomerates, and greater abundance of shale in the northwest. These observations suggest terrestrial deposition in the anthracite region, whereas northwest of the Allegheny front, especially in parts of McKean and Potter counties, deposition was marine. Worm burrows, arthrophycid structures, and productid brachiopods suggest deposition in a littoral zone.

Currents are indicated in the anthracite region by widespread ripple marks, crossbedding, scouring, shale-chip breccias, and oriented plant remains. The consistent current pattern from old land to shore line based on cross-bedding and pebble data favors fluviatile deposition. Coal pods and carbonaceous shales suggest deposition partly in swampy localities and small lakes on a low-lying coastal plain.

Absence of high-grade metamorphic or igneous rock fragments indicates that these rocks were not exposed in the source area. The abundant quartz pebbles and lesser amounts of shale, siltstone, sandstone, quartzite, chert, phyllite, and mica schist fragments show that clastic sediments of all textures associated with low-rank metamorphic rocks were exposed in the source area.

Petrography of the Sandstones

Sandstones from 14 widely spaced localities were studied in thin section. Quartz forms 50-80 per cent of the samples. Detrital quartz occurs as well-rounded or subrounded grains up to 2 mm in diameter, averaging between 0.25 and 0.5 mm. Secondary overgrowths join with other overgrowths to form a quartz mosaic interrupted by crushed rock fragments. Sericite related in origin to the shale fragments has replaced some of the quartz, as shown by the sutured outline of the host quartz.

Rock fragments and matrix together form half the rock volume. Shale is the most abundant type of rock fragment, followed by siltstone and low-rank metamorphic rocks such as quartzite, slate, phyllite, and schist. Certain cryptocrystalline aggregates may be chert. Detrital outlines are in general well rounded. Maximum diameters of the rock fragments are similar to those of quartz, but the minimum diameters are rarely as small as the smallest quartz.

The matrix is similar in character and composition to that of the rock fragments, suggesting that the matrix materials were at least partially derived from crushing of shale particles. In some cases only part of a rock fragment was rounded. The remainder of the fragment filled irregular openings in the confining quartz mosaic. Some phyllitic pebbles which contain sericite showed flowage and alignment of the sericite parallel to outlines of confining quartz grains or adjacent rock fragments. Some rounded shale fragments have been elongated by compaction and have flowed irregularly from points of compression without totally losing their original detrital outlines. In many cases torn and crushed rock fragments grade into an amorphous matrix. In many places the detrital quartz grains are enlarged

by secondary quartz, which must have been deposited in voids. The absence of silt or clay in such voids is difficult to explain if silt and clay were deposited with the quartz sand. It is concluded that the matrixlike materials that appear to fill some voids are formed by the crushing and squeezing of rock fragments and that less than 2 per cent (estimated) is true silt or clay deposited with the mineral and rock fragments of sand size.

Muscovite occurs as conspicuous flakes with regular outlines except for the ends, which are frayed. Mica does not exceed 3 per cent of the rock. It is generally more than 1 mm in diameter, is most abundant in the coarser grades, and shows bending and fracturing. Fractures are perpendicular or at a high angle to the bedding plane and suggest compaction rather than folding. Specimens from the gently folded Pocono of the Allegheny Plateau likewise exhibit bent micas and support the view that compaction caused deformation of the micas. There is no evidence of other grains replacing or being replaced by muscovite. The muscovite plates lie parallel to the bedding planes but in thin sections cut perpendicular to bedding planes follow a sinuous path through the rock, the course being altered by mechanical action in the grains following deposition. For these reasons muscovite, exclusive of its occurrence in rock fragments, is considered detrital.

Biotite is present in most thin sections but was not always tallied in the point-count traverses. It occurs in plates with regular boundaries except for the frayed ends—similar to muscovite. Biotite does not, in most cases, form more than a fraction of 1 per cent of the rock. Grains average about 0.3 mm in diameter.

Opaque constituents do not commonly form more than 2–3 per cent of the rock. Except for iron oxide, most of the material is unrecognizable. Some is organic, perhaps carbonaceous. This is suggested by the carbonized plant material seen in outcrop. Shapes are irregular, bleblike and polyhedral. The carbonaceous grains are less than 0.125 mm.

Minor accessories form less than 1 per cent of the rock. They consist of sphene (in part altered to leucoxene), zircon, golden-brown tourmaline, blue indicolite, chlorite, and feldspar. Except for chlorite and leucoxene, all the grains are well rounded, are commonly fractured, and have diameters less than 0.25 mm.

Tourmalines are the most abundant minor constituents. Of the two varieties in the Pocono, the golden-brown variety is more common. This was also reported by Krynine (1946, p. 76). Zircon and sphene are next in abundance.

Chlorite occurs as isolated smears; its lack of detrital outlines suggests that it is secondary. The feldspar is plagioclase probably of low calcic or subcalcic composition as judged by extinction of the twin lamellae. It is highly weathered and abraded; thus optical determination is difficult. It does not exceed 0.125 mm in diameter.

Dickey (1941, p. 18) in a heavy-mineral study of the Pocono formation reported the rarity of metamorphic minerals. Garnet, kyanite, staurolite, sillimanite, andulusite, amphibole, pyroxene, the epidotes, and carbonates are rare or absent.

The micropetrology suggests a source area consisting of a sedimentary sequence of shale, siltstone, sandstone, and low-grade metamorphic rocks such as quartzite, slate, phyllite, and mica schist. The lack of igneous rock fragments and of high-grade metamorphic minerals precludes a plutonic terrain.

The rounding of the quartz grains, where visible apart from the overgrowths, suggests long transportation or repeated reworking. Concentrations of only the most stable heavy minerals such as sphene, zircon, and tourmaline also indicate a long history of transportation through one or more sedimentary cycles. Lack of feldspars suggests absence of an igneous terrain and a long history of abrasion, or a rigorous climate, or both.

With the aid of a microprojector, measurements were made of 200 grains in each of 8 thin sections. The number of grains measured was such that additional data did not change appreciably the shape of the size-distribution curve. The largest diameter of each grain was recorded, and the number frequency, in per cent, was calculated for various Udden classes (Fig. 5).

Sandstones of the Pocono formation are medium-grained but include some finer and coarser materials. The modal class is generally the 0.25–0.50 mm grade (Fig. 5). The next most important class may occur on either side of this mode. Although there is a symmetrical distribution of the classes, the size distribution is skewed toward the finer sizes. Peakedness is not marked except in sample P-76.

Although the Pocono sand ranges over seven Udden classes, about 95 per cent of the distribution falls in five or six classes. Some of

the fine grains may be particles torn from the crushed-rock detritus, erroneously weighting that part of the frequency distribution. Emery (1955) made thin-section mechanical analyses of the Pocono formation and found a bimodal distribution. He did not indicate where the modes occur.

Sorting[2] of the Pocono is fair to good. It does not reach the excellent sorting of a beach or dune sand but is well above that of a till or graywacke. Comparisons of Pocono histograms were made with 20 samples of river sands listed by Udden (1914). These sands, although analyzed in terms of weight frequency, were in the same size range as those of the Pocono and showed the distribution extending over 4 to 10 classes; 16 distributions were spread over 5 to 9 classes. They were generally unimodal and approximately normal. The over-all characteristics are similar to the Pocono.

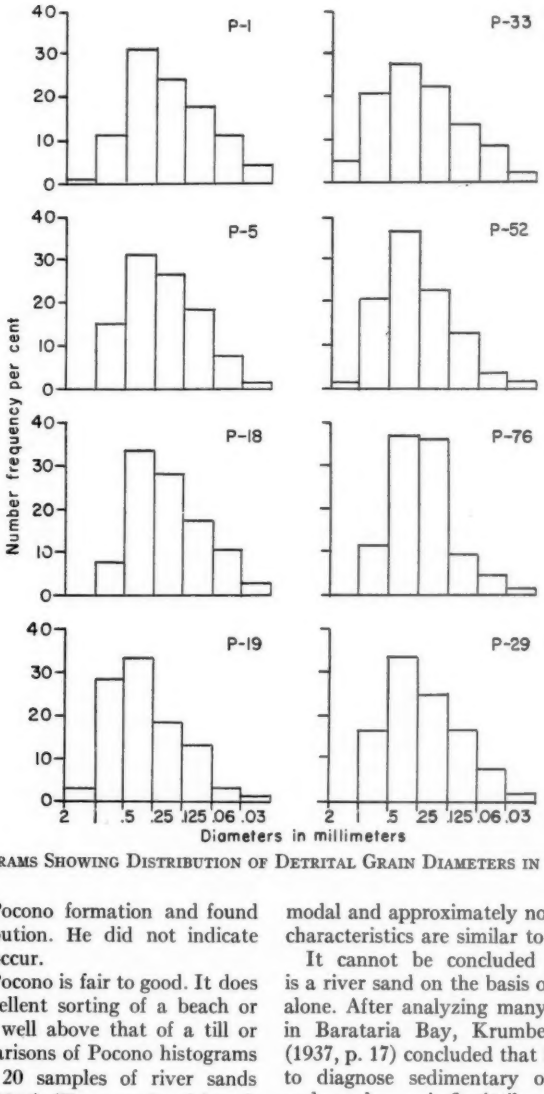

FIGURE 5.—HISTOGRAMS SHOWING DISTRIBUTION OF DETRITAL GRAIN DIAMETERS IN POCONO FORMATION

It cannot be concluded that the Pocono is a river sand on the basis of the size analyses alone. After analyzing many clastic sediments in Barataria Bay, Krumbein and Aberdeen (1937, p. 17) concluded that it was not possible to diagnose sedimentary origin solely from such analyses. A fluviatile origin, however, is possible and appears likely (as compared with glacial, beach, or aeolian) but must be checked against other evidence.

From a point count, percentage composition of minerals was recalculated to 100 per cent

[2] Numerical sorting values of P. D. Trask (p. 230–232 *in* Krumbein and Pettijohn, 1938) are not given here; only a qualitative evaluation is made.

Total amount of quartz included both detrital grain and overgrowth. Indistinct detrital outlines made it difficult to determine the amount lost by solution and that added by infiltration or internal rearrangements. The rock fragments and matrix were summed as rock fragments. These values were plotted on Figure 6. Two samples (P9 and P19) fell in

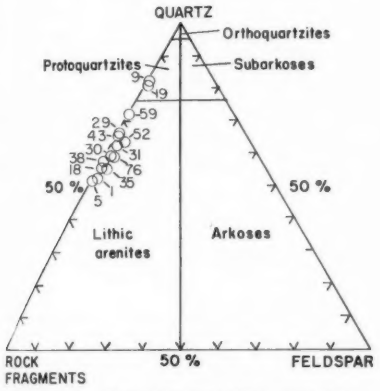

FIGURE 6.—PETROGRAPHIC CLASSIFICATION OF POCONO SANDSTONES

Triangular diagram illustrates positions of Pocono samples in the ternary classification scheme of rock fragments-feldspar-quartz. Two samples lie within the protoquartzite field. Remainder are lithic arenites. Numerals represent sampling localities (*see* B. R. Pelletier, 1957, unpub. Ph.D. thesis, The Johns Hopkins Univ.). Diagram after L. D. Clark *in* Pettijohn, 1957b, p. 292.

the protoquartzite field, and the remainder in the lithic arenite field as defined by Pettijohn (1954, p. 364). If 30 per cent of the quartz is due to overgrowths or cement, position of the rocks in the diagram is modified, but the general classification would remain unaltered.

CROSS-BEDDING

General Statement

The Pocono cross-bedding consists of planes (dominantly tabular plates) inclined at angles to the bedding. The foreset beds show little or no concavity and rarely become tangential to strata underlying the cross-bedding unit. Accordingly the cross-bedding in the Pocono is planar (McKee and Weir, 1953, p. 385). It has also been commonly referred to as torrential bedding. Although some cross-laminations are less than 12 inches long, more commonly they are 1–20 feet long and, rarely, are greater. Troughlike cross-laminated units form only 2–3 per cent of all cross-bedding.

In some parts of the Pocono, units separated by one or more layers of normal bedding may be cross-bedded. In other places several cross-bedded units occur in vertical succession. Such successive units have been called "cosets" (McKee and Weir, 1953, p. 382). Although the lengths of individual laminae were not measured, the stratigraphic thickness (scale) of the cross-bedded unit was recorded wherever the attitudes were determined. Although some cross-bedded units are wedge-shaped, most layers are uniformly thick.

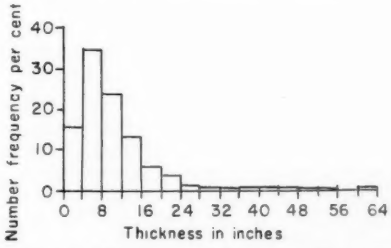

FIGURE 7.—HISTOGRAM SHOWING FREQUENCY DISTRIBUTION OF CROSS-BEDDING THICKNESSES IN POCONO FORMATION

Cross-Bedding Scale

The scale of the cross-bedding for each locality was determined by averaging the thicknesses of all units measured at that locality. (These averages are listed by the author, 1957, Ph.D. Thesis, The Johns Hopkins Univ.) A thickness-frequency distribution is shown in Figure 7.

The cross-beds are thickest in the anthracite region, where they average 18 inches. Westerly and northerly from this region the cross-bedded units thin, with local exceptions. In northwestern Pennsylvania the beds average 3–4 inches thick; inasmuch as Schwarzacher (1953, p. 326) found that cross-bedding thickens toward the source, it is clear that the Pocono source area lay southeast of the anthracite region.

Cross-Bedding Azimuths

Tilt-corrected cross-bedding readings are recorded in the author's Ph.D. thesis (1957, The Johns Hopkins Univ.). The azimuths of each locality were plotted as a rose diagram

or circular histogram. The number frequency (per cent) was shown for 30-degree class intervals. In some cases the class interval proved too small for the number of azimuth measurements available. The 30-degree interval was, however, used for all localities. The histograms were plotted on a regional map (Pl. 1).

In many places, the currents (represented by the dip azimuths) moved from the southeast toward the west and north. Some histograms demonstrate reversals in direction. If the deposit is fluvial, this is to be expected, as rivers commonly meander, change course, or join a main stream at diverse angles. Nevertheless, westerly to northwesterly trends are dominant.

Histograms show graphically the distribution of azimuths and reveal local deviations from the prevailing current direction. Many local anomalies, however, tend to disguise the regional trend. The current pattern may be simplified by showing only the average direction for each locality. Because data are circulary dispersed, calculation of the mean presents some problems, because this involves the application of a linear technique to circular (or periodic) data. The arithmetic mean is affected by the choice of origin used in making the calculation (Jizba, 1953; Chayes, 1954; Curray, 1956; Pincus, 1956).

A vector summation of the azimuths was made, because the result is independent of the choice of origin. Rather than construct the vectors graphically, the sines and cosines of the azimuths were taken from standard tables and algebraically summed. Reiche (1938) used this method, which was later elaborated upon by Curray (1956) and Pincus (1956).

At certain localities a wide scatter of cross-bedding azimuths is evident, whereas at others the azimuths are confined to a narrow range. Reiche (1938, p. 913) used a consistency ratio[3] to measure this scatter. This ratio is defined as the length of the resultant divided by the number of the individual unweighted vectors. If all vectors had the same orientation, their summed length would be that of the resultant vector, and the ratio would have a value of unity. If 50 per cent of the vectors are oppositely directed to the remaining 50 per cent, the ratio is zero, and the mean direction is undeterminable. All other distributions have an intermediate ratio. For progressively greater scatter or dispersion, the values of the ratio become progressively smaller than 1 but never less than zero.

The histograms show the current variability at each locality. The standard deviation is generally used as a measure of spread if the distribution is normal. Very few of the collected data seem to meet this requirement, and more readings may be necessary to show a normal distribution. Most of the histograms of heavily sampled localities, including the composite of the entire Pocono, appear to be normal, so that bimodalism may be due to sampling. Because of accident of exposure, an outcrop may not exhibit the inclined traces of the cross-bedding where the cross-bedding plane strikes parallel to the general bedding (Pettijohn, 1957a, p. 477). Such cross-beds would be overlooked, thus failing to give a normal appearance to the frequency histogram.

F. Chayes (Oral communication), Curray (1956), and Pincus (1956) have demonstrated that, once the vector mean is obtained, the standard deviation may be calculated about it instead of the arithmetic mean. This was done for those localities (23 in all) that had 40 or more readings each. The standard deviation is defined by W. E. Cochran and R. L. Stearman (1956, unpub. syllabus, The Johns Hopkins Univ.) as:

$$s = \sqrt{\frac{(x - \bar{x})^2}{n - 1}}$$

where s is the standard deviation, x is the observation, $\bar{x}$ is the mean of the observations, and n is the sample size. Results of the calculation are given in Table 1. They are compared with the vector magnitudes (or consistency) from the same locality. The inverse relationship of spread to vector magnitude is apparent. The standard deviations of 13 of the 23 localities fall within the 45-degree to 65-degree range. The highest standard deviation is 94.3, and the lowest is 27.3.

Standard deviation of aeolian cross-bedding was calculated by Reiche (1938, p. 915); those localities in which more than 40 cross-bedding measurements were made were compared to similar data in the Pocono (Table 1). Schwarzacher (1953, p. 322) calculated standard deviations of three distributions of marine cross-beds with more than 40 readings and

[3] Consistency ratio in terms of per cent is called vector magnitude (Curray, 1956); also called vector strength (H. J. Pincus, Personal communication).

obtained values of 44.6°, 42.6°, and 28.1° respectively. Reiche's and Schwarzacher's results fall within the same range of standard deviations calculated for the Pocono.

Twenhofel (1926, p. 444) stated that inclinations in dunes were directed in all parts of the compass because of variable winds. This is contradicted by statistical summaries of several hundred readings taken over many localities in various formations. Shotton's (1937, p. 548) measurements of direction of presumed aeolian cross-lamination were grouped within 160° of arc. Wright (1956, p. 418) found that similar measurements in the Chuska sandstone were grouped almost entirely in a single hemisphere. Reiche (1938) also showed the predominance of cross-bedding inclination in two quadrants. Furthermore, Reiche's data are similar to those of Stokes (1953; 1954), Lowell (1955), Potter (1955), Potter and Olson (1954), Olson and Potter (1954), Whitaker (1955, p. 765), J. S. Schlee (1956, unpub. Ph.D. thesis, The Johns Hopkins Univ.) Pettijohn (1957a, p. 476), and the writer; all exhibit similarities of spread and the occurrence of a chief mode. It is concluded that presumed aeolian cross-bedding, at present, cannot be distinguished from presumed fluvial cross-bedding on the basis of statistics alone.

The circular histograms (Pl. 1) summarize current directions (cross-bedding azimuths) at many localities. Although all current-direction measurements were made on beds of Pocono age, the strata studied probably vary in stratigraphic position within the formation. Hence the histograms may record vertical as well as geographic variation. In many areas, only the top of the Pocono section was seen; in others, only the base. Commonly one part was sampled more heavily than another.

Two complete sections were selected to determine if the sampling procedure used gave results comparable to those derived by the sampling of an entire section. These were Mauch Chunk (Jim Thorpe) at the eastern end of the anthracite region, and Berry Mountain at the Susquehanna Water Gap. Both sections were measured, and the stratigraphic intervals at which cross-bedded units occurred were recorded.

The tilt-corrected cross-bedding dip azimuths were plotted at successive 200-foot stratigraphic intervals in the Berry Mountain section (Fig. 8). A vector mean was obtained from each subsample and compared with the vector mean of the whole section. Deviation of the submeans from the locality mean is in general less than 20°. The Mauch Chunk section gave similar results. The lack of precise stratigraphic control of the Pocono study, therefore, does not appear to alter significantly the paleocurrent pattern deduced from cross-bedding measurements.

TABLE 1.—COMPARISON OF STANDARD DEVIATION AND VECTOR MAGNITUDE

(For localities with 40 or more cross-bedding readings)

Locality	Number of readings	Standard deviation	Vector magnitude %
1	108	94.3°	14.87
2	69	51.3°	83.84
3	70	63.7°	55.59
5	62	58.1°	66.62
6	96	89.8°	27.20
7	42	91.1°	30.71
9	46	57.2°	55.30
12	145	54.8°	69.71
15	52	85.0°	32.37
19	46	50.7°	65.72
20	42	35.7°	85.60
34	42	45.2°	70.81
60	48	71.5°	43.92
104	58	69.1°	46.64
106	86	53.6°	65.24
108	52	61.1°	59.9
111	42	84.2°	15.74
114	40	63.0°	65.71
122	44	27.3°	76.04
137	46	51.3°	69.98
190	46	47.3°	74.35
210	42	30.5°	84.88
252	40	56.9°	50.85

It is concluded that, at a given geographic site, current directions were generally consistent through Pocono time. Cross-bedding measurements of partial sections are therefore fairly reliable indicators of current direction for an entire section. The marked bimodal distribution of cross-bedding azimuths observed at several localities may be due to inadequate sampling.

Local geographic variations are shown in the plot of the mean current vectors for each station tion (Fig. 9). Because the current pattern is generally apparent, no recourse was made to further statistical analyses to interpret a trend. There is less variation in the anthracite region than on the Allegheny Plateau. In the Broadtop coal basin and Allegheny Mountains of southwestern Pennsylvania and Maryland, the

variability is between that shown in the hard-coal basin and the plateau. Variation of the mean cross-bedding direction from station to station appears to increase in the down-current direction and may, therefore, reflect the declining gradient of the streams from the highland to the coastal plain. The meanders presumably become larger and more numerous.

A statistical summary of this variation could be calculated and compared with modern streams. R. Brinkman (Oral communication) did this for European streams and found that the variation did increase in a downstream direction.

Local variations, particularly in districts on the ancient coastal plain, may obscure the regional trend of current direction. In order to emphasize the broader picture, areal moving averages[4] were computed, and the current trends thus obtained were plotted at grid intersections as arrows (Fig. 10). Currents moved westerly and northwesterly from the anthracite region. The direction was dominantly to the west and somewhat northwest across Pennsylvania and Maryland. Along the eastern limits of the map, two or possibly three local divergences suggest major current sources, but data from stratigraphic studies are needed to support this idea. It is concluded that currents moved down a paleoslope (an ancient regional slope) from southeast to northwest.

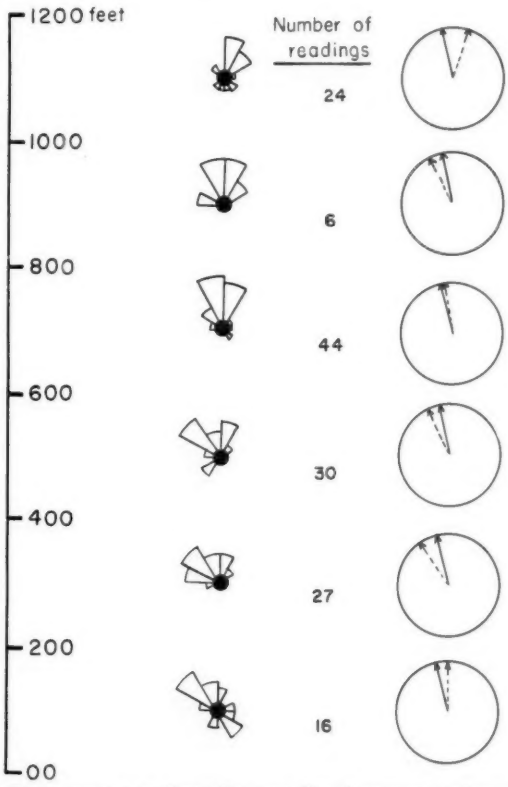

FIGURE 8.—VERTICAL DISTRIBUTION OF CROSS-BEDDING DIP AZIMUTHS AT SUSQUEHANNA WATER GAP, THROUGH BERRY MOUNTAIN, PENNSYLVANIA

Histograms show frequency per cent of cross-bedding azimuths plotted in 30° classes. Full arrow is locality mean; broken arrow is submean at respective 200-foot intervals.

[4] Certain grids contain more locality averages than others. Thus unequal numerical weight is put on these grids when the moving average is constructed.

Cross-Bedding Inclinations

Cross-bedding inclination is the dihedral angle between the cross-bedding and true bedding planes. The tilt-corrected inclination of the cross-bedding ranges from 4° to 55°. Higher tilt-corrected inclinations occur in the folded layers of the Appalachian Mountains than in the gently dipping beds of the Allegheny Plateau. Moreover, such higher inclinations, which were associated with southerly dipping beds, occur in northerly directed cross-bedding. Conversely, in the northerly dipping beds, the north-dipping cross-bedding inclinations were less than those of the south-dipping inclinations. It is clear, therefore, that the inclination is a function of (1) the amount of folding or tilting of the bedding proper, and (2) the relationship between the orientation of the cross-bedding planes and the direction of tilt of the true bedding.

To study the effect of orientation on the deformation of cross-bedding, the dip directions of the tilt-corrected cross-bedding were grouped in four quadrants (Fig. 11). Quadrants I and III are perpendicular to the strike of the true bedding at any outcrop. Cross-bedding dip azimuths (indicated by arrows) are directed northerly in quadrant I and southerly in III. Quadrants II and IV parallel the strike of the true bedding. Cross-bedding dip azimuths are directed easterly in quadrant II and westerly in IV.

The average inclinations of the cross-bedding were also plotted by quadrants for different amounts of tilt and grouped according to their occurrence in a northerly or a southerly dipping bed (Table 2). For example, in beds that dipped from 0° to 30° south, the 501 cross-beds in quadrant I (northerly directed inclinations) had a mean inclination of 19.45°. For the same amount of tilt, the 216 cross-beds in quadrant

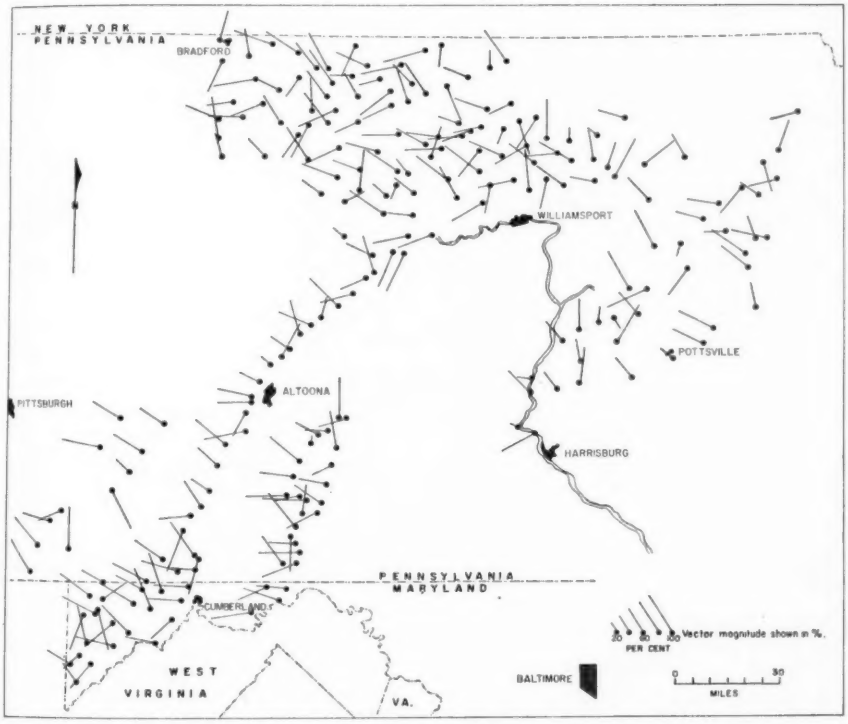

FIGURE 9.—VECTOR MEANS OF TILT-CORRECTED CROSS-BEDDING DIP AZIMUTHS IN POCONO FORMATION

Vectors indicate mean current direction at given localities during Pocono time. Greatest station-to-station variability shown in northwest, least in southeast.

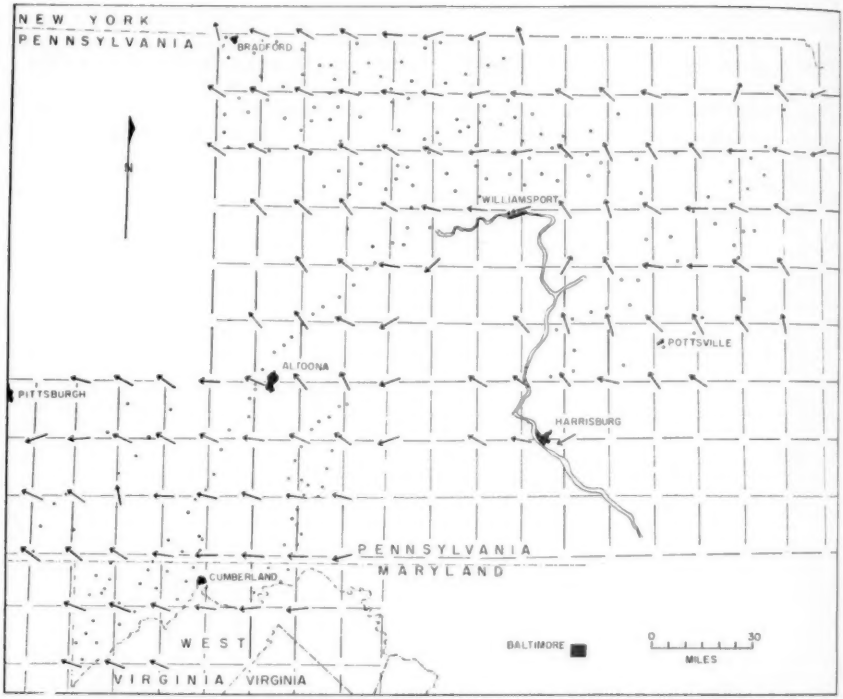

FIGURE 10.—MOVING AVERAGE OF VECTOR MEANS SHOWING REGIONAL CURRENT PATTERNS

Observation points shown by dots; mean vector based on data from four quadrangles shown by arrows placed at centers of respective four-quadrangle areas.

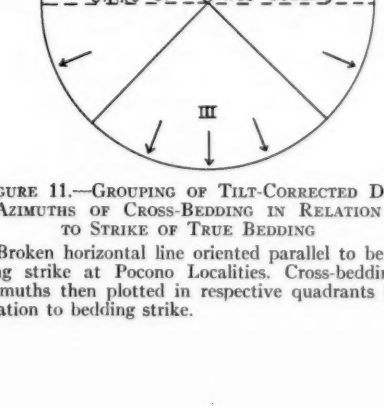

FIGURE 11.—GROUPING OF TILT-CORRECTED DIP AZIMUTHS OF CROSS-BEDDING IN RELATION TO STRIKE OF TRUE BEDDING

Broken horizontal line oriented parallel to bedding strike at Pocono Localities. Cross-bedding azimuths then plotted in respective quadrants in relation to bedding strike.

II (southerly directed inclinations) had a mean inclination of 18.02°. Similar data are tabulated for quadrants III and IV. The inclination of cross-beds in strata that dip northerly from 0° to 30° was similarly analyzed.

In beds tilted 30°–60° the mean inclinations of the cross-beds were plotted in their respective quadrants with reference also to their occurrence in a northerly or southerly dipping bed. This operation was repeated for tilt ranging from 60° to 90° and for overturned beds. All values are summarized in Table 2. Averages of of cross-bedding inclination, with one exception, are lower in beds that dip northerly than in those dipping southerly.

In order to investigate further the relationship between angles of inclination of cross-bedding and amount of deformation, the inclinations, regardless of their orientation, were averaged for the four different amounts of tilt described above. Thus four averages were calculated for all cross-bedding inclinations in

southerly dipping beds and four for those in northerly dipping beds (Table 3). The inclinations of the cross-bedding are generally lower in the north-dipping beds. As shown in Table 2, the difference is more marked in the more steeply dipping beds.

Finally, a mean cross-bedding inclination was computed by averaging the pairs of values in Table 3. Thus for 0°–30° of folding the average inclination of the cross-beds in the northerly dipping beds was averaged with that of the southerly dipping limb. Inclinations were averaged in this manner to avoid unnecessary weighting by the unequal number of readings on different limbs of the folds. Four means obtained (Table 4) show a small rise in average inclination as the amount of deformation is increased.

The Pocono data are similar to data from other areas and formations (Table 4). Although exact comparison is not possible, a similar increase in inclination with increasing deformation is apparent.

Histograms to illustrate Pocono data in Table 4 appear in Figure 12. Cross-bedding inclinations greater than 30°, indicated by shading, are considered abnormal. Cross-bedding formed in an aqueous environment rarely exceeds 30° in inclination. Aeolian sands have steeper foresets than do aqueous deposits. The cross-bedded conglomerates and the pebbles exceeding 1 inch in diameter, however, preclude an aeolian origin of the Pocono beds.

The percentage of inclinations in excess of 30° is calculated for various degrees of folding (Table 5). Here also the increase in inclination with increase in deformation is seen.

Appalachian folding in the coal basins of Pennsylvania and Maryland is considered to be the flexure type, which involves concentric bedding of the limbs as defined by E. Cloos (1947, p. 902). As a result of a petrofabric study, R. E. Fellows (1943, unpub. Ph.D. thesis, The Johns Hopkins Univ.) reported that on an average, less than 14 per cent of the quartz in the quartzose sandstones has recrystallized. Only after 22 per cent of the quartz has recrystallized is a preferred lineation apparent and can the rock be called a tectonite. It is difficult, therefore, to explain why increasing angles of inclination of cross-bedding should correlate with increasing deformation.

TABLE 2.—VARIATION OF MEAN TILT-CORRECTED CROSS-BEDDING INCLINATIONS

Amount of tilt	Direction of dip of true bed	Occurrences of tilt-corrected cross-bedding inclinations							
		Quadrant I		Quadrant II		Quadrant III		Quadrant IV	
		No. of beds	Mean	No. of beds	Mean	No. of beds	Mean	No. of beds	Mean
0°–30°	south	501	19.45°	216	18.02°	163	15.47°	417	16.81°
	north	794	15.28°	424	17.08°	171	19.13°	826	16.58°
30°–60°	south	211	19.90°	71	16.00°	117	16.40°	110	19.96°
	north	137	19.59°	23	13.47°	6	14.17°	116	18.89°
60°–90°	south	155	20.29°	25	19.96°	12	18.67°	58	20.24°
	north	122	20.07°	45	15.33°	19	17.26°	26	18.50°
>90°	south	17	28.28°	5	36.0°	—	—	—	—
	north	62	15.35°	14	13.43°	28	27.89°	80	25.73°

TABLE 3.—VARIATION OF MEAN CROSS-BEDDING INCLINATIONS

Northerly dipping beds are compared to southerly dipping beds for different amounts of folding

Amount of tilt	Direction of dip of true bed	Mean inclination of cross-bedding for all quadrants
0°–30°	south	17.86°
	north	16.44°
30°–60°	south	18.59°
	north	18.68°
60°–90°	south	20.16°
	north	18.62°
>90°	south	30.04°
	north	21.62°

TABLE 4.—VARIATION OF MEAN CROSS-BEDDING INCLINATIONS IN OTHER FORMATIONS

Geological formation	Number of measurements	Mean dip of bedding	Mean inclination of cross-beds	Author
Pennsylvanian (Illinois and vicinity)	531	0°	16.5°	Potter and Olson (1954)
Lorrain quartzite (Bruce Mines, Ontario)	119	19°	20.2°	Pettijohn (1957)
Baraboo quartzite (Wisconsin)	283	46°	23°	Brett (1955)
Lorrain quartzite (Lacloche, Ontario)	32	77°	25.8°	Pettijohn (1957)
Sturgeon quartzite (Michigan)	80	ca90°	28.1°	Trow (1948, Ph.D. thesis, Univ. of Chicago)
Pocono (Maryland and Pennsylvania)	3512	15°	17.15°	This report
Pocono (Maryland and Pennsylvania)	791	45°	18.63°	This report
Pocono (Maryland and Pennsylvania)	462	75°	19.39°	This report
Pocono (Maryland and Pennsylvania)	206	90°	25.83°	This report

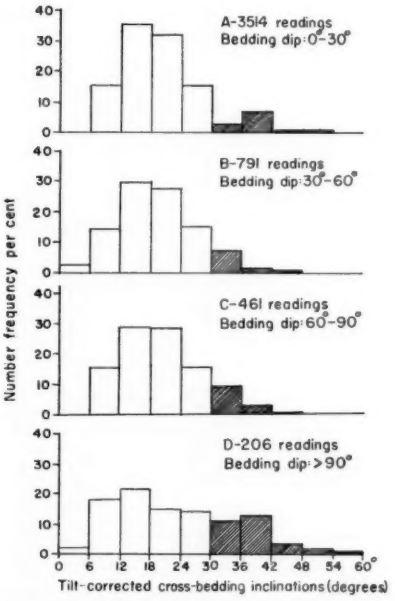

FIGURE 12.—FREQUENCY DISTRIBUTION OF TILT-CORRECTED CROSS-BEDDING INCLINATIONS OF POCONO FORMATION GROUPED ACCORDING TO DIFFERENT AMOUNTS OF TILT

Owing to the concentric nature of the folding, upper beds move relatively upward over the lower beds. This movement initiated a concentric shear between the bedding planes. There is no evidence, such as an easily visible foliation or lineation, to establish the existence of this concentric shear within the bed. Northerly dipping cross-bedding foresets, if affected by the shear, should become less steeply inclined (in relation to original attitude) on the south flank of the syncline and more steeply inclined on the north flank. This has been observed in the Pocono formation. The converse has been observed with southerly directed cross-bedding; the inclination increases on the south flank and decreases on the north flank of the syncline. This effect of folding on cross-bedding inclinations is illustrated by Pettijohn (1957a, p. 474), but the mechanics of the process are obscure.

Origin of Cross-Bedding

Sorby (1859) was among the first to note that currents produced ripples and that deposition on the lee side of ripples produced cross-bedding. Illies (1949, p. 97) witnessed ripple formation in streams and commented that deposition of sand occurred on the lee slopes of ripples at angles between 27° and 30° to the horizontal. Cross-bedding formed by such ripple development is generally less than 6 inches thick. This does not agree with the majority of measurements of the cross-bedding in the Pocono formation.

The association of cross-bedding and the movement of giant ripples, sand waves, and sand bars appears to pertain to the origin of Pocono cross-bedding. This is suggested by the prominences or dunes (Gilbert, 1899, p. 139), the giant sand waves (Kindle, 1917, p. 55), perhaps some of the mega-ripples (Bucher, 1919, p. 258), the plateaulike sand bars (Twenhofel, 1926, p. 443), the terracelike bodies of granular sediments (Shrock, 1948, p. 244) and the transverse bars (Sundborg, 1956,

p. 207). All such features seem to be related, if not identical, phenomena.

Cross-bedding in the Pocono is similar to that formed in transverse bars inasmuch as (1) cross-bedded units are generally bounded by parallel planes which originally approximated horizontality as judged by their relationship with the general bedding, (2) the tops of the cross-beds of the Pocono are truncated, (3) dune crests are not observed in association with the torrential cross-beds, (4) cross-bedded units generally extend across the entire length of the outcrop, which is commonly greater than 30 feet, and this is comparable to the "wave length" of the bars, (5) direction of inclination of the foreset beds is predominantly downcurrent (as inferred from textural and stratigraphic studies), (6) inclination direction in one cross-bedding unit is not necessarily the same in preceding or succeeding units, (7) average thickness of the Pocono cross-bedded units is 6–18 inches and is comparable to the cross-bedded thicknesses in sand-bar deposits. It is concluded that torrential cross-bedding in the Pocono is formed in transverse sand bars, which arise during periods of flood when the sediment load and velocity of the stream are greater.

Primary Linear Structures

Oriented Plant Remains

Macerated plant remains occur in parallel to subparallel orientation on certain bedding planes. Linear stemlike fragments are a fraction of an inch wide and 3–4 inches long and exceptionally as much as 14 inches long with a 3-inch diameter. Similar features have been described and figured from the Unter Vinxbachtal, Germany, by H. Cloos (1938) and mapped by Bausch van Bertsbergh (1940, p. 337).

Large fragments parallel asymmetric ripple marks in outcrops at Duncannon. A similar phenomenon was described by H. Cloos (1938). Orientation of plant fragments, therefore, appears due to lodgement in ripple troughs. If deposition of sand on the lee side of current ripples produces cross-bedding, then the trend of the ripples should be perpendicular, or nearly so, to the current direction. Thus oriented plant stems should be useful in establishing the direction of current, but they will not indicate the sense.

The attitude of the bed containing the oriented plant remains was measured with the Brunton compass. The trend of the plant fragment was also measured by holding the compass in a horizontal position and aligning the axis of the compass parallel to the length of the plant. All readings were plotted on the Schmidt stereonet and rotated about the strike of the bed to horizontality an amount equal to the dip of the bed. This corrected for tilt. All fragments lay in the plane of the bedding, and thus no additional correction for plunge of the fragments was necessary.

Table 5.—Per Cent of Cross-Beds With Tilt-Corrected Inclinations Greater than 30° (Pocono Formation)

Amount of folding	Per cent of cross-bedding inclinations exceeding 30°
0°–30°	9.66
30°–60°	9.90
60°–90°	11.9
>90°	29.1

Most bedding planes containing oriented plant fragments did not have more than 2 or 3 square feet exposed. The trends of all fragments in the area of such exposures were measured individually. At certain localities, more than one bed contained oriented plant fragments. The mean plant orientation in these beds was calculated and recorded. At each locality, all plant orientations were plotted on a single rose diagram (Fig. 13). Data for the various localities implies a consistency in direction of current flow either in a northwest or southeast direction.

The mean plant orientation in the anthracite region, based on 325 plant remains, is N.69°E., indicating the passage of ancient currents northerly or southerly along a bearing of 339° or 159° over that area. The sense of current direction must be determined from the cross-bedding. Clearly the azimuth of 339°, based on the mean of all oriented plants, is consistent with the cross-bedding data.

The dispersion or scatter of the oriented plant stems is much smaller than the spread of cross-bedding dip azimuths. Standard deviations of the oriented plant stems range from 25.3° to 49.9°. The small spread of the oriented plant fragments may be due in part to sampling. Only 2 or 3 square feet of a bedding plane

was involved in the sampling of plants, whereas several yards of cross-bedding layers in many beds extending over 1000 feet was involved in sampling the cross-beds. Thus greater variation can be expected from cross-bedding measurements than from the plant stems.

gular outline of the furrows and ridges, the preferred orientation of such features, and the fact that furrows are the reverse of the ridges on a split slab all suggest that current lineation is due to irregular fracturing or jointing along preferred directions. The main direction of this

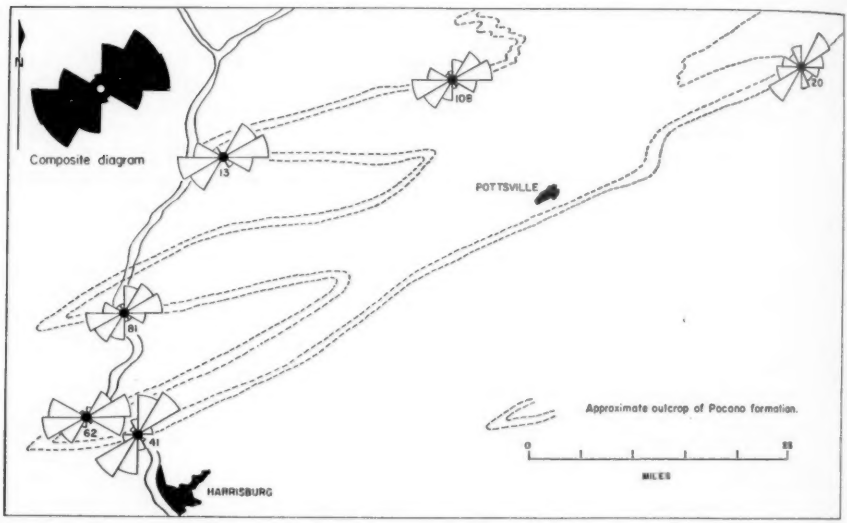

FIGURE 13.—ORIENTATION OF PLANT REMAINS IN THE POCONO FORMATION, ANTHRACITE REGION
Data are plotted in 30° classes on the basis of number frequency per cent. Numeral beside rose diagram represents number of plant remains recorded at that locality.

Primary Current Lineation in Sandstones

Primary current lineation (the "parting lineation" of Crowell, 1955, p. 1357) in sandstones is described by Sorby (1859, p. 138), H. Cloos (1938, p. 358) and Stokes (1947, p. 52; 1953, p. 21; 1954, p. 9). This feature consists of flat furrows or windrows along bedding planes, alternating with ridges which have the same outlines and height (or depth) as the furrows. The furrows on one slab are the ridges on the companion slab.

In general, successive bedding planes show current lineation. At a quarry near Galeton, Pennsylvania, 14 layers within a stratigraphic thickness of 4 feet showed primary current lineations. Primary current lineation is common, but only at Galeton was the structure abundant enough to compare it statistically with other current indicators.

The furrows and ridges, although irregular in outline, commonly are elongated. The trend of this elongation was measured with the Brunton compass. The elongated and somewhat rectan-

fracturing coincides with the current direction as obtained from cross-bedding.

Stokes (1947) observed similar features on the dry sandy beds of intermittent streams in Colorado. No cross-bedding or rippling of the sands was present. He attributed the primary current lineation to slow, almost laminar, flow with sufficient turbulence to lift the grains. Had there been swifter waters, ripple marks and cross-beds would have formed, and had there been laminar flow, grains would not have moved.

A thin section cut parallel to a bedding plane with current lineation was studied to determine if any preferred orientation of sand grains was present. Most grains were equidimensional; no preferred orientation could be observed. It is inferred from the observations of Stokes that primary current lineation is a feature of sedimentation, but it is not known if such features are a response to preferred dimensional orientation or to packing of the component sand grains.

Primary current lineation was measured and statistically analyzed in the same manner as were oriented plant remains. The measurements do not distinguish between the ends of the furrows and ridges. Tilt-corrected trends are recorded as follows: 155°, 163°, 166°, 165°, 172°, 169°, 159°, 154°, 156°, 143°, 151°, 163°, 160°, and 150°. Mean orientation calculated from the above readings is 159° or 339°. Therefore the paleocurrents moved along a bearing of 339° in a northerly or southerly direction. Sense of direction cannot be obtained solely from the lineation.

Only 4° separate the means obtained from cross-bedding and from primary lineation. Lineation azimuths when combined with cross-bedding measurements are excellent guides in reconstructing ancient slopes and current trends.

The primary lineations are restricted to a narrow range, with a standard deviation of 7.6°. Although one station is insufficient to judge its consistency as a current indicator, Stokes (1947, p. 54) reports its reliability over larger areas.

Ripple Marks

Ripple marks occur throughout the Pocono formation but nowhere are abundant enough to use as indicators of current direction. Because they also are linear features, their trends may be analyzed in the same manner as both primary current lineation and oriented plant stems. Oscillation ripples will indicate only the direction, but current ripples will give the sense of direction, as the steep slope is the lee slope.

South of Scranton, Pennsylvania, five beds exhibited ripple marks. Four sets of ripples were asymmetric with trends of 258°, 249°, 242°, and 275°. One oscillation ripple had a trend of 210°. The mean trend is 246°. Asymmetry of the ripples indicates a northwesterly current direction. Because current ripples trend approximately perpendicular to the current direction, the latter is inferred to have an azimuth of 336°. This value is 78° from the mean dip azimuth of the cross-bedding but is in closer agreement with the moving average value of 310°.

Maximum Pebble Sizes

Direction of Transport

Many workers (for example, Sternberg, *in* Barrell, 1925, p. 325) have observed that pebbles decrease in size in a down-current direction. Such decreases in pebble diameters can indicate the direction of sedimentary transport. From this, a probable source area can be deduced.

The decreasing values of the sand-shale ratio reflect the decrease of grain diameters in a down-current direction. The mean grain diameter is a better indicator of current direction than the sand-shale ratio, as it has, quantitatively, a sharper expression of size changes over a broad area. However, it is a time-consuming task to sample every layer of a thick formation, make a mechanical analysis in thin section of each sample, and then apply the necessary correction factors to get true grain diameters. Therefore, only the coarsest fractions (the pebble beds and conglomerates) were examined. The pebbles could be recognized easily at the outcrop and could be measured rapidly.

Pettijohn (1957b, p. 249) used E. H. Kurk's data (1941, unpub. M. S. thesis, Univ. of Chicago) to demonstrate a relationship between mean grain diameter of a detrital population and the diameter of the maximum grain or pebble. From this relationship it appeared that the largest class varied directly with the mean size for various populations. Therefore, instead of measuring the pebble sizes of an entire conglomerate at each locality and calculating the mean of these pebbles, it is faster and easier to measure the largest pebble only. Because the average pebble size decreases in a down-current direction, and because of the relationship of maximum size to population mean, it seemed reasonable that the direction of decreasing size of the largest pebbles would indicate the down-current direction. This principle was applied to both Pocono and Pottsville conglomerates.

The largest diameter visible in the quartz pebble was measured. This was done because (1) the same diameter or apparent diameter was measured each time, (2) it was more practical to look for increasingly larger diameters than for progressively smaller ones.

It was found that the largest diameters of the 10 largest pebbles were generally within a few millimeters of each other in size. The 10 largest pebbles were chosen to reduce any excessive value introduced by an extraordinarily large pebble; also, that number facilitated rapid handling of data.

The average of the 10 largest quartz pebbles was recorded for each locality. In the southeast area of the anthracite region the largest pebbles

averaged 45–60 mm in length, whereas in the western and northwestern areas, they averaged only 10–15 mm.

The diameters of the largest pebbles have been plotted (Fig. 14) in three major classes: 0–25 mm, 25–50 mm, and 50–75 mm. A progressive decrease in size from southeast to northwest is apparent. In the southeast, the largest and intermediate classes are interspersed; in the central area the intermediate and smallest classes are present; in the western and northerly parts only the smallest class is found. The Pocono data (Fig. 14) indicate that currents traveled northward and westward down an ancient regional slope.

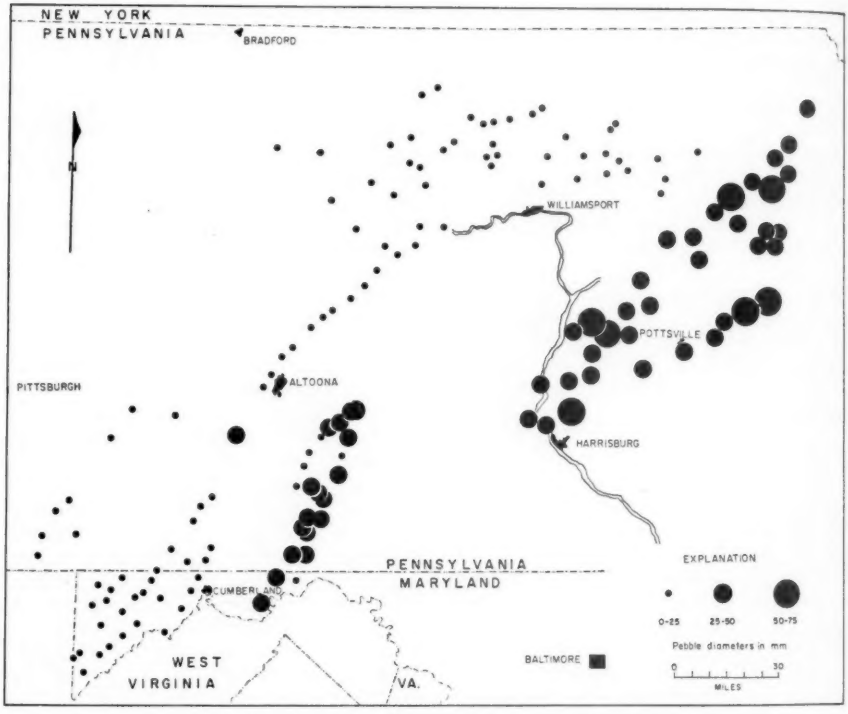

FIGURE 14.—DISTRIBUTION OF PEBBLE SIZES IN THE POCONO FORMATION

A moving average based on a 15-minute grid (Fig. 16) shows averages plotted at the grid intersections, based on the averages previously recorded. The averages, contoured in 10-mm intervals, depict the dip of the paleoslope. The progressive decrease from 60 mm in the southeast to 10 mm in the west and northwest indicates that the ancient regional slope was highest southeast of the present anthracite region and declined toward the west and northwest across Maryland and Pennsylvania. Possibly it extended westerly across northern Virginia and West Virginia and northwesterly across parts of New York.

Distance of Transport

To estimate distance of sedimentary transport the current direction and the rate of detrital size decrease must be known. The current direction is based on cross-bedding measurements; the size decrease of pebbles is based on measurements of diameters at various localities along a line parallel to the current direction.

Crustal shortening is involved in the folding or faulting. Folded or tilted strata must be "unfolded", and the relative horizontal distances adjusted according to the amount of folding. After this adjustment, a direct plot of log sizes (y) of pebbles against distances (x) parallel to the current direction can be made. Such a size-distance curve can be extrapolated

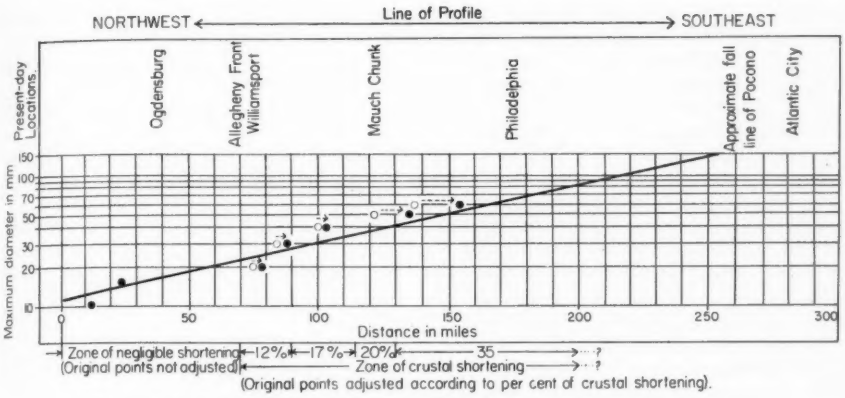

FIGURE 15.—LOG MAXIMUM PEBBLE SIZE AND DISTANCE, POCONO FORMATION

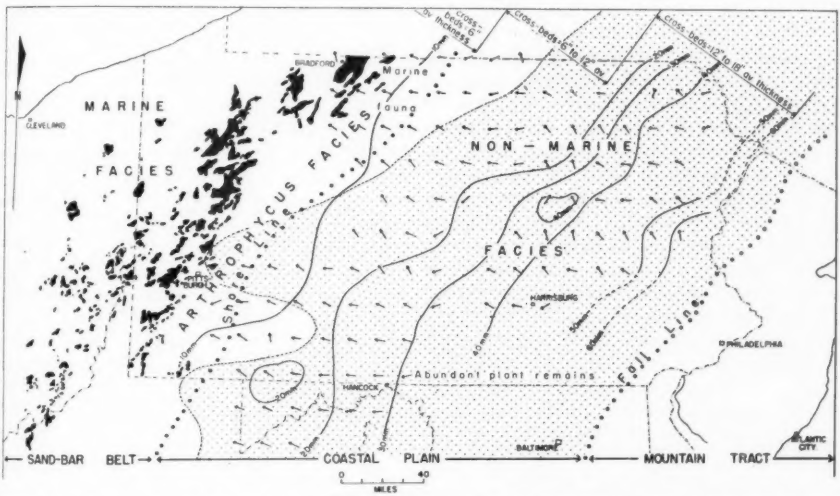

FIGURE 16.—SEDIMENTARY TRENDS AND GENERAL PHYSIOGRAPHIC DIVISIONS DURING POCONO TIME IN THE CENTRAL APPALACHIANS

Shore line shown is approximate average position early in the epoch. Sand-shale ratio greater than 2 shown by stipple, maximum pebble diameters shown by contours in mm, and inferred current directions by small arrows. Note relationship of oil pools (shown in black) of the Upper Devonian-Lower Mississippian to the sedimentary trends.

to intersect y at a value considered to represent the maximum diameter of the pebbles at the source area. Distances can then be read directly from the curve. The rate of pebble-size decrease can be formulated from such data.

To determine the distance of transport of pebbles in the Pocono formation, a line was constructed transversely to the pebble-size contours and, hence, parallel to the current direction. This line or profile extended from the northwest on the Allegheny Plateau southeasterly across the Allegheny front and the eastern part of the anthracite region in the vicinity of Mauch Chunk. Because the line crossed folded sediments, adjustments for crustal shortening were made. Size values were plotted on semilogarithmic paper using logarithmic diameters of pebbles on the ordinate and the linear distance in miles on the abscissa.

E. Cloos (1940, p. 847) calculated crustal

shortening in the anthracite region by reconstructing beds to a prefolding length. His data from 143 sections were applied, with some modification by the present writer, to localities in the Pocono formation.

Crustal shortening northwest of the Allegheny front was considered negligible. Data on crustal shortening in the anthracite region were incomplete. To overcome this shortcoming, this area was divided into zones parallel to the structural trends. In each zone, E. Cloos' estimates for crustal shortening were averaged. The distances along the profile crossing the pebble-size contours were adjusted accordingly (Fig. 15).

Plumley (1948, p. 543) showed that pebbles in the 128-256 mm class are the largest carried by streams emerging from their canyons in the Black Hills. J. S. Schlee (1956, unpub. Ph.D. thesis, The Johns Hopkins Univ.) found that the maximum size of the pebbles was in the 64–128 mm class where the Potomac emerged from the Piedmont and discharged gravel onto the coastal plain. It seems reasonable, therefore, that 150 mm, or about 6 inches, was the probable maximum size of the pebbles of the Pocono streams where these streams discharged into the Pocono basin. Extrapolation of the size-distance curve to intersect the 150 mm ordinate locates the Pocono fall line[5] in the vicinity of Atlantic City, New Jersey. The fall line has been drawn to parallel the Pocono sedimentary strike.

The distance to the fall line can be calculated according to Sternberg's Law; $W = W_o e^{-ax}$, where W is the weight of the pebble at distance x. Quantity W_o is the initial weight of the pebble, e is the base of the natural logarithms, and a is the coefficient of size reduction. About 1875 Sternberg (cited in Barrell, 1925, p. 327) concluded that the wearing down of a pebble is proportional to its weight in water and the distance traveled. Barrell (1925, p. 328) recognized the exponential nature of the law and put it into equation form. This exponential down-current size decrease has also been noted by Krumbein (1937, p. 580), Plumley (1948, p. 546), and others (Krumbein and Pettijohn, 1938, p. 209; Pettijohn, 1957b, p. 529).

Sternberg's Law can also be expressed in terms of diameters; thus $Y = Y_o e^{-ax}$ where Y is the diameter of pebble at distance x and Y_o is the initial diameter of the pebble. The coefficient a must be determined from observations with known Y, Y_o, and x. This value is substituted in the equation, and the size for different values of x can be predicted.

In calculating the distance to the Pocono fall line, the map distance between the 50 mm and 60 mm contours was chosen. This was done because (1) both contours occurred in the same arbitrary zone of crustal shortening and (2) lengthening of stream course due to meandering would be less here than in areas farther north. An adjusted value of 25 miles for crustal shortening was represented by x. Knowing Y and Y_o from the contours, the value of a was calculated to be 0.0072. Substituting this in the equation and letting Y_o be 150 mm and Y be 60 mm, distance x from the 60 mm contour to the fall line is determined. The calculated value is 127 miles, which places the fall line of the Pocono conglomerate 30–40 miles southeast of Atlantic City. Values from the curve are lower probably due to insufficient adjustments for crustal shortening.

Sternberg's Law expresses the decrease in average pebble size in a down-current direction. In the Pocono and Pottsville studies the maximum pebble sizes at each locality decreased in the down-current direction. Field data were applied to the equation, and the distances were calculated to the respective source areas of Pocono and Pottsville conglomerates. These distances were in general agreement with those obtained by extrapolating the size-distance curves of maximum pebble diameters. It is concluded that Sternberg's Law can also apply to the decrease in maximum pebble sizes in a down-current direction.

Pocono Sedimentation

Sedimentary (Depositional) Strike

The original sedimentary or depositional strike was deduced from the paleocurrent pattern. Figure 16 illustrates several aspects of sedimentation during Pocono times. A dominant current pattern directed from the southeast near Philadelphia to the west and northwest is indicated, and the depositional strike, therefore, is normal to the current flow.

The depositional strike is parallel to the isopachs, to contours of equal maximal pebble sizes, to equal sand-shale ratios, and to lines depicting equal thickness of the cross-bedded units. In the direction of sedimentary transport the isopachs decrease in value, cross-bedding units thin, pebble diameters decrease in size,

[5] Pocono fall line refers to a line which paralleled the old mountain front of early Mississippian time. It was located, presumably, at the point where mountain rivers emerged from their canyons and discharged sediments onto a gently sloping coastal plain.

the sand-shale ratio diminishes, and abundant land plants in the southeast give way to a marine fauna in the northwest.

Major Facies

Terrestrial facies.—It has been established that Pocono deposition in the east and southeast was fluviatile. Also, it was suggested, on the basis of coal pods and carbonaceous silt and shale, that deposition took place partly in swampy areas such as a coastal plain. The terrestrial facies is characterized by a sand-shale ratio greater than 2 and by features listed under gross lithology, where such features apply to outcrops in southeastern Pennsylvania.

Arthrophycus facies.—The term *Arthrophycus* facies is introduced to connote a facies thought to be characteristic of near-shore[6] or shore-line environments. It is bounded on one side by terrestrial deposits and on the other by marine beds. The *Arthrophycus* facies overlaps each. Amsden (1955, p. 68) described the same facies in the Lower Silurian of eastern United States and Canada. Sediments passed from a dominantly terrestrial facies westerly and northerly into an *Arthrophycus* facies and then into normal marine beds.

Caley (1940), and Williams (1919), report the Lower Silurian beds of Ontario change to a marine facies in the northwest. The writer (1953, unpub. M. S. thesis, McMaster Univ.) studied the Grimsby sandstone in southern Ontario and observed the transition described by Caley, Williams, and others. From the Grimsby studies an assemblage of characteristics were recorded that closely resemble those of the Pocono *Arthrophycus* facies. The *Arthrophycus* facies is characterized by current ripples, oscillation ripples, interference ripples, small-scale cross-bedding, shale-chip braccias, irregular bedding planes, scour features, possible mud cracks, marine organisms in beds at nearby localities, plant remains, burrowing organisms, *Arthrophycus*[7] or similar fossil, sand-shale ratio of less than 2:1, minor quartz pebble beds or conglomerates, and red beds in adjacent formations. These characteristics, and the position of this facies between marine and nonmarine facies, make it most certainly the product of a near-shore environment.

It is concluded from the Grimsby and Pocono studies, as well as from those by Amsden and other stratigraphers, that a transitional environment of deposition from terrestrial to marine may be characterized by the so-called *Arthrophycus* facies. Combined with a study of paleocurrents, the terrestrial may be separated from the marine, and the location of each predicted.

Marine facies.—A marine fauna in northwest Pennsylvania has been noted in drill cores (Fettke, 1949) and in outcrop (Willard, 1946, p. 785, and the writer). The assemblage noted by Willard includes three brachipod species and certain structures resembling *Fucoides graphica* and *Arthrophycus*. The writer found *Productus* in central McKean County. Busch (*in* Dickey *et al.*, 1943, appendix C) lists fauna in Venango County, northwestern Pennsylvania. The list includes 36 species of brachiopods, 5 species of pelecypods, and 1 species of gastropod.

There are no crinoids or blastoids in the Mississippian rocks of northwestern Pennsylvania, yet echinoids are abundant in rocks of the same age in the Mississippi Valley. Writing of the Pocono fauna, Busch states that

> "... their [the echinoids] absence is probably due to the turbid sand-mud environments which attended the deposition of these sediments. Any hardy form able to withstand a clastic depositional environment would upon death probably have their calyx plates disarticulated as a result of wave agitation."

The Pocono was not studied west of the central part of McKean County; therefore, only a brief description of the marine facies is given. Outcrops in McKean County are mainly shales, with minor thicknesses of sandstone. The sand-shale ratio is less than 2:1. The prominent structures are ripple marks, minor irregular and penecontemporaneously slumped or rolled sandstone beds, and cross-bedding rarely exceeding 6 inches in thickness. The cross-bedding averages 3 inches in thickness and is commonly associated with ripple marks having an amplitude of 2–3 inches or less. Bedding planes are irregular and lack the fine stratification attributed to deposition in quiet waters. Discontinuous sand bodies have been described in many well records and have been identified as offshore bars. Formation of offshore bars in the Upper Devonian of northwestern Pennsylvania is described by Dickey *et al.* (1943, p. 32).

[6] The term near shore could be an alternative to *Arthrophycus* facies. The latter term was chosen as *Arthrophycus* or a similar fossil occurs in a given section which exhibits shallow marine characteristics or continental features or both.

[7] The true *Arthrophycus* as recognized in Silurian rocks does not occur in the Pocono. The Pocono form resembles it in size and shape but not in morphological detail. Priority of facies designation is given to the Silurian form.

Paleogeography

General Setting

The study area is divided into (1) a highland source area, (2) a coastal plain, and (3) a sea area (Fig. 16). The mountain tract or highland source area is separated from the coastal plain by a fall line; the coastal plain is separated from the marine body by a shore line. Because abundant plant remains and large pebbles are common in central and southeastern Pennsylvania and because a marine fauna and finer clastics are present in northwestern Pennsylvania, it is reasonable to infer that a highland source area lay to the southeast and a marine body lay to the northwest. The uniform northwesterly trend of the paleocurrent vectors and the consistent decrease in maximum pebble sizes to the northwest confirm the paleogeographic reconstruction of Figure 16.

Fall Line

The Pocono fall line represents the approximate position of the fall line in early Mississippian time as related to Pocono sedimentation. Similarly the Pottsville fall line represents the approximate position of the fall line in early Pennsylvanian time as related to Pottsville sedimentation.

The distance from sampling localities in Figure 15 to the Pocono fall line was estimated from the pebble measurements; its trend was considered to parallel the sedimentary strike. The position of the Pocono fall line (Fig. 16) is not strictly correct, as no allowance was made for crustal shortening. Its true position as calculated from Sternberg's Law lay 30–40 miles off the present Atlantic Coast. It was drawn parallel to the sedimentary strike. Rivers emerging from the mountain tract farther southeast deposited coarse gravels (150 mm maximum size) in the region adjacent to the mountain front.

Coastal Plain

The coastal plain extends from the fall line to the shore line. The uniform azimuths of the current vectors in the anthracite region suggest that a steeper gradient may have existed in the upper part of the coastal plain and that stream meandering was slight. Toward the shore line, the greater variation in the current vectors probably reflects a greater meandering of the streams in the extreme lowlands where the gradient is low. Coastal swamps and small lakes probably existed in this area.

The coastal plain (Fig. 16) generally coincides with a sand-shale ratio of 2:1 or more. This coincidence is only approximate, because an unconformity has eliminated many of the upper sandy beds in northwestern Pennsylvania. The 2:1 ratio line should swing more to the northwest and more closely parallel the sedimentary strike based on other attributes.

Shore Line

The shore line is difficult to define, as it shifted through time, owing to tectonism and changes in sea level. It may be better to refer to the shore line as a shore zone in this case. To indicate an ancient shore line, only an approximate position can be drawn, and it represents only one of many possible locations between known terrestrial and marine beds deposited during a given geologic time interval.

The shore line shown in Figure 16 is believed to approximate the average position in early Pocono time. It was drawn parallel to the sedimentary strike throughout the Pocono and separates the known occurrence of marine fossils from the plant-bearing Pocono.

Summary of Pocono Sedimentation

The greatest thickness of the Pocono are southeast of a line between Hancock, Maryland, and Harrisburg, Pennsylvania. Thinning to the northwest partly supports this conclusion. Because of erosion to the east, it is not known if the Pocono was thicker in that direction.

Southeast of the Pocono fall line lay an upland area consisting of normal sedimentary clastic and low-rank metamorphic rocks. A river system or systems arising in this area crossed the fall line and spread gravel and sand over a northwestward-sloping plain. The alluvial materials decreased in size with distance of sedimentary transport. The fluvial deposits were thickly bedded and as distance from the source area increased became more thinly bedded.

As the streams left the steeper, upper coastal plain, their courses became irregular, and they probably developed wide meanders. In this lower zone of the coastal plain, pebbles have decreased to less than 10 mm, and cross-bedding units average less than 6 inches in thickness. The sand-shale ratio has decreased to less than 2:1. Along the shore line, these streams formed

local deltas, which may have coalesced to make a deltaic plain.

The discharge of the various streams, predominantly mud with a lesser volume of sand, was responsible for neritic marine deposits. Sufficient sand was not contributed to form a continuous sheet; instead lenses and discontinuous sheets of sand were interbedded and capped by shale. These lenses and sheets tended to form in belts paralleling the shore line.

These sand lenses—barrier beaches and offshore bars—have become traps for the accumulation of oil and gas (Fig. 16). Their distribution and orientation coincides with known pools of Late Devonian—Early Mississippian age in northwest Pennsylvania (Jones and Heeren, 1953), and in adjacent West Virginia and Ohio (Pepper *et al.*, 1945; Demarest, 1946; Demarest and de Witt, 1948).

The location, orientation, and shape of the oil pools in the offshore sand bars are an integral part of the sedimentary pattern (Fig. 16). The oil pools of northwestern Pennsylvania are independent of structure and seem to be offshore bars (Levorsen, 1954, p. 205). Perhaps known belts of oil pools can be extended and new ones predicted by applying the principles outlined in this report.

Mid-Paleozoic Sedimentation

Outline of Study

The cross-bedding and pebble sizes of strata underlying and overlying the Pocono formation in western Maryland and Pennsylvania were also recorded. Cross-bedding attitudes were recorded at 13 exposures of the Upper Devonian and at 5 of the Mississippian (Mauch Chunk) and 7 of the Lower Pennsylvanian. The maximal pebble size of the Pottsville conglomerate was also recorded at 17 localities. The studies were made in order to make comparisons with the Pocono. The pebble measurements were made to establish the distance to the Pottsville fall line.

Cross-Bedding

The cross-bedding measured was of the planar or torrential, type and was processed in the same manner as the Pocono cross-bedding. The Mauch Chunk data were grouped with the Pottsville data so that inferred current patterns of the Pocono could be compared to those of the pre- and post-Pocono times. Composite diagrams of these stages, together with the mean current direction of each, are given in Figure 17.

The mean current direction for the Upper Devonian is 304°; for the Pocono it is 290°; and for the Mauch Chunk and Lower Pennsylvanian it is 295°. The means, therefore, fall within a range of 14°. The shift in current directions during this long period of geologic time was at best very small; the prevailing trend was northwest.

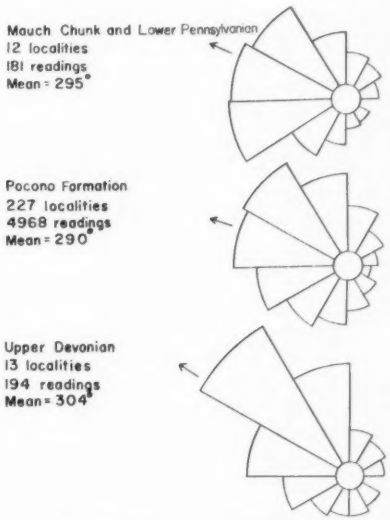

Figure 17.—Variation of Current Directions in Mid-Paleozoic Times

Mean current direction is indicated by small arrows. They are vector means of the cross-bedding dip azimuths.

Maximum Pebble Size in the Pottsville Conglomerate

Large pebbles of the Pottsville quartz conglomerates averaged 5 inches in diameter (illustrated by Wood, 1956). In the present study the white vein quartz pebbles were measured in the same manner as those in the Pocono.

The progressive decrease in size from southeast to northwest is apparent. From 125.8 mm at Pottsville (on the southern rim of the anthracite region), these averages decrease to 81 mm at Aristes in the opposite limb of the synclinorium, to 45.3 mm at the Allegheny front, and to less than 25 mm at Bradford.

A northwest-southeast profile of the pebble sizes was drawn approximately through the distribution of the Pottsville sampling localities and parallel to the current trends. Average

pebble diameters were plotted on semi-logarithmic paper and plotted in the same manner as the Pocono data; crustal shortening was considered (Fig. 18).

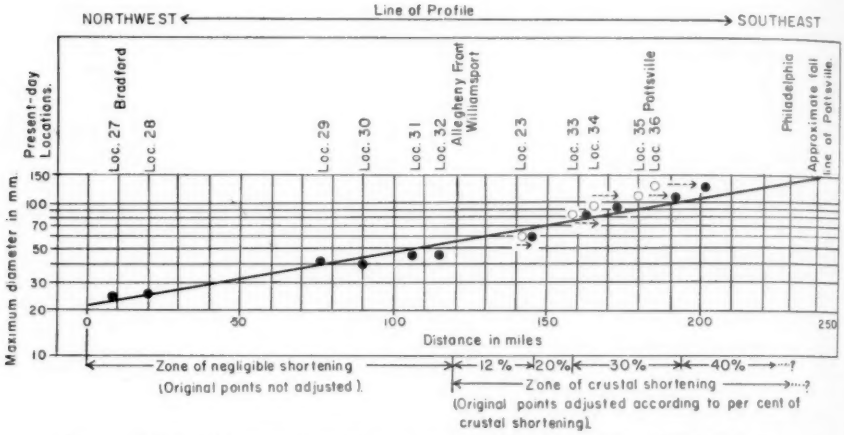

FIGURE 18.—LOG MAXIMUM PEBBLE SIZE AND DISTANCE, POTTSVILLE CONGLOMERATE

TABLE 6.—COMPARISON OF AVERAGE QUARTZ PEBBLE SIZES IN THE POCONO WITH THOSE OF THE POTTSVILLE

Locality	Pebble diameters in mm	
	Pocono	Pottsville
Pottsville	46.9	125.8
Aristes	41.3	81.8
Forest City	42.6	79.4
Mocanaqua	29.7	58.0
Babours	19.4	45.3
Pleasant Valley	15.1	45.3
Morris	14.0	40.0
Asaph	12.0	42.9

Distance of transport was calculated from Sternberg's Law. To determine the value of x, two localities were selected from the southeastern outcrops. The method of selecting these points was similar to that used in the Pocono study; that is, the points fell in the same zone of average crustal shortening. The respective maximum pebble diameters at these points are 92.7 mm (y) and 107.6 mm (y_o), and the adjusted distance (x) between them is 19 miles. The value calculated for a is 0.0078. A maximum diameter of 150 mm was chosen for pebbles occurring at the fall line. The corrected distance to the fall line from the 107.6 mm point is 60 miles. This places the fall line in the vicinity of Philadelphia. It probably is parallel to the prevailing sedimentary strike of the Applachian deposits.

Shift of the Fall Line

The fall line of the Pottsville conglomerate is 100–120 miles northwest of the Pocono fall line, indicating a marked horizontal shift parallel to the direction of sedimentary transport. This shift was suspected, as the pebbles of the Pottsville conglomerate are larger than those of the Pocono at any given locality (Table 6). Localities in Table 6 are listed in order of their occurrence across the sedimentary strike in the down-current direction beginning with Pottsville in the southeast and ending with Asaph in the northwest on the Allegheny Plateau. The table shows coarser pebbles in the Lower Pennsylvanian than in the Lower Mississippian and a decrease in pebble sizes in both formations in the same general direction of sedimentary transport (Fig. 19).

Construction of the size-distance curve indicated that the fall line had shifted but not necessarily the major body of the pre-Pocono ancestral source area. Diastrophism appears to have acted at widely spaced geologic intervals and to have progressively shifted to the northwest generally parallel with present Applachian trends.

Summary of Mid-Paleozoic Sedimentation

In Late Devonian times, sediments were transported from southeast of the anthracite

region westerly and northwesterly across Maryland, West Virginia, eastern Ohio, Pennsylvania, and parts of New York. Because the lithology and assemblage of structures is similar to those in parts of the Pocono, it is thought that part of the Upper Devonian was deposited by rivers. Uplift occurred at the close of the Devonian in northeastern Pennsylvania. The disconformable contacts exhibit scours up to 3 feet deep and several feet wide. In western Maryland and southern Pennsylvania there is no evidence of uplift. Beds are gradational, and a contact cannot be accurately located.

Pocono deposition began southeast of Atlantic City. Coarse conglomerates overlie the Upper Devonian sandstones, which suggests that the fall line shifted after the Devonian uplift. Clastic sediments were carried west and northwest by a system of rivers. Sedimentation at the close of Pocono time was mainly on land.

Information on the Mauch Chunk, although scarce, suggests a continuation of clastic deposition. A slight invasion of the sea from the west is indicated by the eastward-thinning wedge of Loyalhanna limestone in southwestern Pennsylvania and western Maryland.

Two major breaks are indicated between the Pottsville and underlying Pocono and Mauch Chunk. Tilting from the northwest exposed the upper sandy beds of the Pocono and Mauch Chunk to later erosion. Another major uplift in the southeast is indicated by the heavy conglomerate overlying Mauch Chunk sandstones, which are underlain by the lighter conglomerates of the Pocono. Sedimentary transport continued to the northwest and was dominantly terrestrial.

Although the writer's studies in the Pottsville were incomplete, the similarity to the Pocono of structures and textures and the presence of plants suggest the same environment of deposition. After each uplift the river systems eroded the gravels they had previously deposited and carried them farther downstream. A similar process was suggested by P. D. Krynine (unpub. Distinguished Lecture before Pacific Section A.A.P.G., 1943) from petrographic evidence.

With each uplift the whole sedimentary system shifted currentward. The ancestral source area is not known to have moved as a body. The fall line was moved by erosion and river transportation originally initiated by uplift.

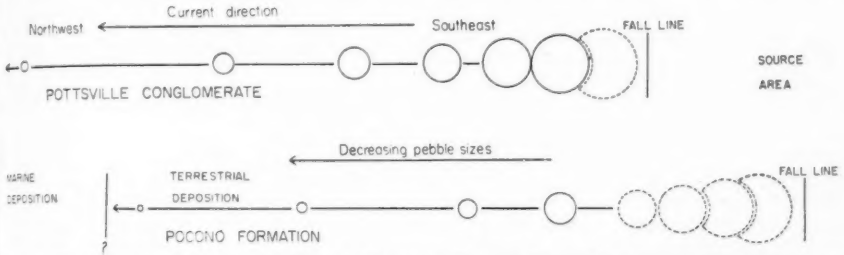

FIGURE 19.—SCHEMATIC DIAGRAM SHOWING MAXIMUM PEBBLE SIZES, POSITION OF FALL LINES, AND SHORE LINES OF POCONO AND POTTSVILLE

Full circles represent pebble diameters occurring at the outcrop. Broken circles represent inferred pebble occurrences presumably eroded.

CONCLUSIONS

Currents in the central Appalachians during mid-Paleozoic times originated in a highland area in the vicinity of the present Atlantic coast. They passed northwesterly across Maryland, Pennsylvania, and neighboring States. The relative postions of the different facies remained fairly constant with a notable shift toward the northwest.

Southeast to northwest, certain trends in the Pocono were noted: the thickness decreased, the sand-shale ratio decreased, diameters of quartz pebbles in the conglomerates decreased, percentage of quartz conglomerate decreased, average thickness of cross-bedded layers decreased, the facies changed from continental to marine, and the conglomerates appeared to ascend the section. Quartz pebbles of the Pottsville conglomerate decreased in size toward the northwest, and at any given locality Pottsville pebbles were larger than those of the Pocono. From this relationship a northwesterly shift in the sedimentary pattern was inferred.

Major westerly and northerly current directions were inferred from ripple marks, parting lineation, and oriented plant stems, which indicated a southeasterly or northwesterly cur-

rent direction; cross-bedding dip azimuths representing current directions indicated such currents were directed mainly to the west and north, and the contoured moving average of the pebble diameters indicated that the paleoslope dipped northwest. Station-to-station variation of the mean current direction increased from the southeast to the northwest. At a given locality, however, current directions were generally consistent during Pocono time. The same inference can be made from cross-bedding studies of the Upper Devonian, Upper Mississippian, and Lower Pennsylvanian beds.

The Pocono rock is a lithic arenite with a matrix consisting of crushed rock fragments mostly of local derivation; for the most part it is fluviatile, and the source area probably consisted of sedimentary and low-rank metamorphic rocks. Cross-bedding in the Pocono is for the most part torrential and was probably formed in sand waves or bars in rivers during floods. The average dip of tilt-corrected cross-beds in gently folded strata is 17° but varies with intensity of folding and position of cross-bed on limbs of folds. The standard deviation of cross-bedding dip azimuths at a given locality ranges from 27° to 94° but commonly ranges from 45° to 65°.

A statistical study of the spread of cross-bedding azimuths at a given locality may not indicate origin of the related rock; primary linear features such as parting lineation in sandstones, oriented plant stems, and ripple marks can indicate current direction but must be applied in conjunction with primary current structures having a vector quality; areal variation of the larger pebbles of a conglomerate rather than the mean of the conglomerate population can be used to infer the paleoslope; extrapolation of the curve of log pebble diameters versus linear distance can be used to give approximate distances to source areas in cases where the average pebble diameter at two or more localities on a line approximately parallel to the current direction is known; the moving average of scalor and vector quantities can be used to depict paleoslopes and regional sedimentary trends; facies studies together with current indicators can be used to interpret paleogeography; the integral relationship of oil reservoirs to the sedimentary pattern may be used in petroleum exploration and development once the sedimentary pattern is known.

References Cited

Amsden, T. W., 1955, Lithofacies map of Lower Silurian deposits in central and eastern United States and Canada: Am. Assoc. Petroleum Geologists Bull., v. 39, p. 60–74

Barrell, J., 1913, The Upper Devonian delta of the Appalachian geosyncline: Am. Jour. Sci., 4th ser., v. 36, no. 215, p. 429–472

—— 1925, Marine and terrestrial conglomerates: Geol. Soc. America Bull., v. 36, p. 279–342

Bausch van Bertsbergh, J. W., 1940, Richtungen der Sedimentation in der rheinischen Geosyncline: Geol. Rundschau, v. 31, p. 328–364

Bolger, R. C., and Grouse, H. V., 1953, Surface and subsurface structure of the Driftwood Quadrangle, Pa.: Pa. Geol. Survey Bull. M36, 4th ser., 32 p.

Brett, G., 1955, Cross-bedding in the Baraboo quartzite, Wisconsin: Jour. Geology, v. 63, p. 143–148

Bucher, W. H., 1919, On ripples and related sedimentary surface forms and their paleogeographic interpretation: Am. Jour. Sci., 4th ser., v. 47, p. 241–269

Caley, J. F., 1940, Paleozoic geology of the Toronto-Hamilton area, Ontario: Geol. Survey Canada Mem. 224, 284 p.

Chayes, F., 1954, Discussion: Effect of change of origin on mean and variance of two-dimensional fabrics: Am. Jour. Sci., v. 252, p. 567–570

Cloos, Ernst, 1940, Crustal shortening and axial divergence in the Appalachians of southeastern Pennsylvania and Maryland: Geol. Soc. America Bull., v. 51, p. 845–872

—— 1947, Oölite deformation in the South Mountain fold, Maryland: Geol. Soc. America Bull., v. 58, p. 843–918

Cloos, Hans, 1938, Primare Richtungen in Sedimenten der rheinschen Geosyncline: Geol. Rundschau, v. 29, p. 357–367

Crowell, J. C., 1955, Directional-current structures from the Prealpine flysch, Switzerland: Geol. Soc. America Bull., v. 66, p. 1351–1384

Curray, J. R., 1956, Analysis of two-dimensional orientation data: Jour. Geology, v. 64, p. 117–131

Demarest, D. F., 1946, Map of the Berea and Murrysville sands of northeastern Ohio, western Pennsylvania, and northernmost West Virginia: U. S. Geol. Survey Oil and Gas Inv., Prelim. map no. 49

Demarest, D. F., and de Witt, W., 1948, Map of the Berea and Murrysville sands of southeastern Ohio, northern West Virginia, and southwestern Pennsylvania: U. S. Geol. Survey Oil and Gas Inv., Prelim. map no. 89

Dickey, P. A., 1941, Oil geology of the Titusville quadrangle Pennsylvania: Pa. Geol. Survey Bull. M22, 4th ser., 91 p.

Dickey, P. A., Sherrill, R. E., and Matteson, L. S., 1943, Oil and gas geology of the Oil City quadrangle, Pennsylvania: Pa. Geol. Survey Bull. M25, 4th ser., 201 p.

Ebright, J. R., 1952, The Hyner and Ferner anticlines and adjacent areas: Centre, Clinton and Lycoming counties, Pennsylvania: Pa. Geol. Survey Bull. M35, 4th ser., 32 p.

Emery, J. R., 1955, The application of a discriminant function to a problem in petroleum geology (Abstract): Am. Assoc. Petroleum Geologists, Soc. Economic Geologists, and Soc. Economic Paleontologists and Mineralogists annual meeting program, p. 110

Fettke, C. R., 1949, Well-sample records: Pa. Topog. Geol. Survey

Gilbert, G. K., 1899, Ripple-marks and cross-bedding: Geol. Soc. America Bull., v. 10, p. 135–140

Haff, J. C., 1938, Preparation of petrofabric diagrams: Am. Mineralogist, v. 23, p. 543–574

Illies, Henning, 1949, Die Schragschichtung in fluviatilen und litoralen Sediment, ihre Ursachen, Messung und Auswertung: Mitt. Geol. Staatsinstitut, Heft 19, p. 89–109

Jizba, Zdenek V., 1953, Mean and standard deviation of certain geologic data—a discussion: Am. Jour. Sci., v. 251, p. 899–906

Jones, T. H., and Heeren, Lillian, 1953, Oil and gas fields of Pennsylvania: Pa. Geol. Survey, 4th ser., map 8

Kindle, E. M., 1917, Recent and fossil ripple mark: Geol. Survey Canada Mus. Bull. 25, p. 1–56

Krumbein, W. C., 1937, Sediments and exponential curves: Jour. Geology, v. 45, p. 577–601

—— 1956, Regional and local components in facies maps: Am. Assoc. Petroleum Geologists Bull., v. 40, p. 2163–2194

Krumbein, W. C., and Aberdeen, Esther, 1937, The sediments on Barataria Bay: Jour. Sed. Petrology, v. 7, p. 3–17

Krumbein, W. C., and Pettijohn, F. J., 1938, Manual of sedimentary petrography: 1st ed., New York, Appleton-Century-Crofts Inc., 549 p.

Krynine, P. D. 1946, The tourmaline group in sediments; Jour. Geology, v. 54, p. 65–87

Levorsen, A. I., 1954, Geology of petroleum: San Francisco, W. H. Freeman and Co., 703 p.

Lowell, J. D., 1955, Application of cross-stratification studies to problems of uranium exploration, Chuska Mountains, Arizona: Econ. Geology, v. 50, p. 177–185

McKee, E. D., and Weir, G. W., 1953, Terminology for stratification and cross-stratification in sedimentary rocks: Geol. Soc. America Bull., v. 64, p. 381–390

Miller, R. L., 1956, Trend surfaces: their application to analysis and description of environments of sedimentation: Jour. Geology, v. 64, p. 425–446

Olson, J. S., and Potter, P. E., 1954, Variance components in some basal Pennsylvanian sandstones of the Eastern Interior Basin; Statistical methods: Jour. Geology, v. 62, p. 26–49

Pepper, J. F., Demarest, D. F., de Witt, W., and Holt, R. D., 1945, Map of the Berea sand of northern Ohio: U. S. Geol. Survey Oil and Gas Inv. Prelim. map no. 39

Pettijohn, F. J., 1954, Classification of sandstones: Jour. Geology, v. 62, p. 360–365

—— 1957a, Paleocurrents of Lake Superior Precambrian quartzites: Geol. Soc. America Bull., v. 68, p. 469–480

—— 1957b, Sedimentary rocks: 2d ed., New York, Harper and Brothers, 718 p.

Pincus, H. J., 1956, Some vector and arithmetic operations on two-dimensional variates, with application to geological data: Jour. Geology, v. 64, p. 533–557

Plumley, W. J., 1948, Black Hills terrace gravels: a study in sediment transport: Jour. Geology, v. 56, p. 526–577

Potter, P. E., 1955, Petrology and origin of the Lafayette gravel: Jour. Geology, v. 63, p. 1–38

Potter, P. E., and Olson, J. S., 1954, Variance components in some basal Pennsylvanian sandstones of the Eastern Interior Basin: Geological application: Jour. Geology, v. 62, p. 50–73

Read, C. B., 1955, Floras of the Pocono formation and Price sandstone in parts of Pennsylvania, Maryland, West Virginia and Virginia: U. S. Geol. Survey Prof. Paper 263, 30 p.

Reiche, P., 1938, An analysis of cross-lamination: the Coconino sandstone: Jour. Geology, v. 46, p. 905–932

Schwarzacher, W., 1953, Cross-bedding and grain size in the Lower Cretaceous sands of East Anglia: Geol. Mag., v. 90, p. 322–330

Shotton, F. W., 1937, The lower Bunter sandstone of North Worcestershire and East Shropshire: Geol. Mag., v. 74, p. 534–553

Shrock, R. R., 1948, Sequence in layered rock: 1st ed., New York, McGraw-Hill Book Co., 507 p.

Sorby, R. C., 1859, On the structures produced by the currents present during the deposition of stratified rocks: The Geologist, v. 2, p. 137–147

Stokes, W. L., 1947, Primary lineation in fluvial sandstones: a criterion of current direction: Jour. Geology, v. 55, p. 52–54

—— 1953, Primary sedimentary trend indicators as applied to ore finding in the Carrizo Mountains, Arizona, and New Mexico: U. S. Atomic Energy Comm. Tech. Rept. RME-3043, pt. 1, 48 p.

—— 1954, Some stratigraphic sedimentary and structural relations of uranium deposits in the Salt Wash sandstone: U. S. Atomic Energy Comm. Tech. Rept. RME-3102, 50 p.

Sundborg, Ake, 1956, The River Klaralven, a study of fluvial process: Geog. Ann., arg. 38, h. 2–3, p. 127–316

Twenhofel, W. H., 1926, Treatise on sedimentation: 1st ed., Baltimore, The Williams and Wilkins Company, 661 p.

Udden, J. A., 1914, Mechanical composition of clastic sediments: Geol. Soc. America Bull., v. 25, p. 655–744

Weller, J. M. *et al.*, 1948, Correlation of the Mississippian formations for North America: Geol. Soc. America Bull., v. 59, p. 91–196

Whitaker, J. C., 1955, Direction of current flow in some lower Cambrian clastics in Maryland: Geol. Soc. America Bull., v. 66, p. 763–766

White, D., 1934, The age of the Pocono: Am. Jour. Sci., 5th ser., v. 27, p. 265–272

Willard, B., 1946, Continental-marine Mississippian relations in northern Pennsylvania: Geol. Soc. America Bull., v. 57, p. 781–796

Williams, M. Y., 1919, The Silurian geology and faunas of Ontario peninsula and Manitoulin and adjacent islands: Geol. Survey Canada Mem. 111, 195 p.

Wilmarth, M. G., 1938, Lexicon of geologic names of the United States, Pt. 2., M-Z: U. S. Geol. Survey, 2396 p.

Wood, G. H., 1956, Subdivision of Pottsville formation in southern anthracite field, Pennsylvania: Am. Assoc. Petroleum Geologists Bull., v. 40, p. 2669–2688

Wright, H. E., Jr., 1956, Origin of the Chuska sandstone, Arizona-New Mexico: a structural and petrographic study of a tertiary eolian sediment: Geol. Soc. America Bull., v. 67, p. 413–434

GEOLOGICAL SURVEY OF CANADA, OTTAWA, ONTARIO, CANADA

MANUSCRIPT RECEIVED BY THE SECRETARY OF THE SOCIETY, JUNE 4, 1957

PROJECT GRANT 723-56

Short Notes

BULLETIN OF THE GEOLOGICAL SOCIETY OF AMERICA
VOL. 69, PP. 1065-1070, 3 FIGS. AUGUST 1958

CRATER HILL LAVA FLOW, ZION NATIONAL PARK, UTAH

BY RICHARD L. THREET

Introduction

Of the numerous, sub-Recent basaltic lava flows and associated cinder cones which dot the landscape of southwestern Utah, perhaps the Crater Hill lava flow has the most vividly and completely displayed geologic record. For about five miles along Utah State Highway 15, the benches on the north side of the Virgin Valley are capped by a basalt sheet more than 200 feet thick; and from viewpoints along the highway near Grafton or on the mesas on the south side of the valley it is evident that this lava flowed down into the Virgin Valley from the vicinity of Crater Hill. Crater Hill is a typical scoria mound which rises more than 600 feet above a mesa developed on Shinarump conglomerate, about 3 miles north of Grafton, at the southwest corner of Zion National Park (Fig. 1).

The Crater Hill lava flow covers approximately 4100 acres, to a depth which must be roughly equal to the thickness of the exposed edges of the basaltic sheet. Deepening of the Virgin Valley and its tributaries has exposed extensively the base of the flow as a cast of the ancient valley bottom and sides, developed chiefly in Moenkopi red beds; and it is possible to estimate the positions and elevations of the various parts of the valley system buried beneath the flow. Accordingly, it appears that the average thickness of the lava sheet must be at least 300 feet, with a maximum of 500 feet.

The considerable thickness and extent of the Crater Hill lava flow, together with local variations in textures and structures of the basalt, apparently led the late H. E. Gregory (1950, p. 138) to postulate multiplicity of flows and a complex geologic history:

> The lava and volcanic agglomerate that cap the cliffs along the Virgin River between Dalton and Coalpits Washes are the edges of sheets that farther north form benches ½ to 3 miles wide. Where its base is exposed the lava rests indifferently on gravel beds of ancient streams, on accumulations of lava boulders cemented with calichelike material, on sandstones of the Shinarump conglomerate, and on shales of the Moenkopi. In consequence of the flows the former rough topography developed in tilted beds has been transformed into fairly level surfaces which locally are marked by roughly circular mounds 20 to 30 feet high and shallow craterlike depressions. The field relations show that the lavas are of at least two ages and came from more than one source. For the flows exposed between Dalton Wash and Grafton a vent may have been near the road 3 miles west of Grafton, where the igneous mass, 200 feet thick, is broken into columns tilted toward the top and bordered by fractured masses of country rock and agglomerate. (See fig. 76) Still earlier flows from unknown sources must have supplied the rounded and angular igneous boulders on which the basalt rests. The youngest volcanic rocks came from Crater Hill, a cone that stands 600 feet above a platform of sedimentary conglomerate, near the western edge of Coalpits Wash. The crater rim of this symmetrical cone consists mainly of clastic material, and its slopes are strewn with lapilli, fragments of scoriaceous lava, and bombs. From breaches in the cone lava emerges and flows eastward over the sandstone wall of Coalpits Wash and southward over the lavas from earlier eruptions. As at Gray Knoll, the vent at Crater Hill produced lava and, as the final stages of eruption, clastic materials. The intermingling of ash and basalt suggests the possibility of alternation in periods of quiet and of explosive eruption.

Gregory's study of the Crater Hill lava flow was necessarily a very small part of his lifelong reconnaissance of the Colorado Plateaus, and he did not give details of the "field relations" which "show that the lavas are of at least two ages and came from more than one source." The benched or steplike character of the southern margin of the lava sheet might suggest two or more flows with different degrees of resistance to erosion, but detailed examination shows that development of a bench is due to erosional stripping of an intensely shattered upper zone from a columnar-jointed lower zone of lava. There is nowhere a slaggy or rusty interval between the two zones, such as might be expected if more than one flow were represented. The development of an irregular "hackly" fractured zone above a columnar-jointed basal zone is rather typical of thick

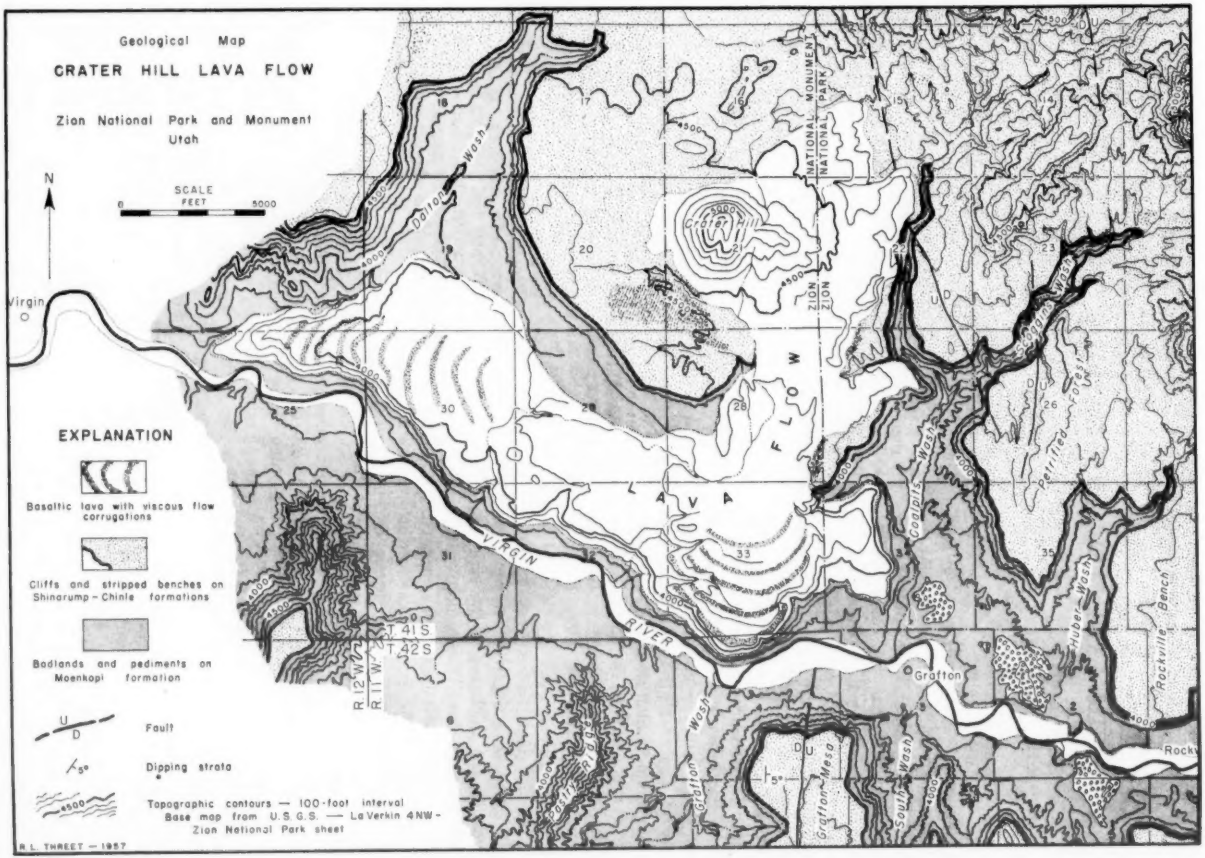

FIGURE 1.—GEOLOGIC MAP OF THE CRATER HILL LAVA FLOW

Small patches which interrupt the Moenkopi pattern north and east of Grafton represent terrace remnants of old course of Virgin River prior to lava flow. North-northeasterly linear shading immediately southwest of Crater Hill represents intense jointing of uppermost Shinarump ledges; joint pattern is not visible elsewhere, in lower Shinarump or in weak Chinle shales surrounding Crater Hill.

The area shown on [illegible] Zion National Park in July 1956 (personal communication, Carl E. Jepson, Chief Park Naturalist,

[illegible] sheets of [illegible] shattering [illegible] chilled ba[illegible] formation [illegible] Gregory [illegible] "agglome[illegible]

[illegible] Shon[illegible] light [illegible] Exc[illegible] there [illegible] be at [illegible]

[illegible] else [illegible] "big, [illegible] volca[illegible] near [illegible] igne[illegible] colu[illegible] frac[illegible] erat[illegible] has [illegible] form[illegible] the [illegible] slop[illegible] sha[illegible] The [illegible] "ti[illegible] the[illegible]

sheets of basalt—apparently by flowage and shattering of a "slush" of lava moving over chilled basal portions of the flow, just short of formation of a true flow breccia. Evidently Gregory mistook the hackly zone of the flow for "agglomerate", for there seems to be nothing

find the "intermingling of ash and basalt" which led Gregory to suggest "the possibility of alternation in periods of quiet and of explosive eruption."

Although aerial photographs (U.S. Dept. Agr. Production and Marketing Adm., 1952,

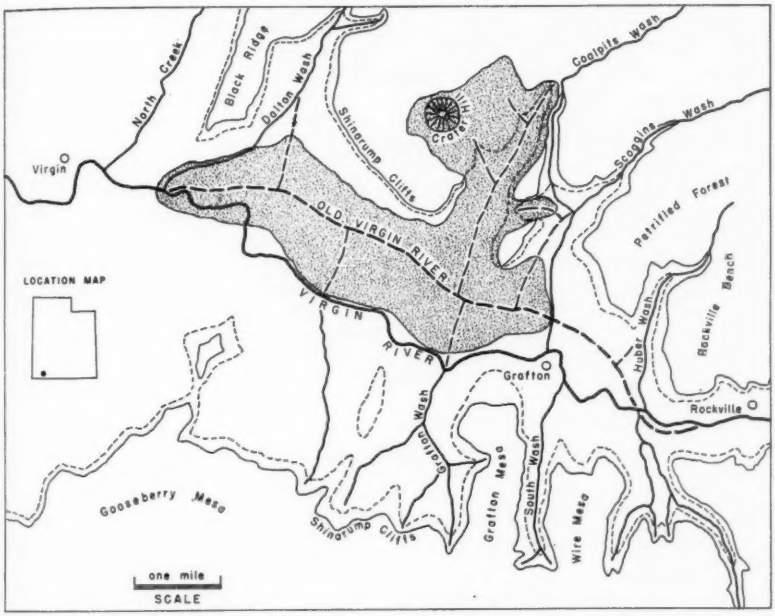

FIGURE 2.—MAP OF ORIGINAL EXTENT OF CRATER HILL LAVA FLOW (stippled)

Showing pre-flow drainage (heavy dashed lines) and probable position of Shinarump cliffs at that time (light dashed lines), in relation to present cliffs and drainage (solid lines).

Except for removal of about 100 acres of the terminus of the flow, by the Virgin River and Dalton Wash, there seems to have been little erosional modification of the original margin of the flow. The lava sheet must be at least 500 feet thick over the axis of the old Virgin River.

else exposed in the vicinity illustrated in his "fig. 76" which could suggest agglomerate or volcanic breccia. Furthermore, the "vent . . . near the road 3 miles west of Grafton, where the igneous mass, 200 feet thick, is broken into columns tilted toward the top and bordered by fractured masses of country rock and agglomerate," illustrated in the same photograph, has a more reasonable explanation as columns formed perpendicular to the cooling base of the flow which molded itself locally to the sloping sides of an ancient gully in the Moenkopi shales.

In typical fashion of comparable vents, "the vent at Crater Hill produced lava and, as the final stages of eruption, clastic materials." The present writer, however, was unable to

Washington County, Utah, DIH-9K-55, 9K-99) faintly reveal viscous-flow corrugations of the lava surface (concentric wrinkles in the "skin" of an expanding, thinning lobe, caused by thrust from the faster-moving, thicker stream behind) in two main lobes of the Crater Hill lava sheet, the continuity of the surface seems to indicate only a splitting of a single stream of lava which spilled over the Shinarump cliffs and into the ancient Coalpits Wash. The positions and orientation of the flow structures indicate that the flow from Crater Hill split, about 1½ miles northwest of Grafton; a blunt lobe pushed on southward across the Virgin Valley, and the main flow streamed 4 or 5 miles westward downvalley. Apparently an ancient extension of Pastry Ridge, a spur from

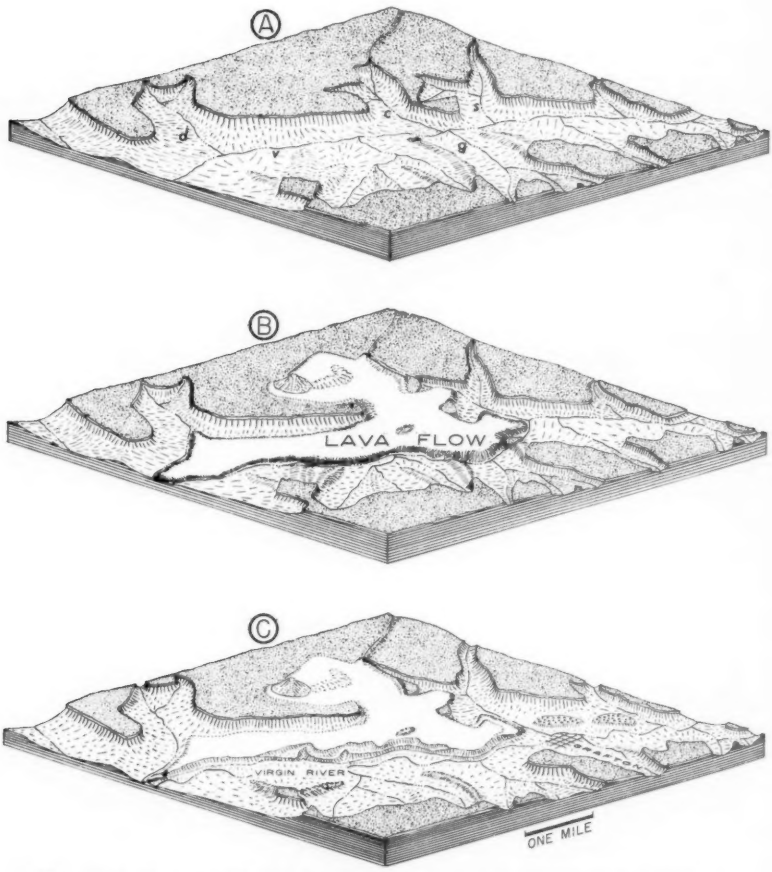

FIGURE 3.—SERIES OF BLOCK DIAGRAMS, LOOKING NORTHEASTWARD ACROSS THE VIRGIN VALLEY, BETWEEN ROCKVILLE AND VIRGIN CITY

Showing effects of Crater Hill lava flow on topography and drainage.

(A) Topography prior to lava flow: Virgin River (v) flowed out of portals of Mukuntuweap (Zion) and Parunuweap canyons (immediately east of area shown), across a broad lowland on Moenkopi shales, between 700-foot cliffs capped by Shinarump conglomerate. Dalton (d), Coalpits (c), and Scoggins (s) washes entered northeast side of Virgin Valley through separate canyons cut into Shinarump benches (stippled). As at present Virgin River was generally flowing much nearer cliffs along north side of the valley, in response to regional northeastward dip and accompanying greater vulnerability of the southern cliffs to erosion. Grafton Wash (g) and other streams from south wall of valley flowed essentially in their present courses but extended nearly a mile farther north.

(B) Topography immediately after eruption and lava flow: Shinarump mesa had been punctured by eruption; lava streamed principally eastward down stripped dip slope and spilled over rim of mesa, into old Coalpits Wash. In spite of main outflow down Coalpits Wash, viscous lava filled the canyon and spilled across the narrow mesa divide, into old Scoggins Wash; main stream of lava flow continued down into Virgin Valley. One lobe pushed southward across valley and nearly a mile up old Grafton Wash; main lobe streamed westward down the old Virgin Valley, flooding locally into Dalton Wash and the broad tributary valley west of Grafton Wash. A minor lobe of the flow pushed eastward, up the confluence of the old Scoggins Wash and Virgin River, north of Grafton.

As a result of the extensive lava dams, streams were diverted into flow-marginal courses, where they have cut down to essentially their present positions. The lower portion of Dalton Wash was diverted almost a mile westward, into the consequent trench between the steep front of the flow and the south slopes of Black Ridge, burying the old basaltic talus from the ancient lava cap of Black Ridge (Gregory, 1950, p. 138). The old canyon of Coalpits Wash was obliterated, and Coalpits Wash was diverted sharply southward across

the south side of the valley, split the flow; a broken arch of the lava surface in the SW¼ NW¼ sec. 33 may be due to settling of a relatively thin and brittle part of the flow around the flanks of a buried knob on the old divide at the junction of the two lobes.

Geomorphology of the Flow

Inasmuch as there has been a general erosional lowering of the valleys since outpouring of the Crater Hill lava flow, it is to be expected that much of the evidence of pre-lava stream courses has been destroyed. Chiefly around the margins of the basalt sheet, the old surfaces over which the lava flowed are preserved and exposed in cross section by recent erosion. The locally thickened parts of the flow are rather closely aligned with segments of present drainage or with strips of gravel-capped terraces which mark the former courses of streams. Furthermore, along the axis of the main stream of the lava flow, the surface of the lava sheet is depressed, apparently because of greater outflow along old valleys beneath the flow or because of differential compaction or collapse of thicker parts of the flow along old valleys.

These various lines of evidence, with textural and structural features discussed earlier, have been synthesized into a map of the relationship of present drainage to former drainage (Fig. 2) and a series of block diagrams which show topographic changes associated with the lava flow (Fig. 3).

Age and Origin of the Flow

The usual stratigraphic methods of dating Recent and sub-Recent lava flows (terrace sequences and associated fossils, artifacts and associated archeological remains, dendrochronology, Carbon-14) cannot be used yet for precise determination of the age of the Crater Hill lava flow. Degree of weathering and erosion of the lava sheet and cinder cone may indicate very roughly the age of the flow, in comparison with dated flows and cinder cones under comparable conditions in adjacent areas. The Crater Hill lava flow and cinder cone seem to show a degree of preservation comparable to the Stage III basaltic lavas of the Uinkaret Plateau (Koons, 1945, p. 156–159) and the San Francisco Mountain area (Colton, 1937, p. 8) of northern Arizona, which are believed to be post-Iowan in age (Sharp, 1942, p. 502).

Although apparently erosion has modified Crater Hill only slightly and the lava surface still retains faint evidence of flow structures and other surficial irregularities, the Crater Hill volcanic features are much less fresh in appearance than are the 1000-year old basaltic flows which have been dated near Sunset Crater (Colton, 1937, p. 33) and elsewhere in northern Arizona and western New Mexico. Therefore, as the age of the Crater Hill flow probably is between a few thousand and a few tens of thousands of years, dating may be within the reach of the Carbon-14 method, if charred vegetation or driftwood can be found in the old soils and stream gravels beneath the flow.

Whatever the exact age of the Crater Hill flow, these basaltic eruptions and lava flows in the Kolob and adjacent plateaus are clearly recent features, related chiefly to the abundant joints and faults which shatter the western portion of the Colorado Plateaus. While most of the basaltic cones and vents in the Zion Park region appear to be located along master joints or intersections of joints, there seems to be no such obvious joint or fault control of the Crater Hill vent. On the other hand, Crater Hill is situated on the shoulder of a small monocline (thrown down about 300 feet, to the east, on opposite sides of the main lava stream in the NE¼ sec. 28) which trends southerly and becomes an antithetically faulted monocline south of the Virgin River. It is not

---

the mesa to Scoggins Wash, cutting a narrow and straight gorge through the Shinarump conglomerate to become established as an accordant tributary. Both streams were further diverted into a more easterly course around the lobe of lava at the confluence of old Scoggins Wash and Virgin River.

Most important of all, the ancient Virgin River was diverted into a lava-marginal course between Grafton and the present mouth of Dalton Wash, across former projections of Pastry Ridge and similar spurs extending from the south side of the Virgin Valley. Although there may have been temporary ponding and alluviation of the valley, subsequent erosion seems to have removed all evidence.

(C) Present topography: Virgin River and tributaries have cut down approximately 200 feet around margin of lava flow, removing projections of former ridges and mesas on south side of valley, causing general retreat of Shinarump cliffs along the valley sides, cliffing the southern margin of the lava flow, as hackly jointed upper part of flow is stripped from columnar-jointed base, and exposing old surface beneath the lava sheet. (Old topography exposed beneath lava flow along highway on north side of Virgin River is actually part of former *south* side of Virgin Valley.) Gravel-capped terraces north and east of Grafton mark former course of Virgin River, through inversion of relief.

known at what point the fault dies out northward, beneath the lava flow, but dying out of the fault and northwestward curvature of the crest of the monoclinal flexure, near the site of Crater Hill, may have focused the piercing activity of ascending molten rock and determined the spot at which the lava broke through the Shinarump ledge. The stripped Shinarump bench which emerges southward from beneath Crater Hill is intensely shattered; one set of fractures trends northeasterly, and a less conspicuous set trends northwesterly—apparently in response to perforation of the mesa caprock and eruption of the lava flow.

Acknowledgments

This brief study was made as part of an investigation of geologic structure and geomorphology of the Colorado Plateau margin in southwestern Utah (summers, 1954–1955), under Grant No. 491 of the National Science Foundation. The writer was assisted in the field by R. L. Lantz.

References Cited

Colton, Harold S., 1937, The basaltic cinder cones and lava flows of the San Francisco Mountain volcanic field, Arizona: Museum N. Ariz. Bull., No. 10, 49 p.

Gregory, H. E., 1950, Geology and geography of the Zion Park region, Utah and Arizona: U. S. Geol. Survey Prof. Paper 220, 200 p.

Koons, E. Donaldson, 1945, Geology of the Uinkaret Plateau, northern Arizona: Geol. Soc. America Bull., v. 56, p. 151–180

Sharp, Robert P., 1942, Multiple Pleistocene glaciation on San Francisco Mountain, Arizona: Jour. Geology, v. 50, p. 481–503

Department of Geology, University of Utah, Salt Lake City, Utah

Manuscript Received by the Secretary of the Society October 29, 1957

BULLETIN OF THE GEOLOGICAL SOCIETY OF AMERICA
VOL. 69, PP. 1071-1073 AUGUST 1958

DEFINITION OF VOLCANIC BRECCIA

BY RICHARD V. FISHER

Common usage of the term breccia by most geologists limits it to a rock composed of angular fragments. The lower-size limit of the fragments is generally set at 2 mm, the limiting size for granules and larger particles (Wentworth, 1922; 1935). Logically it should follow that a volcanic breccia is a breccia composed of angular volcanic fragments larger than 2 mm.

Norton (1917, p. 162), in his classification of breccias, includes volcanic breccias under the heading of subaerial breccias, although he does not set a size limit for the fragments. He further subdivides volcanic breccias (p. 170) into *flow breccia*, which forms by fragmentation of lava during its flow, and *tuff breccia* "made up of fragmental products of explosive eruptions."

Reynolds (1928, p. 97–107) in a modified version of Norton's classification includes volcanic breccias under the heading of *breccias of igneous origin* and as genetic subtypes names *explosion breccias*, *flow breccias*, and *intrusion breccias*, although the heading "volcanic breccia" is not used in the classification.

Wentworth and Williams (1932, p. 51–52) define a volcanic breccia as a *pyroclastic* rock composed of angular volcanic fragments exceeding 32 mm which were solidified before aerial flight and deposition, a definition which apparently excludes volcanic breccias that form by processes other than explosive, such as flow breccias, breccias formed by extrusions of solid lava through a volcanic vent (autobreccias of Curtis, 1954), and breccias formed by the subaerial action of water such as mudflow action (lahars; Van Bemmelen, 1949, p. 191) or by short transportation of volcanic fragments by stream action.

Twenhofel (1950, p. 319) uses the term volcanic breccia in the same sense as Wentworth and Williams—*i.e.*, pyroclastic—but has modified the size limits. He regards the lower limit as 4 mm (fine-grained volcanic breccia). This size restriction is also used by Gilluly, Waters, and Woodford (1951, p. 606).

Kemp (1952, p. 36) considers 1 cm as the lower-grade limit for particles in volcanic breccias and is followed by Emmons *et al.* (1955, p. 432). Some authors have used 1 mm as the lower-grade limit.

Although many authors today follow Wentworth and Williams, the term loses much of its usefulness because of these various definitions' not only in the matter of grade size but, far more importantly, in the matter of genetic implications. Indeed, in the most recent glossary of geologic terms (American Geological Institute, 1957), volcanic breccia has been defined as a "more or less indurated *pyroclastic rock* (author's italics) consisting chiefly of accessory and accidental angular ejecta 32 mm or more in diameter lying in a fine tuff matrix."

It is commonly recognized that volcanic breccias may originate in a variety of ways (Anderson, 1933, p. 215–276; Wentworth and Williams, 1932, p. 32–33; Gilluly, Waters, and Woodford, 1951, p. 606), and apparently most geologists use the term in a broad sense, but in most classifications it is limited to pyroclastic rocks, regardless of common usage (Heinrich, 1956, p. 53; Emmons, Theil, Stauffer, and Allison, 1955, p. 432; Williams, Turner, and Gilbert, 1954, p. 149; Lahee, 1952, p. 269; Twenhofel, 1950, p. 319; Spock, 1953, p. 59; Pirrson and Knopf, 1947, p. 112; Johannsen, 1939, p. 7; Hatch, Rastall, and Black, 1950, p. 258). There obviously is a confusing discrepancy between classification and usage.

Anderson (1933, p. 246), following Lacroix, has reviewed the variety of ways in which volcanic breccias can originate and has arranged their origins in the following manner:

I. Volcanic breccias not transported by water
  A. Crumbling of a dome (*brèches d'écroulement*)
  B. Intrusion (massive *pépérites*)
  C. Friction
  D. Crumbling of advancing lava flow (blocky lava)
  E. Eruptions
    a. Vulcanian
    b. Pelean (*nuées ardentes*)
    c. Ultra-vulcanian (Bandai-san)
  F. Dry avalanche (Vesuvius)

II. Volcanic breccias transported by water
  A. Eruptions
    a. Through a crater lake
    b. Melting of ice and snow
    c. Following heavy rains
    d. Accompanied by heavy rains
  B. Not related to eruptions
    a. Collapse of the dam of a crater lake

b. Heavy rains falling on unconsolidated ejecta
c. Rapid melting of snow and ice (Mount Shasta)

Since there can be great differences in the environments of deposition of the various types of extrusive coarse-grained fragmental volcanic rocks, and since the term volcanic breccia used in a broad sense is extremely useful, it should be made clear that "volcanic breccia" includes all types of volcanic breccias composed of large angular volcanic fragments, regardless of origin. The *definition* should include rocks of such diverse origins as mudflow breccias and block breccias, both types of which are volcanic breccias though certainly not pyroclastic in origin.

TABLE 1.—PROPOSED GRADE-SIZE LIMITS FOR VOLCANIC BRECCIA

Grade size (mm)	Pyroclastic terminology	Sediment-volcanic terminology
>32	Pyroclastic breccia and Agglomerate	Volcanic breccia and Volcanic conglomerate
32–4	Lapilli tuff	
4–2	Tuff <4 mm.	

Discussion

Since "volcanic breccias" formed by fluviatile processes are "true" sedimentary rocks, the grade-size limitations of a generalized term should be considered. It is herein proposed that 2 mm be set for the lower-grade-size limit of fragments composing volcanic breccias, but that established grade sizes for the purely pyroclastic volcanic breccias be retained—*i.e.*, 32 mm (Table 1). Further, it is proposed that *pyroclastic breccia* (a term used by Macdonald, 1953, p. 177) be used for the "volcanic breccia" of Wentworth and Williams.

In keeping with a broad meaning of the term volcanic breccia, the matter of matrix is important. Volcanic breccias may be sedimentary in origin, hence will have a "sandy" or "muddy" matrix; they may be pyroclastic in origin with a tuffaceous matrix, or have a vesicular and pumiceous matrix common to the products of glowing avalanches (Williams, 1949, p. 23); or they may be caused by fragmentation of flowing lava, with the result that particles may be stuck together by adherence of once-plastic surfaces, and thus be "open-structured" (Macdonald, 1953, p. 177). Also, matrix may be formed during movement of a lava flow by mutual abrasion of particles, thereby causing fine sand and dust to develop within the interstices of the fragments (Macdonald, 1953, p. 177; Curtis, 1954, p. 463). The term volcanic breccia should be defined to include any type of volcanic breccia, with or without a matrix.

Normally the fragments of a volcanic breccia are composed of volcanic material. Occasionally, however, loose rock of any origin may be incorporated within a brecciating flow as it moves along the surface of the ground. Upon solidification, the flow breccia may be composed in part of nonvolcanic fragments set in a volcanic matrix. This type of breccia should also be included under the term volcanic breccia.

A proposed definition for volcanic breccia which would enable a geologist to use it for any type of volcanic breccia, regardless of origin, is suggested as follows:

> A volcanic breccia is a rock composed predominantly of angular volcanic fragments greater than 2 mm in size set in a subordinate matrix of any composition and texture, or with no matrix; or composed of fragments other than volcanic set in a volcanic matrix.

If this, or a similar definition, were to be accepted, then a statement such as "a field of volcanic breccias" would not imply "a field of volcanic rocks of explosive origin," but instead "a field of breccias composed of volcanic fragments." To the author, the use of the term in the latter sense is a far better representation of the facts, for many volcanic "fields" are composed of volcanic breccias of all modes of origin, not just pyroclastic.

References Cited

American Geological Institute, 1957, Glossary of geology and related sciences: Nat. Acad. Sci.-Nat. Research Council, 325 p.

Anderson, C. A., 1933, The Tuscan formation of northern California with a discussion of the origin of volcanic breccia: Univ. Calif. Pub., Bull. Dept. Geol. Sci., v. 23, no. 7, p. 215–276

Curtis, G. H., 1954, Mode of origin of pyroclastic debris in the Mehrten formation of the Sierra Nevada: Univ. Calif. Pub., Bull. Dept. Geol. Sci., v. 29, no. 9, p. 453–502

Emmons, W. H., Thiel, G. A., Stauffer, C. R., and Allison, I. R., 1955, Geology: New York, McGraw-Hill Book Co., Inc., 638 p.

Gilluly, J., Waters, A. C., and Woodford, A. O., 1951, Principles of geology: San Francisco, Freeman and Company, 631 p.
Hatch, F. H., Rastall, R. H., and Black, M., 1950, The petrology of the sedimentary rocks: London, Thomas Murby and Company, 383 p.
Heinrich, E. W., 1956, Microscopic petrography: New York, McGraw-Hill Book Co., Inc., 296 p.
Johannsen, A., 1939, A descriptive petrography of the igneous rocks: vol. I, Univ. Chicago Press, 2d ed., 318 p.
Kemp, J. F., 1952, A handbook of rocks, Grout, F. F. *editor*: 6th ed., New York, D. Van Nostrand Co., Inc., 300 p.
Lahee, F. H., 1952, Field geology: 5th ed., New York, McGraw-Hill Book Co., Inc., 883 p.
Macdonald, G. A., 1953, Pahoehoe, aa, and block lava: Am. Jour. Sci., v. 251, p. 169–191
rton, W. H., 1917, Studies for students: A classification of breccias: Jour. Geology, v. 25, p. 160–194
Pirsson, L. V., and Knopf, A., 1947, Rocks and rock minerals: New York, John Wiley and Sons, Inc., 349 p.
Reynolds, S. H., 1928, Breccias: Geol. Mag., v. LXV, no. 3, p. 97–107
Spock, L. E., 1953, A guide to the study of rocks: New York, Harper and Brothers, 256 p.
Twenhofel, W. H., 1950, Principles of sedimentation: 2d ed., New York, McGraw-Hill Book Co., Inc., 673 p.
Van Bemmelen, R. W., 1949, The geology of Indonesia: v. 1A, Hague, Martinus Nijhoff, 732 p.
Wentworth, C. K., 1922, A scale of grade and class terms for clastic sediments: Jour. Geology, v. 30, p. 377–392
—— 1935, The terminology of coarse sediments: Nat. Research Council Bull. 98, p. 225–246
Wentworth, C. K., and Williams, H., 1932, The classification and terminology of the pyroclastic rocks: Nat. Research Council Bull. 89, p. 19–53
Williams, H., 1949, Geology of the MacDoel quadrangle: Calif. State Bur. Mines and Geology, Bull. 151, 78 p.
Williams, H., Turner, F. J., and Gilbert, C. M., 1954, Petrography: San Francisco, Freeman and Company, 406 p.

Univ. of California, Santa Barbara College, Goleta, Calif.

Manuscript Received by the Secretary of the Society, February 3, 1958